Systematic Analysis of Molecular Mechanisms in Glomerular Proteinuria in Humans

---

Dissertation

zur

Erlangung der naturwissenschaftlichen Doktorwürde
(Dr. sc. nat.)

vorgelegt der

Mathematisch-naturwissenschaftlichen Fakultät

der

Universität Zürich

von

Kontheari Sen

von Langnau am Albis ZH

Promotionskommission

Prof. Dr. Carsten A. Wagner (Vorsitz)
Prof. Dr. Clemens D. Cohen (Leitung der Dissertation)
Prof. Dr. Johannes Loffing
Prof. Dr. Matthias Kretzler
Prof. Dr. Rudolf P. Wüthrich

Zürich, 2018

TABLE OF CONTENTS

ZUSAMMENFASSUNG

Neben der hohen individuellen Belastung für den Patienten, stellen die chronischen Nierenerkrankungen eine relevante Herausforderung für die Gesundheitssysteme dar. Die chronische Niereninsuffizienz ist sowohl mit dem Risiko des Fortschreitens der Niereninsuffizienz bis zur Dialysepflicht als auch mit der Entwicklung kardiovaskulärer Komplikationen verbunden. Dabei stellt das Vorliegen einer hohen Proteinurie einen der wenigen etablierten Risikoindikatoren für die Entwicklung einer terminalen Niereninsuffizienz mit erhöhter kardiovaskulärer Morbidität und Mortalität dar. Das Ziel dieser Doktorarbeit war es, neue Gentranskripte zu identifizieren, die an der Entwicklung von humanen Nierenerkrankungen beteiligt sind, indem Genexpressionsprofile der Europäischen Renalen cDNA Bank-Kröner-Fresenius-Biopsiebank (ERCB-KFB) mit den neuesten technischen und bioinformatischen Methoden analysiert wurden. Da das Vorhandensein von Proteinurie von hoher klinischer Relevanz ist, konzentrierten sich unsere Studien hauptsächlich auf erworbene proteinurische Glomerulopathien, wie Minimal Change Disease (MCD), fokal-segmentale Glomerulosklerose (FSGS) und membranöse Glomerulonephropathie (MGN).

Zunächst generierten wir einen humanen renalen Datensatz an glomerulär überexprimierten Gentranskripten, REGGED, mit 677 Genen von bereits bekannter und unbekannter glomerulärer Relevanz. Dieser Datensatz war die umfassendste humane glomeruläre Genexpressionsdatenbank zum Zeitpunkt ihrer Veröffentlichung.

Chronische Hypoxie trägt zur Entstehung von Nierenfibrose bei und es wird vermutet, dass sie an der Entwicklung der Nephrosklerose (NSC), der sogenannten hypertensiven Nephropathie, beteiligt ist. Wir haben spezifische Studien durchgeführt, um die biologischen Prozesse einer Hypoxie-bedingten Nierenschädigung bei NSC zu verstehen. Dabei fanden wir das Hypoxie-induzierte Gentranskript Chemokin C-X-C-Motivrezeptor 4 (CXCR4) prominent in Glomeruli von NSC-Patienten induziert. In NSC-Biopsien zeigte CXCR4, ein bekanntes Zielgen der Hypoxie-induzierten Transkriptionsfaktoren, immunhistochemisch eine starke Positivität in Podozyten, die auch eine nukleäre Positivität für den Hypoxie-induzierbaren Faktor-1α (HIF1α) aufwiesen. Diese Daten weisen auf eine transkriptionelle Aktivität von HIF1α in Glomeruli bei NSC hin.

In einem weiteren Schritt wurde mit unserem REGGED-Datensatz ein glomeruläres Gentranskript mit hoher Induktion in den progressiven Glomerulopathien FSGS und MGN selektiert. Unter den matrizellulären Molekülen war Periostin (POSTN) am stärksten in

diesen progressiven und sklerosierenden Glomerulopathien induziert. Wir konnten erstmals zeigen, dass Periostin in gesunden Glomeruli konstitutiv exprimiert ist und bei Entwicklung einer chronischen Niereninsuffizienz stark induziert wird. So zeigte seine Expression eine negative Korrelation mit der klinisch gemessenen Nierenfunktion bei humanen proteinurischen Glomerulopathien. Stimulationsexperimente an murinen Mesangialzellen mit TGF-β1, einem bekannten Stimulator für die Periostin-Expression in anderen Zellen, führten zu einer robusten Induktion von Periostin. Menschliche und murine Mesangialzellen, die mit Periostin inkubiert wurden, reagierten mit Proliferation. Nieren von Periostin-defizienten Mäusen zeigten vergrösserte Glomeruli und wiesen ein proliferatives Mesangium auf. Die Serumproben dieser adulten Periostin-defizienten Mäuse zeigten eine signifikant abnehmende Nierenfunktion, was auf eine Relevanz von Periostin in der Nierenentwicklung hinweist. Wir nutzten die etablierten Techniken zur Periostin-Analyse auch zur Untersuchung dieses matrizellulären Moleküls bei der peritonealen Fibrose bei niereninsuffizienten Patienten, die mit Peritonealdialyse behandelt wurden. In diesen Patienten fand sich Periostin in fibrotischen Bereichen des Peritoneums stark positiv gefärbt, und auch die Periostinkonzentration stieg im Dialysat mit Dauer der Peritonealdialysetherapie signifikant an.

In Patienten mit spezifischen proteinurischen Nierenerkrankungen mit primärer Podozytendysfunktion kann die Therapie mit Glukokortikoiden zu einer prompten Verbesserung der Proteinurie führen. Dies weist auf einen direkten glomerulären Glukokortikoideffekt in diesen Podozytopathien hin. Auf der Suche nach einem glomerulären REGGED-Gentranskript mit bekannter glukokortikoid-abhängiger Genregulation fanden wir TSC22D3 bei proteinurischen Glomerulopathien supprimiert exprimiert. In humanen Nieren, in diesem Fall Transplantatnephrektomien, waren Podozyten und einige distale Tubuli immunhistochemisch positiv für TSC22D3 gefärbt. Die Western-Blot-Analysen zeigten eine Expression von TSC22D3 in humanen und murinen Podozyten. Die TSC22D3-Expression konnte in diesen Zellen dosisabhängig durch Zugabe von Glukokortikoid gesteigert werden. Zum besseren Verständnis der Rolle von TSC22D3 wurden Isoformen des TSC22D3-Drosophila-Homologs *bunched* in Drosophila-Larven unter verschiedenen Fütterungs-bedingungen untersucht. Hierbei zeigten sich Hinweise auf eine funktionelle Interferenz zwischen den verschiedenen Isoformen.

Zusammenfassend haben wir eine hochspezifische glomeruläre Genexpressionsdatenbank etabliert und für Untersuchungen zur Pathogenese der humanen Nephrosklerose, der matrizellulären Biologie bei progressiven Nierenerkrankungen und zur Podozytenbiologie bei steroid-sensitiven Glomerulopathien genutzt.

SUMMARY

Beside considerable restriction to the patient's individual life and overall poor prognosis, chronic kidney disease (CKD) also burdens the health care system with high costs. CKD patients are prone for progression to end-stage renal failure and development of cardiovascular complication. Proteinuria is one of the few established prognostic indicators for disease progression, cardiovascular morbidity and overall mortality. The aim of this PhD study was to identify novel renal gene transcripts involved in human CKD development by analyzing gene expression profiles from samples of the European Renal cDNA Bank-Kröner-Fresenius Biopsy Bank (ERCB-KFB) using most recent technical and bioinformatical tools. As proteinuria is of specific clinical relevance our studies mainly focused on acquired proteinuric glomerulopathies namely minimal change disease (MCD), focal-segmental glomerulosclerosis (FSGS) and membranous glomerulonephropathy (MGN).

Using a comparative strategy of microdissected nephron segments, we first established a human renal glomerulus-enriched gene expression dataset (REGGED) containing 677 genes of known and previously unknown glomerular relevance. This dataset was proven to be the most comprehensive human glomerular gene expression database at the time of publication.

Chronic hypoxia contributes to renal fibrosis and was hypothesized to be involved in nephrosclerosis (NSC), also known as hypertensive nephropathy. We performed specific studies to comprehend the biological processes of hypoxia-related renal injury in NSC. We found a hypoxia-associated gene expression profile in glomeruli from NSC patients not seen in controls. The expression of chemokine C-X-C motif receptor 4 (CXCR4), a known gene regulated by hypoxia-induced transcription factors (HIF), was found to be prominently induced in NSC glomeruli. In NSC biopsies, CXCR4 protein showed an enhanced staining in podocytes of NSC glomeruli, associated with a nuclear positivity of the hypoxia-inducible factor-1α (HIF1α) suggesting a transcriptional activity of HIF1α.

In a further step, our REGGED dataset was used to select a glomerular gene transcript with highest induction in progressive proteinuric glomerulopathies, namely FSGS and MGN. Among matricellular genes, periostin (POSTN) was found to be maximally induced in these progressive, sclerosing glomerulopathies. In further studies, periostin was found to be constitutively expressed in healthy glomeruli with a maximal induction with development of renal failure. Its expression correlated negatively with renal function in human proteinuric glomerulopathies. Stimulation experiments performed on murine mesangial cells with TGF-β1, a known stimulator for periostin expression, resulted in a robust induction of periostin.

Human and murine mesangial cells exposed to periostin responded with proliferation. In kidneys from periostin-deficient mice, glomeruli were enlarged and showed a proliferative mesangium. Serum data from these adult periostin-deficient mice indicated a reduced renal function suggesting developmental relevance of periostin in the kidney. We took the studies on the matricellular molecule periostin further to peritoneal fibrosis in peritoneal dialysis patients. In these patients with end-stage renal disease, periostin was positively stained in fibrotic areas of the peritoneum and periostin concentrations in the dialysate significantly increased with time on treatment.

In patients with specific proteinuric renal diseases with primary podocyte dysfunction, the treatment with glucocorticoids may lead to a prompt improvement of proteinuria. This suggests a direct glomerular effect of glucocorticoids in such podocytopathies. Seeking for a glomerulus-enriched gene transcript with known glucocorticoid-induced gene regulation, we found TSC22D3 to be repressed in human proteinuric glomerulopathies. In human kidney specimen, i.e. transplant nephrectomies, podocytes and some distal tubules were stained positive for TSC22D3. Western blot analysis showed expression of TSC22D3 in human and murine podocytes. Its expression could be induced by application of glucocorticoids in a dose-dependent manner. To better understand the biology of TSC22D3, isoforms of the TSC22D3 drosophila homolog *bunched* were studied in drosophila larvae under various feeding conditions, suggesting a functional interference among the different isoforms.

In conclusion, we generated a unique glomerulus-enriched gene expression dataset and used this for studies on the pathobiology of glomerular nephrosclerosis, matricellular biology in progressive glomerulopathies and glucocorticoid-dependent glomerular gene transcripts in steroid-sensitive glomerulopathies.

INTRODUCTION

1. CHRONIC KIDNEY DISEASE

The kidneys perform several important tasks, including the removal of excess fluid and metabolic waste products such as urea, creatinine, uric acid and toxins from the blood and the maintenance of homeostasis [1]. This includes the regulation of electrolyte levels such as calcium, sodium and potassium, and the control of acid-base balance. Certain essential hormones are produced by the kidney such as calcitriol (1,25-dihydroxy-vitamin D_3), erythropoietin (EPO) and renin. The latter plays a major role in controlling blood volume and blood pressure by regulation of the angiotensin aldosterone system. Each human kidney is composed of about one million nephrons. The nephron forms the working unit of the kidney and consists of a renal body (the glomerulus with a tuft of capillaries and the Bowman's capsule) and an associated renal tubule system (containing the proximal tubule, loop of Henle, distal and collecting tubule). These organs filtrate about 180 liters of primary urine daily from the glomerular capillaries into the renal tubules and produce approximately 2 liters of urine. The urine results from glomerular filtration and following tubular reabsorption of sodium, water and specific solutes and secretion of metabolism products and other substances [2]. Whereas glomerular filtration is mainly influenced by the netto sum of various pressures and resistances, the tubular reabsorption includes passive and active mechanisms through osmosis and transporters (e.g. ENaC; SGLT1/2; GLUT1/2) [3-6]. The glomerular filtration barrier consists essentially of three layers: the capillary endothelium with its glycocalyx, the negatively charged basement membrane and the podocytes, which also form the inner wall of the Bowman's capsule [7]. While the basement membrane consists of collagen and glycoproteins, the podocytes form between their foot processes a slit diaphragm. The filtration barrier appears to be permeable only to molecules up to a certain size, i.e. smaller than albumin.

The glomerular filtration rate (GFR), an important clinical parameter to define renal function, is defined as the volume of blood that is filtered by all glomeruli per unit time. It is a measure for the elimination capacity of the kidneys and a GFR greater than 90 milliliters per minute is considered as "normal" in most populations. Clinical guidelines recommend estimating GFR (eGFR) by a measurement of serum creatinine, a waste product created by the muscles. The eGFR calculation should be based on the CKD-EPI (Chronic Kidney Disease Epidemiology

Collaboration [8]) or the MDRD (Modification of Diet in Renal Disease [9]) study equation. Both equations are considering the same four variables age, gender, race and serum creatinine concentration. Compared to the gold standard GFR measurement using radioactive ^{125}I-iothalamate the CKD-EPI equation gives the most accurate estimation for GFR greater than 60 milliliters per minute, but the MDRD study equation is still used in 92% of US laboratories as its accuracy is close to that of the CKD-EPI [10].

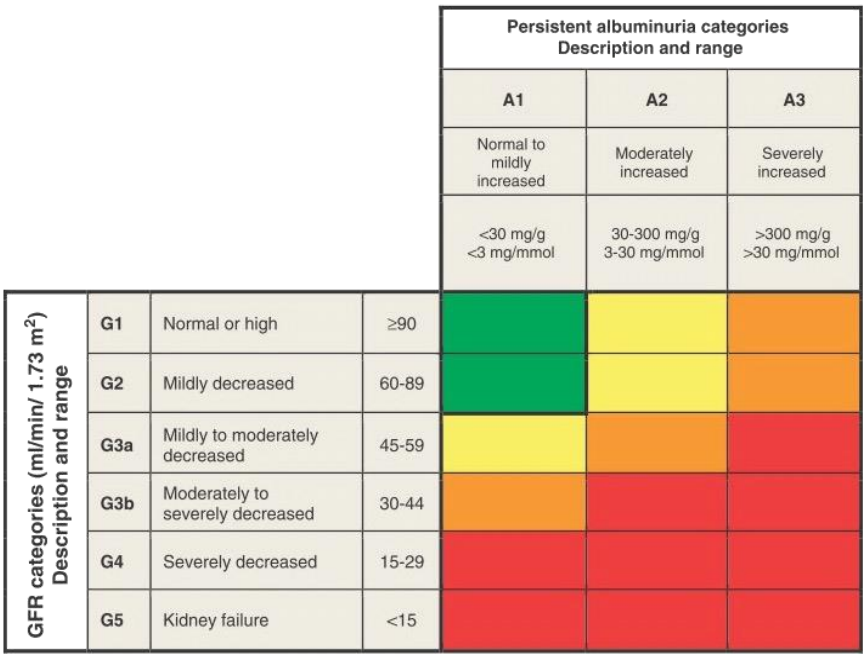

Figure 1: Prognosis of CKD by GFR and albuminuria

Risk for prognosis of CKD and end-stage renal disease (ESRD) is predicted by GFR category ranging from normal (eGFR > 90 ml/min, G1) to kidney failure (eGFR < 15 ml/min, G5) and by severity of albuminuria (A1 to A3).

Green: low risk; yellow: moderately increased risk; orange: high risk; red: very high risk. Taken and adapted from KDIGO 2012 – Clinical Practice Guideline for the Evaluation and Management of Chronic Kidney Disease, Levin A. et al., Kidney Int 2014 [11].

Chronic kidney disease (CKD) is defined as either kidney damage or a glomerular filtration rate (GFR) below 90 milliliters per minute for more than three months [12]. Kidney damage includes structural alterations and abnormalities in blood or urine e.g. hematuria and proteinuria [13]. Proteinuria, the loss of protein into the urine, is the most common marker of kidney damage indicating glomerular damage. The main protein in human blood plasma is albumin.

CKD is currently categorized in specific stages based on the presence of albuminuria (A) and the reduction of GFR (G) (see Figure 1) [11, 12]. In stages G1 and G2 GFR may be normal or mildly decreased. Additional pathological changes such as glomerular and interstitial fibrosis or tubular atrophy appear beside the decreased GFR in stages G3 to G4 [14]. According to this classification system, dialysis patients with end-stage renal disease (ESRD) are diagnosed as CKD stage G5. With the latest KDIGO classification albuminuria is integrated in the CKD classification, categorizing albuminuria (A) into grades 1 to 3. For instance, individuals with normal GFR (category G1) but with severe albuminuria (category A3) are referred to the category of high risk for cardiovascular diseases and ESRD (see Figure 1) as albuminuria has been proven to be a crucial contributor to renal disease.

Signs and symptoms of CKD may include edema, especially the swelling of the legs and eye puffiness due to fluid retention, high blood pressure and fatigue. Also anemia, shortness of breath from fluid accumulation in the lungs or metabolic acidosis, loss of appetite and bone disease occur [14, 15].

CKD can be caused by a variety of clinical factors including toxins, autoimmune diseases and glomerulopathies, infections, abnormalities of the urinary tract and genetic alterations but the major causes are diabetes mellitus and hypertension [16, 17]. Diabetes can harm the kidneys by causing damage to the glomerular capillaries leading to diabetic kidney disease [18], whereby in the advanced stage of diabetic kidney disease (DKD), proteinuria and diffuse glomerulosclerosis is observed [19]. Furthermore, increasing of individuals with obesity (body-mass index higher than 25 and waist circumference more than 102 cm for men and more than 88 cm for women) and the growing aging population are further risk factors that can explain the increasing prevalence of CKD [12, 20, 21]. The progression of renal disease occurs with advancing age as a natural loss of renal mass starts with the age of 40 years by reducing the glomeruli about 10% in each ten years [22].

CKD was extensively studied in rodents in the remnant kidney model with 5/6 nephrectomy [23, 24]. This nephrectomy model results in progressive hyperperfusion, hyperfiltration, hypertrophy and glomerulosclerosis. Glomerular hyperfiltration, one of the key processes in progressive renal injury, showed in a recent study with renal biopsies from patients diagnosed with diabetic kidney disease, a close association with increased glomerular filtration surface [25]. This may explain the initial increased GFR in these patients although urinary albumin level is elevated.

In the last decade, several studies on genomic and transcriptomic level identified new factors that are involved in CKD [26-34]. In a genome-wide association study (GWAS) polymorphisms in *MYH9* and *APOL1* were associated with nondiabetic ESRD in African-Americans [30, 31]. Variants in *MYH9* and *APOL1* have been identified as risk variants for developing progressive CKD in individuals with African descent. The CKDGen consortium performed a meta-analysis of GWAS data from Caucasian patients and found 13 novel loci (e.g. *SLC7A9*, *SLC34A1*, *DAB2*) associated with kidney function, the GFR, and CKD. Single nucleotide polymorphisms (SNPs) at these loci may have influence on the renal function [35]. Mutations in the *UMOD* gene are allied with decline in renal function and cause the autosomal dominant tubulointerstitial kidney disease [36-38]. A further study based on the data from the CKDGen consortium and the CARe consortium, identified *CUBN* as a gene locus for microalbuminuria in Caucasians as well African Americans irrespective of associated disorders such as diabetes [39].

1.1. Early intervention and therapeutic approaches

Medical treatment of CKD and CKD-related diseases causes one fifth of the entire annual medicare costs in the United States and the expenses are rising continually [16, 40-44]. Patients with CKD are at an increased risk not only for end-stage renal disease (ESRD), but also for cardiovascular disease (CVD) (Framingham Heart Study) [13, 45]. In the earlier stages of CKD (2 to 3) statin therapy showed to lower low-density lipoprotein (LDL) cholesterol levels and consequently reduced cardiovascular events in these patients [46].

Several studies showed that proteinuric patients have an increased risk of progressive renal failure compared to non-proteinuric CKD patients and that progression rate correlates with the degree of residual proteinuria [47-49]. The administration of drugs such as angiotensin converting enzyme inhibitors (ACEi) and angiotensin receptor blockers (ARB) allow control of blood pressure and proteinuria in CKD patients [50, 51]. The reduction in proteinuria in the first months of treatment with drugs that inhibit the renin-angiotensin-aldosterone system (RAAS) is associated with long-term kidney function protection, independently from the effect of the antihypertensive drug [52-55]. The ONTARGET study (Ongoing Telmisartan Alone and in Combination with Ramipril Global Endpoint Trial), a multicenter randomized controlled trial, examined the impact of combined administration of angiotensin receptor blockers (ARB) and angiotensin converting enzyme inhibitors (ACEi) in hypertensive patients with established atherosclerotic vascular disease [51]. Both the combined and the solely administration reduced hypertension and proteinuria equally well, but in the combined administration more adverse side-effects such as hyperkalemia were observed and long-term use indicated to worse renal function [51, 56-58].

A five-year period study with normotensive and normoalbuminuria patients with type 1 diabetes, showed that early blockade of the renin-angiotensin system did not prevent nephropathy progression [55]. As cardiovascular disease is one of the leading causes for morbidity and mortality in CKD patients, early intervention with low-salt and low-fat diet, blood pressure control and smoking cessation is recommended [59, 60].

Further, metabolic bone disease is a common complication of chronic kidney disease (CKD) in the progressed stages 4 to 5. It is caused by disturbance of bone and mineral metabolism in consequence of hyperphosphatemia, hypocalcemia and decreased levels of active vitamin D [14, 61]. The abnormalities in bone morphology is leading to higher incidences of fractures, and hyperphosphatemia has been found to be a mortality risk factor in patients with CKD [62]. In these patients very high levels of fibroblast growth factor 23 (FGF-23) and parathyroid hormone (PTH) are measured [63, 64]. Faul et al. demonstrated in a large cohort of CKD patients that circulating FGF-23 is highly associated with left ventricular hypertrophy (LVH) and risk for mortality [65].

Recent studies have indicated that renal klotho expression is markedly suppressed in CKD in mice and humans suggesting that decreased klotho expression may also be involved in the pathophysiology of CKD [66]. The klotho gene (*KL*) is predominantly expressed in kidney, where it functions as a co-receptor for FGF-23. FGF-23 is a bone-derived hormone that suppresses phosphate reabsorption and 1,25-dihydroxyvitamin D_3 (vitamin D) synthesis in the kidney and decreases expression and secretion of PTH. Mice lacking either FGF-23 or klotho exhibit hyperphosphatemia [67]. These findings correspond to human studies whereby decrease of urinary klotho protein levels was observed in patients with early stage CKD (stage 1 and 2) suggesting urinary klotho as an early biomarker of progression [68, 69].

Chronic kidney disease (CKD) is a worldwide public health problem with an increasing incidence and prevalence with various implications (see above) [44]. Earlier detection and suitable treatment is essential for slowing the progression of CKD.

As a consequence, three parameters should be screened for kidney disease: blood pressure, protein or albumin in the urine and glomerular filtration rate (GFR).

2. PROGRESSION OF CHRONIC KIDNEY DISEASE

Chronic kidney disease affects more than 13% of the population in the United States as well as in Europe and a certain proportion of cases progress to end-stage kidney failure [16, 42]. Progression of renal disease is characterized, apart from decline of GFR, by glomerulosclerosis, interstitial leukocyte infiltration, tubular atrophy, and tubulointerstitial fibrosis [70-73]. Thus, involvement of both, the glomeruli and the tubulointerstitium, contributes to progression of renal disease.

Halbesma et al. performed a study to develop and validate a "Renal Risk Score" for the general population [74]. The prediction model contained eGFR, age, urinary albumin excretion, systolic blood pressure and known hypertension. In this study, the first sign of kidney damage is decline of eGFR. Renal dysfunction characterized by a progressive decline of the glomerular filtration rate (GFR < 60 ml per minute) is often accompanied by proteinuria, the loss of protein in the urine (Figure 1).

As previously mentioned, other risk factors for CKD progression are high blood pressure (>130/80 mmHg), hyperglycemia (diabetes mellitus), obesity, dyslipidemia and tobacco use [75, 76]. Hallan et al. identified in an epidemical study, the combination of reduced eGFR and albuminuria or proteinuria as a powerful predictor of progression to ESRD [77].

The activation of the renin angiotensin aldosterone system (RAAS) also contributes to glomerular and tubulointerstitial remodeling and injury, in part through generation of reactive oxygen species [78]. Numerous cytokines and growth factors appear to modulate progression of glomerular and tubulointerstitial scarring since altered gene expression has been found in progressive renal scarring (e.g. PAI-1; PPAR-γ; PDGF; TGF-β; Ang II) [79-83].

Progression factors can be distinguished in clinical and histological factors:

2.1. Clinical factors

2.1.1. Proteinuria

The presence of proteinuria is associated with an increased risk for CKD and cardiovascular disease, as shown by many studies [15, 75, 84]. High proteinuria is defined as urinary protein excretion of greater than 3.5 grams per day and is one symptom of the nephrotic syndrome [85]. Independently of the underlying causes, chronic proteinuric glomerulopathies have in common the loss of selectivity of the glomerular barrier. Proteins with a molecular weight below 60 kDa usually pass freely through the glomerular basement membrane and are actively reabsorbed within the tubular system [86]. The severity of proteinuria depends on the damage of the glomerular capillary wall and the intraglomerular pressure. The intraglomerular pressure is controlled by the afferent and efferent arterioles and may be normalized by reduction of the systemic blood pressure. A blood pressure less than 130/80 mmHg is recommended for a better clinical outcome of CKD with high proteinuria [12].

Proteinuria is not only a strong marker for renal outcome, but also a marker for increased cardiovascular risk [86-88]. Urinary proteins themselves may induce proinflammatory and profibrotic effects that directly contribute to chronic tubulointerstitial damage. Induction of tubular chemokine expression and complement activation lead to inflammatory cell infiltration in the interstitium and persistent fibrogenesis [18]. In animal models, overload albumin (protein) causes interstitial inflammation and fibrosis, and induces expression of a number of inflammatory and fibrogenic mediators such as RANTES, monocyte chemotactic protein 1 and interleukins [89, 90].

2.1.2. Other clinical factors

Other contributors to progression are high glucose (diagnosed diabetes), hypertension and nephrotoxic drugs (e.g. cyclosporine) such as non-steroidal anti-inflammatory drugs (NSAIDs) [91-93]. In diabetes, decreased insulin sensitivity and hyperinsulinemia, in conjunction with hypertension, contribute to glomerular mesangial expansion, podocyte remodeling, loss of slit pore diaphragm integrity, and basement membrane thickening. Therefore, control of blood pressure and diabetes is an important key in treatment of CKD.

2.2. Histological factors

Involvement of both, the glomeruli and the tubulointerstitium, contributes to progression of renal disease as observed in kidney biopsies taken from patients with CKD [71].
Many cellular and molecular events beyond the production of matrix components promote the progression of fibrotic injury, and are actually responsible for the progressive loss of kidney function [94]. In patients with CKD, the histopathological presentation of tubular damage is often characterized as tubular injury and atrophy.
In the glomerulus, matrix accumulation, proliferation or loss of mesangial and endothelial cells, and the alteration and loss of functional podocytes are observed [71]. Therefore, all three glomerular cell types, the endothelial cells, mesangial cells and podocytes, are contributing to the fibrotic process.

2.2.1. Renal fibrosis

Renal fibrosis, characterized by glomerulosclerosis and tubulointerstitial fibrosis, is the final common manifestation of chronic kidney disease (CKD) [19]. The pathogenesis of renal fibrosis is a progressive process which leads to end-stage renal failure. Many cellular and molecular events, such as tubular atrophy, vascular rarefaction and hypoxia, promote the progressive loss of kidney function and determine the outcome of renal fibrosis. The loss of podocytes is considered as a major determinant and prognostic indicator for glomerular sclerosis [70].

It is generally accepted that activated fibroblasts (myofibroblast-phenotype) are responsible for excessive extracellular matrix (ECM; type I and III collagen, fibronectin) deposition leading to interstitial fibrosis [79, 95-97]. These alpha smooth muscle actin (α-SMA) expressing cells are recognized as a predictor of fibrotic progression in renal disease [98]. Type I collagen, one of the major fibrillar collagens, is involved in fibrosis but the mechanisms of transcriptional activation of the gene in kidneys remain unclear [99, 100]. A further central mediator, transforming growth factor beta (TGF-β), up-regulates many fibrogenic factors positively such as connective tissue growth factor by Smad2 or Smad3 molecules [17, 101, 102]. *In-vitro* studies with human fibroblasts showed that TGF-β induces α-SMA and actin-associated proteins that are participating in the formation of stress fibers, cell contractility and spreading [103, 104]. Overexpression of active TGF-β1 in mice causes

mesangial expansion, interstitial fibrosis, decreased GFR and progressive proteinuria [105]. However, therapies that target TGF-β are still non-effective and have very limited effects on renal fibrosis [106]. In an early TGF-β-independent Smad pathway, the renin-angiotensin system is involved in the development of vascular sclerosis by activating Smad3 through Angiotensin II (Ang II) [107, 108].

A further relevant contributor to kidney fibrosis progression appears to be hypoxia. Hypoxia leads to tubulointerstitial ischemic damage, which results in the loss of peritubular capillaries [109, 110]. Activation of the hypoxia-inducible factor (HIF) pathway by induction of vascular endothelial growth factor (VEGF) or stabilization of HIF proteins promotes renal fibrosis [111-115].

An innovative approach to identify progression factors was developed by Ju et al. [33]. There, intrarenal mRNA expression signatures predicted progressive renal fibrosis in mice and could be transferred to data from humans with CKD.

2.3. End-stage renal disease and renal replacement therapy

End-stage renal disease (ESRD) is defined as advanced chronic kidney disease. According to the classification system of KDIGO, dialysis patients with ESRD are diagnosed as CKD stage 5 [11]. Uremia is one main clinical symptom that occurs in patients with chronic renal failure. ESRD with uremic syndrome is characterized by impairment of acid-base and hormone metabolism, which results in disturbance of blood pressure and degradation of metabolism products such as urea and creatinine. Symptoms are uremic odor of breath and skin (uremic fetor), pruritus and discoloration of skin tone. Further implications of renal failure include edema, hypertension, cardiac arrhythmias, renal anemia, renal osteopathy and myopathy [116]. Renal replacement therapy is needed in these patients [117]. In 2006, the NKF workgroup updated the guidelines for initiating dialysis at the estimated glomerular filtration rate (eGFR) below 15 mL/min/1.73 m^2. According to the IDEAL study, early initiation of dialysis in patients with stage 5 CKD had no benefit on clinical outcome or survival prolongation [118, 119]. In the United States, approximately 40% of patients starting dialysis had diabetic kidney disease [40].

2.3.1. Hemodialysis

Hemodialysis (HD) prolongs life for patients with ESRD by restoring the intracellular and extracellular fluid balance, electrolyte homeostasis and acid-base equilibrium. This is obtained by the diffusion of molecules in solution across a semipermeable membrane along an electrochemical concentration gradient. Uremic toxins are eliminated from the blood and transported into the dialysate and important solutes such as bicarbonate are returned into the blood. Complications and side effects of HD include hypotension, muscle cramps, and advanced atherosclerosis. Most symptoms associated with the uremic syndrome are eliminated but it is not possible to replace the kidney function entirely [120, 121]. Longer session lengths and more frequent hemodialysis proved to be beneficial for phosphorus serum levels and therefore could prevent the typical bone disorder caused mainly by hypophosphatemia in these patients [122].

2.3.2. Peritoneal dialysis

Peritoneal dialysis (PD), an alternative therapy to hemodialysis (HD), is used by more than 272,000 patients with ESRD worldwide [123], accounting for approximately 11% of the dialysis population [124]. Concerns about patient survival on HD in comparison with PD may have led nephrologists to select this type of dialysis for their patients [125-127]. A prospective study with HD and PD patients showed that residual GFR is better maintained in PD patients [128].

PD involves the exchange of solutes and fluid between the peritoneal capillaries and the intraperitoneal dialysis solution across the peritoneal membrane. It requires placement of a peritoneal dialysis catheter for repeated dialysate exchange. The development of alterations in the peritoneal membrane, peritoneal sclerosis and fibrosis, is a major chronic complication of PD treatment. These alterations are characterized by vascular changes (increased number of vessels) and by thickening of the submesothelial zone (fibrotic altering) [129, 130]. The cause of peritoneal fibrosis is not clear, but human and murine studies suggested that mainly uremia induces fibrotic changes in the peritoneum [131, 132]. Furthermore, the bio-incompatible peritoneal dialysis solutions composed of glucose, glucose degradation products or/and advanced glycation end products and the acidic pH promote chronic inflammation and fibrotic altering [133].

A rare complication of long-term peritoneal dialysis is encapsulating peritoneal sclerosis (EPS) [131, 134]. Formation of a fibrous cocoon encapsulating the bowel leads to acute gastrointestinal obstruction. The mortality in patients with EPS is high (25-50%) and no established treatment is available.

2.3.3. Renal transplantation

Kidney transplantation is the third and for several reasons preferable renal replacement therapy. The majority of renal transplant recipients are already on dialysis at the time of transplantation [135]. Although life-long immunosuppressive therapy is needed to prevent allograft rejection, renal transplantation represents the best option for most patients with ESRD with respect to survival, quality of life and control of whole body homeostasis. In the last decades, progress in renal transplantation was achieved and organ survival rate has improved remarkably.

Ongoing studies are searching for clinical and histological markers to predict the outcome of transplantation [136]. Beside immunological factors the GFR, fibrotic lesions and age of allograft recipient and donor seem to be important. Strikingly, 50% of allograft loss cases are due to death of the recipient mainly caused by associated disorders [137, 138]. Clinically, renal allograft biopsies are evaluated by the Banff classification which defines five categories of renal transplantation pathology [139]. The purpose is to detect first signs of renal dysfunction and therefore to prevent transplant rejection.

3. GLOMERULONEPHROPATHIES

Current data from the United States and Europe indicate that diabetes mellitus (primarily type 2), hypertension and glomerulonephritis are major causes for the development and progression of renal diseases [40]. In all three entities the glomerulus, the filter unit of the kidney, is primarily affected. The glomerulus consists of three layers: the fenestrated endothelium and glycocalyx, the specific glomerular basement membrane and the glomerular epithelial cells, also called podocytes (Figure 2). The latter play an important role in the selective permeability of the filter barrier as these cells with their interdigitating foot processes, form the slit diaphragm. One common clinical finding due to dysfunction of this construct in progressive kidney diseases is proteinuria, the excessive loss of protein with the urine [140-143]. As mentioned previously, podocyte dysfunction may be caused by genetic and/or environmental factors (e.g. diabetes, hypertension or aging) [144].

Glomerular diseases account for up to 60% for end-stage renal disease (ESRD) in the industrialized world [40]. The signs and symptoms of glomerular disease include: reduced glomerular filtration rate (GFR), proteinuria and/or hematuria. Clinically, these pathophysiological features are distinguished into two main syndromes. The nephrotic syndrome is characterized by massive proteinuria (more than 3 grams per day) and edema, whereas the nephritic syndrome is accompanied by leukocytic infiltration and inflammation of the capillaries leading to hematuria, the loss of erythrocytes in the urine. Glomerular diseases with nephrotic syndrome can be divided into primary and secondary etiologies. Primary caused glomerulonephropathies (GNs) have an acute onset as symptoms such as proteinuria with or without nephrotic syndrome occur in a previously healthy person. Idiopathic, primary GNs with a nephrotic syndrome include minimal change disease (MCD), focal-segmental glomerulosclerosis (FSGS) and membranous glomerulonephropathy (MGN). Secondary caused GNs are associated with certain infections (e.g. HIV/AIDS, hepatitis B and C), drugs (cyclosporine A, non-steroidal anti-inflammatory drugs (NSAIDs)), systemic disorders (e.g. systemic lupus erythematosus (SLE)) or diabetes mellitus. Several hereditary disorders may be associated with genes with prominent glomerular relevance such as Alport's syndrome or Nail-Patella syndrome (mutations in *COL4A5* and *LMX1B*, respectively) and direct podocyte biology (see below).

Furthermore, chronic glomerulonephropathies (GNs) are classified into non-proliferative and proliferative types. The proliferative type is characterized by an increased number of glomerular cells, especially the mesangial cells, and usually leads to nephritic syndrome. IgA

nephropathy (Berger's disease) is the most common type of a proliferative GN in adults worldwide [140, 145].

3.1. Main acquired proteinuric glomerulonephropathies

There are three main causes for primary idiopathic nephrotic syndrome, minimal change disease (MCD), focal-segmental glomerulosclerosis (FSGS) and membranous glomerulonephropathy (MGN) (Figure 2) [143].

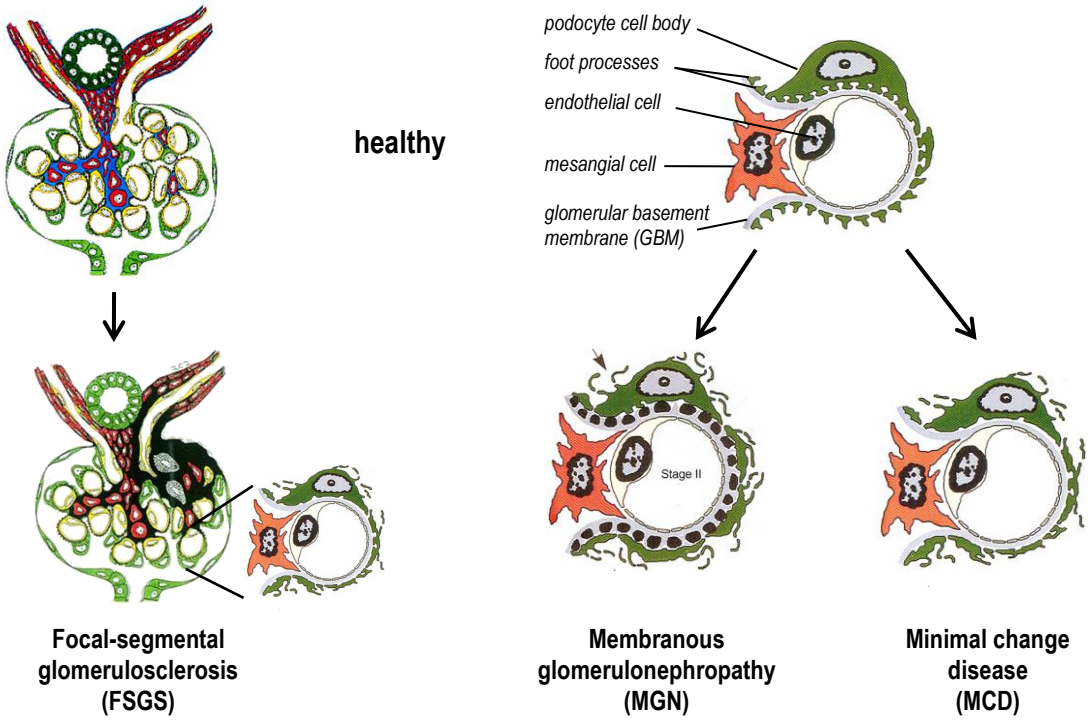

Figure 2: Acquired proteinuric glomerulonephropathies

The main proteinuric glomerular diseases are focal-segmental glomerulosclerosis (FSGS), membranous glomerulonephropathy (MGN) and minimal change disease (MCD). The renal filtration barrier consists of three layers, the glomerular fenestrated endothelial cells, the negatively charged glomerular basement membrane (GMB) and podocytes with their foot processes. One common finding is the loss of the functional podocytes, which leads to alterations of the permselectivity barrier of the glomerular capillary wall, allowing increasing loss of plasma proteins into the urine. Taken and adapted from Primer on Kidney Diseases, Greenberg et al., National Kidney Foundation 2009.

These GNs have no increase in number of cells, and are therefore grouped into the non-proliferative type. These renal diseases show one common pathological finding: the loss of the highly differentiated phenotype of podocytes, which are required for the function of the filter barrier.

The progressive renal diseases such as FSGS and MGN have a high risk of ESRD whereas MCD reveals a good remission opportunity with immunosuppressive treatments such as steroid therapy (corticosteroids) with no loss of GFR. Steroid-sensitive GNs may be identified on renal biopsy with only minimal changes without immunoglobulin deposits.
Although treatments with steroids, calcineurin inhibitors, cyclophosphamide (CYC) and rituximab (RTX) are efficient in the majority of cases, certain patients are non-responders due to genetic alterations (e.g. steroid-resistant GNs). GNs caused by genetic abnormalities are predominantly associated with mutations in podocyte genes (e.g. nephrin (*NPHS1*), podocin (*NPHS2*), α-actinin-4 (*ACTN4*), phospholipase C epsilon 1 gene (*PLCE1*), Wilms tumor suppressor gene (*WT1*), *TRPC6*) [146-151].

3.1.1. Minimal change disease (MCD)

This form of glomerulonephropathy causes 80% of nephrotic syndrome (NS) in children, but only 20% in adults. In clinical practice, about 95% of MCD patients respond to immunosuppressive therapy such as corticosteroids, alkylating agents (e.g. cyclophosphamide), calcineurin inhibitors (e.g. cyclosporine or tacrolimus) or monoclonal antibody rituximab. On electron microscopy, a "fusion" of podocyte foot processes is visible only as apparent histological abnormality (Figure 2). Despite significant progress in understanding the kidney ultrafiltration barrier, the molecular mechanism remains unclear. Earlier studies showed an association with personal or familial history of atopy [152]. However, this podocyte injury in MCD is reversible, so that progressive loss of renal function is rare. The absence of any glomerular abnormality on light microscopy and the complete remission of proteinuria on corticosteroid treatment easily distinguished MCD from FSGS [153].

Animal models of MCD are induced with puromycin aminonucleoside (PAN) low-dose injections, which are leading to proteinuria, foot process effacement and responsiveness to steroids [154, 155]. Garin et al. showed that the expression of podocyte-specific B7-1 was highly present in the urine of MCD patient but not in those with idiopathic FSGS and therefore suggesting urinary B7-1 as a specific marker for MCD [156].
In 2010, the abundance of c-maf inducing protein (c-mip) in podocytes of patients with MCD was reported. Transgenic mice overexpressing c-mip in podocytes developed proteinuria without morphological alterations, inflammatory lesions or cell infiltration [157]. In a recent study, a role of angiopoietin-like-4 (ANGPTL4) in glucocorticoid-sensitive nephrotic syndrome was identified [158]. Up-regulated expression of ANGPTL4 was found in the serum and in podocytes in experimental rodent models of MCD. Sera from human patients with MCD confirmed the result. Rats overexpressing ANGPTL4 in podocytes develop albuminuria, loss of specificity of the glomerular basement membrane (GBM) as well as podocytes foot processes effacement, supposing a causative role of ANGPTL4 in MCD. Clement et al. suggest that ANGPTL4 in MCD might represent a podocytes-derived factor that may act in an autocrine or paracrine manner [158].

3.1.2. Focal-segmental glomerulosclerosis (FSGS)

In FSGS, beside foot process effacement as in MCD, certain foci of glomeruli within the kidney are affected by lesions such as sclerosis and hyalinization of the arterioles. In the affected segments hyaline deposition around the shrinking capillary loops and increased mesangial fibrillar material without any cellular proliferation is found. While the majority of MCD patients respond to steroid therapy, most of FSGS patients are resistant to corticosteroids. Compared with MCD, idiopathic FSGS is associated with steroid resistance and higher risk of progression for renal failure. Originally, the histological diagnosis of FSGS required the identification of segmental sclerotic lesions in at least one glomerulus [159, 160]. FSGS is one of the leading causes for ESRD, especially in African-Americans and Hispanics [161]. In African-Americans, genetic variants in the *MYH9* and *APOL1* locus have been associated with high risk for progression of FSGS and its outcome [30, 31].

FSGS may be a primary idiopathic or secondary GN caused by drug abuse or HIV infection. Hereditary FSGS is caused by mutations in podocyte genes such as nephrin (*NPHS1*) or podocin (*NPHS2*) responsible for the Finish-type congenital nephrotic syndrome and autosomal recessive familial FSGS, respectively. Autosomal dominant FSGS with adult onset is caused by a mutation in α-actinin 4 (*ACTN4*) leading to altered actin-cytoskeleton interaction [162]. It has also been hypothesized that circulating factors in plasma are causing FSGS, as there is a significantly high risk of recurrence of FSGS in renal transplants observed [163, 164]. In 2011, a study of the group of Jochen Reiser identified serum soluble urokinase receptor (suPAR) as a potential circulating causative factor that is elevated in the serum of approximately two-thirds of primary FSGS patients, but not in patients with other glomerular diseases [165]. Circulating suPAR activates β3 integrin (ITGB3) in podocytes, which has been shown to be involved in podocytes foot process effacement.

3.1.3. Membranous glomerulonephropathy (MGN)

MGN is the most common cause for nephrotic syndrome in adults. Microscopically, MGN is characterized by a thickened glomerular basement membrane (GBM) with formation of subepithelial immune deposits within which results in dysfunction of the glomerulus and causing massive proteinuria. The involved immune complexes consist of IgG4 and other antigens [166]. In earlier studies in a rat model of MGN (Heymann's nephritis), antibodies directed against megalin were discovered [167]. However, megalin is not expressed in human podocytes. Debiec et al. characterized a fetomaternal disease in which antibodies to neutral endopeptidase (*NEP*) caused the development of MGN in fetus of *NEP* deficient mothers [29, 168]. Therefore, NEP deficiency should also be considered in patients developing de-novo MGN after renal transplantation.

In 2009, the anti-phospholipase A2 receptor (*PLA2R*) was identified as a major target autoantigen in adult idiopathic MGN [28, 169, 170]. Circulating anti-PLA2R IgG4 were found in sera from 70% of patients with primary idiopathic MGN but not in those with secondary MGN or other GNs. Immunofluorescence staining localized PLA2R in normal human podocytes, which was further confirmed by positive staining with Wilms Tumor 1 (*WT1*). Currently, the anti-B cell agent rituximab is one of the promising therapy options for idiopathic MGN. In a cohort study, rituximab treatment correlated with a decline of anti-PLA2R autoantibodies in MGN patients with a complete or partial remission. Low anti-PLA2R autoantibody titers might represent a potential biomarker for positive treatment response [169, 171, 172].

Furthermore, two autoantibodies against aldose reductase (AR) and mitochondrial superoxide dismutase 2 (SOD2) were discovered to be present in serum and glomeruli from patients with MGN [27]. Recently performed genome-wide association studies of single-nucleotide polymorphisms (GWAS) in patients from Caucasian ancestry with idiopathic MGN identified coding and non-coding regions of HLA-DQA1 and PLA2R1 as risk alleles. PLA2R1 is present in normal podocytes and in immune deposits in patients with idiopathic MGN [26, 173]. All these findings support the concept of circulating autoantibodies binding to glomerular antigens expressed on podocytes and may explain the onset of MGN.

4. EUROPEAN RENAL cDNA BANK-KRÖNER-FRESENIUS BIOPSY BANK

Towards the end of the 20th century, experimental models and gene expression analysis have become evermore an important research tool in renal research as several genes have been identified with key relevance for renal function [36, 112, 174-177]. The renal biopsy and the succeeding histological examination are routine clinical and diagnostic gold standard in nephrology. In nephrology, research methods such as immunohistochemistry, light and electron microscopy are well established, but gene expression analysis will provide an improvement in routine diagnostic information regarding diagnosis, treatment response and prognosis of disease progression.

Hence, in 1998, an international multicenter study, the European Renal cDNA Bank-Kröner-Fresenius Biopsy Bank (ERCB-KFB) was initiated to enable the systematic analysis of gene expression in human kidney biopsies. The objectives were defined as follows:
1.) Improving understanding of transcriptional mechanisms involved in human renal disease, 2.) Identifying diagnostic and prognostic markers in renal biopsies, and 3.) Supporting the renal scientific community by translational research [178].
Nevertheless, a kidney biopsy is still an invasive procedure despite considerable developments in recent years. The development of highly sensitive detection methods is therefore required for the molecular analysis of multiple RNAs from small amounts of tissue (see standardized protocol) [179]. Two methods have been established in recent years to investigate which genes are transcribed in a tissue: Quantitative real-time RT (reverse transcriptase)-PCR (polymerase chain reaction) and microarrays. The first method is very sensitive, even the smallest amounts by amplification of a specific nucleic acid sequence can be quantified [180]. Microarrays allow simultaneous analysis of thousands of cDNAs [181]. Including clinical data in the further parallel analysis (e.g. laboratory values, histology) at time of biopsy and at subsequent dates, it may be possible to correlate the expression pattern of certain genes with clinical outcome or response to therapy (Figure 3) [178, 182].
In particular, gene expression studies based on renal biopsies have made an important contribution to understanding the role of transcriptional regulation in renal disease [176, 183, 184]. With the variety of data from animal models, it is increasingly important to verify the results with respect to their applicability to humans. Often this is done by morphological methods such as histology and immunohistochemistry [185]. The ERCB-KFB offers the

possibility of comparison to another level. By this time more than forty international clinical centers are part of this comprehensive study and over 2900 renal biopsies have been collected. Since its initiation several publications in respectable journals have been emerged from and high reproducibility has been confirmed [110, 176, 178, 182, 184, 186, 187].

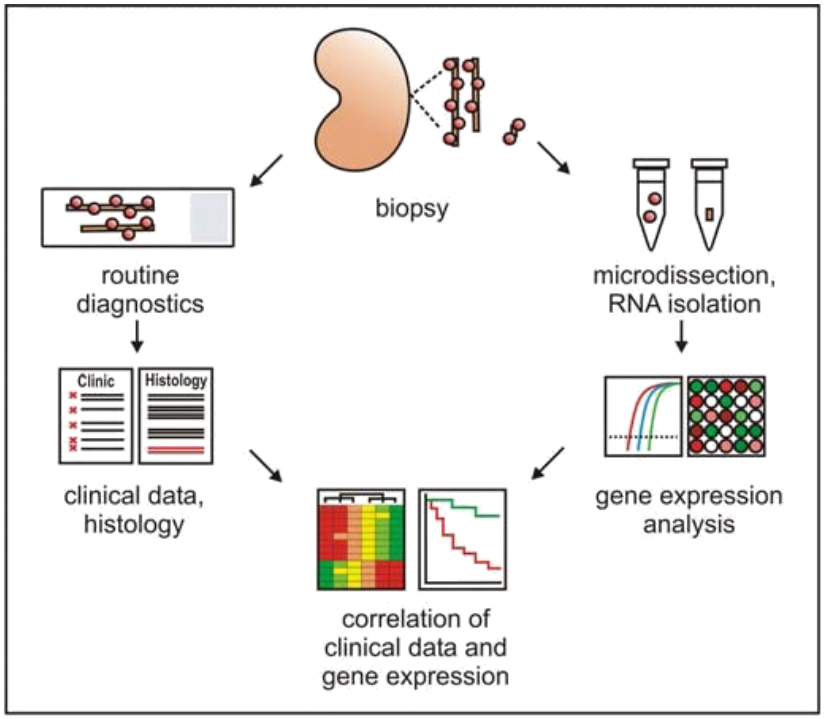

Figure 3: Outline of the European Renal cDNA Bank-Kröner-Fresenius Biopsy Bank (ERCB-KFB)

Immediately after renal biopsy, a minimum of 10% of the biopsy specimen is separated and stored in RNA preservative. Under a stereomicroscope, glomeruli and tubulointerstitial compartments are divided by manual microdissection. The gene expression analysis is performed by real-time RT-PCR or microarrays. Clinical characteristics of the patients are collected in parallel to enable integrative analysis of the gene expression data [182].

To cite as an example, the working group of Susan Quaggin examined a mouse model of rapidly-progressive glomerulonephritis (RPGN) with glomerular deletion of Von Hippel-Lindau gene (Vhlh) and noted the induction of hypoxia-associated cellular processes such as necrotizing glomerular crescents [188]. The investigation of RPGN patients with microdissected glomeruli from the ERCB-KFB yielded the same gene expression pattern as in animal models. Although the pathogenic mechanism of RPGN in humans remains unclear, from these findings may result new therapeutic approaches for blocking the specific hypoxia-induced gene Cxcr4 by extending the survival of mice knowing that hypoxia is a key mechanism in the pathogenesis of renal disease. The finding that hypoxia is a central mechanism in the pathogenesis of kidney disease, was also approved from the work of Higgins et al. where the expression of hypoxia-induced renal factor HIF-1α enhances renal fibrosis in mice [113]. Once more using data from the ERCB-KFB has been shown that this pathomechanism seems to be applicable for humans. Thus, the main goals of the ERCB-KFB are both, generating hypotheses on the nature of kidney diseases and translating results from animal models to humans, and to identify pathophysiological processes in human renal diseases for a better clinical outcome. This approach might reveal new findings on molecular level, which can be made in clinical knowledge.

5. PURPOSE AND PREFACE

In the last two decades, several studies brought a lot for the understanding of the mechanisms involved in CKD development. However, most data still come from animal models and translation to human CKD is often not given. The initial aim of this PhD project was to identify gene transcripts involved in human CKD by analyzing gene expression profiles based on samples of the ERCB-KFB using most recent technical and bioinformatical tools (e.g. Bibliosphere, DAVID, Ingenuity etc.). The fact that not only the GFR, but also proteinuria has essential influence on the progression of CKD, prompted us to mainly focus on proteinuria in acquired proteinuric glomerulopathies, namely MCD, FSGS and MGN (see 3.). A systematic analysis of the molecular mechanisms involved in glomerular proteinuria is necessary to comprehend the biological processes behind:

For that purpose, a human renal glomerulus-enriched gene expression dataset, REGGED, was generated to filter for glomerular gene transcripts of interest. REGGED implicates the most known glomerular markers compared to other published reports on human glomerular expression at the time of publication, which confirms the high validity and excellent quality of this database [174, 189-191]. The chapter I shows the published results from this international collaboration study including *in-vitro* validation experiments.
Chronic hypoxia contributes to renal fibrosis associated with preceding microvasculature dysfunction in several rodent studies and was hypothesized to be involved in nephrosclerosis (NSC), also known as hypertensive nephropathy [192, 193]. In chapter II, we performed specific studies to comprehend the biological processes of hypoxia-related renal injury. We found induced glomerular expression of genes regulated by the hypoxia-inducible factors (HIFs) in NSC such as the chemokine C-X-C motif receptor 4 (CXCR4). In NSC biopsies, CXCR4 showed an enhanced expression in podocytes with an associated nuclear positivity of the hypoxia-inducible factor-1α (HIF1α) suggesting a transcriptional activity of HIF1α.

In a further step, our REGGED dataset was used to select a glomerular gene transcript with a high induction in progressive proteinuric glomerulopathies such as FSGS and MGN. Matricellular proteins such as SPARC are known to contribute to the progression of human nephropathies [194, 195]. To achieve a better comprehension for the pathobiology of progressive proteinuric diseases, a systematic analysis of the matricellular protein POSTN (Periostin) was conducted. POSTN (Periostin), also known as osteoblast-specific factor 2

(OSF-2) was systematically analyzed and found to be expressed in healthy glomeruli with the highest induction in the progressive diseases FSGS and MGN. In the chapters III and IV, studies on POSTN and fibrosis/fibrotic alterations, a hallmark of renal disease progression, were performed by using different methodical approaches. In chapter III renal biopsies taken from patients with proteinuric glomerulopathies in various phases of disease progression were analyzed, compared to clinical data and confirmed by *in-vitro* experiments. As expected, POSTN was strongly associated with the progression of proteinuric diseases. The chapter IV continued the experiments with biopsies and clinical data from patients on peritoneal dialysis (PD) with or without developed encapsulating peritoneal sclerosis (EPS). Periostin concentrations in dialysate of PD patients without signs of EPS significantly increased with time of treatment. The chapter V contains functional studies on POSTN including *ex-vivo* examinations of a periostin-deficient mouse. The kidneys of periostin-deficient mice showed enlarged glomeruli and a proliferative mesangium suggesting worse renal function. This was confirmed by measuring the serum data such as the blood urea nitrogen level.

Patients with primary podocyte-injured renal diseases such as MCD are treated with glucocorticoids and a part of them respond rapidly with improvement of proteinuria or even full remission. The detection of REGGED gene transcripts repressed in proteinuric glomerulopathies with glomerular expression and glucocorticoid-induced regulation would give new insights to podocyte dysfunction. The glucocorticoid-induced leucine zipper TSC22D3 showed a significant repression in all three proteinuric diseases and was found to be expressed in podocytes of human nephrectomy biopsies. In chapter VI, the preliminary results of the second candidate gene transcript TSC22D3 are presented. Several studies indicated that TSC22D3 has a key role in anti-inflammatory and immunosuppressive processes. Different research approaches from cell culture experiments with multiple rodent and human cell lines to an experimental model of Drosophila flies were pursued with promising results.

This work contains both published data (chapters I-IV) and preliminary results (chapters V-VI).

CHAPTER I

Systematic analysis of a novel human renal glomerulus-enriched gene expression dataset

Maja T. Lindenmeyer, Felix Eichinger, Kontheari Sen, Hans-Joachim Anders, Ilka Edenhofer, Deborah Mattinzoli, Matthias Kretzler, Maria P. Rastaldi, Clemens D. Cohen

PLoS ONE 5(7): e11545; doi:10.1371/journal.pone.0011545

OPEN ACCESS Freely available online

PLoS one

Systematic Analysis of a Novel Human Renal Glomerulus-Enriched Gene Expression Dataset

Maja T. Lindenmeyer[1,2], Felix Eichinger[3], Kontheari Sen[2], Hans-Joachim Anders[4], Ilka Edenhofer[1], Deborah Mattinzoli[5], Matthias Kretzler[3], Maria P. Rastaldi[5], Clemens D. Cohen[1,2]*

1 Division of Nephrology, University Hospital Zurich, Zurich, Switzerland, **2** Institute of Physiology with Zurich Center of Integrative Human Physiology, University of Zurich, Zurich, Switzerland, **3** Department of Medicine, University of Michigan, Ann Arbor, Michigan, United States of America, **4** Medizinische Poliklinik, University of Munich, Munich, Germany, **5** Renal Research Laboratory, Fondazione IRCCS Policlinico & Fondazione D'Amico per la Ricerca sulle Malattie Renali, Milan, Italy

Abstract

Glomerular diseases account for the majority of cases with chronic renal failure. Several genes have been identified with key relevance for glomerular function. Quite a few of these genes show a specific or preferential mRNA expression in the renal glomerulus. To identify additional candidate genes involved in glomerular function in humans we generated a human renal glomerulus-enriched gene expression dataset (REGGED) by comparing gene expression profiles from human glomeruli and tubulointerstitium obtained from six transplant living donors using Affymetrix HG-U133A arrays. This analysis resulted in 677 genes with prominent overrepresentation in the glomerulus. Genes with *'a priori'* known prominent glomerular expression served for validation and were all found in the novel dataset (e.g. CDKN1, DAG1, DDN, EHD3, MYH9, NES, NPHS1, NPHS2, PDPN, PLA2R1, PLCE1, PODXL, PTPRO, SYNPO, TCF21, TJP1, WT1). The mRNA expression of several novel glomerulus-enriched genes in REGGED was validated by qRT-PCR. Gene ontology and pathway analysis identified biological processes previously not reported to be of relevance in glomeruli of healthy human adult kidneys including among others axon guidance. This finding was further validated by assessing the expression of the axon guidance molecules neuritin (NRN1) and roundabout receptor ROBO1 and -2. In diabetic nephropathy, a prevalent glomerulopathy, differential regulation of glomerular ROBO2 mRNA was found. In summary, novel transcripts with predominant expression in the human glomerulus could be identified using a comparative strategy on microdissected nephrons. A systematic analysis of this glomerulus-specifc gene expression dataset allows the detection of target molecules and biological processes involved in glomerular biology and renal disease.

Citation: Lindenmeyer MT, Eichinger F, Sen K, Anders H-J, Edenhofer I, et al. (2010) Systematic Analysis of a Novel Human Renal Glomerulus-Enriched Gene Expression Dataset. PLoS ONE 5(7): e11545. doi:10.1371/journal.pone.0011545

Editor: Gordon Chua, University of Calgary, Canada

Received March 23, 2010; **Accepted** June 16, 2010; **Published** July 12, 2010

Funding: The work was supported by the Swiss National Science Foundation (32-122439/1) and the Else Kroener-Fresenius Foundation (A62/04) to CDC. The funders had no role in study design, data collection and analysis, decision to publish, or preparation of the manuscript.

Competing Interests: The authors have declared that no competing interests exist.

* E-mail: clemens.cohen@access.uzh.ch

Introduction

The majority of renal diseases leading to end-stage renal diseases (ESRD) are initiated by glomerular alterations [1]. Hereditary, immune-mediated and metabolic disorders can cause such glomerulopathies, but the understanding of the pathomechanism of the most common glomerular diseases is still limited.

The renal glomerulus is capable of filtering large volumes of plasma while efficiently retaining most proteins within the circulation [2]. The development and maintenance of normal glomerular structure and function requires successful signaling and coordination between all glomerular cells, as shown by the critical requirement for vascular endothelial growth factor-A (VEGFA) production by podocytes for normal endothelial and mesangial cell development and function [3,4].

Podocytes are a unique cell type in the glomerulus [5]. Several genetic studies clearly demonstrated that mutations of proteins, which are preferentially or specifically expressed in this cell type, can cause renal disease leading to the disruption of the filtration barrier, rearrangement of the actin cytoskeleton and ultimately glomerular failure (e. g. α-actinin-4, nephrin, podocin) [6]. Additional studies revealed that proteins regulating the plasticity of the podocyte actin cytoskeleton, such as podocalyxin [7], FAT1 [8], Nck1 and Nck2 [9], synaptopodin [10] and Cathepsin L [11], are also crucial for the function of the glomerular filtration barrier. But also signaling mechanisms in the podocyte including signals from the slit diaphragm (SD) or from the glomerular basal membrane (GBM) are important (e.g. PLCE1, TRPC6, PTPRO, ILK, uPAR [12,13,14]). Transcriptional regulation of genes expressed in the glomerulus plays a key role for functional integrity. Transcription factors that have been associated with glomerular disorders include WT1, FOXC2, LMX1B, TCF21, PAX2 and others [15]. Furthermore the composition and charge of the GBM (e.g. LAMB2, COL4A3, −4, −5), the endothelial cells with their unique fenestration (e.g. EHD3) [6] and the mesangial cells play a crucial role. Studies could outline important species-dependent differences in glomerular gene expression, e.g. megalin was shown to be the target autoantigen in experimental Heyman nephritis is absent from the human glomerulus, whereas PLA2R seems to be a target autoantigen in human idiopathic membranous nephropathy [16]. As the glomerular transcriptome of rodents and humans show significant differences, a reliable and comprehensive human data set is required.

Identification of additional human glomerular-enriched genes and proteins as well as molecular mechanisms and gene networks represent a promising approach to the understanding of

development and function of the glomerulus and its derangement in glomerular diseases.

In the present study, gene expression profiles from human glomeruli and tubulointerstitium obtained from transplant living donors were compared to each other in order to generate a human renal glomerulus-enriched gene expression dataset (REGGED). REGGED aims to facilitate the identification of gene products and mechanisms important in regulation of renal glomerular structure and function. The mRNA expression for several novel glomerular-enriched genes was verified by qRT-PCR. Gene ontology analysis by Database for Annotation, Visualization and Integrated Discovery (DAVID), as well as the Kyoto Encyclopedia of Genes and Genomes (KEGG) database identified pathways and gene categories well-known to be associated with glomerular biology but additionally pathways not previously reported to be involved in glomeruli of healthy human adult kidneys. Axon guidance, identified by this means as a biological process in human mature glomeruli, was used to validate our approach and the expression of the axon guidance molecules neuritin (NRN1) and roundabout receptor ROBO1 and -2.

In summary, REGGED represents a resource for the glomerular research community to interrogate genes identified by *in vitro* systems, rodent models, or human genetic screens for their enrichment in the glomerular compartment. It further will help to prioritize biological processes in functional studies on glomerular biology.

Results

Generation of a human renal glomerulus-enriched gene expression dataset (REGGED) and comparison with published data sets

To identify genes restricted to or enriched in the glomerulus, we compared gene expression profiles of isolated human glomeruli with the tubulointerstitial compartment from biopsies of living donors using Affymetrix HG-U133A arrays. By application of the algorithms given in the Methods section a total of 817 probesets were identified as being glomerular-enriched. After removing unannotated probesets and redundant probesets a list of 677 glomerular-overrepresented genes remained (Supplementary Table S1). For validation of the dataset an arbitrary list of known genes with specific or pronounced expression in the renal glomerulus of different species was generated and compared with REGGED (Supplementary Table S2). Known prominent glomerular transcripts such as CDKN1, DAG1, DDN, EHD3, MYH9, NES, NPHS1, NPHS2, PDPN, PLA2R1, PLCE1, PODXL, PTPRO, SYNPO, TCF21, TJP1, WT1 were all found in the novel expression dataset REGGED (Figure 1) [15,17,18,19,20,21,22,23,24,25]. In a next step, a comparative analysis of different expression platforms was performed. To this end we focused on human data sets and used data published by Chabardes-Garonne et al [26], Higgins et al. [27], Cuellar et al [28], and Nyström et al. [29]. The two SAGE profiling analyses by Chabardes-Garonne and Nyström identified 153 [26] and 492 genes [29], respectively, as being predominantly expressed in the glomerulus compared with other parts of the nephron. The Stanford cDNA microarray profiling by Higgins et al. resulted in 102 [27] glomerular markers, while the plasmid library by Cuellar identified 205 [28] glomerular-enriched genes. Table 1 summarizes the characteristics of the 5 analyses including the present study. The comparison of the 5 different approaches is illustrated in Figure 1 and Supplementary Table S3. REGGED contains a number of genes with established function in glomerular biology, which were not previously found in human data sets (e.g. FYN, MYH9, PDPN) [13,20,30,31]. Similar to He et al [32], who compared rodent and human data sets, only 6 genes were identified in all studies, namely the podocyte-expressed genes CDKN1C, PTPRO, SPARC, and PLAT, the endothelial marker EMCN, and the mesangial-expressed IGFBP5.

Gene Ontology and Pathway Analysis

As gene lists per se need to be integrated in a functional context, we mapped the REGGED genes into different biological categories according to gene ontology (GO). A relative ranking of the association of the various GO-categories with respect to the gene list was carried out employing DAVID, a web-based tool developed for GO-ranking. Although GO enrichment analysis has some limitations [33], it is an efficient means to extract the biological meaning behind large gene list. DAVID analysis of all 677 glomerular-enriched genes yielded 197 GO-categories (Supplementary Table S4; cut-off p-value 0.05, Fold enrichment >1.5). To receive a more comprehensive and structured view of the annotation terms a DAVID clustering analysis under high stringency conditions was performed resulting in ten annotation clusters matching the statistical criteria [($p<0.05$), fold enrichment >1.5 and an enrichment score of at least 2.0]. Each of these clusters was composed of at least 3 annotation terms, with an enrichment score of 2.01–7.34 (Supplementary Table S5 and Supplementary Figure S1). As an example functional cluster 2 is shown in more detail in Figure 2; it is composed of ten GO terms that apply to identical sets of genes.

Subsequently, the aforementioned DAVID annotation tool was used for identification of putative KEGG pathways associated with glomerular biology. The glomerular-enriched genes could be mapped to 105 pathways, 12 of which were significantly enriched with glomerular-associated genes ($p<0.05$, Fold enrichment >1.5) (Supplementary Table S6). For instance, we found the KEGG terms "regulation of actin cytoskeleton", "focal adhesion" and "tight junction" to be significantly enriched pathways, which are known to be of relevance for glomerular biology. Interestingly, "axon guidance", one of the GO terms associated with glomerular-enriched genes, was also pinpointed in the KEGG pathway analysis.

Comparison with neuronal related genes and genes mainly expressed in smooth muscle cells as well as in muscle and heart

Several studies have shown that glomerular podocytes and neurons share some specific characteristics. For instance, both cells are highly arborized, have a common cytoskeletal organization and signaling processes, and share several expression-restricted proteins, such as NPHS1, LRRC7, PTPRO, KHDRBS3, or SYNPO [34,35]. We therefore conducted a digital differential display analysis to compare normal adult brain cDNA libraries (total of 27,891 sequences) with other tissue libraries except for testis (143,877 sequences). Testis libraries were excluded because of the significant similarity of its transcriptome to the one of brain [36]. DDD takes advantage of the UniGene database by comparing the number of times that sequences from different libraries are assigned to a particular UniGene cluster. This analysis produced 186 UniGene clusters that were potentially specific to the brain pool. Combining this list of UniGene clusters with a literature-derived list of neuronal related molecules [37], we generated a list of 414 neuronal/brain-associated genes (Supplementary Table S7) and compared it with REGGED. This comparison revealed that 38 of the 414 neuron/brain-associated

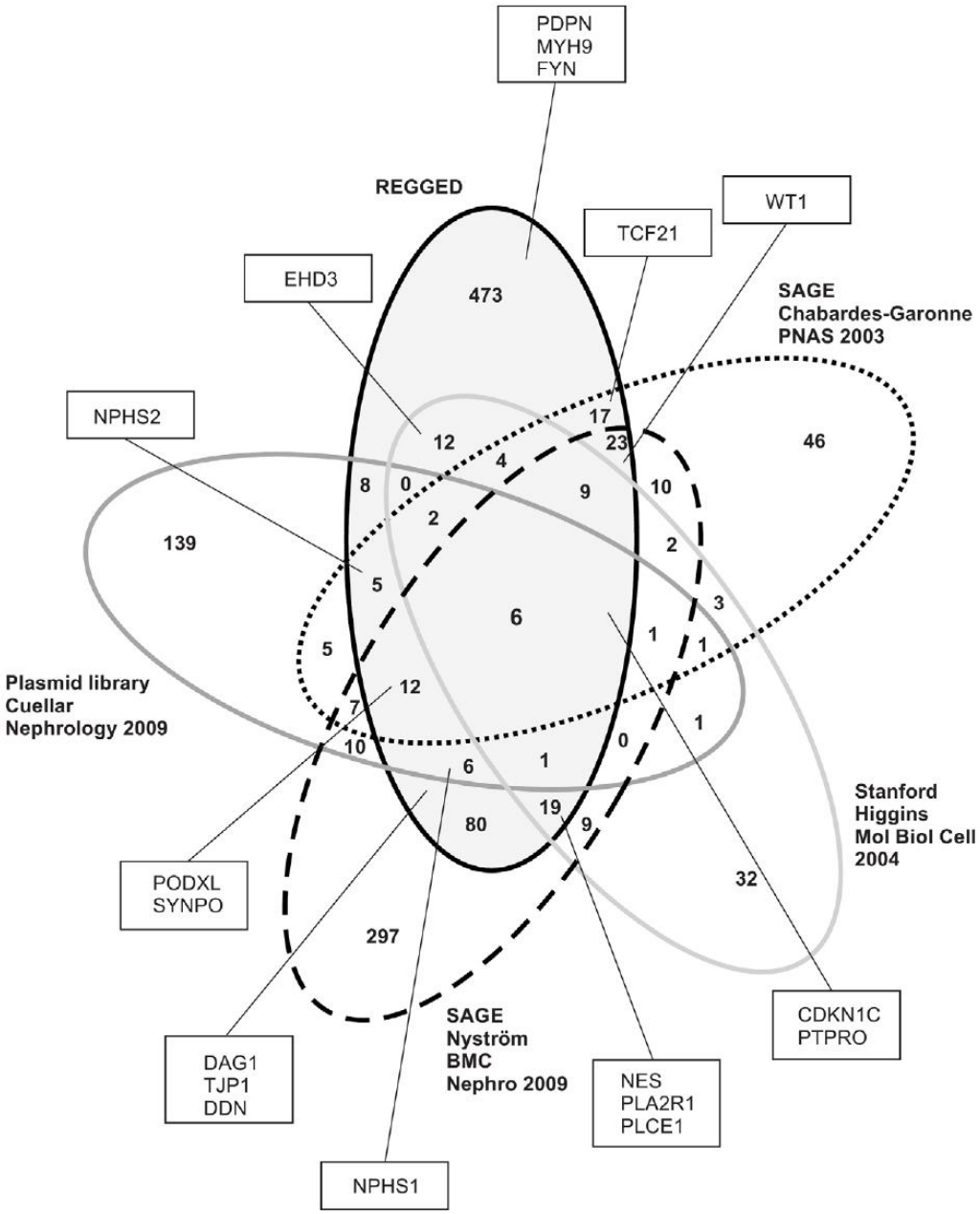

Figure 1. Venn diagram for five human glomerular data set reports. Established glomerular genes are shown in squares. REGGED is the only data set covering all such preselected glomerular gene products. The overlap among the five glomerulus-enriched gene lists is limited (see Table 1).
doi:10.1371/journal.pone.0011545.g001

genes were present in the glomerular dataset (Supplementary Table S8).

More and more studies have demonstrated that myosin or smooth muscle-related molecules participate in glomerular biology and development of renal disease [20,30,38,39]. We therefore conducted two further DDD analyses comparing a coronary artery smooth muscle cell cDNA library (total of 7,220 sequences) or normal adult muscle and heart cDNA libraries (total of 12,861 sequences) with other tissue libraries (176,036 and 163,171 sequences, respectively). These analyses resulted in 90 and 161 UniGene clusters, respectively, which were potentially enriched in smooth muscle cells or muscle and heart. Comparison of the

Table 1. Summary of the characteristics of the five methods.

Investigator	Method	Species	Total Features on the platform	Glomerulus-enriched genes reported	Selection criteria	Reference
Chabardes-Garonne et al	SAGE profiling	Human	50 000 tags	153	$P<0.01$, seven-fold or more difference with at least three nephron libraries	[26]
Higgins et al	Stanford cDNA microarray profiling	Human	41.859 probes	102	Cluster analysis, genes predominantly expressed in glomeruli than others	[27]
Cuellar et al	cDNA library (Plasmid cloning)	Human	5000 clones	205	Sequence analysis and comparison with UniGene database	[28]
Nystrom et al	SAGE profiling	Human	22907 tags	492	Comparison to pooled SAGE libraries for non-glomerular tissues and cells	[29]
Lindenmeyer et al	Affymetrix HG-U133A	Human	22283 probesets	677	Comparison of isolated glomeruli with tubulointerstitial compartment from biopsies of living donors	

doi:10.1371/journal.pone.0011545.t001

smooth muscle cell dataset with REGGED revealed an overlap of 9 genes (Supplementary Table S9). For the comparison of the muscle and heart dataset with REGGED an overlap of 17 genes was found (Supplementary table S10) including genes previously reported to be expressed in the glomerulus such as GSN, NEBL or TNNC1 [40,41]. As expected, MYH9, for which genetic variants were found to be associated with non-diabetic end-stage renal disease [20,30], is missing in these lists as it encodes a non-muscle myosin chain.

Validation by real-time RT-PCR

DDD as well as GO and KEGG analyses revealed axon guidance-related genes to be overrepresented in the renal glomerulus. We decided to focus on 4 selected neuronal associated genes in closer detail: neural proliferation differentiation and control 1 (NPDC1), neuritin (NRN1), roundabout receptor 1 and 2 (ROBO1, ROBO2, the latter not on the HG-U133A array and therefore not in REGGED, but found in rodent glomeruli by [42]). For initial further validation real-time RT-PCR was performed on an independent cohort of microdissected samples of allograft donors. Figure 3 displays the results for NPDC1, NRN1, ROBO1 and ROBO2 mRNA expression. The abundance of all these genes was significantly higher in glomeruli than in the tubulointerstitium ranging from approximately 9-fold (NPDC1) to 130-fold (ROBO2).

Protein expression of neuritin (nrn1) and robo1 in cultured podocytes and in healthy human control kidneys

The protein expression of neuritin and roundabout receptor 1, both known to be involved in axon guidance and neurite outgrowth, was assessed by Western blot in podocytes. Both proteins, robo1 and neuritin, were found to be expressed on protein level in a human podocyte cell line; human brain lysate served as a positive control (Figure 4A and B).

Immunofluorescence experiments were performed to analyze the cellular localization of robo1 and neuritin in podocytes (Figure 5) as both proteins were well expressed on mRNA level in these cell types. In undifferentiated immortalized podocytes (33°C), a cytoskeletal staining for robo1 was found, while in differentiated cells (37°C) a more intense staining of the cell border was observed (Figure 5A). For neuritin a cytoskeletal staining pattern could be observed in undifferentiated and differentiated cells, in the latter a more pronounced staining of stress fibers was seen (Figure 5B).

To evaluate the protein expression of both axon guidance molecules *in vivo*, immunofluorescence staining for robo1 and neuritin was performed on an independent set of healthy control kidneys. For robo1 expression in the glomerulus could be detected, while the staining was either completely absent or showed a minimal scattered positivity in the tubulointerstitial compartment. Neuritin showed a clear staining of the glomerulus, but also some positive signal in the tubulointerstitium (Figure 6A and B). This is consistent with REGGED and the qRT-PCR experiments indicating an enhanced but not specific glomerular expression of neuritin in the human adult healthy kidney.

Regulation of mRNA for the axon guidance molecules NRN1, ROBO1 and ROBO2 in different renal diseases

To investigate intrarenal disease associated regulation of NRN1, ROBO1 and ROBO2 mRNA, we assessed the renal expression on microdissected glomeruli of cohorts with diabetic nephropathy (DN), nephrosclerosis (NSC), focal-segmental glomerulosclerosis (FSGS), membranous glomerulonephropathy (MGN) and pre-transplant biopsies. Compared to normal glomeruli obtained from living donors we found a significantly lower expression of ROBO2 mRNA in DN and a trend towards a decreased expression in FSGS patients. ROBO1 and NRN1 mRNA showed no significant change in the disease cohorts (Figure 7).

Discussion

We compared microarray gene expression data from human glomeruli and tubulointerstitium obtained from transplant living donors to generate a human renal glomerulus-enriched gene expression dataset which contained 677 glomerulus-enriched or -restricted genes.

Comparison of our study with earlier reports of human glomerular-enriched databases using different techniques resulted in a limited overlap (Figure 1). This is in accordance with a meta-analysis performed by He et al [32] comparing different platforms and species. These results suggest that the differences may result from the different technical platforms, glomerular isolation protocols, normalization and processing of the raw data as well as different categorization criteria. In our study we used the Affymetrix platform which identified the highest number of glomerulus-enriched genes compared to the other techniques, again in accordance with the

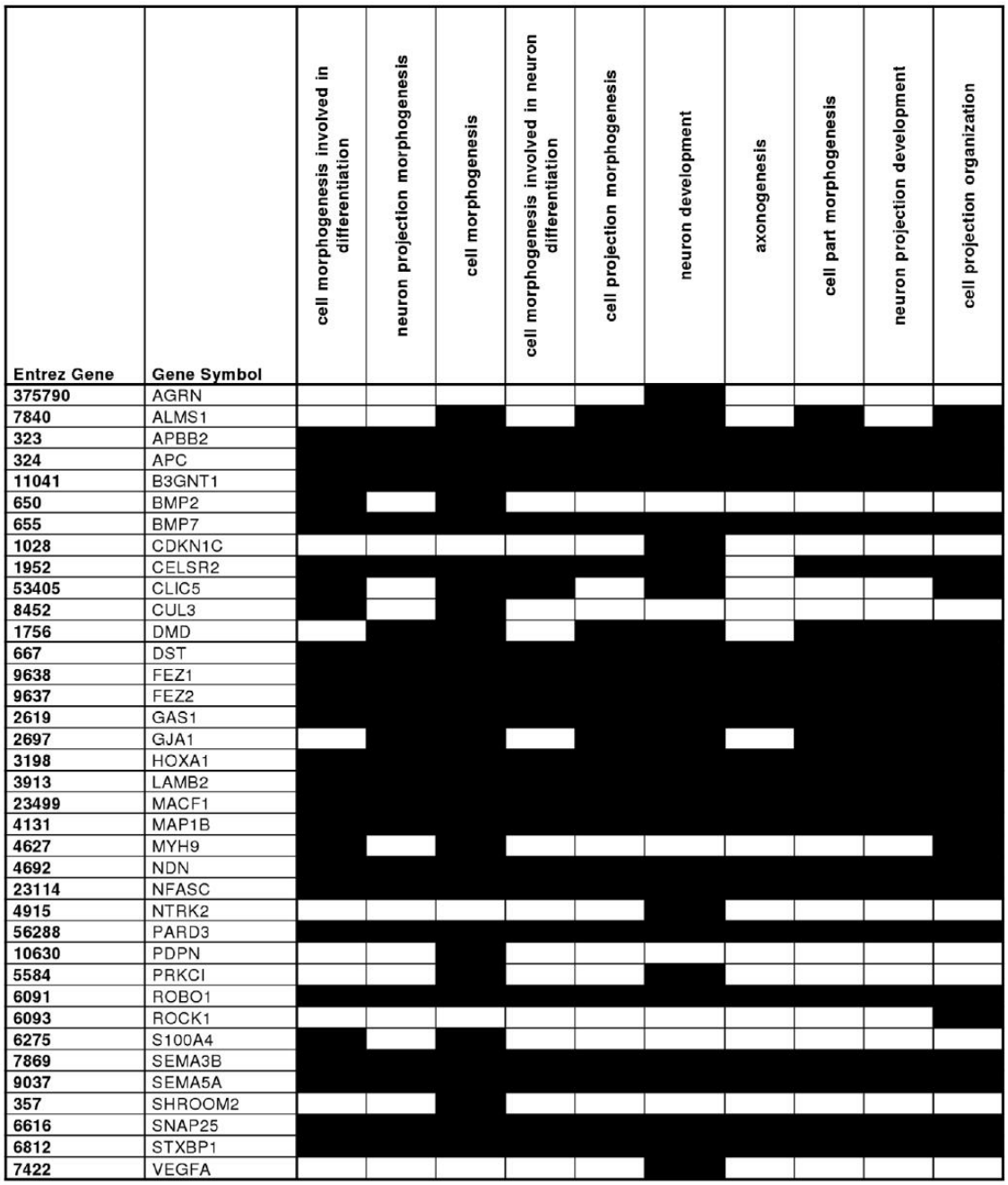

Figure 2. DAVID Functional Cluster Analysis – genes involved in functional cluster 2. Genes which are involved in the respective biological GO-term are shown in black.
doi:10.1371/journal.pone.0011545.g002

report of He et al. [32]. REGGED was in comparison to the other human databases clearly enriched for known podocyte- and glomerulus-enriched genes as summarized in Figure 1. Furthermore REGGED contained some genes, such as PDPN, FYN or MYH9, which are known to be of relevance for glomerular biology, but were missing in the other human databases.

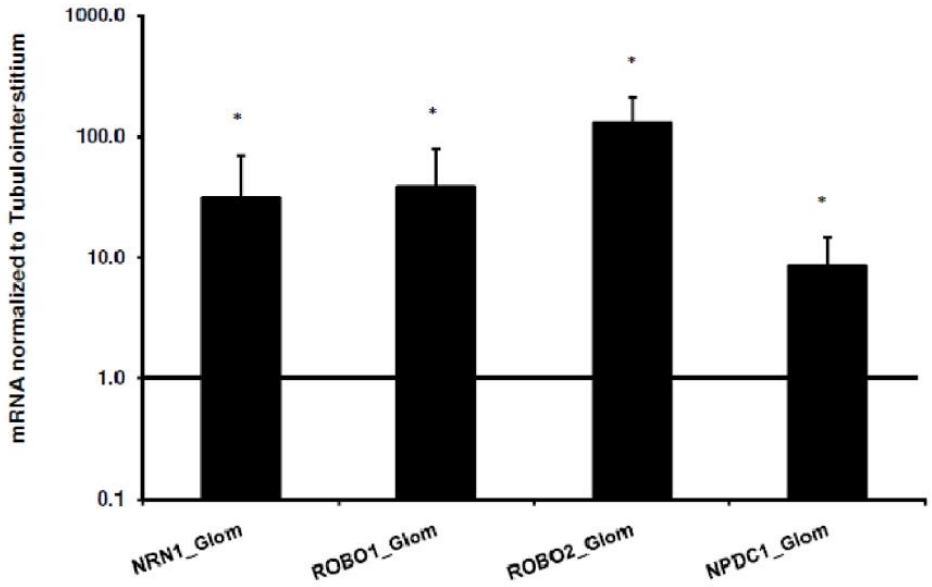

Figure 3. Evaluation of neuron-associated genes by real-time RT-PCR. Expression of NRN1, ROBO1, ROBO2, and NPDC1 mRNA in an independent cohort of microdissected samples of allograft donors normalized to the tubulointerstitial expression (n = 10). * $p<0.05$; ** $p<0.01$. The data shown are normalized to the mean of the two reference genes, GAPDH and 18S rRNA.
doi:10.1371/journal.pone.0011545.g003

To gain further information about the biology represented by this gene set we performed GO and pathway analysis using DAVID and the KEGG database. From GO-analysis, cytoskeleton-associated GO categories were identified as being significantly enriched in the glomerular dataset, which was further confirmed by the KEGG-pathways "regulation of actin cytoskeleton", "focal adhesion", and "tight junction". This is in accordance with several reports indicating that the function of podocytes, one of the three intrinsic glomerular cell types, is dependent on the plasticity of its unique and complex cytoskeletal architecture [43] and that podocyte injury with disruption of their specialized functions leads to proteinuria and foot process effacement.

One characteristic of podocytes is that except in collapsing FSGS the differentiated podocytes do not proliferate. Once podocytes are mature and terminally differentiated they remain in a quiescent state and express cyclin-dependent kinase inhibitors p27 and p57, which are present in REGGED, and do not express markers of proliferation (cyclin A, cyclin D, and Ki-67) [44]. This feature of cell cycle arrest may be the cause why the GO-analysis of the current glomerular dataset revealed several GO categories associated with cell cycle, cell growth and cell death.

Several studies have shown that podocytes share some similarities with neuronal cells. Both cells possess a highly arborized morphology, share many common cytoskeletal proteins such as synaptopodin, drebrin and densin resulting in a common cytoskeletal organization, have a common machinery for process formation [45] and express proteins primarily or exclusively found in neurons and podocytes, e.g. nephrin [46], glomerular epithelial protein 1 (GLEPP1) [47], synaptic vesicle molecule Rab3A and its effector rabphilin-3A [37], the RNA processing protein Sam68-like mammalian protein 2 (SLM2) [34] and the ubiquitin C-terminal hydrolase-L1 (UCH-L1) [48]. DDD analysis showed an enrichment of neuronal associated genes, and gene ontology as well as pathway analysis confirmed an association between neurons and glomeruli by identifying processes such as "neurogenesis" and "axon guidance" as being significantly overrepresented in this glomerular dataset. We selected 4 neuronal genes, which are associated with axon guidance (NRN1, ROBO1, ROBO2) or the control of proliferation and differentiation of neural cells (NPDC1). qRT-PCR analysis on human biopsies confirmed the overrepresentation of these genes in the glomerulus. Of interest, a human glomerular enrichment was only recently reported for NRN1 and NPDC1 [29] but not for ROBO1 and -2.

As "axon guidance" was one of the processes shown to be significantly overrepresented in REGGED, we focused in the further course of the study on genes involved in axon guidance, a process that has not been previously described in the glomerulus of healthy human adult kidneys. Neuritin (NRN1) is a glycosylphosphatidylinositol-anchored protein that is induced by neuronal activity and by the neurotrophins BDNF and NT-3. It promotes neurite outgrowth and arborization as well as neuronal survival [49,50]. In this study we found neuritin to be enriched in the glomerulus. By immunoblotting and -fluorescence we could demonstrate the expression of neuritin in cultured human podocytes and in glomeruli of healthy human kidneys. Previous studies revealed the involvement of neuritin in tumorigenesis by promoting changes in cell morphology, anchorage-independent growth and tumor formation [51] and demonstrated that its expression could be induced in endothelial cells by hypoxia, implicating a role of neuritin in vessel pathfinding and network formation [52]. Recent studies showed that neuritin expression increased following ischemia and reperfusion in rats [53] and that it mediates NGF-induced axonal regeneration and is deficient in experimental diabetic neuropathy [54].

For ROBO1 and -2 mRNA a glomerular overexpression of up to 100 fold compared to the tubulointerstitium could be observed (Figure 3). Supporting the mRNA results we found by immunoblotting and -fluorescence a clear presence of robo1 in cultured

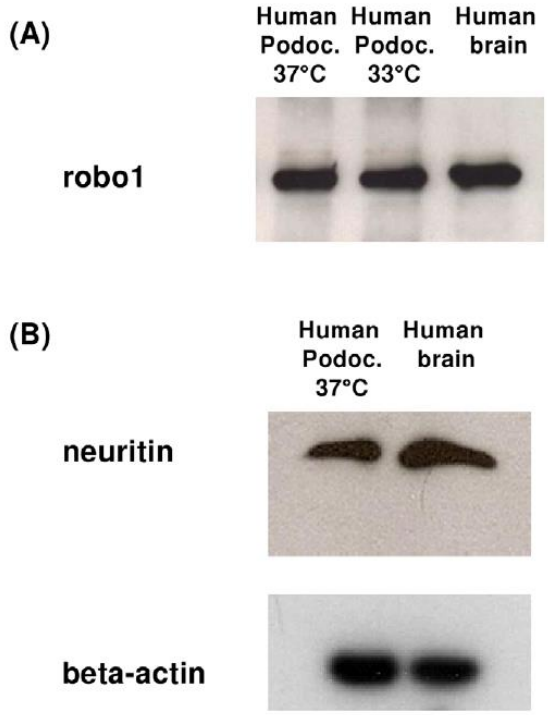

Figure 4. Western Blot analysis of robo1 (A) and neuritin (B) in human podocytes. For robo1 (A) and neuritin (nrn1) (B), a band of the expected size was found in a human podocyte cell line; human brain lysate served as a positive control. Beta-actin was used as an internal loading control.
doi:10.1371/journal.pone.0011545.g004

human podocytes and in glomeruli of healthy human control kidneys. Robo1 and -2, members of the roundabout receptor family, are single-transmembrane receptors that respond to secreted slit proteins and act as repellents regulating the migration of neurons and axons, but are also involved in inhibition of leukocyte chemotaxis, tumor angiogenesis and endothelial cell migration [55,56,57]. It is known that robo and slit genes are not only expressed in the brain, but can be found in a range of tissues. Previous rodent studies could demonstrate that the slit and robo gene families are expressed in the developing murine kidney and that disruption of the slit-robo signaling is associated with congenital anomalies of the kidney and urinary tract [58,59,60]. Furthermore Fan et al. just recently reported that podocyte-specific deletion of *robo2* in mice developed significant albuminuria which was associated with increased glomerular collagen deposition, mesangial matrix expansion and podocyte foot-process effacement [61]. In accordance with these results are our findings of decreased levels of ROBO2 mRNA in human diabetic nephropathy and focal segmental glomerulosclerosis. It is known that axon extension and guidance require a coordinated assembly of F-actin and microtubules. Different studies showed that the slit-robo transduction pathway acts via a specific family of GTPase-activating proteins (GAPs) named slit-robo GAPs (srGAPS). These srGAPs further transmit the signal to the actin cytoskeleton controlling Rho GTPases such as CDC42 or rac1 and thus provide a direct link between slit-robo signaling and actin cytoskeleton [62]. Studies from Kobayashi et al showed that alterations of the activity of the rho family small GTPases leads to changes in actin filament assembly and in foot process formation [45]. In this context, the finding of robo1 and -2 in podocytes indicate a possible role in the regulation of the complex cytoskeletal structure of these cells which is also strengthened by the presence of srGAPs and downstream targets of the slit-robo signaling pathways in our REGGED.

In conclusion, we successfully generated a human glomerulus-enriched gene expression dataset (REGGED) which allowed us to

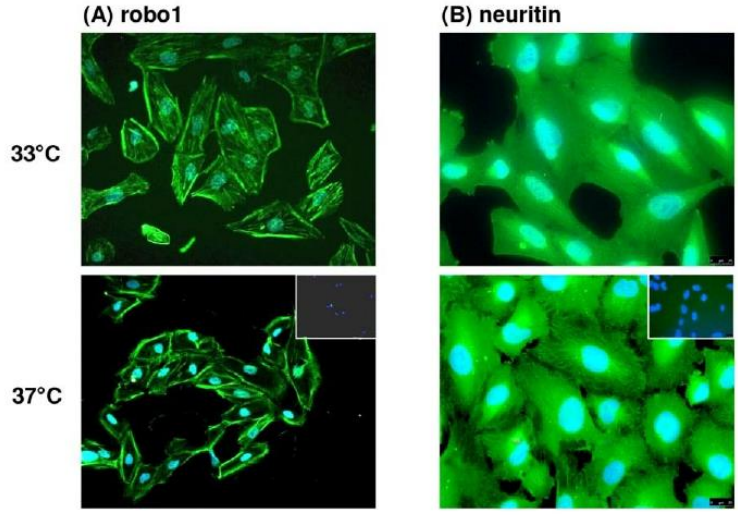

Figure 5. Immunofluorescence of robo1 (A) and neuritin (B) in human podocytes. In undifferentiated, immortalized podocytes (33°C) the expression of robo1 seemed to be more cytoskeletal, while in differentiated cells (37°C) a more intensive staining as well as a more pronounced staining at the cell border was found. For neuritin a cytoskeletal staining pattern could be observed in undifferentiated and differentiated cells with in the latter pronounced staining of stress fibers.
doi:10.1371/journal.pone.0011545.g005

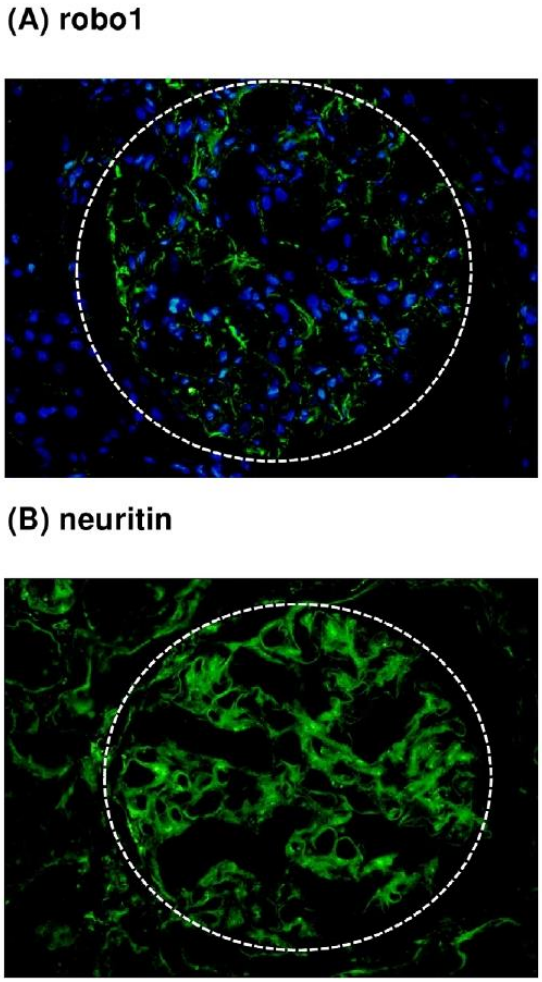

Figure 6. Immunofluorescence of robo1 (A) and neuritin (B) in human control kidneys. Immunofluorescence for robo1 (A) shows a constitutive expression in glomeruli, while there is no expression in the tubulointerstitium. Immunostaining for neuritin (B) shows a clear glomerular expression associated to some positivity in the tubulointerstitium. The hatched line displays the glomerular contour (indirect immunofluorescence, DAPI nuclear counterstain, 200X).
doi:10.1371/journal.pone.0011545.g006

identify novel genes expressed predominantly in the human glomerulus. Pathways which have not previously been associated with glomerular biology were identified. A systematic analysis of this dataset allows the detection of target molecules and biological processes involved in glomerular biology and renal disease. We believe that REGGED will fuel ongoing and future research on glomerular biology and disease.

Materials and Methods

Renal biopsies for mRNA analysis

Human renal biopsy specimens were procured in an international multicenter study, the European Renal cDNA Bank-Kroener-Fresenius biopsy bank (ERCB-KFB, see appendix for participating centers [63]). Renal biopsies were obtained after written consent and approval of the ethics committee and in the frame of the European Renal cDNA Bank approved by the specialized subcommittee for internal medicine of the cantonal ethics committee of Zurich. All kidney donors had normal renal function, no proteinuria and no arterial hypertension. Glomeruli and the tubulointerstitial specimen were microdissected as described previously [63]. The data discussed in this publication have been deposited in NCBI's Gene Expression Omnibus [64] and are accessible through GEO Series accession number GSE21785 (http://www.ncbi.nlm.nih.gov/geo/query/acc.cgi?acc = GSE21785) and will also be made available online at http://www.nephromine.org.

For validation of the microarray data, qRT-PCR on biopsies from an independent cohort of living donors (LD, n = 10) was performed. Furthermore, cohorts of patients with diabetic nephropathy (DN, n = 14), focal segmental glomerulosclerosis (FSGS; n = 17), membranous nephropathy (MGN; n = 17), nephrosclerosis (NSC; n = 14) and controls (living donors (LD) n = 8) were used for gene expression analysis by qRT-PCR (Supplementary Table S11).

Target preparation

RNA was isolated as described previously [63]. Total RNA was reverse-transcribed (RT) and linearly amplified according to a protocol previously reported for tubulointerstitial specimen [65] and glomeruli [66], respectively. The fragmentation, hybridization, staining and imaging were performed according the Affymetrix Expression Analysis Technical Manual.

Microarray Data Analysis

Normalization. To compare the respective glomerular and tubulointerstitial gene expression profiles we performed background adjustment, quantile normalization and probeset summarization using Robust Multichip Analysis (RMA) using RMAexpress version 0.3 [67] with settings from previous studies [65].

Comparison. The comparison of tubulointerstitial and glomerular expression relies on the assumption that only a small subset of genes shows compartment specific expression and as a corollary almost all show equal expression. However, as glomerular and tubulointerstitial specimen were hybridized to the microarrays separately, we had to consider the possibility of systematic error leading to pairwise different expression values of the genes. For example, a positive shift of the glomerular data would make genes with truly similar expression appear to have higher expression in glomeruli. Therefore an adjustment of the data prior to any analysis is crucial to avoid the introduction of false positives and false negatives. Standard normalization methods are designed to remove rather minor technical variation evenly distributed across samples. As we have experienced a more pronounced effect on the two blocks of data we decided to normalize the sets separately and subsequently adjust the data as follows using a linear function.

While the underlying causes of this error type can be complex and hard to discern, a linear function provides a sensible starting point. In detail, this means to find an additive factor (difference of base expression) and a multiplicative one (difference in dynamic range) and apply this function to one of the datasets. By subsequent subtraction of the tubulointerstitial from the glomerular dataset we expected to find many values close to 0, the ones with positive result being our candidates for preferential glomerular expression.

To determine the factors, we calculated the mean of each probeset across all the samples in each condition, resulting in an aggregate expression profile for glomeruli and tubulointerstitium. After sorting

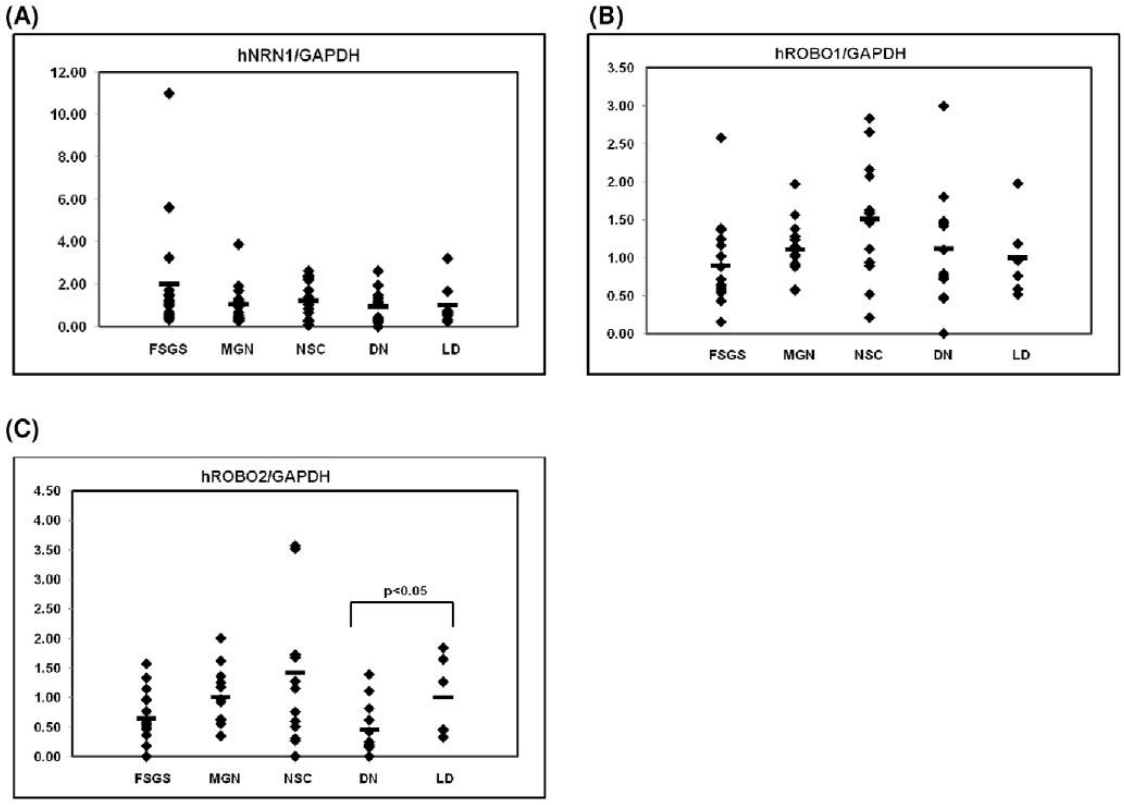

Figure 7. Glomerular mRNA expression of NRN1, ROBO1 and 2 mRNA in human DN, NSC, FSGS and MGN. Levels of mRNA for NRN1 (A), ROBO1 (B) and ROBO2 (C) were quantified in microdissected glomeruli from controls (n = 8), patients with established DN (DN, n = 14), NSC (n = 14), FSGS (FSGS, n = 17) and from patients with MGN (n = 17). ROBO2 was significantly down-regulated in diabetic nephropathy compared to control samples as indicated by the respective p-value, while ROBO1 and NRN1 showed no regulation. The graphs show expression ratios of each gene normalized to hGAPDH.
doi:10.1371/journal.pone.0011545.g007

both by ascending expression level of tubulointerstitium, we generated a line of best fit, its slope (multiplicative factor) and intercept (additive factor) for both datasets (glomeruli: $y = 0.1641x+2.8035$, tubulointerstitium: $y = 0.1771x+1.5913$). To adjust tubulointerstitium to glomeruli we multiplied each value by $(0.1641/0.1771) = 0.9265951$ and added $(2.8035-1.5913) = 1.3022$. To minimize effects of sorting, we repeated the same procedure after sorting by the glomeruli data and used the means of slope and intercept for the final adjustment function ($y = 0.9392425x + 1.17905$). Next we subtracted the corrected tubulointerstitial from glomerular expression values and calculated the standard deviation of this difference. The selection criterion for preferential glomerular expression was set as an expression difference exceeding twice this standard deviation (mean + 2*SD = 1.76) resulting in a dataset of 817 glomerular-enriched probesets. After removing unannotated probesets and redundant probesets a list of 677 glomerular-overrepresentated genes remained (Table S1).

Digital Differential Display (DDD)

DDD, a bioinformatic tool available at the National Center for Biotechnology Information (www.ncbi.nlm.nih.gov/UniGene/info_ddd.html), analyzes the frequencies of cDNA and expressed sequence tag (EST) in expression libraries [34]. The DDD tool was used to compare human cDNA libraries of indicated organs or cells (i. e. normal adult brain, coronary artery smooth muscle cells, muscle and heart) with other organ cDNA libraries except testis as described previously [34].

Analysis of biological processes and pathways

GOs and pathways were identified using a combination DAVID Bioinformatics database from the NIAID, NIH (Version 2010) (http://david.abcc.ncifcrf.gov/) [68,69] and the KEGG database from the University of Kyoto (http://www.genome.jp/kegg/kegg2.html) [70,71].

To obtain a more structured biological picture the functional annotation cluster analysis tool of DAVID was applied on REGGED. This analysis tool measures relationships among the annotation terms by using *Kappa*-statistics and is able to organize and cluster redundant and heterogeneous annotation terms into functional annotation groups which can provide a better understanding of the biological meaning for the given dataset [33].

For all DAVID analyses a p-value (Ease score) of 0.05 and fold enrichment of at least 1.5 was used as standard cut-off level. As gene reference background the Affymetrix HT human genome U133A available in DAVID was used [33,69].

Quantitative real-time RT-PCR

Reverse transcription and qRT-PCR was performed as reported earlier [63]. Pre-developed TaqMan reagents were used for human NRN1 (Hs00213192_m1), NPDC1 (Hs00209870_m1), ROBO1 (Hs00268049_m1) as well as the housekeeper genes (Applied Biosystems Europe, Rotkreuz, Switzerland). For the human ROBO2 (NM_002942), the following oligonucleotide primers (300 nmol/L) and probe (100 nmol/L) were used: sense primer 5′- ATTGAGGCTTTCAGCCAATCA-3′, antisense primer 5′- TGATCGCTCTGACCATGAATAAGT-3′; fluorescence labeled probe (FAM) 5′- TGAGCAACAGCTGGCAGACCGTG-3′. The expression of candidate genes was normalized by two reference genes, 18S rRNA and GAPDH, giving comparable results. The mRNA expression was analyzed by the delta delta Ct method for renal compartment analysis or standard curve quantification for disease-specific expression analysis.

Western Blot

Robo1: Cultured human glomerular epithelial cells [72] were harvested with lysis buffer A (2% Triton, 150 mM NaCl, 100 mM HEPES, 2 mM EGTA, 2 mM Na_3VO_4, and Complete Protease Inhibitor Cocktail [Roche, Mannheim, Germany]). Extracted proteins were boiled in loading buffer for 5 min, resolved by 6% SDS-PAGE under reducing conditions, and transferred to an Immobilon-P membrane (Millipore, Eschborn, Germany).

Neuritin: Cultured human podocytes [72] were lysed with buffer B (150 mM NaCl, 1% Nonidet P-40, 0.5% DOC, 0.1% SDS, 50 mM Tris, pH 8.0, 100 mM DTT, 6M Urea and Complete Protease Inhibitor Cocktail [Roche, Mannheim, Germany]. Extracted proteins were heated for 15 min at 37°C, resolved by 16% Tricine-SDS-PAGE, containing 6M Urea [73] under reducing conditions, and transferred to an Immobilon-P membrane (Millipore, Eschborn, Germany).

Equal loading and transfer efficiency were verified by staining with 2% Ponceau S. Membranes were blocked overnight with Tris-buffered saline (TBS)/3% fat-free skim milk and then incubated with either a polyclonal rabbit anti-robo1 (Abcam, Cambridge, UK) diluted 1:500 overnight at 4°C, or polyclonal rabbit anti-neuritin (Lifespan Biosciences, Seattle, WA, USA) diluted 1:500 overnight at 4°C and rinsed with TBS that contained 0.1% Tween 20. For detection, a donkey anti-rabbit IgG ECL antibody, HRP conjugated (1:10000, 1 hour at room temperature; GE Healthcare, Chalfont St. Giles, UK) and enhanced chemiluminescence substrate (PerkinElmer, Waltham, MA, USA) were used. Membranes were also probed with anti-beta-actin antibody (A 5316, 1:5000, Sigma-Aldrich, Germany) as internal loading control.

Immunofluorescence staining of human podocytes

Cells were fixed with 2% paraformaldehyde and 4% sucrose at room temperature for 10 min. The cells were then washed once with PBS, permeabilized with 0.3% Triton X-100 for 10 min and incubated with blocking solution (2% FCS, 2% BSA, 0.2% fish gelatin) for 30 min, before further incubation with a polyclonal rabbit anti-robo1 (Abcam, Cambridge, UK) or a polyclonal rabbit anti-neuritin antibody (Lifespan Biosciences, Seattle, WA, USA) for 1 h. For immunofluorescence detection, Alexa Fluor 488 goat anti-rabbit IgG secondary antibody (Invitrogen, Molecular Probes, Paisley, UK) were used at a dilution of 1:200. For nuclear counterstaining, tissue sections were mounted with Vectashield with DAPI (Vector Laboratories, Burlinghame, CA, USA).

Immunofluorescence staining of human control kidneys

Kidney tissue was obtained from the healthy pole of kidneys removed because of small and localized tumors. For immunofluorescence, the unfixed renal tissue was embedded in OCT (optimum cutting temperature cryoembedding matrix) (Tissue-Tek, Electron Microscopy Sciences, Società Italiana Chimici, Roma, Italy), snap-frozen in a mixture of isopentane and dry ice, and stored at −80°C. Indirect immunofluorescence was performed on 5-µm-thick tissue cryosections fixed in cold acetone with the primary antibodies rabbit anti-robo1 and rabbit anti-neuritin (both from Novus Biologicals, DBA Italia, Milan, Italy). Sections were incubated for 30 min with a fluorescent-labelled goat anti-rabbit secondary antibody (Alexafluor 488; Invitrogen, Milan, Italy) and nuclei counterstained by DAPI. Specificity of antibody labelling was demonstrated by the lack of staining after substituting proper control immunoglobulins (Rabbit primary antibody isotype control, Invitrogen) for the primary antibodies. Slides were mounted with Fluorsave aqueous mounting medium (Calbiochem, VWR International, Milan, Italy). Images were acquired by a Zeiss Axioscope 40FL microscope, equipped with AxioCam MRc5 digital videocamera and immunofluorescence apparatus (Carl Zeiss SpA, Arese, Mi, Italy), and recorded using AxioVision software 4.3.

Statistics

Experimental data are given as mean ± SD. Statistical analysis was performed using Kruskall-Wallis and Mann-Whitney U tests (SPSS 17.0, SPSS Inc., Chicago, IL). P-values less than 0.05 were considered to indicate statistically significant differences.

Supporting Information

Figure S1 DAVID Functional Annotation Cluster Analysis - genes involved in functional clusters. The terms involved in the respective functional annotation clusters are described in Table S5. Genes which are involved in the respective functional annotation cluster are shown in black.
Found at: doi:10.1371/journal.pone.0011545.s001 (0.06 MB PDF)

Table S1 Renal glomerulus-enriched gene expression dataset (REGGED). 677 renal genes were identified to be enriched in the human glomerulus.
Found at: doi:10.1371/journal.pone.0011545.s002 (0.72 MB DOC)

Table S2 List of known podocyte-, mesangial- and endothelial-specific markers as well as validated glomerular gene and protein expression data.
Found at: doi:10.1371/journal.pone.0011545.s003 (0.35 MB DOC)

Table S3 Comparison of the 5 different approaches. 1 indicates the presence of the gene, 0 indicates the absence of the gene in the respective dataset. Sum: indicates in how many of the databases the respective gene is found.
Found at: doi:10.1371/journal.pone.0011545.s004 (0.24 MB XLS)

Table S4 Prominent biological aspects found by DAVID analysis
Found at: doi:10.1371/journal.pone.0011545.s005 (0.36 MB DOC)

Table S5 DAVID Functional Annotation Cluster Analysis
Found at: doi:10.1371/journal.pone.0011545.s006 (0.13 MB DOC)

Table S6 KEGG pathways
Found at: doi:10.1371/journal.pone.0011545.s007 (0.04 MB DOC)

Table S7 Neuron/brain-associated gene list
Found at: doi:10.1371/journal.pone.0011545.s008 (0.40 MB DOC)

Table S8 Neuron/brain-associated genes present in the REGGED
Found at: doi:10.1371/journal.pone.0011545.s009 (0.07 MB DOC)

Table S9 Smooth muscle cell associated gene list. Genes marked in bold font are present in REGGED.
Found at: doi:10.1371/journal.pone.0011545.s010 (0.10 MB DOC)

Table S10 Muscle- and heart associated gene list. Genes marked in bold font are present in REGGED.
Found at: doi:10.1371/journal.pone.0011545.s011 (0.16 MB DOC)

Table S11 Clinical and histological characteristics. Clinical and histological characteristics of patients and biopsies, respectively, with established diabetic nephropathy, focal segmental sclerosis and living donors analyzed by real-time RT-PCR (P) and oligonucleotide array based gene expression profiling (A) (for living donor). * = blood pressure before biopsy [mmHg].
Found at: doi:10.1371/journal.pone.0011545.s012 (0.15 MB DOC)

Acknowledgments

We thank Stefanie Gaiser for excellent technical assistance.

We thank all participating centers of the European Renal cDNA Bank-Kroener-Fresenius biopsy bank (ERCB-KFB) and their patients for their cooperation. Active members at the time of the study: Clemens David Cohen, Holger Schmid, Michael Fischereder, Lutz Weber, Matthias Kretzler, Detlef Schlöndorff, Munich/Zurich/AnnArbor/New York; Jean Daniel Sraer, Pierre Ronco, Paris; Maria Pia Rastaldi, Giuseppe D'Amico, Milano; Peter Doran, Hugh Brady, Dublin; Detlev Mönks, Christoph Wanner, Würzburg; Andrew Rees, Aberdeen; Frank Strutz, Gerhard Anton Müller, Göttingen; Peter Mertens, Jürgen Floege, Aachen; Norbert Braun, Teut Risler, Tübingen; Loreto Gesualdo, Francesco Paolo Schena, Bari; Jens Gerth, Gunter Wolf, Jena; Rainer Oberbauer, Dontscho Kerjaschki, Vienna; Bernhard Banas, Bernhard Krämer, Regensburg; Moin Saleem, Bristol; Rudolf Wüthrich, Zurich; Walter Samtleben, Munich; Harm Peters, Hans-Hellmut Neumayer, Berlin; Mohamed Daha, Leiden; Katrin Ivens, Bernd Grabensee, Düsseldorf; Francisco Mampaso(†), Madrid; Jun Oh, Franz Schaefer, Martin Zeier, Hermann-Joseph Gröne, Heidelberg; Peter Gross, Dresden; Giancarlo Tonolo; Sassari; Vladimir Tesar, Prague; Harald Rupprecht, Bayreuth; Hermann Pavenstädt, Münster; Hans-Peter Marti, Bern.

Author Contributions

Conceived and designed the experiments: CDC. Performed the experiments: MTL FE KS IE DM MPR. Analyzed the data: MTL FE MPR CDC. Contributed reagents/materials/analysis tools: HJA MK. Wrote the paper: MTL FE MPR MK CDC.

References

1. USRDS (2009) U.S. Renal Data System, USRDS 2009 Annual Data Report: Atlas of End-Stage Renal Disease in the United States. Bethasda, MD: National Institutes of Health, National Institute of Diabetes and Digestive and Kidney Diseases.
2. Haraldsson B, Nystrom J, Deen WM (2008) Properties of the glomerular barrier and mechanisms of proteinuria. Physiol Rev 88: 451–487.
3. Eremina V, Cui S, Gerber H, Ferrara N, Haigh J, et al. (2006) Vascular endothelial growth factor a signaling in the podocyte-endothelial compartment is required for mesangial cell migration and survival. J Am Soc Nephrol 17: 724–735.
4. Eremina V, Sood M, Haigh J, Nagy A, Lajoie G, et al. (2003) Glomerular-specific alterations of VEGF-A expression lead to distinct congenital and acquired renal diseases. J Clin Invest 111: 707–716.
5. Pavenstadt H, Kriz W, Kretzler M (2003) Cell biology of the glomerular podocyte. Physiol Rev 83: 253–307.
6. Kwoh C, Shannon MB, Miner JH, Shaw A (2006) Pathogenesis of nonimmune glomerulopathies. Annu Rev Pathol 1: 349–374.
7. Schmieder S, Nagai M, Orlando RA, Takeda T, Farquhar MG (2004) Podocalyxin activates RhoA and induces actin reorganization through NHERF1 and Ezrin in MDCK cells. J Am Soc Nephrol 15: 2289–2298.
8. Moeller MJ, Soofi A, Braun GS, Li X, Watzl C, et al. (2004) Protocadherin FAT1 binds Ena/VASP proteins and is necessary for actin dynamics and cell polarization. Embo J 23: 3769–3779.
9. Jones N, Blasutig IM, Eremina V, Ruston JM, Bladt F, et al. (2006) Nck adaptor proteins link nephrin to the actin cytoskeleton of kidney podocytes. Nature 440: 818–823.
10. Asanuma K, Kim K, Oh J, Giardino L, Chabanis S, et al. (2005) Synaptopodin regulates the actin-bundling activity of alpha-actinin in an isoform-specific manner. J Clin Invest 115: 1188–1198.
11. Sever S, Altintas MM, Nankoe SR, Moller CC, Ko D, et al. (2007) Proteolytic processing of dynamin by cytoplasmic cathepsin L is a mechanism for proteinuric kidney disease. J Clin Invest 117: 2095–2104.
12. El-Aouni C, Herbach N, Blattner SM, Henger A, Rastaldi MP, et al. (2006) Podocyte-specific deletion of integrin-linked kinase results in severe glomerular basement membrane alterations and progressive glomerulosclerosis. J Am Soc Nephrol 17: 1334–1344.
13. Huber TB, Benzing T (2005) The slit diaphragm: a signaling platform to regulate podocyte function. Curr Opin Nephrol Hypertens 14: 211–216.
14. Wiggins RC (2007) The spectrum of podocytopathies: a unifying view of glomerular diseases. Kidney Int 71: 1205–1214.
15. Rascle A, Suleiman H, Neumann T, Witzgall R (2007) Role of transcription factors in podocytes. Nephron Exp Nephrol 106: e60–66.
16. Ronco P, Debiec H Antigen Identification in Membranous Nephropathy Moves toward Targeted Monitoring and New Therapy. J Am Soc Nephrol.
17. Achenbach J, Mengel M, Tossidou I, Peters I, Park JK, et al. (2008) Parietal epithelia cells in the urine as a marker of disease activity in glomerular diseases. Nephrol Dial Transplant 23: 3138–3145.
18. Beck LH, Jr., Bonegio RG, Lambeau G, Beck DM, Powell DW, et al. (2009) M-type phospholipase A2 receptor as target antigen in idiopathic membranous nephropathy. N Engl J Med 361: 11–21.
19. Jefferson JA, Shankland SJ (2007) Familial nephrotic syndrome: PLCE1 enters the fray. Nephrol Dial Transplant 22: 1849–1852.
20. Kao WH, Klag MJ, Meoni LA, Reich D, Berthier-Schaad Y, et al. (2008) MYH9 is associated with nondiabetic end-stage renal disease in African Americans. Nat Genet 40: 1185–1192.
21. Marshall CB, Shankland SJ (2006) Cell cycle and glomerular disease: a minireview. Nephron Exp Nephrol 102: e39–48.
22. Patrakka J, Xiao Z, Nukui M, Takemoto M, He L, et al. (2007) Expression and subcellular distribution of novel glomerulus-associated proteins dendrin, ehd3, sh2d4a, plekhh2, and 2310066E14Rik. J Am Soc Nephrol 18: 689–697.
23. Schmid H, Henger A, Cohen CD, Frach K, Grone HJ, et al. (2003) Gene expression profiles of podocyte-associated molecules as diagnostic markers in acquired proteinuric diseases. J Am Soc Nephrol 14: 2958–2966.
24. Schnabel E, Anderson JM, Farquhar MG (1990) The tight junction protein ZO-1 is concentrated along slit diaphragms of the glomerular epithelium. J Cell Biol 111: 1255–1263.
25. Thorner PS, Ho M, Eremina V, Sado Y, Quaggin S (2008) Podocytes contribute to the formation of glomerular crescents. J Am Soc Nephrol 19: 495–502.
26. Chabardes-Garonne D, Mejean A, Aude JC, Cheval L, Di Stefano A, et al. (2003) A panoramic view of gene expression in the human kidney. Proc Natl Acad Sci U S A 100: 13710–13715.
27. Higgins JP, Wang L, Kambham N, Montgomery K, Mason V, et al. (2004) Gene expression in the normal adult human kidney assessed by complementary DNA microarray. Mol Biol Cell 15: 649–656.
28. Cuellar LM, Fujinaka H, Yamamoto K, Miyamoto M, Tasaki M, et al. (2009) Identification and localization of novel genes preferentially expressed in human kidney glomerulus. Nephrology (Carlton) 14: 94–104.
29. Nystrom J, Fierlbeck W, Granqvist A, Kulak SC, Ballermann BJ (2009) A human glomerular SAGE transcriptome database. BMC Nephrol 10: 13.
30. Kopp JB, Smith MW, Nelson GW, Johnson RC, Freedman BI, et al. (2008) MYH9 is a major-effect risk gene for focal segmental glomerulosclerosis. Nat Genet 40: 1175–1184.
31. Matsui K, Breiteneder-Geleff S, Kerjaschki D (1998) Epitope-specific antibodies to the 43-kD glomerular membrane protein podoplanin cause proteinuria and rapid flattening of podocytes. J Am Soc Nephrol 9: 2013–2026.
32. He L, Sun Y, Takemoto M, Norlin J, Tryggvason K, et al. (2008) The glomerular transcriptome and a predicted protein-protein interaction network. J Am Soc Nephrol 19: 260–268.

33. Huang da W, Sherman BT, Lempicki RA (2009) Bioinformatics enrichment tools: paths toward the comprehensive functional analysis of large gene lists. Nucleic Acids Res 37: 1–13.
34. Cohen CD, Doran PP, Blattner SM, Merkle M, Wang GQ, et al. (2005) Sam68-like mammalian protein 2, identified by digital differential display as expressed by podocytes, is induced in proteinuria and involved in splice site selection of vascular endothelial growth factor. J Am Soc Nephrol 16: 1958–1965.
35. Giardino L, Armelloni S, Corbelli A, Mattinzoli D, Zennaro C, et al. (2009) Podocyte glutamatergic signaling contributes to the function of the glomerular filtration barrier. J Am Soc Nephrol 20: 1929–1940.
36. Guo JH, Huang Q, Studholme DJ, Wu CQ, Zhao Z (2005) Transcriptomic analyses support the similarity of gene expression between brain and testis in human as well as mouse. Cytogenet Genome Res 111: 107–109.
37. Rastaldi MP, Armelloni S, Berra S, Calvaresi N, Corbelli A, et al. (2006) Glomerular podocytes contain neuron-like functional synaptic vesicles. Faseb J 20: 976–978.
38. Cove-Smith A, Hendry BM (2008) The regulation of mesangial cell proliferation. Nephron Exp Nephrol 108: e74–79.
39. Morton MJ, Hutchinson K, Mathieson PW, Witherden IR, Saleem MA, et al. (2004) Human podocytes possess a stretch-sensitive, Ca2+-activated K+ channel: potential implications for the control of glomerular filtration. J Am Soc Nephrol 15: 2981–2987.
40. Harvey SJ, Jarad G, Cunningham J, Goldberg S, Schermer B, et al. (2008) Podocyte-specific deletion of dicer alters cytoskeletal dynamics and causes glomerular disease. J Am Soc Nephrol 19: 2150–2158.
41. Miao J, Fan Q, Cui Q, Zhang H, Chen L, et al. (2009) Newly identified cytoskeletal components are associated with dynamic changes of podocyte foot processes. Nephrol Dial Transplant 24: 3297–3305.
42. Takemoto M, He L, Norlin J, Patrakka J, Xiao Z, et al. (2006) Large-scale identification of genes implicated in kidney glomerulus development and function. Embo J 25: 1160–1174.
43. Faul C, Asanuma K, Yanagida-Asanuma E, Kim K, Mundel P (2007) Actin up: regulation of podocyte structure and function by components of the actin cytoskeleton. Trends Cell Biol 17: 428–437.
44. Marshall CB, Shankland SJ (2007) Cell cycle regulatory proteins in podocyte health and disease. Nephron Exp Nephrol 106: e51–59.
45. Kobayashi N, Gao SY, Chen J, Saito K, Miyawaki K, et al. (2004) Process formation of the renal glomerular podocyte: is there common molecular machinery for processes of podocytes and neurons? Anat Sci Int 79: 1–10.
46. Putaala H, Soininen R, Kilpelainen P, Wartiovaara J, Tryggvason K (2001) The murine nephrin gene is specifically expressed in kidney, brain and pancreas: inactivation of the gene leads to massive proteinuria and neonatal death. Hum Mol Genet 10: 1–8.
47. Beltran PJ, Bixby JL, Masters BA (2003) Expression of PTPRO during mouse development suggests involvement in axonogenesis and differentiation of NT-3 and NGF-dependent neurons. J Comp Neurol 456: 384–395.
48. Meyer-Schwesinger C, Meyer TN, Munster S, Klug P, Saleem M, et al. (2009) A new role for the neuronal ubiquitin C-terminal hydrolase-L1 (UCH-L1) in podocyte process formation and podocyte injury in human glomerulopathies. J Pathol 217: 452–464.
49. Naeve GS, Ramakrishnan M, Kramer R, Hevroni D, Citri Y, et al. (1997) Neuritin: a gene induced by neural activity and neurotrophins that promotes neuritogenesis. Proc Natl Acad Sci U S A 94: 2648–2653.
50. Cappelletti G, Galbiati M, Ronchi C, Maggioni MG, Onesto E, et al. (2007) Neuritin (cpg15) enhances the differentiating effect of NGF on neuronal PC12 cells. J Neurosci Res 85: 2702–2713.
51. Raggo C, Ruhl R, McAllister S, Koon H, Dezube BJ, et al. (2005) Novel cellular genes essential for transformation of endothelial cells by Kaposi's sarcoma-associated herpesvirus. Cancer Res 65: 5084–5095.
52. Le Jan S, Le Meur N, Cazes A, Philippe J, Le Cunff M, et al. (2006) Characterization of the expression of the hypoxia-induced genes neuritin, TXNIP and IGFBP3 in cancer. FEBS Lett 580: 3395–3400.
53. Rickhag M, Teilum M, Wieloch T (2007) Rapid and long-term induction of effector immediate early genes (BDNF, Neuritin and Arc) in peri-infarct cortex and dentate gyrus after ischemic injury in rat brain. Brain Res 1151: 203–210.
54. Karamoysoyli E, Burnand RC, Tomlinson DR, Gardiner NJ (2008) Neuritin mediates nerve growth factor-induced axonal regeneration and is deficient in experimental diabetic neuropathy. Diabetes 57: 181–189.
55. Legg JA, Herbert JM, Clissold P, Bicknell R (2008) Slits and Roundabouts in cancer, tumour angiogenesis and endothelial cell migration. Angiogenesis 11: 13–21.
56. Prasad A, Qamri Z, Wu J, Ganju RK (2007) Slit-2/Robo-1 modulates the CXCL12/CXCR4-induced chemotaxis of T cells. J Leukoc Biol 82: 465–476.
57. Wu JY, Feng L, Park HT, Havlioglu N, Wen L, et al. (2001) The neuronal repellent Slit inhibits leukocyte chemotaxis induced by chemotactic factors. Nature 410: 948–952.
58. Piper M, Georgas K, Yamada T, Little M (2000) Expression of the vertebrate Slit gene family and their putative receptors, the Robo genes, in the developing murine kidney. Mech Dev 94: 213–217.
59. Lu W, van Eerde AM, Fan X, Quintero-Rivera F, Kulkarni S, et al. (2007) Disruption of ROBO2 is associated with urinary tract anomalies and confers risk of vesicoureteral reflux. Am J Hum Genet 80: 616–632.
60. Grieshammer U, Le M, Plump AS, Wang F, Tessier-Lavigne M, et al. (2004) SLIT2-mediated ROBO2 signaling restricts kidney induction to a single site. Dev Cell 6: 709–717.
61. Fan KLQG, Wang X, et al. (2009) Robo2 Is a Podocyte Protein Required for Normal Glomerular Filtration Barrier Function. ASN Renal Week 2009, free communication. San Diego: American Society of Nephrology.
62. Ghose A, Van Vactor D (2002) GAPs in Slit-Robo signaling. Bioessays 24: 401–404.
63. Cohen CD, Frach K, Schlondorff D, Kretzler M (2002) Quantitative gene expression analysis in renal biopsies: a novel protocol for a high-throughput multicenter application. Kidney Int 61: 133–140.
64. Barrett T, Troup DB, Wilhite SE, Ledoux P, Rudnev D, et al. (2009) NCBI GEO: archive for high-throughput functional genomic data. Nucleic Acids Res 37: D885–890.
65. Schmid H, Boucherot A, Yasuda Y, Henger A, Brunner B, et al. (2006) Modular activation of nuclear factor-kappaB transcriptional programs in human diabetic nephropathy. Diabetes 55: 2993–3003.
66. Cohen CD, Klingenhoff A, Boucherot A, Nitsche A, Henger A, et al. (2006) Comparative promoter analysis allows de novo identification of specialized cell junction-associated proteins. Proc Natl Acad Sci U S A 103: 5682–5687.
67. Irizarry RA, Bolstad BM, Collin F, Cope LM, Hobbs B, et al. (2003) Summaries of Affymetrix GeneChip probe level data. Nucleic Acids Res 31: e15.
68. Dennis G, Jr., Sherman BT, Hosack DA, Yang J, Gao W, et al. (2003) DAVID: Database for Annotation, Visualization, and Integrated Discovery. Genome Biol 4: P3.
69. Huang da W, Sherman BT, Lempicki RA (2009) Systematic and integrative analysis of large gene lists using DAVID bioinformatics resources. Nat Protoc 4: 44–57.
70. Kanehisa M, Araki M, Goto S, Hattori M, Hirakawa M, et al. (2008) KEGG for linking genomes to life and the environment. Nucleic Acids Res 36: D480–484.
71. Kanehisa M, Goto S, Furumichi M, Tanabe M, Hirakawa M (2009) KEGG for representation and analysis of molecular networks involving diseases and drugs. Nucleic Acids Res.
72. Saleem MA, O'Hare MJ, Reiser J, Coward RJ, Inward CD, et al. (2002) A conditionally immortalized human podocyte cell line demonstrating nephrin and podocin expression. J Am Soc Nephrol 13: 630–638.
73. Schagger H (2006) Tricine-SDS-PAGE. Nat Protoc 1: 16–22.

CHAPTER II

Human nephrosclerosis triggers a hypoxia-related glomerulopathy

Matthias A. Neusser, Maja T. Lindenmeyer, Anton G. Moll, Stephan Segerer, Ilka Edenhofer, Kontheari Sen, Daniel P. Stiehl, Matthias Kretzler, Hermann-Josef Gröne, Detlef Schlöndorff, Clemens D. Cohen

Am J Pathol 2010, 176:594 – 607; doi: 10.2353/ajpath.2010.090268

The American Journal of Pathology, Vol. 176, No. 2, February 2010

DOI: 10.2353/ajpath.2010.090268

Cardiovascular, Pulmonary and Renal Pathology

Human Nephrosclerosis Triggers a Hypoxia-Related Glomerulopathy

Matthias A. Neusser,* Maja T. Lindenmeyer,†‡ Anton G. Moll,‡ Stephan Segerer,†§ Ilka Edenhofer,†‡ Kontheari Sen,‡ Daniel P. Stiehl,‡ Matthias Kretzler,¶ Hermann-Josef Gröne,‖ Detlef Schlöndorff,** and Clemens D. Cohen†‡

From the Clinic and Policlinic for Internal Medicine and the Division of Nephrology,† University Hospital Zurich, Zurich, Switzerland; the Institute of Physiology with Zurich Center of Integrative Human Physiology,‡ and the Institute of Anatomy,§ University of Zurich, Zurich, Switzerland; the Department of Medicine,¶ University of Michigan, Ann Arbor, Michigan; the Department of Cellular and Molecular Pathology,‖ German Cancer Research Center Heidelberg, Germany; and the Department of Medicine,** Mount Sinai School of Medicine, New York, New York*

In the kidney, hypoxia contributes to tubulointerstitial fibrosis, but little is known about its implications for glomerular damage and glomerulosclerosis. Chronic hypoxia was hypothesized to be involved in nephrosclerosis (NSC) or "hypertensive nephropathy." In the present study genome-wide expression data from microdissected glomeruli were studied to examine the role of hypoxia in glomerulosclerosis of human NSC. Functional annotation analysis revealed prominent regulation of hypoxia-associated biological processes in NSC, including angiogenesis, fibrosis, and inflammation. Glomerular expression levels of a majority of genes regulated by the hypoxia-inducible factors (HIFs) were significantly altered in NSC. Among these HIF targets, chemokine C-X-C motif receptor 4 (CXCR4) was prominently induced. Glomerular CXCR4 mRNA induction was confirmed by quantitative RT-PCR in an independent cohort with NSC but not in those with other glomerulopathies. By immunohistological analysis, CXCR4 showed enhanced positivity in podocytes in NSC biopsy specimens. This CXCR4 positivity was associated with nuclear localization of HIF1α only in podocytes of NSC, indicating transcriptional activity of HIF. As the CXCR4 ligand CXCL12/SDF-1 is constitutively expressed in podocytes, autocrine signaling may contribute to NSC. In addition, a blocking CXCR4 antibody caused significant inhibition of wound closure by podocytes in an *in vitro* scratch assay. These data support a role for CXCR4/CXCL12 in human NSC and indicate that hypoxia not only is involved in tubulointerstitial fibrosis but also contributes to glomerular damage in NSC. *(Am J Pathol 2010, 176:594–607; DOI: 10.2353/ajpath.2010.090268)*

Hypoxia is considered a pivotal factor contributing to tubular atrophy and interstitial fibrosis, which are factors for the progression of renal disease.[1] The evidence in support of this hypothesis derives mostly from experimental animal studies.[2–5] Most of these have focused on the tubulointerstitial space with little attention being paid to the glomerulus. The cellular response to hypoxia is largely mediated by heterodimeric transcription factors, the hypoxia-inducible factors (HIFs).[2] The cellular levels of the HIF1α and HIF2α subunits (HIFα) of HIF (gene symbols *HIF1A* and *HIF2A*) are controlled mainly by post-translational protein modification. Under normoxia HIFα is degraded by the von Hippel-Lindau tumor suppressor protein. This process is regulated by oxygen-dependent hydroxylation of HIFα through specific prolyl hydroxylases. Under hypoxic conditions degradation of HIFα ceases and the stabilized protein can function as a transcription factor.[2] In the renal glomerulus, a functional role of HIF1α[6–8] and HIF2α[9] has been documented in podocytes of rodents. Recently, glomerular podocyte-specific deletion of von Hippel-Lindau tumor suppressor protein was achieved in mice, resulting in podocyte-specific overactivity of HIF with induction of HIF target genes.[6,8]

Supported by the Else Kröner-Fresenius Foundation (A62/04 to C.D.C.) and the Swiss National Science Foundation (32-122439/1 to C.D.C.) and in part by the National Institutes of Health (National Institute of Diabetes and Digestive and Kidney Diseases R01-DK081420-01 to D.S.) and the Deutsche Forschungsgemeinschaft (SFB405-B10 to H.-J.G.).

M.A.N., M.T.L., and A.G.M., contributed equally to this work.

Accepted for publication September 29, 2009.

Supplemental material for this article can be found on *http://ajp.amjpathol.org*.

Address reprint requests to Clemens D. Cohen, M.D., Institute of Physiology and Division of Nephrology, University and University Hospital of Zurich, Winterthurerstr. 190 (23-J-74), 8057 Zurich, Switzerland. E-mail: clemens.cohen@access.uzh.ch.

Podocyte-specific HIF activation led to overexpression of chemokine (C-X-C motif) receptor 4 (CXCR4) in podocytes.[8] This was associated with progressive glomerular damage and crescent formation, raising the question of whether hypoxia may also play a prominent role in glomerular pathology.[8]

The aim of the present study was to investigate the potential role of hypoxia in common glomerulopathies such as nephrosclerosis (NSC). NSC constitutes the second most common cause for end-stage renal disease in the Western world, next to diabetic nephropathy.[10] NSC is also known under different synonyms such as hypertensive nephropathy or "benign" nephrosclerosis. The diagnosis of NSC is based on histological criteria including segmental hyalinosis mainly within the walls of afferent arterioles and subendothelial fibrosis of interlobular arteries, as well as focal and segmental glomerulosclerosis and glomerular collapse.[11–13] The exclusion of other known causes of renal disease, such as long-standing diabetes mellitus, autoimmune disease, or exposure to nephrotoxins is part of the diagnostic work-up.[14,15] Arterial hypertension is an important contributory factor but is not a *conditio sine qua non*.[13,14,16] Genetic susceptibility factors may modulate development and progression of glomerular sclerosis. Recently, genetic variants such as single nucleotide polymorphisms in the gene *MYH9*, which encodes nonmuscle myosin heavy chain type II isoform A, were found to be associated with nondiabetic end-stage renal disease in African Americans, probably including a considerable number with NSC.[17–19] Although the pathogenesis of NSC remains to be clearly defined, it has been hypothesized that a prominent pathomechanism in NSC may be glomerular ischemia due to luminal narrowing of the preglomerular arteriole.[20,21]

This situation prompted us to perform systematic analyses on gene expression data sets from microdissected human renal biopsy specimens from patients with NSC. We hypothesized that local hypoxia leading to transcriptional activity of HIF may play a key role in the development and progression of NSC. This activation of HIF target genes may influence, among others, three major processes involved in the progression of renal disease, ie, angiogenesis, fibrosis, and inflammation.[1] This hypothesis is supported by the reported gene expression data, as a large number of known HIF target genes, including CXCR4, are induced in glomeruli from patients with NSC. HIF1α was selected as a marker of hypoxia-associated transcriptional activation and was demonstrated in nuclei of NSC podocytes by immunohistological analysis. These data and supporting *in vitro* studies provide considerable evidence that local hypoxia contributes to the progression of glomerulosclerosis in NSC.

Materials and Methods

Renal Biopsy Specimens for mRNA Analysis

Human renal biopsy specimens were procured in an international multicenter study, the European Renal cDNA Bank-Kröner-Fresenius biopsy bank (see Acknowledgments for participating centers).[22] Biopsy specimens were obtained from patients after informed consent and with approval of local ethics committees. Affymetrix HG-U133A microarrays were hybridized with glomerular cDNA procured from 14 patients with NSC. Specific attention was paid to the clinical and histological criteria of NSC mentioned in the Introduction.[11–15] For diagnosis of NSC, light microscopic and immunofluorescence examination was performed on all samples, and electron microscopic examination was performed on all but three biopsy specimens (NSC1, NSC2, and NSC18). Tumor-free kidney specimens from patients undergoing tumor nephrectomy (TN) served as control tissues. Confirmatory real-time RT-PCR analyses were performed on microdissected glomeruli from biopsy specimens from an independent cohort of patients with NSC (n = 13), primary focal segmental glomerulosclerosis (FSGS) (n = 18), IgA nephropathy (IgAN) n = 15), and minimal change disease (MCD) (n = 12). Pretransplant kidney biopsy specimens from living renal allograft donors (LDs) (n = 6) served as controls. Clinical and histological characteristics of the patients and biopsy specimens are summarized in Table 1.

RNA Isolation, Preparation, and Microarray Experiments

After renal biopsy, the tissue was transferred to an RNase inhibitor and microdissected into glomerular and tubular specimens. Total RNA was isolated from microdissected glomeruli, reverse-transcribed, and linearly amplified according to a protocol reported previously.[23] Fragmentation, hybridization, staining, and imaging were performed according to the Affymetrix Expression Analysis Technical Manual for HG-U133A. Before microarray analysis Robust Multichip Average was applied. To exclude highly variable nonexpressed or low-expressed probe sets we defined a filter cutoff using the highest signal value obtained from a nonhuman Affymetrix control probe set multiplied by a factor of 1.2, corresponding in the current data set to a log2-based value of 6.81.[24] The expression data are made available online at http://www.nephromine.org. Subsequently we analyzed the differential expression with significance analysis of microarrays.[25] The main results were also confirmed in a probe set-independent analysis (ChipInspector, Genomatix, Munich, Germany).[26] In a further step, the probe sets of a group of selected genes above cutoff were hierarchically clustered using dChip software.[27] The Euclidean distance metric was chosen, and clusters were merged using average linkage. Gene lists derived from the literature were mapped to the default Affymetrix annotation using Human Genome Organization gene symbols.

Analysis of Biological Processes

Database for Annotation, Visualization and Integrated Discovery (DAVID, version 2007) is a web- and literature-based functional annotation tool, which allows systematic grouping of biologically related genes from user-classified gene lists, thereby highlighting the most relevant

Table 1. Clinical and Histological Characteristics of Biopsy Specimens from Patients with NSC, FSGS, IgAN, and MCD and Controls

Biopsy group	Number (method)	Sex	Age (years)	BP systolic (mmHg)	BP diastolic (mmHg)	Creatinine (mg/dl)	eGFR (ml/min)	Proteinuria (g/day)
Nephrosclerosis								
NSC	NSC1 (A)	M	47	145	90	2.58	29	2.30
NSC	NSC2 (A)	M	49	146	95	2.66	27	NA
NSC	NSC4 (A)	M	49	120	80	1.60	49	1.80
NSC	NSC5 (A)	M	57	NA	NA	2.40	30	0.10
NSC	NSC6 (A)	M	44	140	80	2.00	39	0.90
NSC	NSC7 (A)	M	63	120	80	2.00	36	0.20
NSC	NSC8 (A)	M	64	125	77	2.10	34	4.90
NSC	NSC11 (A)	M	77	NA	NA	7.46	8	NA
NSC	NSC12 (A)	F	55	150	90	0.74	87	0.20
NSC	NSC13 (A)	F	76	150	60	2.20	23	0.50
NSC	NSC14 (A)	M	47	175	105	3.60	19	3.39
NSC	NSC15 (A)	M	47	160	80	1.10	76	NA
NSC	NSC16 (A)	M	55	160	105	1.53	50	NA
NSC	NSC18 (A)	F	78	125	85	0.73	82	NA
Mean ± SD			58 ± 12			2.3 ± 1.7	42 ± 24	1.6 ± 1.7
Controls								
TN	TN1b (A)	F	59	NA	NA	1	60	no
TN	TN2b (A)	NA	NA	NA	NA	NA	NA	NA
TN	TN3b (A)	F	71	NA	NA	1	58	no
TN	TN4b (A)	NA	NA	NA	NA	NA	NA	NA
Mean ± SD			65 ± 9			1.0 ± 0	59 ± 1	no
Nephrosclerosis								
NSC	NSC1 (P)	M	40	120	80	1.00	88	1.50
NSC	NSC2 (P)	M	61	120	80	2.50	28	0.20
NSC	NSC3 (P)	M	43	150	100	2.20	35	NA
NSC	NSC4 (P)	F	47	150	90	1.50	40	3.30
NSC	NSC5 (P)	M	51	140	80	2.50	29	0.50
NSC	NSC6 (P)	NA	NA	NA	NA	5.00	NA	8.20
NSC	NSC7 (P)	NA	NA	NA	NA	1.10	NA	0.40
NSC	NSC8 (P)	NA	NA	170	80	1.40	NA	NA
NSC	NSC9 (P)	M	75	160	80	12.90	4	NA
NSC	NSC10 (P)	M	56	190	105	1.10	74	NA
NSC	NSC11 (P)	M	52	90	40	3.80	18	0.00
NSC	NSC12 (P)	F	52	NA	NA	0.80	80	NA
NSC	NSC13 (P)	M	59	133	79	4.60	14	0.00
Mean ± SD			54 ± 10			3.1 ± 3.3	41 ± 29	1.8 ± 2.8
Focal segmental glomerulosclerosis								
FSGS	FSGS1 (P)	M	22	120	80	0.80	128	3.90
FSGS	FSGS2 (P)	F	55	NA	NA	0.80	79	8.40
FSGS	FSGS3 (P)	F	21	130	70	0.70	112	0.60
FSGS	FSGS4 (P)	M	32	125	70	0.80	119	5.50
FSGS	FSGS5 (P)	F	39	160	105	2.70	21	2.50
FSGS	FSGS6 (P)	M	37	145	95	2.00	40	8.80
FSGS	FSGS7 (P)	M	44	140	100	1.38	59	1.30
FSGS	FSGS8 (P)	F	63	160	85	1.30	44	3.99
FSGS	FSGS9 (P)	F	51	120	80	0.79	82	2.00
FSGS	FSGS10 (P)	F	55	130	80	0.60	110	1.90
FSGS	FSGS11 (P)	M	26	130	80	0.96	101	1.65
FSGS	FSGS12 (P)	F	32	120	75	0.69	105	0.66
FSGS	FSGS13 (P)	M	40	170	100	0.90	99	4.50
FSGS	FSGS14 (P)	M	53	120	80	1.20	67	7.00
FSGS	FSGS15 (P)	F	66	NA	NA	1.30	44	3.00
FSGS	FSGS16 (P)	F	31	160	93	1.00	69	6.00
FSGS	FSGS17 (P)	F	67	115	57	0.77	79	13.00
FSGS	FSGS18 (P)	M	23	110	81	0.97	102	3.00
Mean ± SD			42 ± 15			1.1 ± 0.5	81 ± 31	4.3 ± 3.3
Minimal change disease								
MCD	MCD1 (P)	M	25	100	60	0.60	174	0.10
MCD	MCD2 (P)	M	20	NA	NA	1.60	59	2.00
MCD	MCD3 (P)	F	54	130	70	2.40	22	4.90
MCD	MCD4 (P)	M	46	137	82	1.38	59	NA
MCD	MCD5 (P)	F	52	118	69	0.60	112	6.50
MCD	MCD6 (P)	M	36	125	75	0.80	116	13.50
MCD	MCD7 (P)	F	19	NA	NA	0.68	118	NA

(*table continues*)

Table 1. *Continued*

Biopsy group	Number (method)	Sex	Age (years)	BP systolic (mmHg)	BP diastolic (mmHg)	Creatinine (mg/dl)	eGFR (ml/min)	Proteinuria (g/day)
MCD	MCD8 (P)	F	45	NA	NA	0.54	130	14.80
MCD	MCD9 (P)	F	32	125	85	0.70	103	3.00
MCD	MCD10 (P)	M	16	135	100	1.20	84	5.40
MCD	MCD11 (P)	F	20	110	70	0.50	167	6.00
MCD	MCD12 (P)	M	32	150	90	1.30	68	11.00
Mean ± SD			33 ± 14			1.0 ± 0.6	101 ± 45	6.7 ± 4.9
IgA nephropathy								
IgAN	IgAN1 (P)	M	35	130	80	1.40	61	0.30
IgAN	IgAN2 (P)	F	35	120	70	0.72	98	0.28
IgAN	IgAN3 (P)	F	22	120	70	0.90	83	0.70
IgAN	IgAN4 (P)	F	24	130	70	0.60	131	0.70
IgAN	IgAN5 (P)	M	51	120	75	0.80	108	NA
IgAN	IgAN6 (P)	M	35	NA	NA	1.31	66	NA
IgAN	IgAN7 (P)	M	31	150	100	1.10	83	3.00
IgAN	IgAN8 (P)	M	15	120	60	0.90	117	0.80
IgAN	IgAN9 (P)	F	33	120	80	1.50	43	0.49
IgAN	IgAN10 (P)	M	39	NA	NA	1.47	57	1.00
IgAN	IgAN11 (P)	M	19	140	70	0.79	134	4.00
IgAN	IgAN12 (P)	M	37	130	90	1.00	89	1.30
IgAN	IgAN13 (P)	F	50	160	90	0.90	70	1.92
IgAN	IgAN14 (P)	M	36	150	80	4.50	16	3.80
IgAN	IgAN15 (P)	M	49	160	90	0.90	95	10.00
Mean ± SD			34 ± 11			1.3 ± 0.9	83 ± 33	2.2 ± 2.7
Controls								
LD	LD1 (P)	F	35	NA	NA	<1.0	>60	no
LD	LD2 (P)	F	56	NA	NA	<1.0	>60	no
LD	LD3 (P)	M	41	NA	NA	<1.0	>60	no
LD	LD4 (P)	M	62	NA	NA	<1.0	>60	no
LD	LD5 (P)	M	27	NA	NA	<1.0	>60	no
LD	LD6 (P)	NA	NA	NA	NA	<1.0	>60	no
Mean ± SD			44 ± 15			<1.0	>60	no

As controls we used tumor-free tissue from tumor nephrectomy specimens (TN) for the microarray experiments and biopsy specimens from living donor kidneys (LD) for the confirmational real-time RT-PCR experiments. Patients were analyzed by oligonucleotide array (A)-based gene expression profiling [NSC (A): $n = 14$, controls (TN): $n = 4$] and real-time RT-PCR (P) [NSC (P): $n = 13$, FSGS (P): $n = 18$, IgAN (P): $n = 15$, MCD (P): $n = 12$, controls (LD): $n = 6$]. The patients' sex is given as male (M) or female (F). BP, blood pressure; eGFR, glomerular filtration rate (estimated according to the Modification of Diet in Renal Disease formula); NA, not available.

Gene Ontology (GO) terms associated with a given gene list. The significance determination of GO terms in DAVID is based on the Expression Analysis Systematic Explorer, a variant of one-tailed Fisher exact probability.[28] For DAVID analyses, a P value of 0.05 was used as standard cutoff level.

Immunohistological Analysis

HIF1α staining was performed on biopsy specimens from an independent group of 9 patients with NSC and 5 controls (healthy tissue from TN), and CXCR4 staining was performed on biopsy specimens from an independent group of 15 patients with NSC and 5 controls (TN). Costaining was done on biopsy samples from 2 patients with NSC (3 and 11 glomeruli), 2 controls (TN, >20 glomeruli), and 4 patients with FSGS (10 to 34 glomeruli), one of these with a documented *NPHS2* mutation. The following antibodies were used: a rabbit polyclonal antibody to CXCR4 (ab2074, Abcam, Eching, Germany) and monoclonal IgG2b against HIF1α (NB 100-105, Novus Biologicals, Littleton, CO). For costaining, HIF was documented with the tyramide signal amplification system (TSATM Fluorescence System, NEN Life Science Products, Boston, MA). CXCR4 was then visualized by indirect immunofluorescence with an anti-rabbit antibody (AF488, 1:200, Invitrogen, Paisley, UK). Nuclei were stained by the DNA interactive agent DRAQ5TM (Alexis-Axxora, Lörrach, Germany). The staining shown is from a representative sample. The findings for CXCR4 and HIF1α staining in glomerular podocytes that we report were globally present but showed focal accentuation.

For chemokine (C-X-C motif) ligand 12 (CXCL12; also called SDF-1), immunohistochemical analysis was performed as described previously.[29] The primary antibody was a mouse anti-human CXCL12 (clone 79018, R&D Systems, Minneapolis, MN). Immunohistochemical analysis was performed on normal areas collected from TNs ($n = 3$) and biopsy specimens from patients with NSC ($n = 3$). Replacement of the primary antibody by diluent served as a negative control.

Cell Culture Experiments with Hypoxia

We used established cell lines of immortalized murine (K5P5[30]) and human podocytes (A [h63][31] and B [AB81][32]). K5P5, h63, and AB81 cells were cultured as given in the respective references. Normoxia was defined as 20% O_2 in the gas phase, and hypoxia constituted 2.0 and 0.2% O_2, respectively. For oxygen titration, cell cul-

tures were distributed into incubators (Binder, Tuttlingen, Germany) with different oxygen concentrations (2.0 and 20% O_2) or were placed in a hypoxia incubator (In Vivo$_2$ Hypoxia Workstation 400, Ruskinn Technology, Guiseley, UK, flushed with gas [0.2% O_2, 5% CO_2, and 94.8% N_2]) and simultaneously cultured for the indicated time periods. Cells were analyzed at 4 hours for HIF1α, at 24 hours for HIF2α Western blot analysis, and at 24 hours for mRNA expression analysis, respectively. Total cellular RNA was extracted using the Qiagen RNeasy kit (Qiagen, Hombrechtikon, Switzerland). The mRNA expression was analyzed by real-time RT-PCR.

Western Blot

For HIF1α detection, cultured glomerular epithelial cells[30,32] were harvested with lysis buffer (10 mmol/L Tris-HCl [pH 8.0], 0.1% Nonidet P-40, 400 mmol/L NaCl, 1 mmol/L EDTA [pH 8.0], 1 mmol/L dithiothreitol, 1 mmol/L phenylmethylsulfonyl fluoride, and Complete Protease Inhibitor Cocktail [Roche, Mannheim, Germany]). For HIF2α detection, glomerular epithelial cells[30,32] were harvested with a lysis buffer containing 8 M urea (10 mmol/L Tris-HCl [pH 6.8], 1% SDS, 5 mmol/L dithiothreitol, 10% glycerol, 8 M urea, 0.5 mmol/L phenylmethylsulfonyl fluoride, and Complete Protease Inhibitor Cocktail). The protein concentrations were determined by the Bradford method (Bio-Rad Laboratories, Hercules, CA). Extracted proteins were boiled in loading buffer for 5 minutes, resolved by 10% SDS-polyacrylamide gel electrophoreses under reducing conditions, and transferred to an Immobilon-P membrane (Millipore, Eschborn, Germany). Equal loading and transfer efficiencies were verified by staining with 2% Ponceau S. Membranes were blocked overnight with Tris-buffered saline/5% fat-free skim milk and then incubated with a monoclonal mouse antibody raised against human HIF1α (BD Transduction Laboratories, Lexington, KY) diluted 1:1000 overnight at 4°C and rinsed with Tris-buffered saline containing 0.1% Tween 20. Immunoblotting for HIF1α in murine podocytes was performed using polyclonal rabbit anti-HIF1α antibody (1:200, overnight at 4°C, Novus Biologicals). HIF2α was detected using a polyclonal rabbit anti-HIF2α antibody (1:200, overnight at 4°C, Novus Biologicals).

For detection, a horseradish peroxidase-linked anti-mouse IgG antibody (1:2000, 1 hour at room temperature, DAKO, Glostrup, Denmark) and enhanced chemiluminescence substrate (PerkinElmer Life and Analytical Sciences, Waltham, MA) were used. Membranes were also probed with anti-β-actin antibody (A 5316, 1:5000, Sigma-Aldrich, Munich, Germany) as an internal loading control.

In Vitro *"Wound Healing" Assay*

In confluent cell monolayers on collagen-coated six-well plates, a scratch ("wound") was created with a sterile pipette tip. Cells were then incubated for 22 hours with either blocking rabbit anti-rat CXCR4 antibody (5 μg/ml, Torrey Pines Biolabs, East Orange, NJ), which has been shown to be effective in mice,[8] or rabbit immunoglobulin IgG (5 μg/ml, R&D Systems). At 0 hours and after 22 hours, the width of the scratch was measured at the same 10 to 12 points per well in a blinded fashion (n = 12 for each condition). The extent of wound healing is given as a percentage of the original width (1 − mean of measured distances at 22 hours/mean of measured distances at 0 hours).

Quantitative Real-Time RT-PCR

For studies using biopsy samples, reverse transcription and real-time RT-PCR were performed as reported earlier.[33] Predeveloped TaqMan reagents were used for human fibronectin 1 (FN1, NM_002026), human lysyl oxidase-like 2 (LOXL2, NM_002318.2), and the housekeeper genes 18S rRNA, GAPDH, and β-actin (Applied Biosystems, Foster City, CA). The following oligonucleotide primers (300 nmol/L) and probe (100 nmol/L) were used for human CXCR4 (NM_003467.2), sense primer 5′-GGCCGACCTCCTCTTTGTC-3′, antisense primer 5′-CAAAGTACCAGTTTGCCACGG-3′, and fluorescence labeled probe (FAM) 5′-ACGCTTCCCTTCTGGGCAGTTGATG-3′; and for CXCL12 (NM_199168), sense primer 5′-ACCGCGCTCTGCCTCA-3′, antisense primer 5′-CATGGCTTTCGAAGAATCGG-3′, and fluorescence labeled probe (FAM) 5′-TCAGCCTGAGCTACAGATGCCCATGC-3′. The expression of candidate genes was normalized to three reference genes, 18S rRNA, hGAPDH, and β-actin, giving similar results. Data shown are normalized to 18S rRNA, and target gene expression in the control cohort is set as 1. The mRNA expression was analyzed by standard curve quantification.

For *in vitro* studies, reverse transcription was performed as described above. Predeveloped TaqMan reagents were used for human CXCR4 (NM_003467.2) and for the reference gene 18S rRNA (Applied Biosystems). For human and murine vascular endothelial growth factor A (VEGFA and Vegfa, respectively) and murine Cxcr4, the following oligonucleotide primers (300 nmol/L) and probes (100 nmol/L) were used: for human VEGFA (NM_003376), sense primer 5′-GCCTTGCTGCTCTACCTCCAC-3′, antisense primer 5′-ATGATTCTGCCCTCCTCCTTCT-3′, and fluorescence labeled probe (FAM) 5′-AAGTGGTCCCAGGCTGCACCCAT-3′; for murine Vegfa (NM_001025250.3), sense primer 5′-GCTGTGCAGGCTGCTGTAAC-3′, antisense primer 5′-TGATGTTGCTCTCTGACGTGG-3′, and fluorescence labeled probe (FAM) 5′-ATGAAGCCCTGGAGTGCGTGCC-3′; and for murine Cxcr4 (NM_009911.3), sense primer 5′-TGGAACCGATCAGTGTGAGTATATA-3′, antisense primer 5′-GGTGGGCAGGAAGATCCTATT-3′, and fluorescence labeled probe (FAM) 5′-CTGCTTCCGGGATGAAAACGTCCATT-3′. The expression of candidate genes was normalized to 18S rRNA and analyzed by the $\Delta\Delta$Ct method.

Statistics

Experimental data are given as mean ± SD. Statistical analysis was performed using the Mann-Whitney U test and the Welch and Games-Howell test (SPSS 14.0, SPSS,

Chicago, IL). *P* and *q* values <0.05 were considered to indicate statistically significant differences.

Results

Glomerular Expression of Hypoxia-Regulated Genes Is Altered in NSC

Gene expression profiling was performed on isolated glomeruli to study alterations in gene transcript expression in NSC. In choosing the cohort to be examined, specific attention was paid to the histological criteria of NSC and clinical features.[11–15] The clinical characteristics of the patients are provided in Table 1. Glomerular gene expression profiles yielded 14,762 probe sets with expression intensities above cutoff (see *Materials and Methods*). We used unsupervised clustering to visualize the probe sets in a dendrogram. Cluster dendrograms sort samples with the most similar gene expression profiles together with the shortest branches. Clustering all 14,762 probe sets above cutoff resulted in clear segregation of NSC from TN (Supplemental Figure S1, see *http://ajp.amjpathol.org*). The comparison between controls and NSC resulted in 7,381 significantly altered probe sets (Supplemental Table S1, see *http://ajp.amjpathol.org*). These corresponded to roughly 5,711 genes, taking the limitations of the default Affymetrix probe set annotation into account.[34]

To test whether hypoxia-related biological processes previously reported to contribute to deterioration of renal function may be involved in NSC, the data were grouped according to their GO classification.[1] The glomerular gene expression data demonstrated significant overrepresentation of GO terms of two biological processes potentially involved in hypoxia-related kidney damage: angiogenesis (eg, the GO terms "angiogenesis" [GO:0001525] and "vasculature development" [GO:0001944]) (Supplemental Table S2, see *http://ajp.amjpathol.org*) and inflammation (eg, GO terms "immune response" [GO:0006955] and "inflammatory response" [GO:0006954]) (Supplemental Table S3, see *http://ajp.amjpathol.org*). A third process, renal fibrosis, has recently been discussed as being controlled by HIF.[1,3] Because a corresponding GO term does not exist, we used a literature-based list of genes potentially involved in renal fibrosis.[35–38] Of 84 fibrosis-related genes derived from the literature, 83 were represented on the HG-U133A array. Of these, 73 genes showed mRNA expression above the cutoff in the expression array analysis of the glomeruli from NSC biopsy specimens. Of these, 42 (58%) were found to be significantly altered in NSC compared with controls (Supplemental Table S4, see *http://ajp.amjpathol.org*). In summary, GO analyses of the microarray data from glomeruli with NSC support the idea of hypoxia-associated processes being involved in the development of renal disease.

These initial results prompted us to further evaluate the potential role of hypoxia-regulated gene expression in glomeruli from NSC biopsy specimens. A literature-based list of previously reported HIF target genes was generated.[39,40] From a total of 554 HIF target genes, 542 were represented on the HG-U133A array and 476 showed mRNA expression above cutoff. Expression of 290 (61%) of these genes was significantly altered in glomeruli with NSC compared with controls (Supplemental Table S5, see *http://ajp.amjpathol.org*). This number is higher than that observed in patients with FSGS, in whom expression of only 23% of the HIF target genes was found to be changed ($n = 13$, unpublished data). Because HIFα subunits are regulated mainly at the post-translational level, it was not surprising that HIF1A mRNA itself was not significantly altered in glomeruli with NSC (HIF1A, probe set 200989_at, fold change 0.96, NS). HIF2A mRNA was significantly increased (EPAS1, probe set 200879_s_at, fold change 1.25, $q = 0.05$ and 200878_at, fold change 1.57, $q < 0.01$). To further evaluate our hypothesis that hypoxia may play a significant pathophysiological role in NSC, we examined whether expression of HIF-regulated genes might segregate glomerular gene expression in NSC biopsy specimens from that in controls. We used unsupervised clustering to visualize the 476 HIF target genes above cutoff in a dendrogram. This cluster dendrogram of HIF target genes segregated NSC from controls with two distinct branches being identified: one corresponding to the NSC group and the other one to the TN control group (Figure 1). No association of HIF target gene expression with clinical parameters (renal function or proteinuria) or antihypertensive treatment with or without blockade of the renin angiotensin system was observed nor was there a correlation with the histological degree of glomerular scarring on this limited number of patients. Of 25 HIF targets with relevance to renal function, reported by Haase et al,[5] 20 genes showed mRNA expression above cutoff. Expression of 16 (80%) of these was significantly changed in glomeruli with NSC compared with controls (Table 2). Among the HIF targets, which were significantly more abundant in glomeruli with NSC (Table 2 and Supplemental Table S5, see *http://ajp.amjpathol.org*), we found genes representing prominent hypoxia-modulated biological processes such as angiogenesis, fibrosis, and inflammation. VEGFA and its receptor FMS-like tyrosine kinase 1 (FLT1), both with significantly increased transcript levels in glomeruli with NSC, are examples of genes involved in the first process. For early as well as late stages of fibrosis the following genes are prominent indicators: TIMP1 (tissue inhibitor of metalloproteinase 1), SERPINE1 (serpin peptidase inhibitor, clade E, member 1, also called plasminogen activator inhibitor type 1),[4] LOX (lysyl oxidase), and LOXL2 (lysyl oxidase-like 2).[3] Fibronectin (FN1) mRNA, also shown to be up-regulated under hypoxic conditions,[41,42] was strongly increased in glomeruli with NSC. Furthermore, mRNA expression for several collagen α-chains was increased in NSC glomeruli, including the reportedly hypoxia-inducible genes COL1A2, COL4A1, and COL4A2.[4,39] Interestingly, only the embryonic (COL4A1 and COL4A2) and not the mature isoforms of collagen type 4 (COL4A3, COL4A4, and COL4A5) were found to be significantly altered in NSC glomeruli (Supplemental Table S4, see *http://ajp.amjpathol.org*).[43] Finally, among the above processes inflammation emerged as a prominent one in NSC (Supplemental Table S3, see

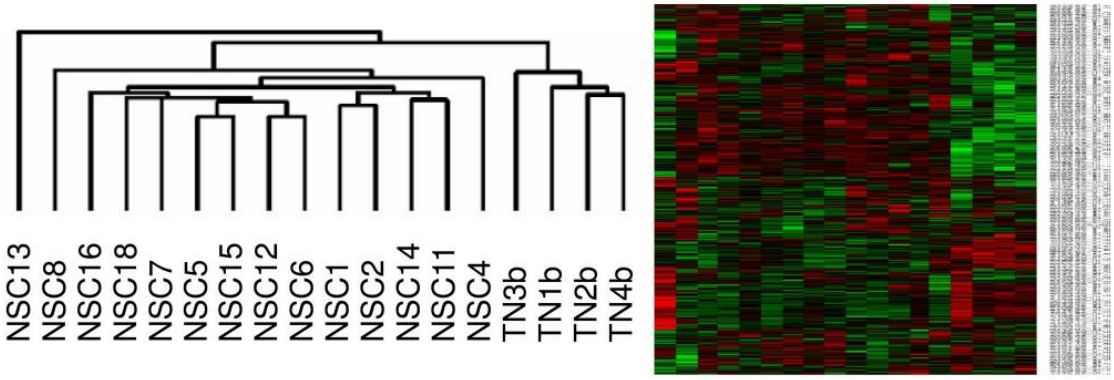

Figure 1. Cluster of HIF target genes in NSC. Unbiased and unsupervised clustering was used to visualize the expressed HIF target genes in a dendrogram. Cluster dendrograms group the patients with the most similar gene expression profiles. The length of the branches represents the dissimilarity. Probe set abundance is displayed on a red-green color scale, with red indicating expression above and green below the mean. This cluster dendrogram uses the HIF target genes to segregate NSC from the healthy controls. Two distinct branches could be identified: one corresponding to the NSC group and the other one to the TN group.

http://ajp.amjpathol.org). In line with this finding, the chemokine receptor CXCR4 was one of the most strongly increased HIF target genes in NSC glomeruli.

Glomerular Induction of CXCR4 mRNA Is Found in NSC, but Not in Other Common Glomerulopathies

From the above-mentioned significantly altered HIF target genes we selected LOXL2, FN1, and CXCR4 for further confirmatory analysis. The glomerular mRNA expression was determined by real-time RT-PCR in an independent cohort of patients with NSC and patients with other glomerulopathies such as FSGS, IgAN, and MCD. Pretransplant allograft biopsy specimens from LDs served as healthy controls (Table 1). A significant induction of LOXL2 mRNA (2.6 ± 1.7-fold, $P < 0.01$) and FN1 mRNA (5.5 ± 3.7-fold, $P < 0.01$) was found in glomeruli with NSC compared with controls. LOXL2 and FN1 mRNA were not found to be consistently induced in glomeruli from patients with FSGS, IgAN, and MCD (LOXL2: FSGS 1.1 ± 0.4, NS, IgAN 1.4 ± 0.9, NS, and MCD 0.9 ± 1.0, NS, compared with controls; FN1: FSGS 1.2 ± 1.6, NS, IgAN 0.9 ± 1.1, MS, and MCD 0.3 ± 0.2, NS, compared with controls) (Figure 2, A and B). The mRNA for CXCR4, one of the most strongly altered HIF target templates in our microarray data set, was also found to be induced in glomeruli of an independent cohort of patients with NSC, but not in those with FSGS, MCD, or IgAN (NSC 2.0 ± 1.1, $P < 0.05$; FSGS 0.6 ± 0.4, NS; IgAN 0.4 ± 0.2, $P < 0.05$; and MCD 0.6 ± 0.5, NS, compared with controls) (Figure 2C). Expression of the known ligand of CXCR4, ie, CXCL12, was not found to be significantly altered in the glomerular microarray data. This result was again confirmed by real-time RT-PCR, which demonstrated only a nonsignificant trend for CXCL12 mRNA induction in NSC (NSC 3.9 ± 4.8, NS; FSGS 1.4 ± 1.5, NS; IgAN 0.9 ± 0.9, NS; and MCD 1.8 ± 1.9, NS). In summary, the real-time RT-PCR studies on independent patient cohorts supported the microarray data and confirmed the glomerular induction of LOXL2, FN1, and CXCR4 mRNA seen on the microarray as potential contributors to hypoxia-induced pathomechanisms in NSC.

HIF1α Shows Nuclear Localization in CXCR4-Positive Podocytes of NSC Biopsy Specimens

To demonstrate the glomerular cell type expressing CXCR4 in NSC, immunohistological analysis was performed on additional biopsy specimens to further study the expression of CXCR4. In NSC biopsy specimens, the CXCR4 protein could be localized to glomerular epithelial cells in all glomeruli with a prominent increase in fluorescence intensity compared with the faint staining for CXCR4 in control kidneys (Figure 3, A–C). As was expected, interstitial mononuclear cells also stained positive for CXCR4 (not shown).

To evaluate whether the CXCR4 protein expression in podocytes of NSC biopsy specimens was associated with HIF1α activation as a general marker of hypoxia-associated transcriptional activation, double staining for both molecules was performed. A faint cytoplasmic staining for HIF1α was occasionally seen in cells of control biopsy specimens. In marked contrast, a robust nuclear HIF1α staining was apparent in podocytes from NSC biopsy specimens and colocalized with staining for CXCR4 (Figure 3, A and B). Because HIF1α is translocated from the cytosol to the nucleus on activation, the localization may indicate transcriptional activity of HIF in these cells.[5] Occasionally tubular epithelial cells showed also a nuclear staining pattern for HIF1α. These cells demonstrated no concomitant CXCR4 staining. In biopsy specimens from patients with the main diagnosis of FSGS, glomerular epithelial cells stained also positive for CXCR4 but with a restrained and heterogeneous nuclear HIF1α positivity. This result is in line with the microarray data reported above, which indicate a more pronounced hypoxia-associated gene regulation in NSC glomeruli than in FSGS glomeruli.

Table 2. Regulation of HIF Target Genes with Relevance to Renal Function

Probe set	Gene symbol (HUGO)	Gene name (from Affymetrix HG-U133A-20080318)	Fold change	*q* value (%)
200966_x_at	*ALDOA*	Aldolase A, fructose-bisphosphate	1.12	4.87
214687_x_at	*ALDOA*	Aldolase A, fructose-bisphosphate	1.13	2.27
201849_at	*BNIP3*	BCL2/adenovirus E1B 19kDa interacting protein 3	0.74	0.73
201848_s_at	*BNIP3*	BCL2/adenovirus E1B 19kDa interacting protein 3	0.80	4.87
205199_at	*CA9*	Carbonic anhydrase IX	0.83	0.88
211919_s_at	*CXCR4*	Chemokine (C-X-C motif) receptor 4	2.37	0.08
209201_x_at	*CXCR4*	Chemokine (C-X-C motif) receptor 4	2.41	0.03
217028_at	*CXCR4*	Chemokine (C-X-C motif) receptor 4	4.23	0.03
209101_at	*CTGF*	Connective tissue growth factor	0.88	18.58
218995_s_at	*EDN1*	Endothelin 1	0.94	22.72
201231_s_at	*ENO1*	Enolase 1, (alpha)	0.89	19.75
217294_s_at	*ENO1*	Enolase 1, (alpha)	1.21	4.87
217254_s_at	*EPO*	Erythropoietin	BC	BC
207257_at	*EPO*	Erythropoietin	BC	BC
222033_s_at	*FLT1*	Fms-related tyrosine kinase 1	1.74	0.03
210287_s_at	*FLT1*	Fms-related tyrosine kinase 1	BC	BC
204406_at	*FLT1*	Fms-related tyrosine kinase 1	BC	BC
203665_at	*HMOX1*	Heme oxygenase (decycling) 1	0.57	0.73
202934_at	*HK2*	Hexokinase 2	1.33	4.87
222305_at	*HK2*	Hexokinase 2	BC	BC
205302_at	*IGFBP1*	Insulin-like growth factor binding protein 1	BC	BC
200650_s_at	*LDHA*	Lactate dehydrogenase A	BC	BC
203510_at	*MET*	Met proto-oncogene	0.62	0.73
211599_x_at	*MET*	Met proto-oncogene	0.84	1.58
213807_x_at	*MET*	Met proto-oncogene	0.84	0.73
213816_s_at	*MET*	Met proto-oncogene	BC	BC
209957_s_at	*NPPA*	Natriuretic peptide precursor A	0.78	0.06
210037_s_at	*NOS2A*	Nitric oxide synthase 2A	BC	BC
205581_s_at	*NOS3*	Nitric oxide synthase 3	BC	BC
200738_s_at	*PGK1*	Phosphoglycerate kinase 1	1.03	19.75
200737_at	*PGK1*	Phosphoglycerate kinase 1	1.18	4.87
217383_at	*PGK1*	Phosphoglycerate kinase 1	1.24	4.87
217356_s_at	*PGK1*	Phosphoglycerate kinase 1	BC	BC
200725_x_at	*RPL10*	Ribosomal protein L10	1.05	10.75
200724_at	*RPL10*	Ribosomal protein L10	1.09	10.75
221989_at	*RPL10*	Ribosomal protein L10	1.33	1.58
217680_x_at	*RPL10*	Ribosomal protein L10	BC	BC
202628_s_at	*SERPINE1*	Serpin peptidase inhibitor	1.20	8.92
202627_s_at	*SERPINE1*	Serpin peptidase inhibitor, clade E	1.26	1.14
201250_s_at	*SLC2A1*	Solute carrier family 2, member 1	0.76	0.07
201249_at	*SLC2A1*	Solute carrier family 2, member 1	BC	BC
201666_at	*TIMP1*	TIMP metallopeptidase inhibitor 1	1.65	0.10
214064_at	*TF*	Transferrin	BC	BC
214063_s_at	*TF*	Transferrin	BC	BC
203400_s_at	*TF*	Transferrin	BC	BC
220109_at	*TF*	Transferrin	BC	BC
208691_at	*TFRC*	Transferrin receptor /// transferrin receptor	0.81	10.75
207332_s_at	*TFRC*	Transferrin receptor /// transferrin receptor	0.85	12.73
210512_s_at	*VEGFA*	Vascular endothelial growth factor	1.06	17.38
212171_x_at	*VEGFA*	Vascular endothelial growth factor	1.11	14.49
211527_x_at	*VEGFA*	Vascular endothelial growth factor	1.31	4.87
210513_s_at	*VEGFA*	Vascular endothelial growth factor	1.38	0.06

Twenty-five of 25 selected HIF targets with relevance to renal function derived from the literature were represented on the HG-U133A array. Twenty of these genes showed mRNA expression above cutoff on the arrays. Of these 20 expressed mRNAs, 16 (80%) were significantly regulated in glomeruli from NSC biopsy samples compared with controls (TN).[5] The fold change indicates the expression of each gene in nephrosclerosis (NSC) glomeruli compared with controls, ie, a fold change of 1.75 refers to an induction of 75% in NSC. BC, below cutoff, see *Materials and Methods* for further detail.

CXCL12, the corresponding ligand of CXCR4, was also found to be expressed in podocytes of NSC biopsy specimens as well as in control tissue (Figure 4). In addition, CXCL12 expression was seen on some tubular epithelial cells and on endothelial cells of larger veins and arteries. The constitutive expression was consistent with the mRNA expression data, indicating no CXCL12 mRNA induction in NSC.

Hypoxia Induces HIFα Protein and CXCR4 mRNA in Podocytes in Vitro

CXCR4 and nuclear HIF1α colocalized to podocytes in double immunofluorescence staining. We therefore studied podocytes *in vitro* to define whether this might represent a functional association. We exposed podocyte cell lines[30–32] to hypoxic culture conditions. By Western blot,

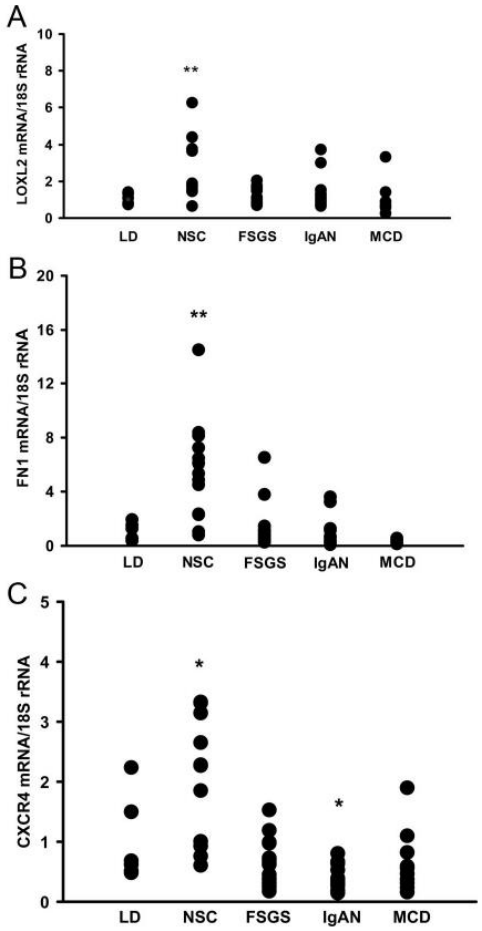

Figure 2. Confirmation of LOXL2, FN1, and CXCR4 mRNA expression in glomeruli with NSC and controls. **A:** LOXL2 mRNA measured by RT-PCR is induced in glomeruli from NSC biopsy specimens. LOXL2 mRNA showed increased expression by quantitative RT-PCR in glomeruli from an independent group of NSC biopsy specimens ($n = 13$). Values were normalized to pretransplant LD control biopsy specimens ($n = 6$) and the housekeeper gene 18S rRNA. In FSGS, IgAN, and MCD, LOXL2 mRNA was not significantly different compared with that in living donor (LD) controls. $^{**}P < 0.01$ compared with controls. **B:** FN1 mRNA is overexpressed in glomeruli from NSC biopsy specimens. Same biopsy cohorts as mentioned in **A**. $^{**}P < 0.01$ compared with controls (LD). **C:** CXCR4 mRNA expression levels are higher in glomeruli from NSC biopsy specimens. Same biopsy cohorts as mentioned in **A**. $^{*}P < 0.05$ compared with controls (LD). FSGS, focal segmental glomerusclerosis; IgAN, IgA nephropathy; MCD, minimal change disease.

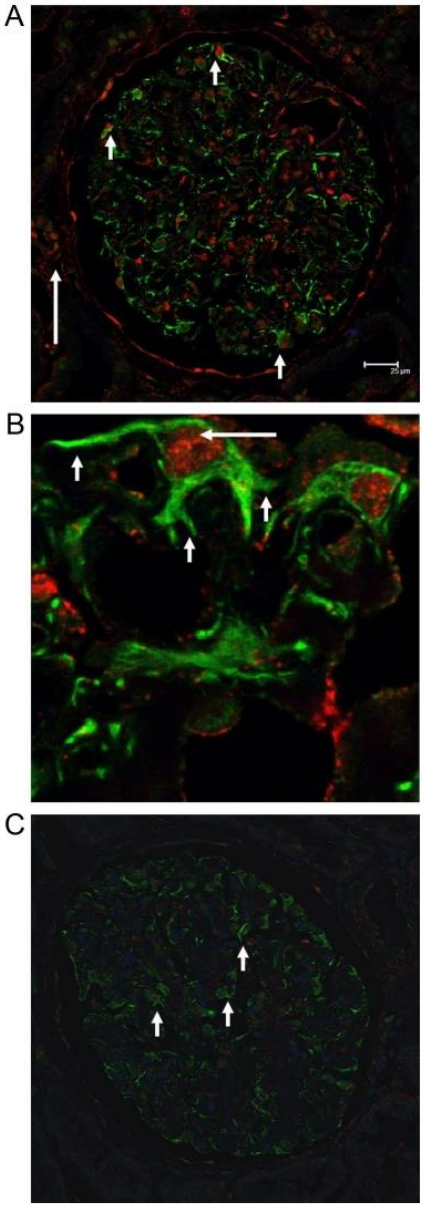

Figure 3. CXCR4 and HIF1α staining in NSC and controls. **A:** CXCR4 and HIF1α staining in glomeruli with NSC. CXCR4 (green staining) and HIF1α (red staining) showed robust expression in podocytes of NSC (**short arrows**). As expected some tubular epithelial cells stained positive for HIF1α (**long arrow**). Interstitial mononuclear cells also stained positive for CXCR4 (not shown). **B:** High magnification of CXCR4 and HIF1α staining in NSC. Higher magnification of glomerular epithelial cells with surface staining for CXCR4 (**short arrows**) and nuclear staining for HIF1α (**long arrow**). **C:** CXCR4 and HIF1α staining in glomeruli from controls. Healthy tissue from TN served as a control, with podocytes showing a faint green CXCR4 background staining (**arrows**) without any HIF1α positivity.

we were able to demonstrate higher HIF1α and HIF2α protein levels under graded hypoxic conditions compared with normoxic controls (see Figure 5, A and B,[32] for human podocytes; murine podocytes not shown). Hypoxic incubation conditions (0.2% and 2% oxygen) resulted in a significant increase in CXCR4/Cxcr4 mRNA in all podocyte cell lines tested compared with 20% oxygen concentration (Figure 6, Table 3). VEGFA/Vegfa mRNA served as a positive control for a hypoxia-induced genes and also showed an induction under hypoxic conditions (Table 3).

As CXCR4 and CXCL12 were both found to be expressed by podocytes, we set out to study a functional role of this receptor/ligand system. Because CXCR4 is known to play a role in guidance of cell migration, we applied an *in vitro* scratch assay on cultured podocytes. In line with a functional relevance of CXCR4/CXCL12 in

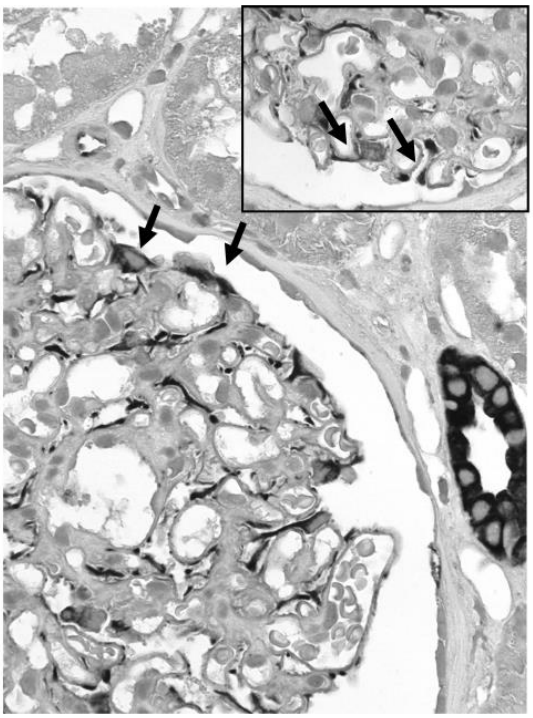

Figure 4. CXCL12 staining in glomeruli with NSC. CXCL12 was localized by immunohistochemical analysis in biopsy specimens from patients with NSC and controls. A prominent CXCL12 expression was found, in a pattern consistent with podocytes. Note the staining of cells on the outer surface of the glomerular basement membrane (**arrows**). Original magnification, ×400. **Inset:** Higher magnification of CXCL12 staining of glomeruli with NSC confirmed expression by podocytes (**arrows**). Original magnification, ×1000.

podocyte biology, a blocking CXCR4 antibody significantly impaired the extent of wound closure in these cells compared with control IgG (23 ± 6% versus 41 ± 13%, $P < 0.01$, $n = 12$ each) (Figure 7).

Discussion

The growing evidence for hypoxia as a modulator of progression of renal disease prompted us to examine its

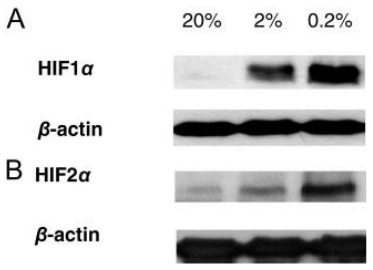

Figure 5. Hypoxia induces HIF1α and HIF2α protein in cultured podocytes. **A:** By Western blot a dose-dependent induction of HIF1α under graded hypoxic conditions (0.2 and 2% O_2) was demonstrated in human podocytes[32] compared with normoxic time controls (20% O_2, at 4 hours). **B:** In addition, HIF2α was found to be stabilized in human podocytes at 0.2 and 2% O_2 compared with 20% O_2 (at 24 hours). β-Actin was used as loading control.

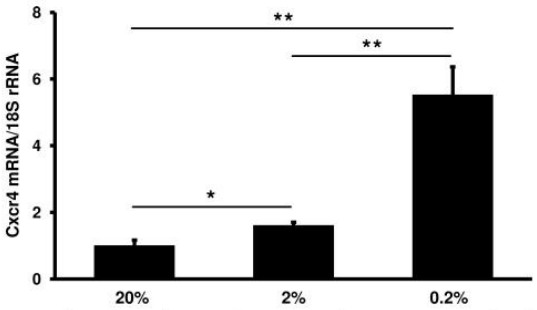

Figure 6. Hypoxia induces Cxcr4 mRNA in podocytes *in vitro*. In cultured murine podocytes, expression of Cxcr4 mRNA was increased after 24 hours at 0.2% O_2 compared with podocytes incubated at 2% O_2 after 24 hours and normoxic (20% O_2) controls ($n = 4$ each). $^*P < 0.05$, $^{**}P < 0.01$, significant differences compared with 20% O_2. $^{**}P < 0.01$, significant difference comparing 0.2 with 2% O_2. For expression data of CXCR4 and VEGFA in human podocyte cell lines exposed to hypoxia, see Table 3.

potential role in human NSC.[1] NSC represents an entity with a poorly understood pathogenesis, even though it is reported to be the second most common cause for end-stage renal disease in the Western world.[10] We found hypoxia-related genes to be clearly induced in glomeruli from patients with NSC. CXCR4, a known target of HIF, was significantly induced in NSC and could be localized to podocytes together with positive nuclear staining for HIF1α as a general indicator for hypoxia-associated transcriptional activity.

The hypothesis-driven analysis of the gene expression data was focused on genes known to be regulated by HIF.[5,39,40] Consistent with the hypothesis that hypoxia is an important factor in NSC, the majority of known HIF target genes were significantly altered in glomeruli from NSC biopsy specimens and segregated them from controls in the unsupervised cluster analysis. Prominent biological processes modulated by hypoxia are angiogenesis, fibrosis, and inflammation. In angiogenesis, VEGFA and its receptor FLT1, both significantly increased in NSC, play a central role (Table 2). VEGFA is an important growth, survival, and repair factor for glomerular capillaries. The induction of VEGFA in the glomeruli of the NSC cohort is consistent with previously reported expression of VEGF mRNA in podocytes in NSC[44] and induction of VEGFA mRNA in cultured podocytes under hypoxia (Table 3). The finding of glomerular VEGFA and FLT1 induction in NSC biopsy specimens is in contrast to the reduced expression of VEGFA recently reported in human diabetic nephropathy both in glomeruli and in the tubulointerstitial compartment, indicating a different pathophysiological mechanism for glomerulosclerosis in NSC and diabetic nephropathy.[33,45] HIF target genes involved in the accumulation of extracellular matrix and fibrosis were also found to be induced in glomeruli with NSC. This finding was confirmed by RT-PCR for FN1, for which HIF-independent regulatory mechanisms are also described,[46] and for LOXL2. LOX, and LOXL2 are documented examples of genes involved in matrix remodeling by cross-linking of collagen fibers. They were recently reported to be induced in a murine model of hypoxia-induced tubulointerstitial fibrosis.[3] Tubulointerstitial

Table 3. Cxcr4/CXCR4 and Vegfa/VEGFA mRNA Expression under Hypoxic Conditions

	20% O_2	2% O_2	0.2% O_2
VegFa/VEGFA			
Murine podocytes	1.00 ± 0.04	1.22 ± 0.08*	2.21 ± 0.41*‡
Human podocytes A	1.00 ± 0.36	3.35 ± 1.70 (NS)	11.97 ± 1.35‡§
Human podocytes B	1.00 ± 0.11	1.36 ± 0.31*	2.23 ± 0.67†‡
Cxcr4/CXCR4			
Murine podocytes	1.00 ± 0.17	1.60 ± 0.10*	5.52 ± 0.85‡§
Human podocytes A	1.00 ± 0.17	9.98 ± 3.29*	19.16 ± 3.56†‡
Human podocytes B	1.00 ± 0.30	1.29 ± 0.35 (NS)	4.41 ± 1.67‡§

Expression of Cxcr4/CXCR4 and Vegfa/VEGFA mRNA in cultured murine (K5P5) and human podocytes (podocytes A [h63] and podocytes B [AB81]) after incubation for 24 hours at 0.2 and 2% O_2 compared with 20% O_2 (n = 4 each for K5P5 and h63 and n = 8 for AB81).
*$P < 0.05$, significant difference compared with 20% O_2.
†$P < 0.05$, significant difference comparing 0.2 with 2% O_2.
‡$P < 0.01$, significant difference compared with 20% O_2.
§$P < 0.01$, significant difference comparing 0.2 with 2% O_2.

LOXL2 mRNA was also found to be induced in various progressive human renal diseases including NSC.[3] Our present data showing increased LOXL2 expression in glomeruli with NSC but not other glomerulopathies may indicate that this hypoxia-inducible enzyme is not only involved in progressive interstitial fibrosis but may also play a role in glomerulosclerosis in NSC. Besides these collagen-associated molecules increased mRNA expression for several collagen α-chains, the known HIF target genes COL1A2, COL4A1, and COL4A2, was prominent in the NSC data set.[39] We observed significant increases only for the fetal isoforms of collagen type 4, ie, COL4A1 and COL4A2, whereas the mature isoforms COL4A3, COL4A4, and COL4A5 were not found to be significantly regulated (Supplemental Table S4, see *http://ajp.amjpathol.org*). The expression of these fetal collagen isoforms resembles that seen in Alport syndrome, in which it has been related to a potentially more vulnerable glomerular basement membrane composition ultimately leading to glomerulosclerosis.[43,47] Such re-expression of fetal collagen genes in glomeruli from adult patients with NSC may be part of an increased cellular plasticity (see below).

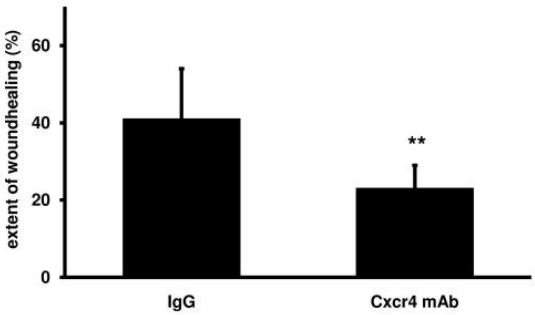

Figure 7. CXCR4 blockade reduces podocyte migration *in vitro* in a wound-healing assay. To assess potential functions of CXCR4 in podocyte migration, a wound-healing assay was performed. Confluent murine podocytes (K5P5) were treated with either blocking anti-CXCR4 antibody or immunoglobulin IgG as control. At 0 hours and after 22 hours, the width of each scratch inflicted at 0 hours was measured in a blinded fashion. The CXCR4 antibody significantly impaired the extent of wound closure compared with controls (23 ± 6 versus 41 ± 13%, **$P < 0.01$, n = 12 each). mAb, monoclonal antibody.

Inflammation is another biological process closely linked to hypoxia and to progression of renal disease.[1,48] The complex interplay between hypoxia and the immune system is nicely illustrated by the example of nuclear factor-κB, a master switch in the inflammatory response: HIF1α has been shown to activate nuclear factor-κB and nuclear factor-κB itself is a transcriptional activator of HIF1α.[48,49] Indeed, inflammatory gene signatures were significantly altered in NSC glomeruli (Supplemental Table S3, see *http://ajp.amjpathol.org*) including major histocompatibility class I and II genes, interleukins, and chemokines. Although glomerular inflammatory cell infiltrates have been observed in NSC,[50] they are not a prominent feature of glomerular NSC.[11,12] In addition, it should be noted that the expression of "inflammatory" genes cannot be directly equated with inflammatory infiltrates, as some of these genes could be regulated on intrinsic glomerular cells, for which our observations with CXCR4 on podocytes may serve as example.

Among the HIF target genes involved in inflammation, the chemokine receptor CXCR4 was found to be prominently induced in NSC glomeruli. Interestingly, induction of CXCR4 mRNA was not seen by RT-PCR in other glomerulopathies such as FSGS, IgAN, or MCD. For IgAN and membranous nephropathy, the absence of prominent CXCR4 expression in glomeruli had been reported previously.[8,51] Although FSGS is characterized by glomerular sclerosis similar to NSC, CXCR4 mRNA was not consistently induced in glomeruli from biopsy specimens of patients with primary FSGS. Although immunohistological analysis also revealed CXCR4 positivity of podocytes in FSGS biopsy specimens, the nuclear HIF1α staining in these biopsy specimens seemed restrained and heterogeneous. In this context, it should be noted that CXCR4 transcriptional regulation also includes HIF- and hypoxia-independent mechanisms.[52–54] In FSGS, the primary pathology may be of direct glomerular origin whereas narrowing of the afferent blood vessels with consecutive glomerular hypoxia may be a central mechanism in NSC. Nuclear HIF1α in podocytes of NSC biopsy specimens can be seen as a biological indicator for hypoxia-associated transcriptional processes. Because nuclear HIF1α was associated with CXCR4 expression in podocytes of NSC biopsy specimens, we went on to study CXCR4

expression in podocytes *in vitro*. In cultured human and murine podocytes, we found a low but constitutive expression of CXCR4/Cxcr4, as was also reported by Huber et al.[51] Hypoxia *in vitro* stabilized HIF1α and HIF2α protein and induced CXCR4/Cxcr4 mRNA expression in podocytes. In our experiments we used HIF1α as a global biological marker of hypoxia. However, HIF2α has been shown to be of specific functional relevance in podocytes.[9] Although providing clear evidence for an activation of hypoxia-associated transcriptional programs in podocytes, our descriptive data do not elucidate which HIFα subunit or mechanism is mainly regulating CXCR4 in podocytes. However, induction of CXCR4 by hypoxia has been reported for several cell types, such as monocytes, macrophages, endothelial cells, cancer cells, and stem/progenitor cells.[52,55–57] Von Hippel-Lindau tumor suppressor protein/HIF-dependent regulation of Cxcr4 on podocytes *in vivo* was elegantly demonstrated in a study by Ding et al[8] in mice with genetically engineered deletion of von Hippel-Lindau tumor suppressor protein in podocytes, leading to glomerular epithelial cell proliferation and extracapillary crescent formation. In this model, interference with CXCR4 signaling prevented the proliferation of the epithelial cells and markedly improved the course of the experimental disease.[8]

Recently, CXCR4 expression on some glomerular parietal epithelial cells of Bowman's capsule has been reported. These parietal cells also express markers for progenitor cells as well as for podocytes.[58–60] In general, CXCR4 is expressed on stem cells and is involved in their recruitment to sites of tissue regeneration.[61–63] Potentially, such podocyte precursors of glomerular parietal epithelial cell origin may be involved in the repopulation of the glomerular tuft during podocyte injury.[58–60,64] CXCR4/CXCL12 guide cell migration in a number of systems (eg, renal morphogenesis (tubulogenesis), neuron/axon development, and tumor metastasis[65–68]). Using an *in vitro* wound healing assay to evaluate CXCR4-dependent migration, we could demonstrate that treatment of cultured podocytes with a blocking CXCR4 antibody significantly impaired *in vitro* wound healing and hence CXCR4-dependent cell migration. Potentially, these *in vitro* data indicate that *in vivo* CXCR4 is involved in the migration of podocytes during hypoxic injury such as that occurring in NSC. Supporting this observation, we found CXCL12 to be expressed in podocytes in adults, as has been recently reported in the developing murine kidney.[8,69] CXCL12 was also reported to be expressed by mesangial cells in the developing human[70] and murine glomerulus.[8] Future studies on the expression of CXCL12 and CXCR4 during glomerular development and disease should provide further insight into the respective roles and interplay of both molecules in the glomerulus.

Finally, the neo-expression of CXCR4 on podocytes in NSC could reflect a change of differentiation of these epithelial cells re-expressing developmental genes. Although considerable controversy exists in the literature, cellular plasticity has been reported for renal cells.[71] Tubular cells may change their differentiation during hypoxia,[3,72] and podocytes have also been reported to be capable of undergoing changes of differentiation *in vitro*.[73,74] We found potential markers for a change of differentiation in the microarray gene expression analysis of glomeruli from NSC, eg, down-regulation of the epithelial marker keratin 1 ($q < 0.01$) and up-regulation of the mesenchymal markers S100 calcium binding protein A4 ($q < 0.01$) and smooth muscle actin, $\alpha 2$ ($q < 0.01$) (Supplemental Table S1, see *http://ajp.amjpathol.org*). These observations could point to a role of hypoxia for potential plasticity in podocyte differentiation.

In summary, our data provide evidence for prominent hypoxia-regulated gene expression in glomeruli from human renal biopsy specimens from patients with NSC. This includes biological processes known to be involved in renal damage such as fibrosis and inflammation. Furthermore, our data indicate a reactivation of developmental processes, pointing to considerable plasticity of podocytes during hypoxic glomerular damage. Our observations expand evidence for the contribution of hypoxia from the previously documented role in interstitial fibrosis and tubular damage to that of glomerular sclerosis in NSC.

Acknowledgments

We thank Claudia Schmidt, Stefanie Gaiser, and Sylke Rohrer for excellent technical assistance. We are indebted to Anissa Boucherot, Almut Nitsche, Bodo Brunner (Sanofi-Aventis Deutschland GmbH, Frankfurt, Germany), and Anna Henger (University of Michigan).

We thank all participating centers of the European Renal cDNA Bank-Kroener-Fresenius biopsy bank and their patients for their cooperation. Active members at the time of the study were Clemens David Cohen, Holger Schmid, Michael Fischereder, Lutz Weber, Matthias Kretzler, and Detlef Schlöndorff, Munich/Zurich/Ann Arbor/New York; Jean Daniel Sraer and Pierre Ronco, Paris; Maria Pia Rastaldi and Giuseppe D'Amico, Milan; Peter Doran and Hugh Brady, Dublin; Detlev Mönks and Christoph Wanner, Würzburg; Andrew Rees, Aberdeen; Frank Strutz and Gerhard Anton Müller, Göttingen; Peter Mertens and Jürgen Floege, Aachen; Norbert Braun and Teut Risler, Tübingen; Loreto Gesualdo and Francesco Paolo Schena, Bari; Jens Gerth and Gunter Wolf, Jena; Rainer Oberbauer and Dontscho Kerjaschki, Vienna; Bernhard Banas and Bernhard Krämer, Regensburg; Moin Saleem, Bristol; Rudolf Wüthrich, Zurich; Walter Samtleben, Munich; Harm Peters and Hans-Hellmut Neumayer, Berlin; Mohamed Daha, Leiden; Katrin Ivens and Bernd Grabensee, Düsseldorf; Francisco Mampaso (deceased), Madrid; Jun Oh, Franz Schaefer, Martin Zeier, and Hermann-Joseph Gröne, Heidelberg; Peter Gross, Dresden; Giancarlo Tonolo, Sassari; Vladimir Tesar, Prague; Harald Rupprecht, Bayreuth; and Hans-Peter Marti, Bern.

References

1. Fine LG, Norman JT: Chronic hypoxia as a mechanism of progression of chronic kidney diseases: from hypothesis to novel therapeutics. Kidney Int 2008, 74:867–872

2. Haase VH: The VHL/HIF oxygen-sensing pathway and its relevance to kidney disease. Kidney Int 2006, 69:1302–1307
3. Higgins DF, Kimura K, Bernhardt WM, Shrimanker N, Akai Y, Hohenstein B, Saito Y, Johnson RS, Kretzler M, Cohen CD, Eckardt KU, Iwano M, Haase VH: Hypoxia promotes fibrogenesis in vivo via HIF-1 stimulation of epithelial-to-mesenchymal transition. J Clin Invest 2007, 117:3810–3820
4. Higgins DF, Kimura K, Iwano M, Haase VH: Hypoxia-inducible factor signaling in the development of tissue fibrosis. Cell Cycle 2008, 7:1128–1132
5. Haase VH: Hypoxia-inducible factors in the kidney. Am J Physiol Renal Physiol 2006, 291:F271–F281
6. Brukamp K, Jim B, Moeller MJ, Haase VH: Hypoxia and podocyte-specific Vhlh deletion confer risk of glomerular disease. Am J Physiol Renal Physiol 2007, 293:F1397–F1407
7. Freeburg PB, Robert B, St John PL, Abrahamson DR: Podocyte expression of hypoxia-inducible factor (HIF)-1 and HIF-2 during glomerular development. J Am Soc Nephrol 2003, 14:927–938
8. Ding M, Cui S, Li C, Jothy S, Haase V, Steer BM, Marsden PA, Pippin J, Shankland S, Rastaldi MP, Cohen CD, Kretzler M, Quaggin SE: Loss of the tumor suppressor Vhlh leads to upregulation of Cxcr4 and rapidly progressive glomerulonephritis in mice. Nat Med 2006, 12:1081–1087
9. Rosenberger C, Mandriota S, Jurgensen JS, Wiesener MS, Horstrup JH, Frei U, Ratcliffe PJ, Maxwell PH, Bachmann S, Eckardt KU: Expression of hypoxia-inducible factor-1α and -2α in hypoxic and ischemic rat kidneys. J Am Soc Nephrol 2002, 13:1721–1732
10. U.S. Renal Data System: USRDS 2008 Annual Data Report: Atlas of Chronic Kidney Disease and End-Stage Renal Disease in the United States. Bethesda, MD, National Institutes of Health, National Institute of Diabetes and Digestive and Kidney Diseases, 2008
11. Tisher CC, Brenner BM: Benign and malignant nephrosclerosis and renovascular disease. Renal Pathology, with Clinical and Functional Correlations, vol 2. Philadelphia, Lippincott, 1994, pp 1202–1203
12. Churg J, Sobin LH: Renal Disease: Benign nephrosclerosis. Classification and Atlas of Glomerular Diseases. Tokyo, Igaku-Shoin, 1982, pp 211–224
13. Marcantoni C, Fogo AB: A perspective on arterionephrosclerosis: from pathology to potential pathogenesis. J Nephrol 2007, 20:518–524
14. Fogo A, Breyer JA, Smith MC, Cleveland WH, Agodoa L, Kirk KA, Glassock R: Accuracy of the diagnosis of hypertensive nephrosclerosis in African Americans: a report from the African American Study of Kidney Disease (AASK) Trial. AASK Pilot Study Investigators. Kidney Int 1997, 51:244–252
15. Schlessinger SD, Tankersley MR, Curtis JJ: Clinical documentation of end-stage renal disease due to hypertension. Am J Kidney Dis 1994, 23:655–660
16. Marcantoni C, Ma LJ, Federspiel C, Fogo AB: Hypertensive nephrosclerosis in African Americans versus Caucasians. Kidney Int 2002, 62:172–180
17. Freedman BI, Sedor JR: Hypertension-associated kidney disease: perhaps no more. J Am Soc Nephrol 2008, 19:2047–2051
18. Kopp JB, Smith MW, Nelson GW, Johnson RC, Freedman BI, Bowden DW, Oleksyk T, McKenzie LM, Kajiyama H, Ahuja TS, Berns JS, Briggs W, Cho ME, Dart RA, Kimmel PL, Korbet SM, Michel DM, Mokrzycki MH, Schelling JR, Simon E, Trachtman H, Vlahov D, Winkler CA: MYH9 is a major-effect risk gene for focal segmental glomerulosclerosis. Nat Genet 2008, 40:1175–1184
19. Kao WH, Klag MJ, Meoni LA, Reich D, Berthier-Schaad Y, Li M, Coresh J, Patterson N, Tandon A, Powe NR, Fink NE, Sadler JH, Weir MR, Abboud HE, Adler SG, Divers J, Iyengar SK, Freedman BI, Kimmel PL, Knowler WC, Kohn OF, Kramp K, Leehey DJ, Nicholas SB, Pahl MV, Schelling JR, Sedor JR, Thornley-Brown D, Winkler CA, Smith MW, Parekh RS: MYH9 is associated with nondiabetic end-stage renal disease in African Americans. Nat Genet 2008, 40:1185–1192
20. Freedman BI, Iskandar SS, Appel RG: The link between hypertension and nephrosclerosis. Am J Kidney Dis 1995, 25:207–221
21. Wang PX, Sanders PW: Mechanism of hypertensive nephropathy in the Dahl/Rapp rat: a primary disorder of vascular smooth muscle. Am J Physiol Renal Physiol 2005, 288:F236–F242
22. Cohen CD, Frach K, Schlondorff D, Kretzler M: Quantitative gene expression analysis in renal biopsies: a novel protocol for a high-throughput multicenter application. Kidney Int 2002, 61:133–140
23. Cohen CD, Klingenhoff A, Boucherot A, Nitsche A, Henger A, Brunner B, Schmid H, Merkle M, Saleem MA, Koller KP, Werner T, Grone HJ, Nelson PJ, Kretzler M: Comparative promoter analysis allows de novo identification of specialized cell junction-associated proteins. Proc Natl Acad Sci USA 2006, 103:5682–5687
24. Schmid H, Boucherot A, Yasuda Y, Henger A, Brunner B, Eichinger F, Nitsche A, Kiss E, Bleich M, Grone HJ, Nelson PJ, Schlondorff D, Cohen CD, Kretzler M: Modular activation of nuclear factor-κB transcriptional programs in human diabetic nephropathy. Diabetes 2006, 55:2993–3003
25. Tusher VG, Tibshirani R, Chu G: Significance analysis of microarrays applied to the ionizing radiation response. Proc Natl Acad Sci USA 2001, 98:5116–5121
26. Cohen CD, Lindenmeyer MT, Eichinger F, Hahn A, Seifert M, Moll AG, Schmid H, Kiss E, Grone E, Grone HJ, Kretzler M, Werner T, Nelson PJ: Improved elucidation of biological processes linked to diabetic nephropathy by single probe-based microarray data analysis. PLoS One 2008, 3:e2937
27. Li C, Wong WH: Model-based analysis of oligonucleotide arrays: expression index computation and outlier detection. Proc Natl Acad Sci USA 2001, 98:31–36
28. Hosack DA, Dennis G Jr, Sherman BT, Lane HC, Lempicki RA: Identifying biological themes within lists of genes with EASE. Genome Biol 2003, 4:R70
29. Segerer S, Heller F, Lindenmeyer MT, Schmid H, Cohen CD, Draganovici D, Mandelbaum J, Nelson PJ, Grone HJ, Grone EF, Figel AM, Nossner E, Schlondorff D: Compartment specific expression of dendritic cell markers in human glomerulonephritis. Kidney Int 2008, 74:37–46
30. Mundel P, Reiser J, Zuniga Mejia Borja A, Pavenstadt H, Davidson GR, Kriz W, Zeller R: Rearrangements of the cytoskeleton and cell contacts induce process formation during differentiation of conditionally immortalized mouse podocyte cell lines. Exp Cell Res 1997, 236:248–258
31. Delarue F, Virone A, Hagege J, Lacave R, Peraldi MN, Adida C, Rondeau E, Feunteun J, Sraer JD: Stable cell line of T-SV40 immortalized human glomerular visceral epithelial cells. Kidney Int 1991, 40:906–912
32. Saleem MA, O'Hare MJ, Reiser J, Coward RJ, Inward CD, Farren T, Xing CY, Ni L, Mathieson PW, Mundel P: A conditionally immortalized human podocyte cell line demonstrating nephrin and podocin expression. J Am Soc Nephrol 2002, 13:630–638
33. Lindenmeyer MT, Kretzler M, Boucherot A, Berra S, Yasuda Y, Henger A, Eichinger F, Gaiser S, Schmid H, Rastaldi MP, Schrier RW, Schlondorff D, Cohen CD: Interstitial vascular rarefaction and reduced VEGF-A expression in human diabetic nephropathy. J Am Soc Nephrol 2007, 18:1765–1776
34. Moll AG, Lindenmeyer MT, Kretzler M, Nelson PJ, Zimmer R, Cohen CD: Transcript-specific expression profiles derived from sequence-based analysis of standard microarrays. PLoS One 2009, 4:e4702
35. Catania JM, Chen G, Parrish AR: Role of matrix metalloproteinases in renal pathophysiologies. Am J Physiol Renal Physiol 2007, 292:F905–F911
36. Eddy AA: Molecular basis of renal fibrosis. Pediatr Nephrol 2000, 15:290–301
37. Eikmans M, Baelde JJ, de Heer E, Bruijn JA: ECM homeostasis in renal diseases: a genomic approach. J Pathol 2003, 200:526–536
38. Zeisberg M, Strutz F, Muller GA: Renal fibrosis: an update. Curr Opin Nephrol Hypertens 2001, 10:315–320
39. Manalo DJ, Rowan A, Lavoie T, Natarajan L, Kelly BD, Ye SQ, Garcia JG, Semenza GL: Transcriptional regulation of vascular endothelial cell responses to hypoxia by HIF-1. Blood 2005, 105:659–669
40. Wenger RH, Stiehl DP, Camenisch G: Integration of oxygen signaling at the consensus HRE. Sci STKE 2005, 2005:re12
41. Milner R, Hung S, Erokwu B, Dore-Duffy P, LaManna JC, del Zoppo GJ: Increased expression of fibronectin and the $\alpha5\beta1$ integrin in angiogenic cerebral blood vessels of mice subject to hypobaric hypoxia. Mol Cell Neurosci 2008, 38:43–52
42. Distler JH, Jungel A, Pileckyte M, Zwerina J, Michel BA, Gay RE, Kowal-Bielecka O, Matucci-Cerinic M, Schett G, Marti HH, Gay S, Distler O: Hypoxia-induced increase in the production of extracellular matrix proteins in systemic sclerosis. Arthritis Rheum 2007, 56:4203–4215
43. Hudson BG, Tryggvason K, Sundaramoorthy M, Neilson EG: Alport's syndrome. Goodpasture's syndrome, and type IV collagen, N Engl J Med 2003, 348:2543–2556
44. Gröne HJ, Simon M, Gröne EF: Expression of vascular endothelial

growth factor in renal vascular disease and renal allografts. J Pathol 1995, 177:259–267
45. Baelde HJ, Eikmans M, Lappin DW, Doran PP, Hohenadel D, Brinkkoetter PT, van der Woude FJ, Waldherr R, Rabelink TJ, de Heer E, Bruijn JA: Reduction of VEGF-A and CTGF expression in diabetic nephropathy is associated with podocyte loss. Kidney Int 2007, 71:637–645
46. Bluyssen HA, Lolkema MP, van Beest M, Boone M, Snijckers CM, Los M, Gebbink MF, Braam B, Holstege FC, Giles RH, Voest EE: Fibronectin is a hypoxia-independent target of the tumor suppressor VHL. FEBS Lett 2004, 556:137–142
47. Gubler MC: Inherited diseases of the glomerular basement membrane. Nat Clin Pract Nephrol 2008, 4:24–37
48. Rius J, Guma M, Schachtrup C, Akassoglou K, Zinkernagel AS, Nizet V, Johnson RS, Haddad GG, Karin M: NF-κB links innate immunity to the hypoxic response through transcriptional regulation of HIF-1α. Nature 2008, 453:807–811
49. Walmsley SR, Print C, Farahi N, Peyssonnaux C, Johnson RS, Cramer T, Sobolewski A, Condliffe AM, Cowburn AS, Johnson N, Chilvers ER: Hypoxia-induced neutrophil survival is mediated by HIF-1α-dependent NF-κB activity. J Exp Med 2005, 201:105–115
50. Imakiire T, Kikuchi Y, Yamada M, Kushiyama T, Higashi K, Hyodo N, Yamamoto K, Oda T, Suzuki S, Miura S: Effects of renin-angiotensin system blockade on macrophage infiltration in patients with hypertensive nephrosclerosis. Hypertens Res 2007, 30:635–642
51. Huber TB, Reinhardt HC, Exner M, Burger JA, Kerjaschki D, Saleem MA, Pavenstadt H: Expression of functional CCR and CXCR chemokine receptors in podocytes. J Immunol 2002, 168:6244–6252
52. Staller P, Sulitkova J, Lisztwan J, Moch H, Oakeley EJ, Krek W: Chemokine receptor CXCR4 downregulated by von Hippel-Lindau tumour suppressor pVHL. Nature 2003, 425:307–311
53. Mori T, Kim J, Yamano T, Takeuchi H, Huang S, Umetani N, Koyanagi K, Hoon DS: Epigenetic up-regulation of C-C chemokine receptor 7 and C-X-C chemokine receptor 4 expression in melanoma cells. Cancer Res 2005, 65:1800–1807
54. Mehta SA, Christopherson KW, Bhat-Nakshatri P, Goulet RJ Jr, Broxmeyer HE, Kopelovich L, Nakshatri H: Negative regulation of chemokine receptor CXCR4 by tumor suppressor p53 in breast cancer cells: implications of p53 mutation or isoform expression on breast cancer cell invasion. Oncogene 2007, 26:3329–3337
55. Schioppa T, Uranchimeg B, Saccani A, Biswas SK, Doni A, Rapisarda A, Bernasconi S, Saccani S, Nebuloni M, Vago L, Mantovani A, Melillo G, Sica A: Regulation of the chemokine receptor CXCR4 by hypoxia. J Exp Med 2003, 198:1391–1402
56. Zagzag D, Krishnamachary B, Yee H, Okuyama H, Chiriboga L, Ali MA, Melamed J, Semenza GL: Stromal cell-derived factor-1α and CXCR4 expression in hemangioblastoma and clear cell-renal cell carcinoma: von Hippel-Lindau loss-of-function induces expression of a ligand and its receptor. Cancer Res 2005, 65:6178–6188
57. Hung SC, Pochampally RR, Hsu SC, Sanchez C, Chen SC, Spees J, Prockop DJ: Short-term exposure of multipotent stromal cells to low oxygen increases their expression of CX3CR1 and CXCR4 and their engraftment in vivo. PLoS ONE 2007, 2:e416
58. Sagrinati C, Netti GS, Mazzinghi B, Lazzeri E, Liotta F, Frosali F, Ronconi E, Meini C, Gacci M, Squecco R, Carini M, Gesualdo L, Francini F, Maggi E, Annunziato F, Lasagni L, Serio M, Romagnani S, Romagnani P: Isolation and characterization of multipotent progenitor cells from the Bowman's capsule of adult human kidneys. J Am Soc Nephrol 2006, 17:2443–2456
59. Ronconi E, Sagrinati C, Angelotti ML, Lazzeri E, Mazzinghi B, Ballerini L, Parente E, Becherucci F, Gacci M, Carini M, Maggi E, Serio M, Vannelli GB, Lasagni L, Romagnani S, Romagnani P: Regeneration of glomerular podocytes by human renal progenitors. J Am Soc Nephrol 2009, 20:322–332
60. Mazzinghi B, Ronconi E, Lazzeri E, Sagrinati C, Ballerini L, Angelotti ML, Parente E, Mancina R, Netti GS, Becherucci F, Gacci M, Carini M, Gesualdo L, Rotondi M, Maggi E, Lasagni L, Serio M, Romagnani S, Romagnani P: Essential but differential role for CXCR4 and CXCR7 in the therapeutic homing of human renal progenitor cells. J Exp Med 2008, 205:479–490
61. Ceradini DJ, Kulkarni AR, Callaghan MJ, Tepper OM, Bastidas N, Kleinman ME, Capla JM, Galiano RD, Levine JP, Gurtner GC: Progenitor cell trafficking is regulated by hypoxic gradients through HIF-1 induction of SDF-1. Nat Med 2004, 10:858–864
62. Lapidot T, Kollet O: The essential roles of the chemokine SDF-1 and its receptor CXCR4 in human stem cell homing and repopulation of transplanted immune-deficient NOD/SCID and NOD/SCID/B2m^{null} mice. Leukemia 2002, 16:1992–2003
63. Ceradini DJ, Gurtner GC: Homing to hypoxia: hIF-1 as a mediator of progenitor cell recruitment to injured tissue. Trends Cardiovasc Med 2005, 15:57–63
64. Appel D, Kershaw DB, Smeets B, Yuan G, Fuss A, Frye B, Elger M, Kriz W, Floege J, Moeller MJ: Recruitment of podocytes from glomerular parietal epithelial cells. J Am Soc Nephrol 2009, 20:333–343
65. Ueland J, Yuan A, Marlier A, Gallagher AR, Karihaloo A: A novel role for the chemokine receptor Cxcr4 in kidney morphogenesis: an in vitro study. Dev Dyn 2009, 238:1083–1091
66. Baudouin SJ, Pujol F, Nicot A, Kitabgi P, Boudin H: Dendrite-selective redistribution of the chemokine receptor CXCR4 following agonist stimulation. Mol Cell Neurosci 2006, 33:160–169
67. Onoue T, Uchida D, Begum NM, Tomizuka Y, Yoshida H, Sato M: Epithelial-mesenchymal transition induced by the stromal cell-derived factor-1/CXCR4 system in oral squamous cell carcinoma cells. Int J Oncol 2006, 29:1133–1138
68. Pujol F, Kitabgi P, Boudin H: The chemokine SDF-1 differentially regulates axonal elongation and branching in hippocampal neurons. J Cell Sci 2005, 118:1071–1080
69. Takabatake Y, Sugiyama T, Kohara H, Matsusaka T, Kurihara H, Koni PA, Nagasawa Y, Hamano T, Matsui I, Kawada N, Imai E, Nagasawa T, Rakugi H, Isaka Y: The CXCL12 (SDF-1)/CXCR4 axis is essential for the development of renal vasculature. J Am Soc Nephrol 2009, 20:1714–1723
70. Gröne HJ, Cohen CD, Gröne E, Schmidt C, Kretzler M, Schlondorff D, Nelson PJ: Spatial and temporally restricted expression of chemokines and chemokine receptors in the developing human kidney. J Am Soc Nephrol 2002, 13:957–967
71. Kaissling B, Le Hir M: The renal cortical interstitium: morphological and functional aspects. Histochem Cell Biol 2008, 130:247–262
72. Neilson EG: Mechanisms of disease: fibroblasts—a new look at an old problem. Nat Clin Pract Nephrol 2006, 2:101–108
73. Li Y, Kang YS, Dai C, Kiss LP, Wen X, Liu Y: Epithelial-to-mesenchymal transition is a potential pathway leading to podocyte dysfunction and proteinuria. Am J Pathol 2008, 172:299–308
74. Sam R, Wanna L, Gudehithlu KP, Garber SL, Dunea G, Arruda JA, Singh AK: Glomerular epithelial cells transform to myofibroblasts: early but not late removal of TGF-β1 reverses transformation. Transl Res 2006, 148:142–148

CHAPTER III

Periostin is induced in glomerular injury and expressed de novo in interstitial renal fibrosis

Kontheari Sen, Maja T. Lindenmeyer, Ariana Gaspert, Felix Eichinger, Matthias A. Neusser, Matthias Kretzler, Stephan Segerer, Clemens D. Cohen

Am J Pathol 2011, 179:1756 –1767; doi: 10.1016/j.ajpath.2011.06.002

The American Journal of Pathology, Vol. 179, No. 4, October 2011

DOI: 10.1016/j.ajpath.2011.06.002

Cardiovascular, Pulmonary, and Renal Pathology

Periostin Is Induced in Glomerular Injury and Expressed *de Novo* in Interstitial Renal Fibrosis

Kontheari Sen,* Maja T. Lindenmeyer,*† Ariana Gaspert,‡ Felix Eichinger,§ Matthias A. Neusser,† Matthias Kretzler,§ Stephan Segerer,†¶ and Clemens D. Cohen*†

From the Institute of Physiology and the Department of Anatomy,¶ University of Zurich, Zurich, Switzerland; the Division of Nephrology† and the Institute of Surgical Pathology,‡ University Hospital Zurich, Zurich, Switzerland; and the Department of Medicine,§ University of Michigan, Ann Arbor, Michigan*

Matricellular proteins participate in the pathogenesis of chronic kidney diseases. We analyzed glomerular gene expression profiles from patients with proteinuric diseases to identify matricellular proteins contributing to the progression of human nephropathies. Several genes encoding matricellular proteins, such as *SPARC*, *THBS1*, and *CTGF*, were induced in progressive nephropathies, but not in nonprogressive minimal-change disease. Periostin showed the highest induction, and its transcript levels correlated negatively with glomerular filtration rate in both glomerular and tubulointerstitial specimen. In well-preserved renal tissue, periostin localized to the glomerular tuft, the vascular pole, and along Bowman's capsule; no signal was detected in the tubulointerstitial compartment. Biopsies from patients with glomerulopathies and renal dysfunction showed enhanced periostin expression in the mesangium, tubular interstitium, and sites of fibrosis. Periostin staining correlated negatively with renal function. α-smooth muscle actin–positive mesangial and interstitial cells localized close to periostin-positive sites, as indicated by co-immunofluorescence. *In vitro* stimulation of mesangial cells by external addition of TGF-β1 resulted in robust induction of periostin. Addition of periostin to mesangial cells induced cell proliferation and decreased the number of cells expressing activated caspase-3, a marker of apoptosis. These human data indicate for the first time a role of periostin in glomerular and interstitial injury in acquired nephropathies. ***(Am J Pathol 2011, 179:1756–1767; DOI: 10.1016/j.ajpath.2011.06.002)***

Matricellular proteins are a class of extracellular matrix (ECM)-related molecules defined by their ability to modulate cell matrix interactions through binding cell surface receptors such as integrins, as well as extracellular growth factors and collagens. Beside their role in constant ECM remodeling, matricellular proteins are key regulators of matrix accumulation, cell–matrix interaction, and fibrosis.[1] Thrombospondins (TSPs, protein symbols: THBSs), osteopontin, secreted protein acidic rich in cysteine (SPARC), and members of the CCN family [eg, connective tissue growth factors (CTGF)] are prominent representatives of this group of molecules.[2] These proteins are highly expressed during development and in very early postnatal tissue. In contrast, expression in healthy adult tissues is usually very low.[2] Areas where matricellular proteins are under intense investigation range from wound healing and fibrosis to inflammation and tumor progression.[3–5] In the kidney, osteopontin, thrombospondins, and SPARC are matricellular proteins reported in the pathogenesis of chronic glomerulopathies and tubulointerstitial alteration.[6–9] As mediators of fibrosis, matricellular proteins represent interesting therapeutic targets to prevent interstitial fibrosis, and by this, development of renal failure.[10]

In a recent study, we generated a comprehensive data set of genes constitutively expressed in the healthy human glomerulus, the renal glomerular gene expression data set (REGGED).[11] Periostin (POSTN), a matricellular protein previously not studied in the glomerulus, was among these glomerular transcripts predominantly and constitutively expressed in healthy glomeruli.[11] Because periostin was reported to be mainly expressed in dis-

Supported by grants from the Else Kröner-Fresenius Foundation (A62/04 to C.D.C.), the Swiss National Science Foundation (32-122439/1 to C.D.C. and 32003B_129710 to S.S.), the Novartis Foundation (09B26 to S.S.), the University of Zurich (Forschungskredit, to S.S.), and Applied System Biology Core, O'Brien Renal Center, University of Michigan (P30 DK081943-01 to M.K. and F.E.).

Accepted for publication June 22, 2011.

Supplemental material for this manuscript can be found at *http://ajp.amjpathol.org* or at doi: 10.1016/j.ajpath.2011.06.002.

Address reprint requests to Clemens D. Cohen, M.D., Institute of Physiology and Division of Nephrology, Winterthurerstrasse 190, CH-8057 Zurich, Switzerland. E-mail: clemens.cohen@access.uzh.ch.

Table 1. Clinical Characteristics of the Patients Whose Biopsies Were Used for Microarray Analyses

Patient cohort	Number	Sex (F/M)	Age (years)	eGFR (mL/min/1.73 m^2)	Creatinine (mg/dL)	Proteinuria (g/day)	Hypertension (yes/no)
MGN Hyb A	21	9/12	53.7 ± 18.0	84.6 ± 40.1	1.0 ± 0.4	4.5 ± 3.1	14/7
MCD Hyb B	5	3/2	36.7 ± 13.5	111.3 ± 54.9	1.0 ± 0.8	8.3 ± 7.0	3/2
FSGS Hyb A*	13	5/8	47.6 ± 16.8	63.4 ± 39.2	1.6 ± 1.1	4.8 ± 2.8	9/4
FSGS Hyb B*	10	7/3	43.3 ± 12.7	81.1 ± 35.1	1.1 ± 0.6	3.5 ± 2.2	8/2
LD Hyb A	14	5/9	53.2 ± 11.3	>90	≤1.0	<0.2	0/14
LD Hyb B	18	9/9	46.8 ± 12.6	>90	≤1.0	<0.2	0/18

*Non-identical glomerular samples from four FSGS patients were hybridized on each array.
eGFR, estimated glomerular filtration rate according to the MDRD (Modification of Diet in Renal Disease) formula; F/M, female/male; FSGS, focal-segmental glomerulosclerosis; Hyb A and B, hybridization on (A) Affymetrix HG-U133A or (B) HG-U133 Plus 2.0, respectively; LD, living donors; MCD, minimal change disease; MGN, membranous glomerulopathy.

eased or fibrotic tissue, we were interested in its expression in diseased glomeruli. We performed a comprehensive screen regarding the expression of matricellular genes in glomeruli from patients with progressive and nonprogressive glomerulopathies. Periostin, although found in REGGED to be constitutively expressed in this compartment of the kidney, showed the highest induction in human glomerular diseases of all of the matricellular proteins. Hence, we followed this finding further and localized periostin protein in renal biopsies and studied the expression of periostin in glomerular cells *in vitro*.

Materials and Methods

Renal Biopsies for mRNA Analysis

Human renal biopsy specimens were collected in an international multicenter study, the European Renal cDNA Bank–Kröner-Fresenius biopsy bank (ERCB-KFB, see *Acknowledgments* for participating centers).[12] Biopsies that were all clinically indicated for proteinuria or renal failure were obtained from patients after informed consent and with approval of the local ethics committees. In two independent hybridization experiments, Affymetrix HG-U133A and HG-U133 Plus 2.0 microarrays (Affymetrix, Santa Clara, CA), respectively, were hybridized with glomerular cDNA procured from a total of 77 patients with proteinuric glomerulopathies such as focal-segmental glomerulosclerosis (FSGS, $n = 19$), membranous nephropathy (MGN, $n = 21$), and minimal change disease (MCD, $n = 5$), as well as pretransplant biopsies from living renal allograft donors as controls ($n = 32$) (Table 1). Confirmatory real-time RT-PCR analyses were performed on microdissected glomeruli from biopsy specimens from additional patients with FSGS ($n = 16$), MGN ($n = 14$), MCD ($n = 8$), proliferative lupus nephritis ISN/RPS III–IV (LN, $n = 20$), and IgA nephropathy (IGAN, $n = 14$) or on tubulointerstitial specimens from patients with FSGS ($n = 25$) or MGN ($n = 28$) (Table 2). Pretransplant kidney biopsies from living renal allograft donors ($n = 6$) served as controls. Clinical and histological characteristics of the patients and biopsies are summarized in Tables 1 and 2.

RNA Isolation, Preparation, and Microarray Experiments

Following renal biopsy, the tissue was transferred to RNase inhibitor and microdissected into glomerular and tubular specimens.[12] Total RNA was isolated from microdissected glomeruli, reverse transcribed, and linearly amplified according to a protocol previously reported.[13] Fragmentation, hybridization, staining, and imaging were performed according to the Affymetrix Expression Analysis Technical Manual (Affymetrix). Microarray analysis was performed using a sequence-specific analysis approach, ChipInspector (Genomatix, Munich, Germany). Here, all probes on the array are individually matched against the genome and all known transcripts thereof.

Table 2. Clinical Data of the Study Population for the Real-Time RT-PCR Studies

Diagnosis	Sex (F/M)	Age (years)	Creatinine (mg/dL)	eGFR (mL/min)	Proteinuria (g/day)
Glomerular specimens					
FSGS	9/7	42.3 ± 15.8	1.1 ± 0.6	83.5 ± 32.2	4.4 ± 3.4
MCD	4/4	33.0 ± 13.7	1.0 ± 0.6	99.7 ± 43.1	5.6 ± 4.7
MGN	7/7	49.9 ± 17.9	1.0 ± 0.4	88.6 ± 39.9	4.2 ± 3.3
LN	18/2	34.2 ± 11.4	1.3 ± 0.6	63.1 ± 24.8	3.1 ± 3.6
IGAN	4/10	33.4 ± 11.5	1.2 ± 1.0	87.2 ± 32.5	2.0 ± 2.7
LD	3/2	49.8 ± 11.6	<1.0	>60	<0.2
Tubulointerstitial specimens					
FSGS	10/15	48.8 ± 18.1	1.8 ± 1.1	59.8 ± 39.2	5.2 ± 4.9
MGN	14/14	60.6 ± 17.0	1.9 ± 1.6	55.4 ± 34.7	6.8 ± 4.9

For one LD patient age and sex were not available, two FSGS and one MGN patient proteinuria at time of biopsy was not reported.
eGFR, estimated glomerular filtration rate according to the MDRD (Modification of Diet in Renal Disease) formula; F/M, female/male; FSGS, focalsegmental glomerulosclerosis; IGAN, IgA nephropathy; LD, living doors; LN, proliferative lupus nephritis ISN/RPS III/IV; MCD, minimal change disease; MGN, membranous glomerulopathy.

Only probes that match to one transcript are retained for further analysis. The input data for the significance analysis of microarrays were single probe values, and the resulting probes showing significantly changed signals are then used to identify the corresponding transcripts described.[14] Parallel analysis using robust multichip average and significance analysis of microarrays gave comparable results.[15]

Quantitative Real-Time RT-PCR

To confirm the microarray results, we performed real-time RT-PCR studies on biopsy samples from an independent cohort of patients (Table 2). Reverse transcription and real-time RT-PCR were performed as reported previously.[12] Predeveloped TaqMan reagents were used for human POSTN mRNA and the housekeeper genes *GAPDH* and *18SrRNA* (Applied Biosystems, Darmstadt, Germany). The mRNA expression was analyzed by standard curve quantification. For *in vitro* studies, reverse transcription was performed as described above. The same predeveloped TaqMan reagents were used. The expression of candidate genes in samples from *in vitro* studies was analyzed by the delta delta Ct method.[12]

Immunohistochemistry

Immunohistochemistry was performed as previously described.[16] In brief, dewaxed and rehydrated tissue sections were incubated in 3% hydrogen peroxide to block endogenous peroxidases. The Avidin/Biotin blocking kit was used to block endogenous biotin (Vector Laboratories, Burlingame, CA). Antigen retrieval was performed in a microwave oven in hydrochloric acid solution with a pH of 0.9.[17] The primary antibody was applied for 1 hour, and incubation with the biotinylated secondary antibody for 30 minutes was followed by the ABC reagent (Vector Laboratories). 3,3′-Diaminobenzidine (Sigma, Taufkirchen, Germany) with metal enhancement (resulting in a black product) was used as a detection system. As previously reported, polyclonal rabbit anti-human periostin antibody was used (RD181045050; Biovendor, Heidelberg, Germany).[18,19] Human transplant nephrectomy tissue with advanced interstitial fibrosis was used to establish the staining protocol. A heat-based antigen retrieval resulted in a very reliable staining pattern. Blocking experiments were performed with a recombinant periostin protein (RD172045100; Biovendor), which completely abolished the signal. Immunohistochemistry for periostin was performed on formalin-fixed, paraffin-embedded renal biopsies from patients with FSGS (n = 5), MGN (n = 12), LN ISN/RPS III, IV, IV/V (n = 6), IGAN (n = 5), and pretransplant biopsies as control (n = 5) (Table 3). Replacement of the primary antibody by diluent served as an additional negative control. The slides stained for periostin by immunohistochemistry were scanned using the MIRAX Midi Digital Slide Scanner (Carl Zeiss MicroImaging, Jena, Germany). The periostin-positive area was quantified on each slide using the HistoQuant software package of the MIRAX Viewer (Release 1.12; Carl Zeiss MicroImaging). The analysis was done separately for glomeruli and tubulointerstitium. The positive area was expressed as percentage of the evaluated area.

Consecutive sections of human transplant nephrectomy tissue were stained for periostin and cell-type markers such as α-smooth muscle actin (α-SMA, M0851; DAKO, Glostrup, Denmark), Wilms tumor 1 (WT1, sc-192; Santa Cruz Biotechnology, Santa Cruz, CA), and platelet endothelial cell adhesion molecule 1 (PECAM1/CD31, M0823; DAKO).

Immunofluorescence

Multicolor immunofluorescence was performed for periostin, α-SMA, and PECAM1 on kidney transplant nephrectomy tissue. The monoclonal antibodies for α-SMA and PECAM1 (M0851 and M0823; DAKO) were visualized with a Cy3-labeled secondary antibody (Invitrogen, Basel, Switzerland). Periostin (RD181045050; Biovendor) was visualized by a biotinylated secondary antibody and labeled with fluorescein isothiocyanate bound to streptavidin (Vector Laboratories). Negative controls consisted of isotype immunoglobulins or non-immune serum (not illustrated).

Cell Culture

Human mesangial cells (HMC)[20] were grown in Dulbecco's modified Eagle's medium (DMEM)+GlutaMAX-I (Gibco, Invitrogen) containing 10% fetal bovine serum (FBS) and 1% penicillin/streptomycin (P/S). Murine mesangial cells (MMC)[21] were grown in DMEM (Gibco, Invitrogen) containing 5% FBS, 1% P/S, 2 mmol/L L-glutamine, and 10 mmol/L HEPES (Gibco, Invitrogen). Cells were incubated at 37°C in a humidified atmosphere of 5% CO_2 in air. All experiments, but for the TGF-β1 stimulation, were performed in both cell lines with comparable results. HMC were not used for TGF-β1 stimulation because the current passages of the cell line showed no appropriate response to external TGF-β1 in control experiments (eg, fibronectin expression).

Western Blot Analysis

Cultured HMC and MMC were harvested with radioimmunoprecipitation assay buffer composed of 150 mmol/L NaCl, 1% (v/v) Nonidet P40, 0.5% (v/v) sodium deoxycholate, 0.1% (v/v) SDS, and 50 mmol/L Tris (pH 8). The protein concentrations of the supernatants were determined by the Bradford method (Bio-Rad Laboratories, Hercules, CA). Extracted proteins were boiled in loading buffer for 5 minutes, resolved by 10% SDS-polyacrylamide gel electrophoresis under reducing conditions, and transferred to an Immobilon-P membrane (Millipore, Eschborn, Germany). Membranes were blocked for 1 hour with Tris-buffered saline/3% fat-free skim milk and then incubated with the polyclonal rabbit antibody raised against human periostin (1:5000; Biovendor) overnight at 4°C and rinsed with Tris-buffered saline containing 0.1% Tween 20. For detection, a horseradish peroxidase–linked anti-rabbit IgG antibody (1:10,000, 1 hour at room temperature; DAKO) and enhanced chemiluminescence

Table 3. Clinical Data of the Patients Selected for Immunohistochemistry and Semiquantitative Data for the Periostin Staining

Diagnosis case no.	Sex	Age (years)	Creatinine (mg/dL)	Proteinuria (g/day)	eGFR (mL/min)	Positive area interstitium	Positve area glomerulus
FSGS-H1	M	36	9.5	0.1	6.7	28.9%	10.7%
FSGS-H2	M	55	3.0	2.0	23.6	8.8%	5.0%
FSGS-H3	M	65	1.6	3.5	45.0	1.7%	12.7%
FSGS-H4	M	29	1.3	0.6	70.7	2.7%	7.2%
FSGS-H5	M	42	0.6	1.5	144.5	0.8%	3.2%
IGAN-H1	F	45	3.2	1.7	16.8	24.9%	24.3%
IGAN-H2	M	26	1.5	0.5	58.4	0.4%	14.9%
IGAN-H3	M	33	1.1	0.4	78.4	0.2%	2.0%
IGAN-H4	M	40	1.0	0.4	87.3	0.2%	7.6%
IGAN-H5	M	16	0.9	3.6	120.6	1.5%	6.8%
LN-H1	F	30	2.2	12.9	28.4	14.9%	20.3%
LN-H2	F	73	1.1	4.5	51.3	2.2%	9.1%
LN-H3	F	22	0.8	1.0	94.9	2.0%	2.1%
LN-H4	F	23	0.8	6.6	98.9	0.2%	9.5%
LN-H5	F	21	0.7	2.6	118.6	6.5%	16.7%
LN-H6	M	43	0.7	9.2	138.2	0.6%	8.8%
MGN-H1	M	38	5.8	3.2	11.6	14.0%	23.5%
MGN-H2	F	80	1.2	13.0	46.0	7.0%	2.7%
MGN-H3	F	59	1.2	7.8	50.0	5.3%	9.2%
MGN-H4	F	66	1.1	2.5	53.0	5.5%	12.4%
MGN-H5	M	67	1.2	3.0	67.2	2.7%	9.8%
MGN-H6	M	68	1.0	3.0	77.4	1.6%	7.8%
MGN-H7	F	65	0.7	5.4	94.3	0.7%	4.1%
MGN-H8	M	33	1.0	11.4	97.0	5.6%	7.1%
MGN-H9	M	66	0.8	17.5	102.3	1.9%	9.3%
MGN-H10	M	50	0.8	5.0	111.9	1.6%	3.7%
MGN-H11	F	30	0.6	4.4	114.8	1.4%	12.8%
MGN-H12	F	47	0.5	4.0	145.1	0.2%	6.9%
Pre-Tx-H1	M	21	NA	NA	NA	0.0%	1.3%
Pre-Tx-H2	M	52	NA	NA	NA	6.7%	13.9%
Pre-Tx-H3	F	42	NA	NA	NA	0.1%	1.4%
Pre-Tx-H4	F	64	NA	NA	NA	0.0%	2.2%
Pre-Tx-H5	M	54	NA	NA	NA	0.3%	6.4%

eGFR, estimated glomerular filtration rate according to the MDRD (Modification of Diet in Renal Disease) formula; F/M, female/male; FSGS, focalsegmental glomerulosclerosis; IGAN, IgA nephropathy; LN, proliferative lupus nephritis ISN/RPS III/IV; MCD, minimal change disease; MGN, membranous glomerulopathy; Pre-Tx, pretransplant biopsy taken before implantation of the allograft.

substrate (PerkinElmer Life and Analytical Sciences, Waltham, MA) were used. β-Actin (Sigma) was used as loading control in Western blot analyses.

TGF-β1 Stimulation

MMC were starved in medium containing 0.5% FBS 24 hours before incubation with 2.5 ng/mL of human TGF-β1 (R+D Systems, Abingdon, UK) for 2, 4, and 6 hours, respectively. This time-dependent analysis showed highest induction at 4 hours, hence dose-dependence was tested at 4 hours with 0.1 to 10 ng/mL TGF-β1. Total cellular RNA was extracted using Qiagen RNeasy kit (Qiagen, Hombrechtikon, Switzerland). The mRNA expression was analyzed by real-time RT-PCR.

Proliferation Assay and Caspase-3 Staining

HMC and MMC were plated at a concentration of 5000 cells per well (60% confluency) on a 96-well plate. The cells were grown initially in DMEM+GlutaMAX-I medium supplemented with 10% FBS and 1% P/S or DMEM containing 5% FBS, 1% P/S, 2 mmol/L L-glutamine, and 10 mmol/L HEPES, respectively. Cells were starved in medium containing 0.5% FBS 24 hours before incubation with 1 to 100 ng/mL recombinant periostin protein for 48 hours. Cell proliferation was measured with the Promega Cell Titer 96 MTS assay method (Promega, Madison, WI).

To study the effect of periostin on apoptosis of mesangial cells, HMC were stained for activated caspase-3. HMC seeded on glass coverslips were starved in medium containing 0.5% FBS 24 hours before incubation with 10 ng/mL recombinant periostin protein or vehicle for 48 hours. Coverslips were fixed in 4% paraformaldehyde and incubated with 0.1% Triton-X 100 in PBS. After blocking with PBS containing 3% BSA and 0.05% NP-40 for 1 hour, the primary caspase-3 antibody (Cell Signaling Technology Inc., Beverly, MA) was applied overnight at 4°C followed by a biotinylated secondary antibody and fluorescein isothiocyanate bound to streptavidin (Vector Laboratories). Quantification of caspase-3–positive and –negative cells was performed by ImageJ (version 1.45e, National Institutes of Health, Bethesda, MD) after mounting with DAPI.

Statistics

Experimental data are given as mean ± SD. Where appropriate, statistical analyses were performed using

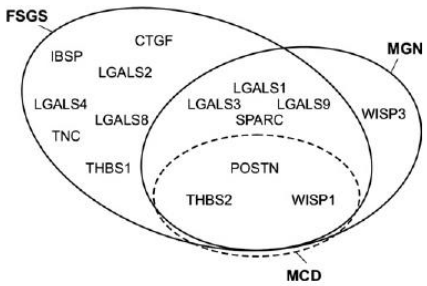

Figure 1. Venn diagram of matricellular proteins induced in proteinuric diseases. Transcript levels of 15 matricellular proteins that were found to be induced in glomeruli from patients with proteinuric diseases are indicated. In both progressive glomerulopathies, FSGS and MGN, more matricellular proteins were induced than in the nonprogressive disease MCD. Periostin, although constantly expressed in this renal compartment, showed the highest induction of all matricellular proteins (see Supplemental Table S1 at *http://ajp.amjpathol.org*). Abbreviations represent the official gene symbols of the matricellular proteins: IBSP, bone sialoprotein; POSTN, periostin; TNC, tenascin-C; WISP1, -3, WNT1 Inducible Signaling Pathway protein-1, -3.

Kruskall-Wallis, Mann–Whitney *U*-tests, and Pearson's correlation using SPSS 17.0 (SPSS., Chicago, IL), respectively. P values < 0.05 were considered to indicate statistically significant differences.

Results

Glomerular Transcriptional Levels of Matricellular Proteins in Proteinuric Diseases

The steady-state mRNA expression of genes encoding matricellular proteins was first studied by microarrays on microdissected glomeruli from renal biopsies of patients with different proteinuric diseases and controls (FSGS, $n = 19$; MGN, $n = 21$; MCD, $n = 5$; controls, $n = 32$, Table 1). The expression of bone sialoprotein, CTGF, CYR61, galectins (LGALS) 1–4, 8, and 9, NOV, osteonectin (SPARC), osteopontin, periostin, tenascin-C, THBS-1 and -2, and WNT1 Inducible Signaling Pathway proteins-1 to -3 were studied. The expression of 15 of these 19 known matricellular proteins was transcriptionally induced in glomeruli from patients with proteinuric diseases (Figure 1; see also Supplemental Table S1 at *http://ajp.amjpathol.org*). Interestingly, the mRNA levels of 12 of these 15 genes were induced in progressive glomerulopathies such as FSGS and MGN, but not in nonprogressive MCD. This would be consistent with a functional role of matricellular proteins in the progression to sclerosis and loss of renal function in acquired nephropathies. The strongest induction was found for periostin, again most prominently in the progressive disease FSGS, less in MGN, and only mild in MCD (FSGS: 2.5-fold compared with living donor samples, MGN: 2.0-fold; MCD: 1.5-fold, all statistically significant compared to controls; see Supplemental Table S1 at *http://ajp.amjpathol.org*).

Localization of Periostin in Well-Preserved Renal Tissue

This strong induction of periostin mRNA was unexpected because we previously found periostin to be constantly expressed in the human glomerulus, making a high fold-change even more significant compared with genes with lower constitutive expression.[11] To confirm first that periostin mRNA is indeed overrepresented in healthy glomeruli compared to the tubulointerstitial compartment, we performed quantitative real-time RT-PCR for periostin mRNA on microdissected glomeruli and tubulointerstitium of pretransplant biopsies from living renal allograft donors ($n = 13$). Consistent with our previous microarray report,[11] periostin demonstrated a 31.1-fold (± 29.8, $P < 0.001$) higher expression in microdissected glomeruli as compared to tubulointerstitial specimens. However, a high variance of steady state expression was observed (Figure 2).

To further study the expression and localization of the periostin protein in renal tissue, immunohistochemistry was established on formalin-fixed, paraffin-embedded renal tissue. Immunohistochemistry for periostin was performed in renal tissue of five biopsies from allografts taken before implantation as controls. The tissue in these biopsies was generally well preserved. As predicted by the mRNA expression, periostin was mainly found in glomerular areas, but not in the tubulointerstitium in these controls (Figure 3, A and B). In glomeruli, the staining was rarely localized within the peripheral glomerular tuft, but was prominent close to the vascular pole. Bowman's capsule was regularly periostin-positive. No expression by tubular epithelial cells was observed. Within the normal tubular interstitium, no periostin staining was present in the pretransplant biopsies, despite very focal sites of interstitial fibrosis (Figure 3B). On the contrary, human transplant nephrectomy tissue with advanced interstitial fibrosis, used to establish the staining protocol, also showed, besides a strong positivity in the glomerular vascular pole and tuft, a prominent periostin signal in regions

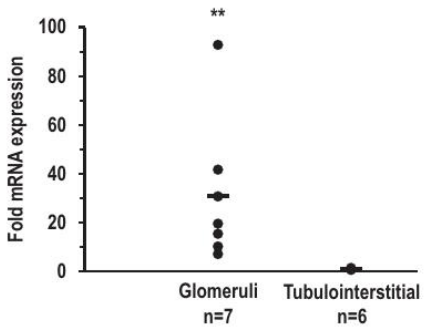

Figure 2. Periostin mRNA is enriched in the glomerular compartment. Expression of periostin mRNA was analyzed by real-time RT-PCR in glomerular and tubulointerstitial samples from pretransplant biopsies. The expression in the glomerular compartment was >30-fold higher compared with the tubulointerstitium. $^{**}P < 0.01$; data shown are normalized to GAPDH, and tubulointerstitial expression was set as 1.

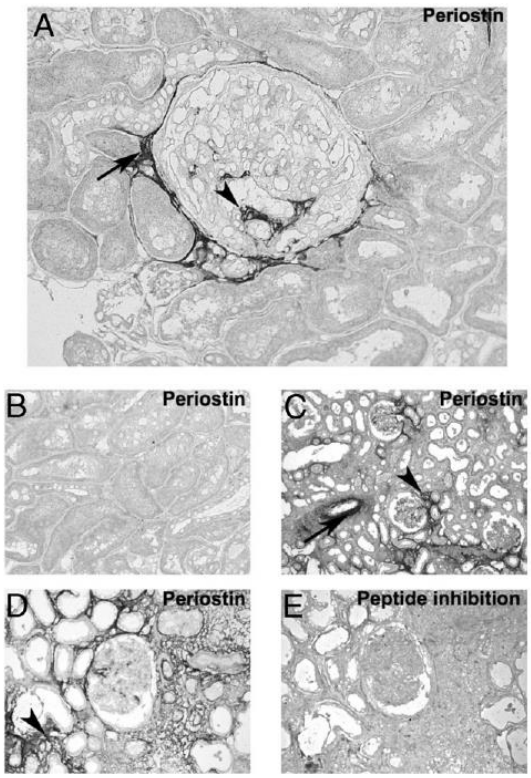

Figure 3. Localization of periostin in human pretransplant biopsies and transplant nephrectomies. Immunohistochemistry was performed with a polyclonal antiserum against periostin (**A–D**) or the combination of antiserum and the corresponding peptide (**E**) on pretransplant biopsies [original magnification, ×250 (**A** and **B**)] and allograft nephrectomies [original magnification: ×100 (**C**); ×250 (**D** and **E**)]. **A:** In well-preserved tissue from pretransplant biopsies, a positivity was rarely found for periostin within the glomerular tuft (**arrowhead**), but commonly at the vascular pole and along the Bowman's capsule (**arrow**). **B:** No periostin staining was detected in the well-preserved tubulointerstitium from pretransplant biopsies. **C** and **D:** In transplant nephrectomies due to chronic dysfunction, periostin was strongly positive in regions with interstitial fibrosis (**arrowheads**) and constitutively expressed in the wall of larger arteries (**arrow** in **C**). **E:** Addition of recombinant periostin completely blocked the specific staining of the primary antibody (consecutive section to **D**).

with interstitial fibrosis in this chronically damaged renal tissue (Figure 3, C and D). Here, periostin was also found in the media of medium-sized arteries (Figure 3C). Specificity of the staining was tested by blocking experiments with recombinant periostin (Figure 3, D and E).

Expression and Localization of Periostin in Different Acquired Glomerulopathies

The periostin mRNA induction in proteinuric glomerulopathies was validated by real-time RT-PCR. Periostin mRNA expression was studied in microdissected glomeruli from patients with FSGS (n = 16), MGN (n = 14), MCD (n = 8), controls (n = 6), and two additional progressive proteinuric diseases, LN (n = 20) and IGAN (n = 14) (Table 2). Corresponding to the microarray data, an induction of periostin was found in progressive glomerulopathies such as LN (12.9 ± 24.1, $P < 0.001$), FSGS (2.3 ± 1.4, $P < 0.05$), but not in MCD (2.8 ± 3.5, NS). In MGN (1.9 ± 1.4, NS), and IGAN (3.3 ± 3.9, NS), a trend for induction was seen but missed significance, potentially due to the above-mentioned considerable variance in periostin steady state expression even in healthy glomeruli (Figure 4, A and B).

Furthermore, periostin was localized by immunohistology in renal biopsies from patients with FSGS (n = 5), MGN (n = 12), proliferative LN ISN/RPS III, IV, IV/V (n = 6), IGAN (n = 5), and controls mentioned above (n = 5). The clinical parameters of the patients are summarized in Table 3. In contrast to the occasional glomerular staining in pretransplant biopsies, periostin was prominently and diffusely present in the glomerular tuft from patients with MGN and LN (Figure 5, A–D). This periostin positivity was consistent with a mesangial distribution (Figure 5, A–D). Additionally, the positivity was found in some biopsies in the periphery of the glomerular capillaries (Figure 5C).

The results from a quantitative image analysis of the periostin staining are summarized in Table 3. All patients with LN demonstrated a prominent and diffuse glomerular staining pattern. In one patient with LN and sequential biopsies, the mesangial positivity clearly increased with

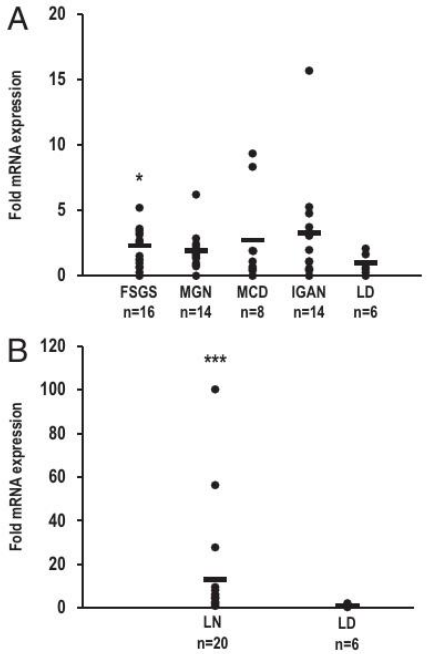

Figure 4. Periostin mRNA expression in different glomerulopathies. Periostin mRNA is induced in progressive glomerulopathies such as FSGS and LN. **A:** The expression of periostin mRNA is shown as fold-change compared with living donors (LD). FSGS, focal-segmental glomerulosclerosis; IGAN, IgA nephropathy; MCD, minimal change disease; MGN, membranous glomerulopathy. **B:** Periostin mRNA showed the highest induction in proliferative lupus nephritis compared with LD. $^{*}P < 0.05$, $^{***}P < 0.001$. Data are shown as fold-change compared to expression in LD (set as 1) and are normalized to GAPDH.

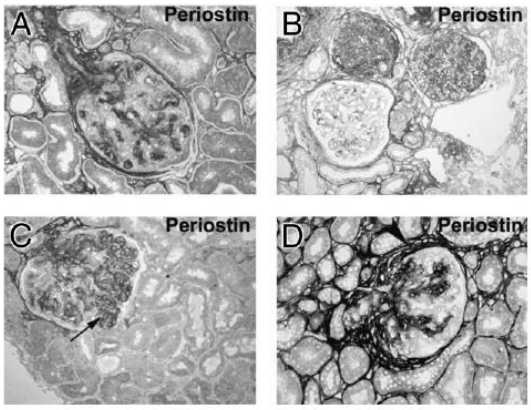

Figure 5. Periostin staining in membranous nephropathy and proliferative lupus nephritis. Immunohistochemistry was performed with a polyclonal antiserum against periostin (**A–D**) on renal biopsies with membranous nephropathy (**A** and **B**), lupus nephritis (**C** and **D**), [original magnification, ×200 (**A–D**)]. **A:** The typical constitutive staining of the vascular pole is illustrated in combination with a prominent staining of the glomerular tuft with a predominant mesangial pattern in a biopsy with membranous nephropathy. **B:** Three glomeruli with different grades of glomerular staining are illustrated ranging from focal staining (left glomerulus), to global staining in a completely sclerosed glomerulus (in the middle). **C** and **D:** In two patients with LN ISN/RPS IV and comparably high proteinuria (7 to 8 g/day), the glomerular periostin staining was similar. However, the tubulointerstitial periostin staining was mild in the patient with preserved eGFR (>60 mL/min; **C**, **arrow:** glomerular periphery) and prominent in the patient with impaired renal function and interstitial fibrosis (eGFR <30 mL/min; **D**, **arrowhead**).

duration of kidney disease and loss of renal function. In FSGS, the periostin staining was found accentuated in areas of sclerosis, but mesangial positivity was found to be similar to that in healthy glomeruli. In IGAN, a disease with no significant mRNA induction found by real-time RT-PCR, the staining was also not significantly different to control tissue.

Periostin Expression in the Tubulointerstitium and in Biopsies with Renal Failure

As described above, the staining of transplant nephrectomies was strongly positive for periostin in the tubular interstitium at sites of fibrosis and interstitial inflammation (Figure 3, C and D). This was also seen in renal biopsies from patients with glomerulopathies and reduced renal function (Figure 5, B and D). In contrast to the periostin-negative tubulointerstitium in healthy renal tissue, the interstitium became increasingly periostin-positive with loss of renal function independent of the type of glomerulopathy. Periostin-positive staining was found most prominently in areas with interstitial matrix accumulation and tubular atrophy. For example, stainings for lupus nephritis patients with comparable amounts of proteinuria but different estimated GFR (eGFR) are shown (Figure 5, C and D). Quantitative image analysis was applied and, in biopsies from patients with an eGFR <30 mL/min, showed a significantly more prominent tubulointerstitial periostin staining than in biopsies with well-preserved renal function (Figure 6 A). This was also indicated by a significant negative correlation between the periostin-positive areas in the interstitium of biopsies from all patients with different nephropathies and the eGFR ($r = -0.695$, $P < 0.001$). Similarly, quantitative analysis of the glomerular signal showed the highest scores for glomerular periostin in biopsies from patients with an eGFR <30 mL/min, and again, a significant negative correlation was found for the periostin-positive glomerular area and eGFR of the patient ($r = -0.472$, $P = 0.01$, Figure 6B). Staining scores of the tubulointerstitial and glomerular areas in each biopsy showed a statistically significant positive correlation ($r = 0.597$, $P < 0.001$).

To further substantiate the negative correlation of periostin expression and eGFR, the more quantitative

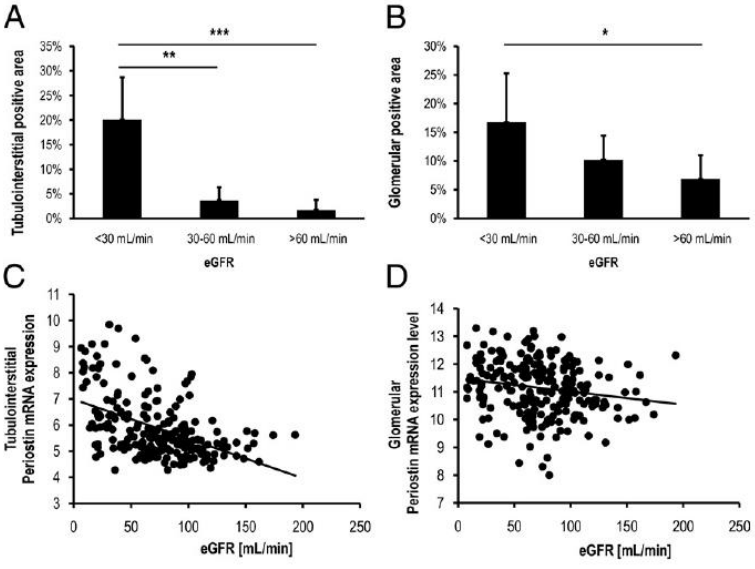

Figure 6. Periostin correlates negatively with renal function. **A** and **B:** Digital image analysis was performed to quantify the periostin-positive area. **A:** Periostin staining was most prominent in the interstitium of biopsies from patients with an eGFR <30 mL/min (**$P < 0.01$ vs. eGFR 30–60 mL/min and ***$P < 0.001$ vs. eGFR >60 mL/min, respectively). **B:** The same enhanced periostin positivity can be seen in the glomerular compartment of biopsies with reduced GFR (*$P < 0.05$ eGFR <30 mL/min vs eGFR >60 mL/min). **C** and **D:** In a comprehensive transcriptomic screen on biopsies from patient with different nephropathies ($n = 221$), periostin mRNA expression was correlated with eGFR of the patients. Intrarenal periostin mRNA levels showed a significant, negative correlation with eGFR in both tubulointerstitium (**C**) and glomeruli (**D**) (tubulointerstitium: $r = -0.47$, $P = 6.9^{-14}$, glomeruli: $r = -0.18$, $P = 8.1^{-03}$).

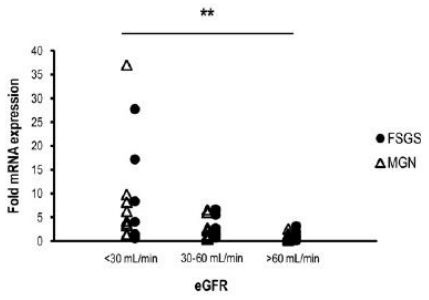

Figure 7. Periostin mRNA expression in tubulointerstitium. Periostin mRNA levels in the tubulointerstitium were quantified by real-time RT-PCR in biopsies from patients with FSGS ($n = 25$) and MGN ($n = 28$), with a wide range of eGFR. Highest periostin mRNA levels were found in biopsies from patients with eGFR <30 mL/min (**$P < 0.01$, data are shown as fold-change compared to the eGFR >60 mL/min group).

data from a comprehensive transcriptomic screen were analyzed.[22] Periostin mRNA expression showed a significant, negative correlation with renal function in both compartments (tubulointerstitium: $r = -0.47$, $P = 6.9^{-14}$, glomeruli: $r = -0.18$, $P = 8.1^{-03}$; $n = 221$) (Figure 6, C and D). No statistically significant correlations were found for the intensity score or mRNA expression with proteinuria or age of the patients, respectively. We also tested the glomerular expression of other matricellular proteins for correlation with renal function. For 6 of 19 genes (including *POSTN*), glomerular expression levels correlated negatively with eGFR (see Supplemental Table S1 at *http://ajp.amjpathol.org*). No correlation with reported levels of proteinuria was observed. To substantiate the tubulointerstitial data from the transcriptomic screen, real-time RT-PCR for periostin mRNA was performed. On microdissected tubulointerstitium from patients with FSGS and MGN with a wide range of eGFR ($n = 25$ and 28, respectively; Table 2), again a significant negative correlation of periostin expression levels with eGFR was seen ($r = -0.374$, $P < 0.01$, Figure 7).

Mesangial Cells Produce Periostin and Respond to It with Proliferation and Reduced Rate of Apoptosis

Periostin is known to be produced in most organs by fibroblasts or fibroblast-like cells.[23] To determine whether this is also true in the kidney, we performed co-immunofluorescence for smooth muscle actin (α-SMA) and periostin in transplant nephrectomies. Periostin localized to the extracellular matrix in close vicinity to α-SMA–positive cells but without overlap of both signals (Figure 8, A–C). Such proximity of both signals has been illustrated previously in other organs (see *Discussion* and Kikuchi et al[24]). Because mesangial cells are the glomerular cells expressing α-SMA during glomerular injury,[25] the staining would indicate that mesangial cells are the source of periostin in the glomerulus. By co-immunofluorescence with PECAM1, an endothelial marker, no overlap or proximity with periostin was seen. Staining of consecutive sections for WT1 (a podocyte marker), PECAM1, and periostin showed also no overlap or common staining pattern. Again, however, a clear proximity of periostin and α-SMA was observed (Figure 8, D–J). These stainings suggest mesangial cells to be the source of glomerular periostin. In the interstitium, a similar proximity of periostin and α-SMA was seen, indicating an expression by interstitial myofibroblasts.[23]

The glomerular staining and periostin induction in disease prompted us to study periostin in mesangial cells *in vitro*. Consistent with the staining pattern, supernatant from both human and murine mesangial cells was found to be positive for periostin by Western blot analysis (Figure 9A). In addition, mesangial cells showed a time- and dose-dependent induction of periostin mRNA when treated with TGF-β1, a known stimulator of periostin in other cell types (Figure 9B). We aimed to translate this finding to human data and looked for association of

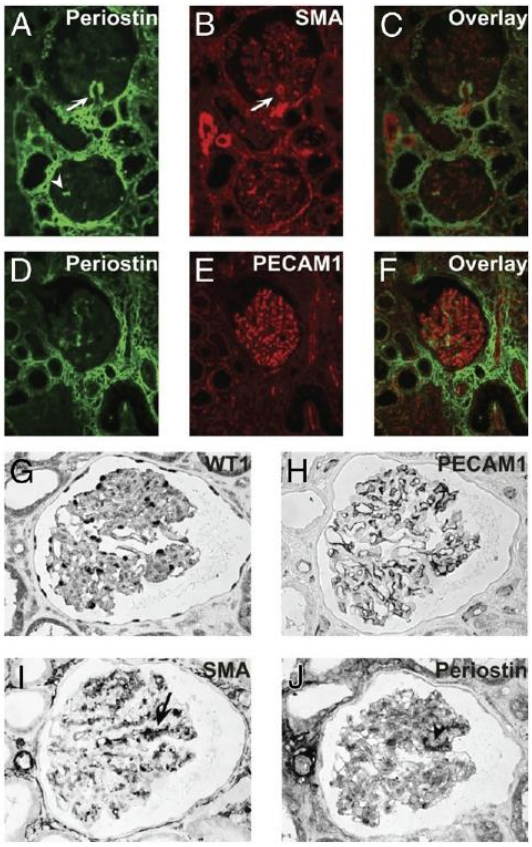

Figure 8. Co-immunofluorescence and consecutive sections for periostin, α-SMA, PECAM1, and WT1. A transplant nephrectomy was stained for periostin (**A**) and α-smooth muscle actin (α-SMA) (**B**). The merge (**C**) indicates no overlap of both signals but clear and consistent proximity of both molecules in both glomeruli (**arrows**) and in the tubulointerstitium. Focal staining in the periphery of glomerular tuft is illustrated by the **arrowhead**. No such proximity or any overlap was seen by co-immunofluorescence for periostin and PECAM1 (**D–F**). Consecutive sections of human transplant nephrectomy tissue were also stained for the cell-type markers WT1 (**G**), PECAM1 (**H**), α-SMA (**I**), and for periostin (**J**). Again, a clear proximity of α-SMA and periostin were observed, illustrated by **arrow** and **arrowhead**, and no overlap or obvious proximity with WT1 or PECAM1.

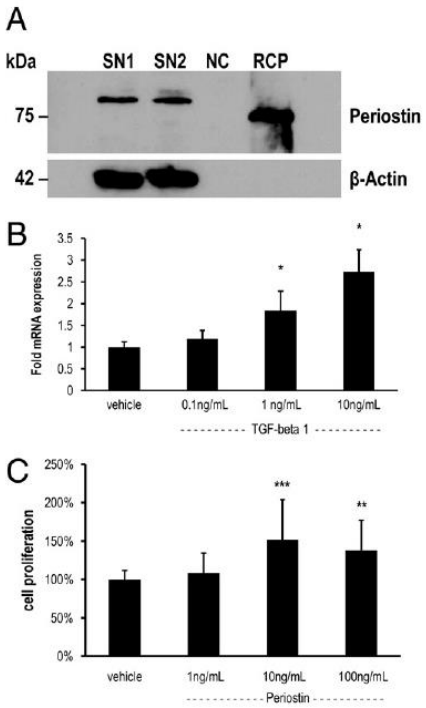

Figure 9. Periostin is produced by mesangial cells *in vitro* and induces cell proliferation. **A:** Western blot analysis for periostin showed a single band of the expected size in human and murine mesangial cell supernatants (SN1, SN2, respectively); a truncated recombinant periostin protein served as positive control (RCP; 75 kDa; Biovendor). Water served as negative control (NC). **B:** Murine mesangial cells were incubated with TGF-β1 at the indicated concentrations for 4 hours. This stimulation led to a dose-dependent induction of periostin mRNA (*$P < 0.05$ vs vehicle control; $n = 4$ each). **C:** Cell proliferation was tested on mesangial cells incubated in the absence and presence of varying concentrations of periostin. Highest proliferative effect was found for 10 ng/mL periostin. The results are shown from human mesangial cells and are summarized from four independent experiments with three to eight stimulations each. **$P < 0.01$, ***$P < 0.001$ versus vehicle control. Murine mesangial cells gave comparable results with highest induction at 10 ng/mL periostin.

TGF-β1 and periostin mRNA levels in human glomeruli. In the comprehensive transcriptomic data set from patients with different nephropathies, TGF-β1 mRNA levels correlated positively with periostin mRNA expression (glomeruli: $r = 0.204$, $P < 0.01$ and tubulointerstitium: $r = 0.168$, $P < 0.001$; $n = 221$). To determine whether periostin accelerates mesangial cell proliferation as it does in other cell types,[24,26] we incubated human mesangial cells for 48 hours with recombinant periostin. This led to a significant increase in proliferation with the highest proliferative effect at a periostin concentration of 10 ng/mL (Figure 9C). Again, we tried to complete this finding by *ex vivo* data; therefore, we scored the histology reports of LN patients ($n = 20$) for mesangial proliferation and compared it with the periostin mRNA levels found by real-time RT-PCR. A trend, although not significant, for higher periostin levels in highly proliferative lupus nephritis was observed [periostin mRNA/GAPDH mRNA ratio in biopsies graded "no or mild proliferation" ($n = 5$): 0.014 $\pm$ 0.01; "moderate" ($n = 11$): 0.032 $\pm$ 0.03; "severe" ($n = 8$): 0.13 $\pm$ 0.18]. Mechanisms that promote cell survival or prevent apoptosis are considered to promote cell proliferation. On different cell types, an antiapoptotic effect of periostin has been reported.[26,27] Accordingly, addition of recombinant periostin significantly decreased the number of cells expressing activated caspase-3, a marker of apoptosis [vehicle treated: 4.5% $\pm$ 2.1% of cells caspase-3 positive; periostin treated: 3.4% $\pm$ 1.5% of cells caspase-3 positive (ie, 24% reduction, $n = 3$, $P < 0.05$)]. These data are in line with our initial finding indicating that mesangial cells, as α-SMA–positive glomerular cells, represent the source and may also be a target cell of glomerular periostin in diseased human renal tissue.

Discussion

Progressive kidney diseases are characterized by ECM deposition in glomeruli and tubular interstitium, vascular rarefaction, inflammatory cell infiltrate, and nephron loss. Matricellular proteins are known to be important regulators of fibrosis, angiogenesis, and cell–matrix interaction in different tissues, including the injured kidney. In healthy kidneys, their expression is low. As such, they became interesting candidates for therapeutic interventions in renal diseases.[8,10] However, the specific role of each matricellular protein in the human kidney has still to be defined. Unexpectedly, we found recently a constitutive expression of the matricellular protein periostin in healthy human glomeruli.[11] This prompted us to study the expression of periostin in different glomerulopathies.

Periostin is currently discussed as a major player in organ fibrosis but is also a critical component of mechanically challenged biological structures such as cardiac valves, annuli, and bone. It was initially isolated as an osteoblast-specific factor that functions as a cell adhesion molecule for preosteoblasts and is thought to be involved in osteoblast recruitment, attachment, and spreading.[28] Periostin was found to be highly expressed in the embryonic periosteum, periodontal ligament, and the developing mouse heart during valve formation.[29,30] Furthermore, under pathological conditions, periostin expression is high during wound healing and in malignant diseases.[2] Knockout of the periostin gene in mice led to growth retardation and skeletal defects in terms of a periodontal disease-like phenotype and severe incisor enamel defects.[30,31] About 14% of these mice died within 2 to 3 weeks after birth as the result of cardiovascular malformations caused by large acellular deposits of ECM in the valves.[30] After myocardial infarction, cardiac healing is impaired in periostin-deficient mice, caused by a reduction of α-SMA–positive cells, impaired collagen fibril formation, and finally, cardiac rupture.[32] Interestingly, mice surviving without ventricular rupture show less cardiac fibrosis and better ventricular performance.[33] Local application of periostin to postischemic myocardium improved also ventricular remodeling and reduced fibrosis.[34]

According to our knowledge, this report is the first detailed evaluation of periostin in normal kidneys and

acquired nephropathies with interstitial fibrosis, whereas previous research on fibrotic conditions focused on myocardial fibrosis and remodeling.[35] Regarding the kidney, a previous report described higher expression of periostin mRNA in cultured human autosomal dominant polycystic kidney disease cyst epithelial cells compared to normal human kidney cells.[19] Periostin was localized to cyst walls in autosomal dominant polycystic kidney disease kidneys, and *in vitro* studies indicated that periostin increases proliferation of cyst epithelial cells via α_V-integrin signaling.

Consistent with our data, the tubulointerstitial compartment of healthy kidneys showed no periostin expression in this study, where no results on the glomerular compartment were reported. Also in concordance with our data, the main positivity in diseased kidneys was found in the extracellular matrix. Wallace et al[19] indicated in their report that periostin was also produced by epithelial cells of cysts in autosomal dominant polycystic kidney disease. Such epithelial positivity was not observed in our study on acquired nephropathies, where α-SMA–positive cells were found in close proximity to periostin-positive ECM. This appears to be consistent with findings on postischemic myocardium, where fibroblasts are the main source of extracellular periostin.[32] Similarly, invasion of α-SMA–positive myofibroblasts correlated with the accumulation of periostin in dermal wounds,[36] and for diseased heart valves, a coexpression of periostin with α-SMA, vimentin, and CD14 was reported.[37]

In healthy human kidneys, the constitutive intraglomerular periostin expression may well originate from mesangial cells. The positivity along the Bowman's capsule could derive from parietal epithelial cells, but this cannot be concluded from the current data. We speculate that in the healthy kidney, glomerular periostin has structural properties like those discussed in heart valves and may be involved in the configuration and stabilization of the vascular pole, glomerular tuft, and Bowman's capsule. These structures are of specific relevance to stabilize the glomerular architecture during capillary circulation and may therefore make use of molecular mechanisms also involved in heart valve architecture. There, periostin seems to be essential for structural integrity during mechanical stress, potentially involving a constant remodeling of the specific tissue and ECM.[38,39] However, further studies are required to address this issue in the renal glomerulus.

The *de novo* periostin expression in the tubular interstitium derives most likely from myofibroblasts as described in postischemic myocardium or diseased heart valves. Migration and proliferation of aortic smooth muscle cells were influenced by both periostin production *per se*, as well as through signaling via integrin and focal adhesion kinase.[40] This again is consistent with the dose-dependent TGFβ1-induced induction of periostin in mesangial cells, a cell type also showing a proliferative response to external periostin. Like other secreted ECM proteins, periostin is found in fibrotic areas and interacts with ECM molecules such as collagens I and V, as well as fibronectin, known to be induced also in renal interstitial fibrosis and glomerulosclerosis.[41–43] Recently, it was shown that periostin also supports bone morphogenic protein-1 (BMP1)-mediated activation of lysyl oxidase (LOX),[44] an enzyme catalyzing covalent cross-linking of collagen fibrils. LOX, together with the related family member LOX-like 2 (LOXL2), has been shown to be involved in glomerulosclerosis and renal interstitial fibrosis.[41,43] In addition, periostin is a ligand for cellular receptors such as integrin $\alpha_v\beta_3$, $\alpha_v\beta_5$, and $\alpha_4\beta_6$. In part, these receptors and the integrin-linked kinase have already been functionally linked to the development of glomerular diseases and proteinuria.[45–47] We speculate that periostin in progressive renal disease is also involved in profibrotic cellular recruitment, and stimulation of ECM production and fibrosis, as is demonstrated in cardiac damage.[33,48] Future interventional studies will show the significance of periostin for interstitial fibrosis and glomerulosclerosis.

In summary, periostin—in contrast to most other matricellular molecules—is constitutively expressed in healthy human glomeruli. Its expression is strikingly increased in glomeruli of patients with progressive proteinuric disease. In patients with loss of renal function and interstitial fibrosis, *de novo* expression of periostin is also found in the tubular interstitium. The expression in both compartments significantly correlates with reduction of glomerular filtration rate. *Ex vivo* and *in vitro* studies indicate that in the glomeruli, mesangial cells produce periostin, which can be induced by TGFβ1. As in the heart, periostin might be involved in the structural integrity of mechanically challenged structures such as the glomerular tuft and vascular pole. The strong induction of periostin in nephropathies suggests that this molecule plays a central role in renal damage and, potentially, in remodeling, similar to its function in cardiac fibrosis and healing.

Acknowledgments

We thank all participating centers of the European Renal cDNA Bank–Kröner-Fresenius biopsy bank (ERCB-KFB) and their patients for their cooperation. We also thank Ilka Edenhofer and Stefanie Gaiser for excellent technical assistance.

Active members at the time of the study are as follows: Clemens David Cohen, Holger Schmid, Michael Fischereder, Lutz Weber, Matthias Kretzler, Detlef Schlöndorff (Munich/Zurich/Ann Arbor/New York); Jean Daniel Sraer, Pierre Ronco (Paris); Maria Pia Rastaldi, Giuseppe D'Amico (Milano); Peter Doran, Hugh Brady (Dublin); Detlev Mönks, Christoph Wanner (Würzburg); Andrew Rees (Aberdeen and Vienna); Frank Strutz, Gerhard Anton Müller (Göttingen); Peter Mertens, Jürgen Floege (Aachen); Norbert Braun, Teut Risler(Tübingen); Loreto Gesualdo, Francesco Paolo Schena (Bari); Jens Gerth, Gunter Wolf (Jena); Rainer Oberbauer, Dontscho Kerjaschki (Vienna); Bernhard Banas, Bernhard Krämer (Regensburg); Moin Saleem (Bristol); Rudolf Wüthrich (Zurich); Walter Samtleben (Munich); Harm Peters, Hans-Hellmut Neumayer (Berlin); Mohamed Daha (Leiden); Katrin Ivens, Bernd Grabensee (Düsseldorf); Francisco Mampaso (Madrid); Jun Oh, Franz Schaefer, Martin Zeier, Hermann-Joseph

Gröne (Heidelberg); Peter Gross (Dresden); Giancarlo Tonolo (Sassari); Vladimir Tesar (Prague); Harald Rupprecht (Bayreuth); Hermann Pavenstädt (Münster); Hans-Peter Marti (Bern); and Peter Mertens (Magdeburg).

References

1. Bornstein P, Sage EH: Matricellular proteins: extracellular modulators of cell function. Curr Opin Cell Biol 2002, 14:608–616
2. Hamilton DW: Functional role of periostin in development and wound repair: implications for connective tissue disease. J Cell Commun Signal 2008, 2:9–17
3. Chiodoni C, Colombo MP, Sangaletti S: Matricellular proteins: from homeostasis to inflammation, cancer, and metastasis. Cancer Metastasis Rev 2010, 29:295–307
4. Llera AS, Girotti MR, Benedetti LG, Podhajcer OL: Matricellular proteins and inflammatory cells: a task force to promote or defeat cancer? Cytokine Growth Factor Rev 2010, 21:67–76
5. Ruan K, Bao S, Ouyang G: The multifaceted role of periostin in tumorigenesis. Cell Mol Life Sci 2009, 66:2219–2230
6. Hudkins KL, Giachelli CM, Eitner F, Couser WG, Johnson RJ, Alpers CE: Osteopontin expression in human crescentic glomerulonephritis. Kidney Int 2000, 57:105–116
7. Taneda S, Pippin JW, Sage EH, Hudkins KL, Takeuchi Y, Couser WG, Alpers CE: Amelioration of diabetic nephropathy in SPARC-null mice. J Am Soc Nephrol 2003, 14:968–980
8. Hugo C, Daniel C: Thrombospondin in renal disease. Nephron Exp Nephrol 2009, 111:e61–e66
9. Mizobuchi M, Towler D, Slatopolsky E: Vascular calcification: the killer of patients with chronic kidney disease. J Am Soc Nephrol 2009, 20:1453–1464
10. Phanish MK, Winn SK, Dockrell ME: Connective tissue growth factor-(CTGF. CCN2): a marker, mediator and therapeutic target for renal fibrosis. Nephron Exp Nephrol 2010, 114:e83–e92
11. Lindenmeyer MT, Eichinger F, Sen K, Anders HJ, Edenhofer I, Mattinzoli D, Kretzler M, Rastaldi MP, Cohen CD: Systematic analysis of a novel human renal glomerulus-enriched gene expression dataset. PLoS One 2010, 5:e11545
12. Cohen CD, Frach K, Schlondorff D, Kretzler M: Quantitative gene expression analysis in renal biopsies: a novel protocol for a high-throughput multicenter application. Kidney Int 2002, 61:133–140
13. Cohen CD, Klingenhoff A, Boucherot A, Nitsche A, Henger A, Brunner B, Schmid H, Merkle M, Saleem MA, Koller KP, Werner T, Grone HJ, Nelson PJ, Kretzler M: Comparative promoter analysis allows de novo identification of specialized cell junction-associated proteins, Proc Natl Acad Sci U S A 2006, 103:5682–5687
14. Cohen CD, Lindenmeyer MT, Eichinger F, Hahn A, Seifert M, Moll AG, Schmid H, Kiss E, Grone E, Grone HJ, Kretzler M, Werner T, Nelson PJ: Improved elucidation of biological processes linked to diabetic nephropathy by single probe-based microarray data analysis. PLoS One 2008, 3:e2937
15. Tusher VG, Tibshirani R, Chu G: Significance analysis of microarrays applied to the ionizing radiation response, Proc Natl Acad Sci U S A 2001, 98:5116–5121
16. Segerer S, Cui Y, Eitner F, Goodpaster T, Hudkins KL, Mack M, Cartron JP, Colin Y, Schlondorff D, Alpers CE: Expression of chemokines and chemokine receptors during human renal transplant rejection. Am J Kidney Dis 2001, 37:518–531
17. Jedlicka J, Soleiman A, Draganovici D, Mandelbaum J, Ziegler U, Regele H, Wuthrich RP, Gross O, Anders HJ, Segerer S: Interstitial inflammation in Alport syndrome. Hum Pathol 2010, 41:582–593
18. Soltermann A, Tischler V, Arbogast S, Braun J, Probst-Hensch N, Weder W, Moch H, Kristiansen G: Prognostic significance of epithelial-mesenchymal and mesenchymal-epithelial transition protein expression in non-small cell lung cancer. Clin Cancer Res 2008, 14:7430–7437
19. Wallace DP, Quante MT, Reif GA, Nivens E, Ahmed F, Hempson SJ, Blanco G, Yamaguchi T: Periostin induces proliferation of human autosomal dominant polycystic kidney cells through alphaV-integrin receptor. Am J Physiol Renal Physiol 2008, 295:F1463–1471
20. Banas B, Luckow B, Moller M, Klier C, Nelson PJ, Schadde E, Brigl M, Halevy D, Holthofer H, Reinhart B, Schlondorff D: Chemokine and chemokine receptor expression in a novel human mesangial cell line. J Am Soc Nephrol 1999, 10:2314–2322
21. Wolf G, Aberle S, Thaiss F, Nelson PJ, Krensky AM, Neilson EG, Stahl RA: TNF alpha induces expression of the chemoattractant cytokine RANTES in cultured mouse mesangial cells. Kidney Int 1993, 44:795–804
22. Bhavnani SK, Eichinger F, Martini S, Saxman P, Jagadish HV, Kretzler M: Network analysis of genes regulated in renal diseases: implications for a molecular-based classification. BMC Bioinformatics 2009, 10 (Suppl 9):S3
23. Conway SJ, Molkentin JD: Periostin as a heterofunctional regulator of cardiac development and disease. Curr Genomics 2008, 9:548–555
24. Kikuchi Y, Kashima TG, Nishiyama T, Shimazu K, Morishita Y, Shimazaki M, Kii I, Horie H, Nagai H, Kudo A, Fukayama M: Periostin is expressed in pericryptal fibroblasts and cancer-associated fibroblasts in the colon. J Histochem Cytochem 2008, 56:753–764
25. Schlondorff D, Banas B: The mesangial cell revisited: no cell is an island. J Am Soc Nephrol 2009, 20:1179–1187
26. Bao S, Ouyang G, Bai X, Huang Z, Ma C, Liu M, Shao R, Anderson RM, Rich JN, Wang XF: Periostin potently promotes metastatic growth of colon cancer by augmenting cell survival via the Akt/PKB pathway. Cancer Cell 2004, 5:329–339
27. Zhu M, Fejzo MS, Anderson L, Dering J, Ginther C, Ramos L, Gasson JC, Karlan BY, Slamon DJ: Periostin promotes ovarian cancer angiogenesis and metastasis. Gynecol Oncol 2010, 119:337–344
28. Takeshita S, Kikuno R, Tezuka K, Amann E: Osteoblast-specific factor 2: cloning of a putative bone adhesion protein with homology with the insect protein fasciclin I. Biochem J 1993, 294 (Pt 1):271–278
29. Kruzynska-Frejtag A, Machnicki M, Rogers R, Markwald RR, Conway SJ: Periostin (an osteoblast-specific factor) is expressed within the embryonic mouse heart during valve formation. Mech Dev 2001, 103:183–188
30. Rios H, Koushik SV, Wang H, Wang J, Zhou HM, Lindsley A, Rogers R, Chen Z, Maeda M, Kruzynska-Frejtag A, Feng JQ, Conway SJ: periostin null mice exhibit dwarfism, incisor enamel defects, and an early-onset periodontal disease-like phenotype. Mol Cell Biol 2005, 25:11131–11144
31. Kii I, Amizuka N, Minqi L, Kitajima S, Saga Y, Kudo A: Periostin is an extracellular matrix protein required for eruption of incisors in mice. Biochem Biophys Res Commun 2006, 342:766–772
32. Shimazaki M, Nakamura K, Kii I, Kashima T, Amizuka N, Li M, Saito M, Fukuda K, Nishiyama T, Kitajima S, Saga Y, Fukayama M, Sata M, Kudo A: Periostin is essential for cardiac healing after acute myocardial infarction. J Exp Med 2008, 205:295–303
33. Oka T, Xu J, Kaiser RA, Melendez J, Hambleton M, Sargent MA, Lorts A, Brunskill EW, Dorn GW 2nd, Conway SJ, Aronow BJ, Robbins J, Molkentin JD: Genetic manipulation of periostin expression reveals a role in cardiac hypertrophy and ventricular remodeling. Circ Res 2007, 101:313–321
34. Kuhn B, del Monte F, Hajjar RJ, Chang YS, Lebeche D, Arab S, Keating MT: Periostin induces proliferation of differentiated cardiomyocytes and promotes cardiac repair. Nat Med 2007, 13:962–969
35. Dorn GW 2nd: Periostin and myocardial repair, regeneration, and recovery. N Engl J Med 2007, 357:1552–1554
36. Jackson-Boeters L, Wen W, Hamilton DW: Periostin localizes to cells in normal skin, but is associated with the extracellular matrix during wound repair. J Cell Commun Signal 2009, 3:125–133
37. Hakuno D, Kimura N, Yoshioka M, Mukai M, Kimura T, Okada Y, Yozu R, Shukunami C, Hiraki Y, Kudo A, Ogawa S, Fukuda K: Periostin advances atherosclerotic and rheumatic cardiac valve degeneration by inducing angiogenesis and MMP production in humans and rodents. J Clin Invest 2010, 120:2292–2306
38. Snider P, Hinton RB, Moreno-Rodriguez RA, Wang J, Rogers R, Lindsley A, Li F, Ingram DA, Menick D, Field L, Firulli AB, Molkentin JD, Markwald R, Conway SJ: Periostin is required for maturation and extracellular matrix stabilization of noncardiomyocyte lineages of the heart. Circ Res 2008, 102:752–760
39. Norris RA, Moreno-Rodriguez RA, Sugi Y, Hoffman S, Amos J, Hart MM, Potts JD, Goodwin RL, Markwald RR: Periostin regulates atrioventricular valve maturation. Dev Biol 2008, 316:200–213
40. Li G, Jin R, Norris RA, Zhang L, Yu S, Wu F, Markwald RR, Nanda A, Conway SJ, Smyth SS, Granger DN: Periostin mediates vascular smooth muscle cell migration through the integrins alphavbeta3 and alphavbeta5 and focal adhesion kinase (FAK) pathway. Atherosclerosis 2010, 208:358–365
41. Higgins DF, Kimura K, Bernhardt WM, Shrimanker N, Akai Y, Hohenstein B, Saito Y, Johnson RS, Kretzler M, Cohen CD, Eckardt KU, Iwano M, Haase

VH: Hypoxia promotes fibrogenesis in vivo via HIF-1 stimulation of epithelial-to-mesenchymal transition. J Clin Invest 2007, 117:3810–3820
42. Lindenmeyer MT, Kretzler M, Boucherot A, Berra S, Yasuda Y, Henger A, Eichinger F, Gaiser S, Schmid H, Rastaldi MP, Schrier RW, Schlondorff D, Cohen CD: Interstitial vascular rarefaction and reduced VEGF-A expression in human diabetic nephropathy. J Am Soc Nephrol 2007, 18:1765–1776
43. Neusser MA, Lindenmeyer MT, Moll AG, Segerer S, Edenhofer I, Sen K, Stiehl DP, Kretzler M, Grone HJ, Schlondorff D, Cohen CD: Human nephrosclerosis triggers a hypoxia-related glomerulopathy. Am J Pathol 2010, 176:594–607
44. Maruhashi T, Kii I, Saito M, Kudo A: Interaction between periostin and BMP-1 promotes proteolytic activation of lysyl oxidase. J Biol Chem 2010, 285:13294–13303
45. Kretzler M, Teixeira VP, Unschuld PG, Cohen CD, Wanke R, Edenhofer I, Mundel P, Schlondorff D, Holthofer H: Integrin-linked kinase as a candidate downstream effector in proteinuria. FASEB J 2001, 15:1843–1845
46. Wei C, Moller CC, Altintas MM, Li J, Schwarz K, Zacchigna S, Xie L, Henger A, Schmid H, Rastaldi MP, Cowan P, Kretzler M, Parrilla R, Bendayan M, Gupta V, Nikolic B, Kalluri R, Carmeliet P, Mundel P, Reiser J: Modification of kidney barrier function by the urokinase receptor. Nat Med 2008, 14:55–63
47. Kang YS, Li Y, Dai C, Kiss LP, Wu C, Liu Y: Inhibition of integrin-linked kinase blocks podocyte epithelial-mesenchymal transition and ameliorates proteinuria. Kidney Int 2010, 78:363–373
48. Teekakirikul P, Eminaga S, Toka O, Alcalai R, Wang L, Wakimoto H, Nayor M, Konno T, Gorham JM, Wolf CM, Kim JB, Schmitt JP, Molkentin JD, Norris RA, Tager AM, Hoffman SR, Markwald RR, Seidman CE, Seidman JG: Cardiac fibrosis in mice with hypertrophic cardiomyopathy is mediated by non-myocyte proliferation and requires Tgf-beta. J Clin Invest 2010, 120:3520–3529

CHAPTER IV

Periostin: a matricellular protein involved in peritoneal injury during peritoneal dialysis

Niko Braun[*], Kontheari Sen[*], M. Dominik Alscher, Peter Fritz, Martin Kimmel, Johann Morelle, Eric Goffin, Achim Jörres, Rudolf P. Wüthrich, Clemens D. Cohen, Stephan Segerer

[*]*Contributed equally*

Perit Dial Int 2013; 33(5):515-528; doi:10.3747/pdi.2010.00259

Peritoneal Dialysis International, Vol. 33, pp. 515–528
doi: 10.3747/pdi.2010.00259

0896-8608/13 $3.00 + .00

PERIOSTIN: A MATRICELLULAR PROTEIN INVOLVED IN PERITONEAL INJURY DURING PERITONEAL DIALYSIS

Niko Braun,[1,2]* Kontheari Sen,[3,4]* M. Dominik Alscher,[1,2] Peter Fritz,[2,5] Martin Kimmel,[1,2] Johann Morelle,[6] Eric Goffin,[6] Achim Jörres,[7] Rudolf P. Wüthrich,[3] Clemens D. Cohen,[3,4]* and Stephan Segerer[3,8]*

Department of Internal Medicine,[1] Division of General Internal Medicine and Nephrology, Robert-Bosch-Hospital, and Institute of Digital Medicine,[2] Stuttgart, Germany; Division of Nephrology,[3] University Hospital, and Institute of Physiology,[4] University of Zurich, Switzerland; Department of Diagnostic Medicine,[5] Division of Pathology, Robert-Bosch-Hospital, Stuttgart, Germany; Division of Nephrology,[6] Saint-Luc UCL Academic Hospital, Brussels, Belgium; Department of Nephrology and Medical Intensive Care,[7] Charité-Universitätsmedizin Berlin, Campus Virchow-Klinikum, Berlin, Germany; and Institute of Anatomy,[8] University of Zurich, Switzerland

♦ ***Background:*** **Periostin is a matricellular protein involved in tissue remodeling through the promotion of adhesion, cell survival, cellular dedifferentiation, and fibrogenesis. It can be induced by transforming growth factor beta and high glucose concentrations. We hypothesized that this protein might be expressed in the peritoneal cavity of patients on peritoneal dialysis (PD) and even more in patients with signs of encapsulating peritoneal sclerosis (EPS).**

♦ ***Method:*** **In this retrospective study, we included peritoneal biopsies from patients on PD with EPS (n = 7) and without signs of EPS (n = 10), and we compared them with biopsies taken during hernia repair from patients not on PD (n = 11) and during various procedures from uremic patients not on PD (n = 6). Periostin was localized by immunohistochemistry, scored semiquantitatively, and quantified by morphometry. Periostin protein concentrations were measured by ELISA in dialysates from 15 patients. Periostin messenger RNA was quantified *in vitro* in peritoneal fibroblasts.**

♦ ***Results:*** **In control biopsies, periostin was present in the walls of larger arteries and focally in extracellular matrix in the submesothelial zone. Patients on PD demonstrated interstitial periostin in variable amounts depending on the severity of submesothelial fibrosis. In EPS, periostin expression was very prominent in the sclerosis layer. The area of periostin was significantly larger in EPS biopsies than in control biopsies, and the percentage of periostin-positive area correlated with the thickness of the submesothelial fibrosis zone. Periostin concentrations in dialysate increased significantly with time on PD in patients without signs of EPS; in patients with EPS, periostin concentrations in dialysate were low and demonstrated the smallest increase with time. *In vitro*, periostin was found to be strongly expressed by peritoneal fibroblasts.**

♦ ***Conclusion:*** **Periostin is strongly expressed by fibroblasts and deposited in the peritoneal cavity of patients with EPS and with simple peritoneal fibrosis on PD. This protein might play a role in the progression of peritoneal injury, and low levels of periostin after prolonged time on PD might be a marker of EPS.**

Perit Dial Int 2013; 33(5):515-528 www.PDIConnect.com
epub ahead of print: 01 Feb 2013 doi:10.3747/pdi.2010.00259

KEY WORDS: Matricellular protein; periostin; peritoneal fibrosis; encapsulating peritoneal sclerosis; simple peritoneal fibrosis.

During peritoneal dialysis (PD), exposure to dialysate (including high glucose, low pH, glucose degradation products) mediates peritoneal injury, with matrix expansion and angiopathy, resulting in so-called simple peritoneal fibrosis (1). This condition is an important cause of technique failure in patients on PD.

Encapsulating peritoneal sclerosis (EPS) is a rare but life-threatening complication of PD. The hallmark of EPS is thickening of the peritoneal membrane by layers of fibrin and fibrosis leading to encapsulation and bowel obstruction. Decreased appetite, weight loss, and signs of inflammation are early but nonspecific symptoms of EPS (2). Later, partial or complete bowel obstruction becomes clinically apparent. Computed tomographic

* These authors contributed equally to this work.

Correspondence to: S. Segerer, Division of Nephrology, University Hospital Zurich, Rämistr. 100, Zurich 8091 Switzerland.
Stephan.segerer@usz.ch
Received 22 October 2010; accepted 22 June 2012

imaging demonstrating peritoneal thickening, bowel tethering, peritoneal calcification, peritoneal enhancement, and loculated fluid collections is important for a diagnosis of EPS (3). The histologic picture of EPS is described as relatively nonspecific. Mesothelial denudation, hemorrhage, vasculopathy, calcification, peritoneal fibroblast swelling, interstitial fibrosis, angiogenesis with increased capillary numbers, and mononuclear cell infiltration have been described as typical (4,5). Fibrin deposits on the peritoneal membrane lead to adhesions and permanent scarring, which finally result in bowel obstruction (3).

Periostin was originally called osteoblast-specific factor 2 and was later renamed because of its intense expression in periosteum and periodontal ligament (6,7). It has a molecular weight of about 90 kDa (7) and mediates cell adhesion via the $\alpha_V\beta_3$ and $\alpha_V\beta_5$ integrins (8). Periostin is a profibrogenic molecule (9) that is involved in angiogenesis (10) and that has been shown to stiffen collagen matrices *in vitro* (11).

During embryogenesis, periostin is involved in the normal development of teeth (12), bones, and the heart (13,14). Mice deficient in periostin demonstrate multiple defects such as incisor enamel defects, an early-onset periodontal-disease-like phenotype, and dwarfism (15). Periostin can be re-expressed in adults under pathologic conditions—for example, in heart failure (16), during myocardial infarction (17), in muscle injury, and in various forms of human cancers [reviewed in Ruan *et al.* (18)]. Our group was able to demonstrate that periostin, which is constitutively expressed in the human glomerular mesangium (19), was *de novo* expressed in tubulointerstitial renal fibrosis and correlated with loss of renal function (20). Recently, increased concentrations of periostin were reported in uremic hearts (21), in rat kidneys with 5/6 nephrectomy, and in urine from patients with chronic kidney disease (22).

High concentrations of glucose and transforming growth factor β (TGF-β) were found to induce periostin (7,23,24), and the presence of those two factors is well described during peritoneal injury related to PD and in patients with EPS (25–27). Periostin might also be involved in the propagation of cellular dedifferentiation, epithelial-to-mesenchymal transition, fibrosis, and angiogenesis in patients on PD. We therefore set out to localize periostin in peritoneal biopsies from patients on PD with EPS and without signs of EPS. We also quantified periostin protein levels in effluent from a second PD patient population. Finally, we quantified the expression of periostin *in vitro* in human peritoneal fibroblasts.

METHODS

STUDY POPULATION

Biopsies from parietal peritoneum were formalin-fixed and paraffin-embedded using routine protocols (28). The study included biopsies from patients on PD without signs of EPS ($n = 10$) and patients on PD with a clinical diagnosis of EPS ($n = 7$, Table 1). Biopsies from a second series of uremic patients, taken at the time of catheter implantation before the start of PD, were also studied ($n = 6$). Control biopsies were taken at the time of hernia repair from patients not on PD ($n = 11$).

Biopsies from patients on PD were obtained at the time of catheter implantation, removal, or correction of a dislocation, or at the time of any abdominal surgery (for example, hernia repair). Patients with an episode of peritonitis within the preceding 6 months were excluded. Biopsies from patients with EPS were taken at the time of peritonectomy. Clinically, all patients with EPS were at a very late stage of the disease, with recurrent abdominal pain caused by chronic bowel obstruction (Table 2). All patients gave informed consent regarding a scientific work-up of tissues taken during routine procedures.

IMMUNOHISTOCHEMISTRY

Immunohistochemistry was performed as previously described (29,30). In brief, paraffin-embedded tissue sections were deparaffinized, rehydrated, and incubated in 3% hydrogen peroxide (to block endogenous peroxidases). Antigen retrieval was performed in HCl (pH 0.9) heated by microwaving for 10 minutes (30). The primary antibody was applied for 1 hour. Incubation with biotinylated secondary reagents (Vector, Burlingame, CA, USA) for 30 minutes was followed by ABC reagent (Vector). As a detection system, we used 3,3'-diaminobenzidine (Sigma, Taufkirchen, Germany) with metal enhancement (resulting in a black-colored product). Nuclei were counterstained with methyl green.

A polyclonal anti-human periostin antibody was used (Biovendor, Heidelberg, Germany). As controls, we used sections from an allograft nephrectomy, including replacement of the antibody by diluent or by nonimmune serum [Figure 1(A,B)]. The latter controls did not demonstrate positive staining [Figure 1(B)]. Antigen retrieval at low pH reduces the nuclear counterstain and therefore nuclei appear "empty." All sections (from controls, PD patients, and EPS patients illustrated in the quantitative figures) were evaluated by an observer blinded to the clinical diagnosis. Sites of positive staining were described, and a semiquantitative scoring system

TABLE 1
Clinical Data for the Biopsy Population

Variable	Study group			
	Normal peritoneum	Uremia	PD	EPS
Biopsies (*n*)	11	6	10	7
Mean age of subjects (years)	58.6±12.7	60.5±9.2	49.9±15.6	54.3±15.4
PD duration (months)[a]	—	—	21.3±26.1	70.6±34.1
Peritonitis (episodes/months at risk)	—	—	6/192	11/494
PD fluid				
Neutral	—	—	1	5
Acidic			1	1
Both or ND			5	4
Icodextrin (*n*)	—	—	1	5
Diabetes (*n*)	—	2	3	3
Smokers	—	1	1	3
PTH [pmol/L (normal: 1.1 – 7.3)]	ND	45.4±24.3	14.1±9.5	45.0±31.6
Urea nitrogen [mg/dL (normal: 10 – 25)]	ND	167.3±24.7	61.4±30.6	39.3±10.6
Creatinine [mg/dL (normal: 0.5 – 1.4)][a]	0.92±0.31	7.3±1.67	7.69±3.77	6.99±2.17

PD = peritoneal dialysis; EPS = encapsulating peritoneal sclerosis; ND = not determined; PTH = parathyroid hormone.
[a] $p < 0.01$.

TABLE 2
Clinical Findings, Laboratory Values, and Peritoneal Dialysis (PD) Characteristics in Seven Patients with Encapsulating Peritoneal Sclerosis

Variable	Incidence [*n* (%)]
Clinical findings	
Pain	7 (100)
Diarrhea	1 (14)
Malnutrition	4 (57)
Ascites/hemoperitoneum	4 (57)
Bowel obstruction	7 (100)
On tamoxifen or immunosuppressants	0 (0)
Laboratory values	
C-Reactive protein > 0.5 mg/dL	5 (71)
PD characteristics	
Transport status	2 High (29) 4 High-average (57) 1 ND (14)

ND = not determined or peritoneal equilibration test more than 6 months in the past.

was used (0 = no or faint focal staining of extracellular matrix; 1 = prominent but focal staining of extracellular matrix; 2 = diffuse staining of extracellular matrix).

The slides stained for periostin by immunohistochemistry were scanned using the Mirax Midi digital slide scanner (Carl Zeiss MicroImaging, Jena, Germany), and the area of periostin positivity was quantified using the HistoQuant module of the Mirax Viewer software (release 1.12: Carl Zeiss MicroImaging). The positive area was expressed as a percentage of the evaluated area.

The submesothelial fibrotic zone was measured using the Leica Application Suite (version 3.4.0: Leica Microsystems, Heerbrugg, Switzerland) in combination with a Leica Microscope (Leica DMRXA2). To illustrate the association with extracellular matrix, consecutive sections were stained with Masson–Goldner trichrome, or sirius red, or both.

DOUBLE IMMUNOFLUORESCENCE

Double immunofluorescence was performed for periostin and alpha-smooth muscle actin (α-SMA). The monoclonal antibody for α-SMA (M0851: Dako, Glostrup, Denmark) was visualized with a Cy3-labeled secondary antibody (Jackson ImmunoResearch, Suffolk, UK). Periostin was visualized with a biotinylated secondary antibody and labeled with FITC bound to streptavidin (Vector). Negative controls consisted of isotype immunoglobulins or nonimmune serum on renal allografts (not illustrated).

STUDIES ON PERITONEAL FIBROBLASTS *IN VITRO*

The isolation and characterization of peritoneal fibroblasts has previously been described in detail (31). Briefly, human peritoneal fibroblasts were isolated

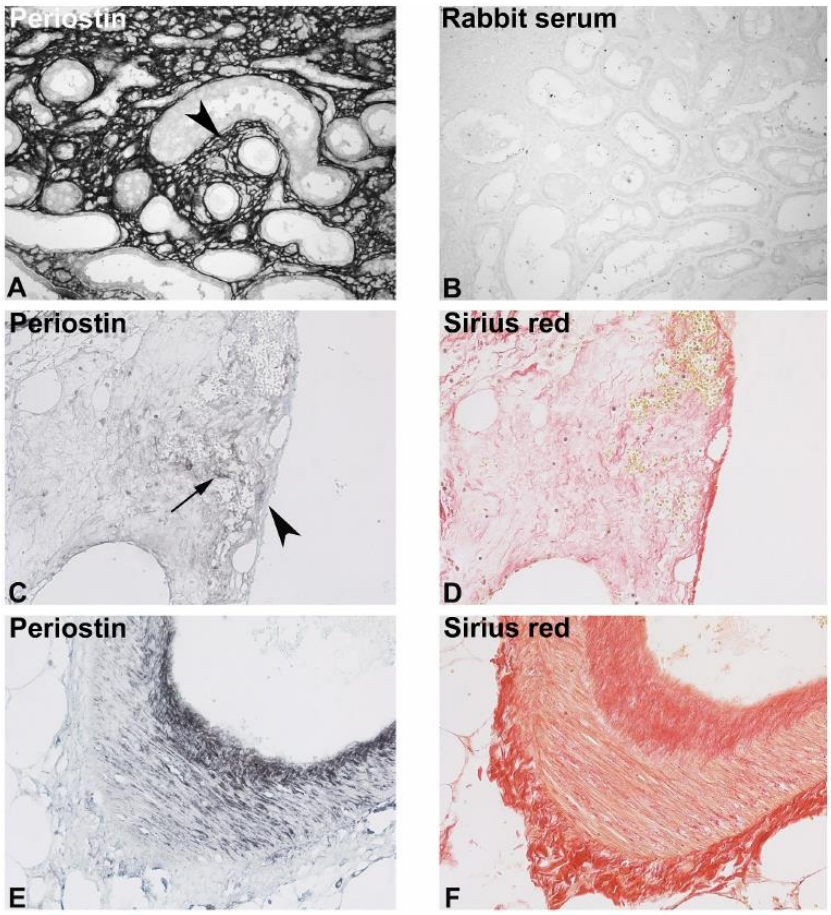

Figure 1 — Periostin in control tissue. Immunohistochemistry (A,C,E) was performed using a polyclonal antiserum against periostin on tissue sections (A,B) from an allograft nephrectomy and (C–F) from a peritoneal biopsy obtained at the time of hernia repair (original magnification 200×). (A) Note the prominent presence of periostin in areas of interstitial fibrosis (arrowhead); (B) no black color product was present when the primary antibody was replaced with non-immune rabbit serum (negative control). (C) In the biopsies, the thin layer of submesothelial fibrotic tissue was commonly negative for periostin (arrowhead), but focal staining for periostin was present within the interstitial tissue (arrow). (E,F) Smooth-muscle cells of arteries in the biopsies were positive for periostin [representative view of same specimen as (C,D)]. (D,F) Consecutive sections of the peritoneal biopsy stained with sirius red.

from specimens of omentum by enzymatic digestion. Cells were grown to confluence and rendered quiescent in serum-free medium for 48 hours. Cells were then exposed to glucose (75 mmol/L) or mannitol (75 mmol/L) for 12 hours, 1 day, 2 days, or 4 days. In a second experiment, the cells were stimulated with tumor necrosis factor α (TNF-α) 1 ng/mL or interleukin 1β (IL-1β) 1 ng/mL for at least 6 hours and up to 3 days. At designated time intervals, total RNA was isolated using RNAzol. Reverse transcription was performed using 1 µg total RNA in a reaction volume of 20 µL. Expression of periostin messenger RNA (mRNA) was quantified by real-time reverse-transcription polymerase chain reaction as previously described (29,32). Pre-developed TaqMan reagents were used for human periostin and the housekeeping genes GAPDH and 18SrRNA (Applied Biosystems, Darmstadt, Germany). Expression of mRNA was analyzed using the delta delta Ct method (25).

QUANTIFICATION OF PERIOSTIN IN DIALYSATE

An ELISA was established to quantify periostin in dialysate, as previously described in Ben *et al.* (33). A

96-well plate was coated overnight at 4°C with 1 µg/mL (0.1 µg per well) monoclonal anti-periostin antibody (MAB2955: R&D Systems, Minneapolis, USA) diluted in 0.05 mol/L carbonate–bicarbonate (C3041: Sigma). After a blocking step with solution containing 3% phosphate-buffered saline with bovine serum albumin for 1 hour at room temperature, undiluted samples were added to the wells for 2 hours at room temperature. A rabbit polyclonal antibody to periostin (Ab14041: Abcam, Cambridge, UK) diluted 1:500 in phosphate-buffered saline was added to the plate for 1 hour at room temperature, followed by a horseradish peroxidase–conjugated goat anti-rabbit immunoglobulin [1:500 dilution in phosphate-buffered saline (BD554021: BD Biosciences, Allschwil, Switzerland)]. As a detection substrate, we used 3,3′,5,5′-tetramethylbenzidine (555214: BD Biosciences), and the reaction was terminated by the addition of 1 N sulfuric acid. Absorbance was measured at 450 nm with an ELISA reader (Infinite 200 Pro: Tecan Schweiz, Männedorf, Switzerland). For determination of periostin levels, a standard curve with diluted recombinant periostin (3548-F2: R&D Systems) at concentrations ranging from 3.125 ng/mL to 50 ng/mL was used. Negative controls included incubation of wells with phosphate-buffered saline or solution containing 3% phosphate-buffered saline with bovine serum albumin.

Samples from 15 patients were available for the study. Patients with fast transport status ($n = 5$) and with low or low-average transport status ($n = 5$) were included. Transport status was assessed during a modified peritoneal equilibration test, using a 3.86% glucose-based dialysate for a 4-hour dwell 4 – 6 weeks after PD start. Five patients who developed EPS were included. For each patient, the first sample after the start of PD, and the last sample before the patient stopped PD were evaluated. In 5 patients (2 with fast transport status and 3 with EPS), intermediate samples during the time course were available.

STATISTICAL ANALYSIS

An observer blinded to the diagnosis completed the semiquantitative scoring of the periostin staining. For comparisons of means, the nonparametric Kruskal–Wallis and Dunn multiple comparison tests were used. Spearman rank correlations were performed for correlations with the thickness of the submesothelial area (InStat software, version 3.05: Intuitive Software for Science, San Diego, CA, USA). A value of $p < 0.05$ was considered significant. Error bars demonstrate the standard error of the mean.

RESULTS

Table 1 summarizes the clinical data for the patient cohort.

PERIOSTIN EXPRESSION

Control Tissue: A total of 11 control biopsies taken during hernia repair in patients not on PD were included [Figure 1(C–F)]. These tissue samples consisted of a thin submesothelial layer covering the fat tissue, with very little interstitial tissue and larger vessels [Figure 1(C,D)]. Periostin was commonly absent from the thin submesothelial area [Figure 1(C,D)]. Faint staining was focally present in some biopsies [Figure 1(C)]. In contrast, constitutive expression of periostin was present in the walls of arteries in the interstitial tissue [Figure 1(E,F)]. In the group of control biopsies, the blinded scoring resulted in a mean score of 1.1 [range: 0 – 2; Figure 2(A)]. The percentage periostin-positive area (including positive vessel walls) was 15% [range: 7% – 33%; Figure 2(B)].

Tissue from Patients on PD Without Signs of EPS: Ten biopsies from patients on PD were included. The severity of fibrosis varied between the biopsies, with a mean submesothelial fibrotic thickness of 188 µm (range: 59 – 599 µm). Periostin was found to be present in the extracellular matrix and the arterial walls. Figure 3 illustrates biopsies with increasing severity of peritoneal fibrosis, from early lesions [Figure 3(A–D)], to lesions of moderate severity [Figure 3(E,F)], to a severe form [Figure 3(G,H)]. Thickness of the periostin-positive layer and percentage of the periostin-positive area increased with the severity of fibrosis (Figure 3).

The presence of periostin ranged from no or minimal staining of extracellular matrix (score 0), to focal staining (score 1), to diffuse presence of periostin [Figure 3(G,H)]. The mean score was 1.3 [range: 0 – 2; Figure 2(A)]. The percentage of periostin-positive area (including positive vessel walls) was 19% [range: 5% – 46%; Figure 2(B)]. There was also a morphologic correlation, though nonsignificant, between the severity of submesothelial thickness and periostin staining. The mean percentage of periostin-positive area in peritoneal biopsies from uremic patients who had not started dialysis was 17% (range: 6% – 27%). That value was not significantly different from those of the other groups studied.

Tissue from PD Patients With EPS: Figure 4 illustrates the 7 biopsies from patients on PD with clinical signs of EPS. The mean thickness of the sclerotic area was 760 µm (range: 418 – 1250 µm; $p = 0.001$ vs controls, $p = 0.05$

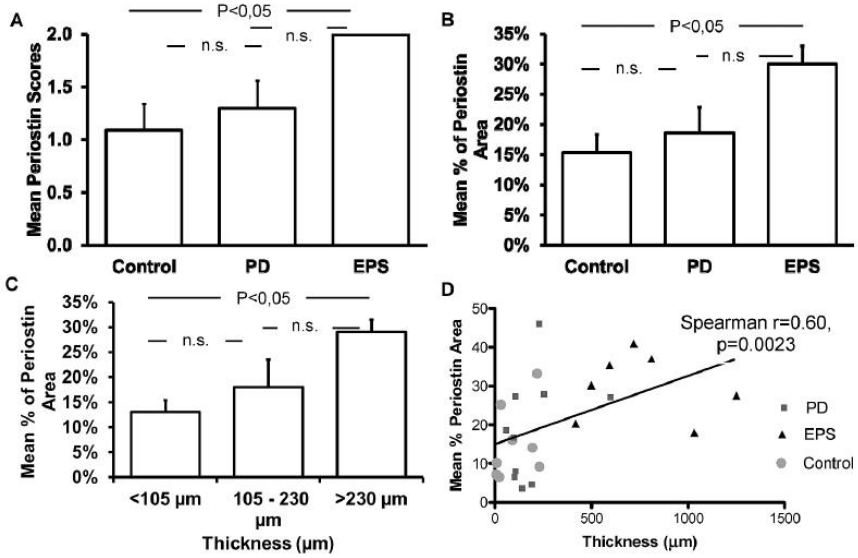

Figure 2 — Quantification of periostin staining. (A) Periostin was scored semi-quantitatively in a blinded fashion as described in the Methods section. Mean scores for the study groups are shown (error bars illustrate the standard error of the mean; n.s. = nonsignificant; PD = peritoneal dialysis; EPS = encapsulating peritoneal sclerosis). (B) Percentage of periostin staining in the submesothelial area for the study groups quantified by morphometry. (C) Percentage periostin-positive area by tertile of submesothelial thickness. (D) Correlation between submesothelial thickness (in micrometers) and the percentage periostin-positive area for the study groups.

vs PD patients). All biopsies demonstrated strong and diffuse staining of the sclerotic zone [Figure 4(A,C)]. The periostin staining appeared in layers of the sclerotic zone [Figure 4(A,B)]. The periostin-positive sclerotic zone was commonly covered by a periostin-negative layer [Figure 4(C,D)]. Entire cross-sections through the thick sclerotic membranes were impressively positive for periostin. By immunohistochemistry, periostin-negative fibroblasts were seen as a negative contrast [Figure 4(E)]. All 7 biopsies were scored as 2 (diffuse periostin staining), which was significantly different compared with the scoring for the controls [Figure 2(A)]. The mean percentage of periostin-positive area in peritoneal biopsies from patients with EPS was 30% [range: 15% – 41%; Figure 2(B)]. The morphometric quantification of periostin demonstrated a significant increase in the percentage of periostin-positive area compared with that in control biopsies [Figure 2(B)]. Using double immunofluorescence (Figure 5), the α-SMA–positive fibroblasts were embedded in the periostin-positive extracellular matrix [Figure 5(G–I)].

ASSOCIATION BETWEEN PERIOSTIN AND SUBMESOTHELIAL FIBROSIS

Figure 3 describes the morphologic association between submesothelial thickness and periostin staining for patients on PD. The mean percentage of periostin-positive staining increased with the severity of submesothelial fibrosis, illustrated in Figure 2(C) for the tertiles of submesothelial thickness (the figure includes all biopsies). Although the number of biopsies included in the present study was low, a significant correlation was observed between the thickness of the submesothelial fibrotic zone and periostin staining as reflected by the semiquantitative score or the percentage of positive area [Figure 2(D)]. A strong overlap was observed between the controls and the PD group [Figure 2(D), left side]. The EPS group had little overlap in thickness [Figure 2(D), right side], but there was some overlap in the percentage of periostin positivity.

PERITONEAL FIBROBLASTS

To further study the expression of periostin by peritoneal fibroblasts, *in vitro* studies were performed using primary peritoneal fibroblasts. Expression of periostin was quantified by real-time reverse-transcription polymerase chain reaction. Prominent expression of periostin mRNA could be documented with threshold cycles (Ct) between 23 and 26 (GAPDH: 19 – 23 Ct). High osmolarity [Figure 6(A)] and exposure to cytokines [Figure 6(B)] did not result in significant regulation of periostin.

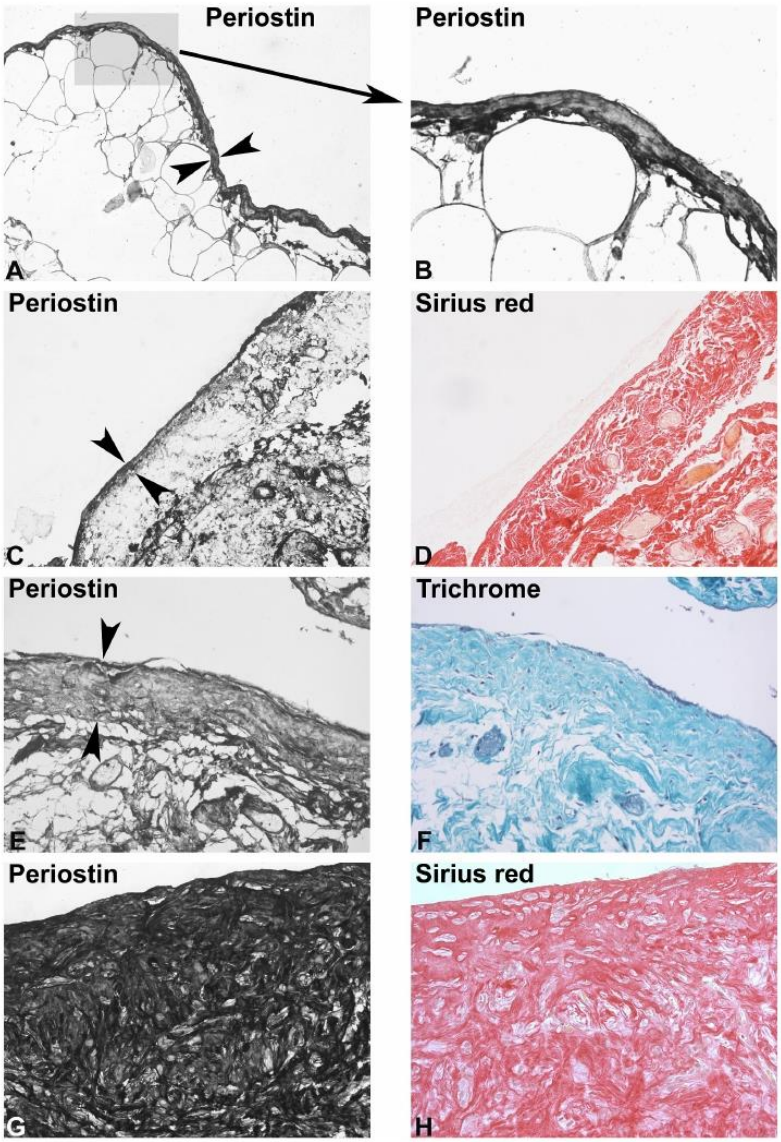

Figure 3 — Periostin in peritoneal dialysis (PD) patients. Peritoneal biopsies from PD patients were stained with (A,B,C,E,G) a polyclonal antibody against periostin, (D,H) Sirius red, and (F) Masson trichrome. Original magnification (A,C–H) 200× and (B) 630×. (A–D) These two biopsies come from the first tertile of submesothelial thickness [described in Figure 2(C)] and demonstrate early peritoneal changes, with periostin staining of the submesothelial sclerotic zone. (E) A moderate form of peritoneal fibrosis [second tertile of submesothelial thickness, indicated by the arrowheads in (A,C,E)]. (G) A severe form of peritoneal fibrosis (third tertile of submesothelial thickness). Note that the basal end of the sclerotic zone is no longer visible at this magnification. Note the prominent increase in the periostin-positive area with the progression of peritoneal fibrosis.

PERIOSTIN QUANTIFICATION IN EFFLUENT

Effluent samples from 15 patients were available for quantification of periostin [Table 3, Figure 6(C)]. For each patient, the first sample available after the start of PD and the last sample before PD withdrawal were included. In patients without EPS, a significantly higher concentration of periostin was present in the last PD effluent than in the initial effluent. Figure 6(C) illustrates periostin protein concentration normalized for its

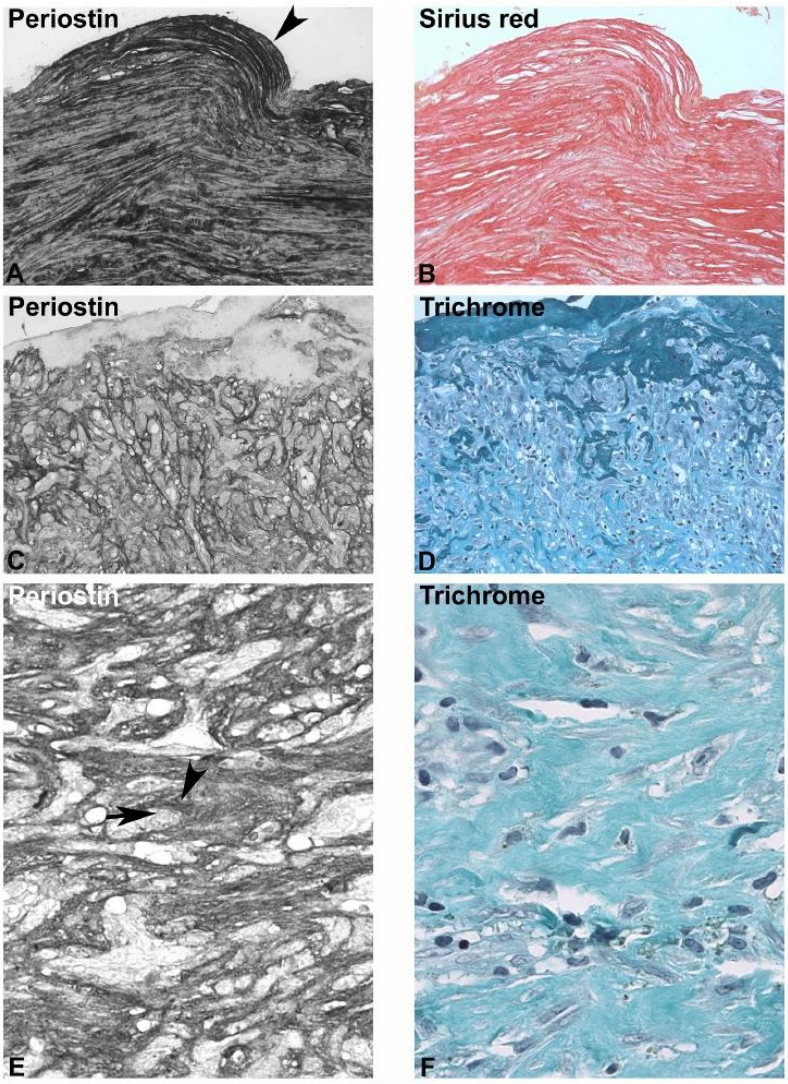

Figure 4 — Periostin in peritoneal dialysis (PD) patients with encapsulating peritoneal sclerosis (EPS). (A,C,E) Immunohistochemistry was performed using a polyclonal antiserum against periostin. Original magnification (A,C) 200× and (E) 630×. Consecutive sections were stained with (B) sirius red or (D) Masson trichrome. Original magnification (D) 200× and (F) 630×. (A,C,E) In all biopsies from patients with EPS, extracellular matrix demonstrated positive severe diffuse staining for periostin. The mesothelial cell layer was absent [arrowhead in (A)]. (A,B) Areas of fibrosis correlated with periostin-positive areas. (E) Fibroblasts and vessels were embedded in a periostin-positive extracellular matrix (arrowhead), therefore appearing in negative contrast (arrow).

concentration in the first effluent in patients without EPS ($p < 0.01$). Low concentrations of periostin were found in the last available effluent from EPS patients [Table 3, Figure 6(C)]. Intermediate samples from 5 patients (2 with fast transport status, and 3 with EPS) were available. The 3 patients with EPS demonstrated only a small nonsignificant rise in effluent periostin concentration (without a significant peak during the time course).

DISCUSSION

The mechanisms and factors underlying so-called simple peritoneal fibrosis and EPS are under intense investigation, but are still incompletely understood (27). Here, we describe a relatively new matricellular protein that is prominently expressed in both lesions. The localization to sites of fibrosis results in a positive association with the

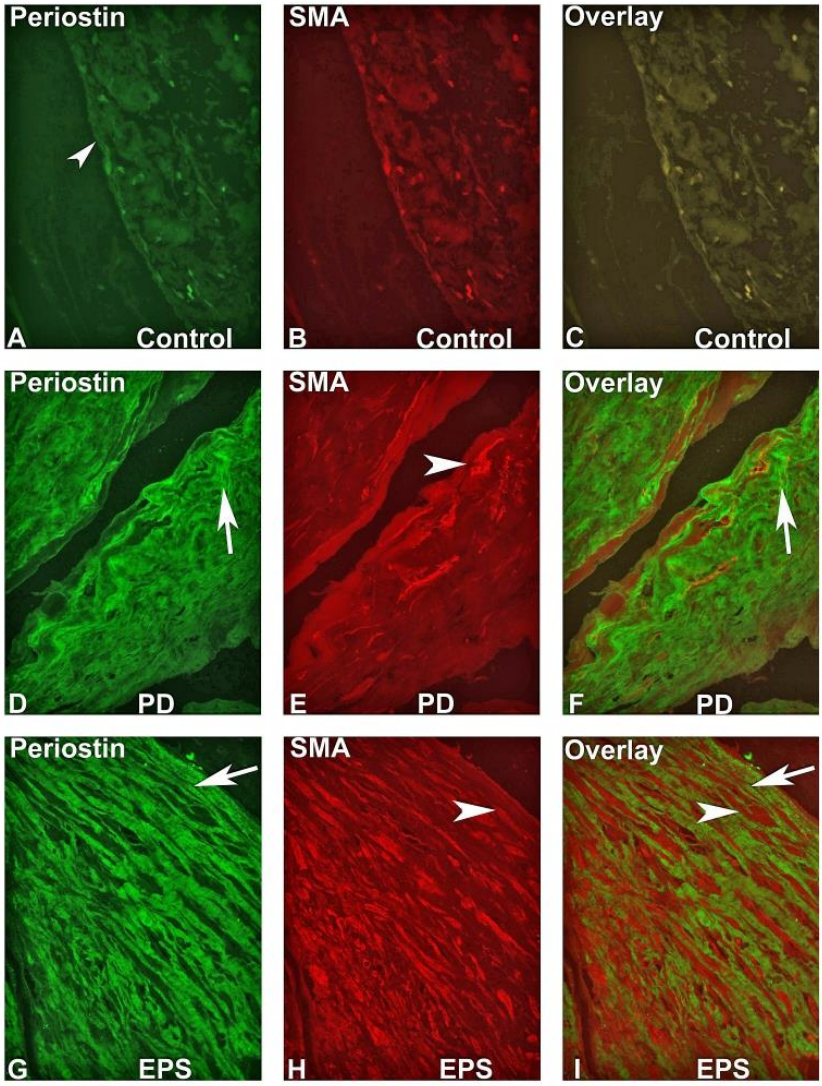

Figure 5 — Double immunofluorescence for periostin and smooth muscle actin (SMA). Double immunofluorescence was performed using (A,D,G) a polyclonal antiserum against periostin and (B,E,H) a monoclonal antibody against SMA on tissue sections from peritoneal biopsies taken (A–C) during hernia repair, (D–F) from patients on PD, and (G–I) from PD patients with encapsulating peritoneal sclerosis (EPS). (C,F,I) Immunofluorescence overlay. All images, original magnification 400×. (A–C) In the control tissue, no positive staining for periostin was evident (arrowhead localizes the tissue border). Prominent staining for periostin (arrow) was present (D) in a patient on PD and (G) in a PD patient with EPS. (E,H) Fibroblasts positive for SMA (red) are embedded in the periostin-positive matrix (arrowheads).

thickness of the submesothelial fibrotic area. Periostin protein localized by immunohistochemistry does not discriminate between EPS and simple fibrosis, but it might be involved in the pathogenesis of both lesions. Only in EPS biopsies was the area of periostin staining significantly increased compared with staining in controls. Biopsies with increased submesothelial fibrosis demonstrated larger areas of periostin staining in patients on PD. On the other hand, periostin in effluent increased with time on PD, but patients with EPS demonstrated low effluent periostin concentrations at the time of EPS diagnosis. Based on our data and the current literature, several hypotheses concerning the role of periostin in peritoneal tissue remodeling can be advanced.

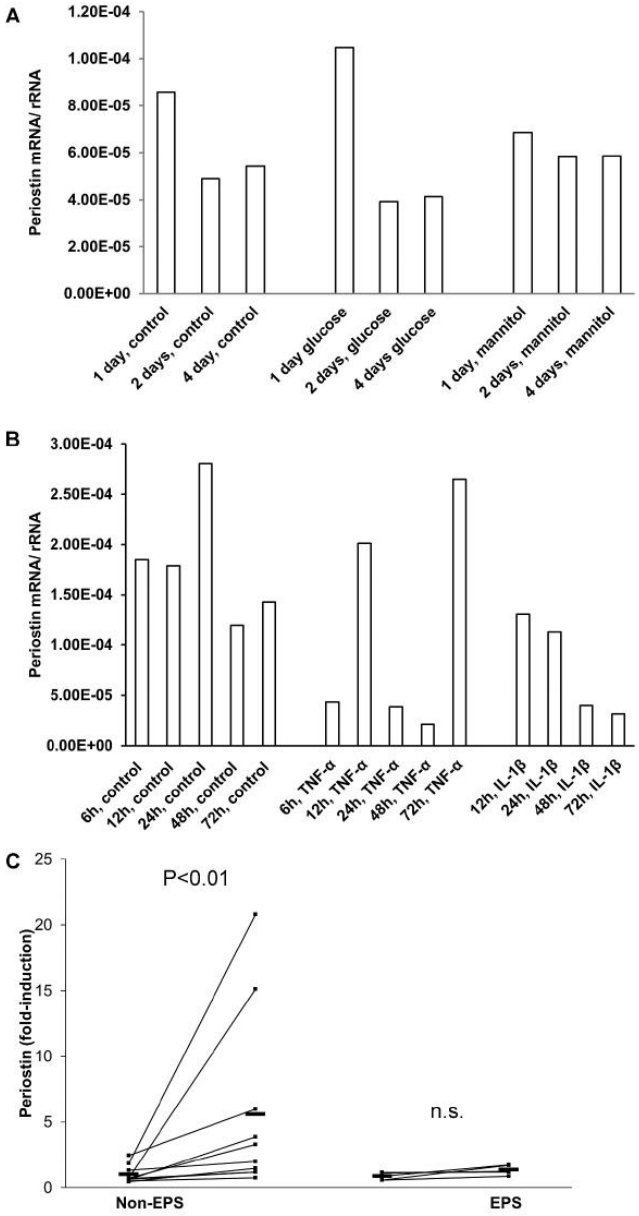

Figure 6 — Quantification of periostin *in vitro* and *in vivo* in effluent. Periostin messenger RNA (mRNA) expression in peritoneal fibroblasts *in vitro* after exposure (A) to glucose or (B) to cytokines as described in the Methods section. Although periostin was prominently expressed by peritoneal fibroblasts, no regulation was detectable under the conditions tested. (C) Periostin was quantified by ELISA in the first and last effluent available from 15 patients. The graph illustrates the factor by which periostin was induced in effluent, normalized to the concentration in the first effluent from patients without encapsulating peritoneal sclerosis (EPS). Significant induction was found in the last available effluent sample from patients without EPS ($p < 0.01$). Patients with EPS demonstrated a low level of periostin in the last effluent sample available (n.s. = nonsignificant).

Simple peritoneal fibrosis and EPS have, in part, overlapping morphology, because EPS develops in long-term PD patients with simple fibrosis. In both processes, the typical features in which periostin might be involved are fibroblast activation with extracellular matrix formation, angiogenesis, and epithelial-to-mesenchymal

TABLE 3
Clinical Characteristics of the Study Population for Periostin in Effluent

Variable	Pts (*n*)	Sex (female)	Age (years)	Time on PD (months)	Periostin Protein	Periostin Induction factor
High transport	5	1	66 (51–80)	31.9 (23–44)	1±0.26	4.9±3.6
Low transport	5	4	54 (28–81)	41.3 (11–80)	1±0.1	7±2.7[b]
EPS	5	1	51 (39–62)	61.5 (34–101)	1±0.15	1.6±0.19
All	15	6	57 (28–81)	44.9 (11–101)	1±0.1	4.5±1.7[c]

PD = peritoneal dialysis; EPS = encapsulating peritoneal sclerosis.
[a] Values expressed as mean and range for age and time on peritoneal dialysis; periostin protein and factor for induction of the protein (± standard error of the mean) in effluent normalized to first effluent for the corresponding group; the "low transport" group combines low and low-average transporters.
[b] $p < 0.05$ compared with first effluent.
[c] $p < 0.001$.

differentiation (27). Periostin staining did not help to distinguish the lesions, but all patients with EPS demonstrated severe diffuse deposition of periostin. Because time on PD was longer in the EPS group, we cannot definitively determine whether the increased periostin expression was a result of the pathogenesis of EPS or simply a reflection of longer time on PD with more prominent lesions of simple fibrosis. We have to acknowledge here the main limitation of our study, which is its small sample size and an absence of significance for both scored and measured periostin protein in biopsies from PD patients.

Transforming growth factor β has been described to be induced during PD and is a key factor in peritoneal fibrosis and fibroblast activation (27). This growth factor directly induces formation of extracellular matrix, but it also induces expression of periostin (7). The prominent expression of periostin in biopsies from patients on PD and with EPS is therefore consistent with data describing induction of TGF-β in PD and EPS. On the other hand, periostin can, *per se*, induce TGF-β expression (11). A vicious cycle can easily be envisioned in which induction of periostin might promote ongoing formation of active TGF-β. Additionally, periostin promotes collagen fibrillogenesis and crosslinking and leads to stiffening of the matrix (11). The expression of matrix metalloproteinase 2 (MMP2), a tissue remodeler, was found to be increased by periostin (34). The presence of MMP2 in PD effluents (35,36) and in experimental peritoneal fibrosis (37) has been described. Expression of MMP2 might therefore be a downstream event. These complex interactions can now be evaluated in future studies.

Angiogenesis and vasculopathy are prominent findings in peritoneal fibrosis associated with PD and might be the driving force in technique failure (38). Vascular endothelial growth factor A (VEGFA) has been shown to be important in that process (38,39). Tumors promote angiogenesis through the release of periostin (40). Periostin mediates angiogenesis through an integrin-dependent induction of vascular endothelial growth factor receptor 2 expression (40). Periostin in the peritoneum might therefore modulate the response of endothelial cells to VEGFA.

The transformation of epithelial cells to cells with fibroblastic appearance during PD has recently attracted much attention (38,41). This transformation might be a source for fibroblasts, the major contributors to extracellular matrix production. Periostin has been shown to promote cellular dedifferentiation and transformation [reviewed in Ruan *et al.* (18)]. Those three processes (dedifferentiation, extracellular matrix deposition, and angiogenesis) show complex interaction because TGF-β is a major mediator of cellular transformation, and mesothelial cells undergoing dedifferentiation demonstrate increased expression of growth factors such as VEGFA (38). Further studies in human and animal models, including knockout mice, are necessary to illuminate the exact role of this protein in the pathogenesis of peritoneal fibrosis during PD.

With time on PD, the amount of periostin in dialysate increased significantly in patients with simple fibrosis. Consistently, the area of periostin staining was associated with submesothelial thickness (also, the mean percentage of periostin in PD patients was not significantly different from that in control subjects). Our first hypothesis, that periostin might be regulated by osmolarity or cytokines (or both) was not confirmed by our *in vitro* experiments. Rather, we found prominent expression, an association with tissue fibrosis, and the presence of myofibroblasts. The increased number of

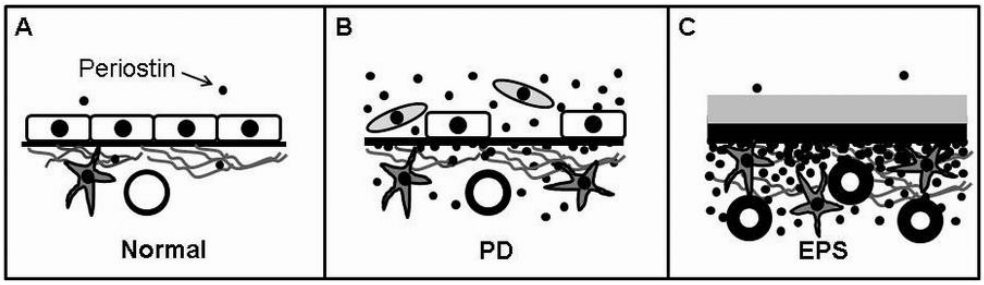

Figure 7 — Hypothetical schema for periostin capture in the peritoneal membrane in encapsulating peritoneal sclerosis (EPS). (A) The normal mesothelial cell layer with some periostin positivity in the submesothelial tissue and the vessel wall. (B) The situation of peritoneal fibrosis during peritoneal dialysis (PD), with loss of mesothelial cells, thickening of the submesothelial zone, increasing deposition of periostin in the extracellular matrix, and a significant amount of periostin in the peritoneal fluid. (C) The situation in EPS, with complete loss of mesothelial cells and formation of a fibrin layer on the mesothelial surface (shown in gray). Deposition of periostin is prominent in the sclerotic zone and sclerotic vessels, but the peritoneal fluid contains only a little periostin, which might be a result of either periostin trapping by the submesothelial extracellular matrix or capture of periostin by the fibrin-positive layer, or both.

fibroblasts might therefore be the main cause of the increased deposition of periostin, rather than increased expression per fibroblast.

An unexpected finding was the low level of periostin in effluent from patients with EPS [Figure 6(C)]. Morphologically, periostin is prominently present in the thick areas of sclerosis found in EPS [Figure 7(C)]. Morphologic features that might help to differentiate EPS from simple fibrosis are deposition of fibrin and increased thickness of the degenerative compact zone (42). Periostin might find its way into effluent in patients on PD without EPS, but not in patients with signs of EPS [Figure 7(B,C)]. Comparing the first and last effluents during the time course of dialysis, patients with EPS demonstrated the smallest increase in periostin. That finding might be related either to the thick deposition of fibrin present on the peritoneal surface or to periostin being "trapped" by the matrix in the compact zone. To determine whether periostin could be a biomarker for EPS development, future experiments should include more longitudinal measurements of periostin in effluent from long-term PD patients at risk for EPS. We had multiple effluent samples only from 3 patients with EPS, and periostin levels were low throughout the time course in those patients.

CONCLUSIONS

Here, we present the first data that localize periostin in the lesions of simple peritoneal fibrosis and EPS in patients on PD. Our hypothesis is that, during peritoneal exposure to PD solutions, induction of TGF-β stimulates fibroblast proliferation and the production and deposition of periostin. The periostin might promote ongoing matrix expansion (fibrosis), angiogenesis, and cellular transformation, resulting in technique failure. That sequence of events is supported by a higher periostin concentration with prolonged time on PD. This hypothesis can now be addressed with *in vitro* and animal models. Finally, periostin might be a suitable therapeutic target to prevent peritoneal remodeling in PD patients.

ACKNOWLEDGMENTS

SS is supported by a grant from Baxter Healthcare, a grant from the Swiss National Science Foundation (SNF 32003B_129710) and by the C.K.M. Stiftung. NB is supported by the Robert-Bosch Foundation and a grant from Baxter Healthcare. CDC is also supported by the Swiss National Science Foundation (32-122439/1). Microscopes were provided by the Center of Microscopy and Image Analysis (University of Zurich). We thank Olivier Devuyst for helping with the acquisition of effluent probes.

DISCLOSURES

The present study was supported by a grant from Baxter Healthcare. SS receives benefits from Roche as a consultant. The remaining authors have no financial conflicts of interest to declare.

REFERENCES

1. Margetts PJ, Bonniaud P. Basic mechanisms and clinical implications of peritoneal fibrosis. *Perit Dial Int* 2003; 23:530–41.
2. Alscher DM, Reimold F. New facts about encapsulating peritoneal sclerosis as a sequel of long-term peritoneal

dialysis—what can we do? *Minerva Urol Nefrol* 2007; 59:269–79.
3. Augustine T, Brown PW, Davies SD, Summers AM, Wilkie ME. Encapsulating peritoneal sclerosis: clinical significance and implications. *Nephron Clin Pract* 2009; 111:c149–54.
4. Honda K, Nitta K, Horita S, Tsukada M, Itabashi M, Nihei H, *et al.* Histologic criteria for diagnosing encapsulating peritoneal sclerosis in continuous ambulatory peritoneal dialysis patients. *Adv Perit Dial* 2003; 19:169–75.
5. Alscher DM, Braun N, Biegger D, Fritz P. Peritoneal mast cells in peritoneal dialysis patients, particularly in encapsulating peritoneal sclerosis patients. *Am J Kidney Dis* 2007; 49:452–61.
6. Takeshita S, Kikuno R, Tezuka K, Amann E. Osteoblast-specific factor 2: cloning of a putative bone adhesion protein with homology with the insect protein fasciclin I. *Biochem J* 1993; 294:271–8.
7. Horiuchi K, Amizuka N, Takeshita S, Takamatsu H, Katsuura M, Ozawa H, *et al.* Identification and characterization of a novel protein, periostin, with restricted expression to periosteum and periodontal ligament and increased expression by transforming growth factor beta. *J Bone Miner Res* 1999; 14:1239–49.
8. Gillan L, Matei D, Fishman DA, Gerbin CS, Karlan BY, Chang DD. Periostin secreted by epithelial ovarian carcinoma is a ligand for $\alpha_V\beta_3$ and $\alpha_V\beta_5$ integrins and promotes cell motility. *Cancer Res* 2002; 62:5358–64.
9. Norris RA, Moreno–Rodriguez R, Hoffman S, Markwald RR. The many facets of the matricellular protein periostin during cardiac development, remodeling, and pathophysiology. *J Cell Commun Signal* 2009; 3:275–86.
10. Zhu M, Fejzo MS, Anderson L, Dering J, Ginther C, Ramos L, *et al.* Periostin promotes ovarian cancer angiogenesis and metastasis. *Gynecol Oncol* 2010; 119:337–44.
11. Sidhu SS, Yuan S, Innes AL, Kerr S, Woodruff PG, Hou L, *et al.* Roles of epithelial cell-derived periostin in TGF-beta activation, collagen production, and collagen gel elasticity in asthma. *Proc Natl Acad Sci U S A* 2010; 107:14170–5.
12. Kii I, Amizuka N, Minqi L, Kitajima S, Saga Y, Kudo A. Periostin is an extracellular matrix protein required for eruption of incisors in mice. *Biochem Biophys Res Commun* 2006; 342:766–72.
13. Norris RA, Kern CB, Wessels A, Moralez EI, Markwald RR, Mjaatvedt CH. Identification and detection of the periostin gene in cardiac development. *Anat Rec A Discov Mol Cell Evol Biol* 2004; 281:1227–33.
14. Kruzynska–Frejtag A, Machnicki M, Rogers R, Markwald RR, Conway SJ. Periostin (an osteoblast-specific factor) is expressed within the embryonic mouse heart during valve formation. *Mech Dev* 2001; 103:183–8.
15. Rios H, Koushik SV, Wang H, Wang J, Zhou HM, Lindsley A, *et al.* Periostin null mice exhibit dwarfism, incisor enamel defects, and an early-onset periodontal disease-like phenotype. *Mol Cell Biol* 2005; 25:11131–44.
16. Asakura M, Kitakaze M. Global gene expression profiling in the failing myocardium. *Circ J* 2009; 73:1568–76.
17. Dobaczewski M, Gonzalez–Quesada C, Frangogiannis NG. The extracellular matrix as a modulator of the inflammatory and reparative response following myocardial infarction. *J Mol Cell Cardiol* 2010; 48:504–11.
18. Ruan K, Bao S, Ouyang G. The multifaceted role of periostin in tumorigenesis. *Cell Mol Life Sci* 2009; 66:2219–30.
19. Lindenmeyer MT, Eichinger F, Sen K, Anders HJ, Edenhofer I, Mattinzoli D, *et al.* Systematic analysis of a novel human renal glomerulus-enriched gene expression dataset. *PLoS One* 2010; 5:e11545.
20. Sen K, Lindenmeyer MT, Gaspert A, Eichinger F, Neusser MA, Kretzler M, *et al.* Periostin is induced in glomerular injury and expressed *de novo* in interstitial renal fibrosis. *Am J Pathol* 2011; 179:1756–67.
21. Pohjolainen V, Rysa J, Napankangas J, Koobi P, Eraranta A, Ilves M, *et al.* Left ventricular periostin gene expression is associated with fibrogenesis in experimental renal insufficiency. *Nephrol Dial Transplant* 2012; 27:115–22.
22. Satirapoj B, Wang Y, Chamberlin MP, Dai T, LaPage J, Phillips L, *et al.* Periostin: novel tissue and urinary biomarker of progressive renal injury induces a coordinated mesenchymal phenotype in tubular cells. *Nephrol Dial Transplant* 2012; 27:2702–11.
23. Zou P, Wu LL, Wu D, Fan D, Cui XB, Zhou Y, *et al.* High glucose increases periostin expression and the related signal pathway in adult rat cardiac fibroblasts [Chinese]. *Sheng Li Xue Bao* 2010; 62:247–54.
24. Bolton K, Segal D, McMillan J, Sanigorski A, Collier G, Walder K. Identification of secreted proteins associated with obesity and type 2 diabetes in *Psammomys obesus*. *Int J Obes (Lond)* 2009; 33:1153–65.
25. Günal AI, Duman S, Sen S, Unsal A, Terzioğlu E, Akçiçek F, *et al.* By reducing TGF beta 1, octreotide lessens the peritoneal derangements induced by a high glucose solution. *J Nephrol* 2001; 14:184–9.
26. Ha H, Lee HB. Effect of high glucose on peritoneal mesothelial cell biology. *Perit Dial Int* 2000; 20(Suppl 2):S15–18.
27. Schilte MN, Celie JW, Wee PM, Beelen RH, van den Born J. Factors contributing to peritoneal tissue remodeling in peritoneal dialysis. *Perit Dial Int* 2009; 29:605–17.
28. Braun N, Alscher DM, Fritz P, Edenhofer I, Kimmel M, Gaspert A, *et al.* Podoplanin-positive cells are a hallmark of encapsulating peritoneal sclerosis. *Nephrol Dial Transplant* 2011; 26:1033–41.
29. Neusser MA, Kraus AK, Regele H, Cohen CD, Fehr T, Kerjaschki D, *et al.* The chemokine receptor cxcr7 is expressed on lymphatic endothelial cells during renal allograft rejection. *Kidney Int* 2010; 77:801–8.
30. Jedlicka J, Soleiman A, Draganovici D, Mandelbaum J, Ziegler U, Regele H, *et al.* Interstitial inflammation in Alport syndrome. *Hum Pathol* 2010; 41:582–93.
31. Witowski J, Jörres A. Peritoneal cell culture: fibroblasts. *Perit Dial Int* 2006; 26:292–9.
32. Cohen CD, Frach K, Schlondorff D, Kretzler M. Quantitative gene expression analysis in renal biopsies: a novel

protocol for a high-throughput multicenter application. *Kidney Int* 2002; 61:133–40.
33. Ben QW, Zhao Z, Ge SF, Zhou J, Yuan F, Yuan YZ. Circulating levels of periostin may help identify patients with more aggressive colorectal cancer. *Int J Oncol* 2009; 34:821–8.
34. Hakuno D, Kimura N, Yoshioka M, Mukai M, Kimura T, Okada Y, *et al.* Periostin advances atherosclerotic and rheumatic cardiac valve degeneration by inducing angiogenesis and MMP production in humans and rodents. *J Clin Invest* 2010; 120:2292–306.
35. Hirahara I, Inoue M, Okuda K, Ando Y, Muto S, Kusano E. The potential of matrix metalloproteinase-2 as a marker of peritoneal injury, increased solute transport, or progression to encapsulating peritoneal sclerosis during peritoneal dialysis—a multicentre study in Japan. *Nephrol Dial Transplant* 2007; 22:560–7.
36. Kurata K, Maruyama S, Kato S, Sato W, Yamamoto J, Ozaki T, *et al.* Tissue-type plasminogen activator deficiency attenuates peritoneal fibrosis in mice. *Am J Physiol Renal Physiol* 2009; 297:F1510–17.
37. Yamamoto D, Takai S, Hirahara I, Kusano E. Captopril directly inhibits matrix metalloproteinase-2 activity in continuous ambulatory peritoneal dialysis therapy. *Clin Chim Acta* 2010; 411:762–4.
38. Devuyst O, Margetts PJ, Topley N. The pathophysiology of the peritoneal membrane. *J Am Soc Nephrol* 2010; 21:1077–85.
39. Braun N, Reimold F, Biegger D, Fritz P, Kimmel M, Ulmer C, *et al.* Fibrogenic growth factors in encapsulating peritoneal sclerosis. *Nephron Clin Pract* 2009; 113:c88–95.
40. Shao R, Bao S, Bai X, Blanchette C, Anderson RM, Dang T, *et al.* Acquired expression of periostin by human breast cancers promotes tumor angiogenesis through up-regulation of vascular endothelial growth factor receptor 2 expression. *Mol Cell Biol* 2004; 24:3992–4003.
41. Kim YL. Update on mechanisms of ultrafiltration failure. *Perit Dial Int* 2009; 29(Suppl 2):S123–7.
42. Sherif AM, Yoshida H, Maruyama Y, Yamamoto H, Yokoyama K, Hosoya T, *et al.* Comparison between the pathology of encapsulating sclerosis and simple sclerosis of the peritoneal membrane in chronic peritoneal dialysis. *Ther Apher Dial* 2008; 12:33–41.

CHAPTER V

PRELIMINARY DATA: Functional studies on periostin

Cell cycle analysis and apoptosis

Our previous studies showed that periostin induces cell proliferation and decreases the number of apoptotic cells (see chapter III) [196].

Material and Methods

To study the effect of periostin on apoptosis, cell cycle analyses were performed by flow cytometry using propidium iodide and annexin V binding (eBioscience, Vienna, Austria). Human and murine mesangial cells (HMC; MMC) were plated on six-well plates. Cells were starved in medium (DMEM; Gibco, Invitrogen) containing 0.5% fetal bovine serum (FBS) 24 hours before exposure for 48 hours to human periostin (100-1000 ng/ml; Biovendor, Heidelberg, Germany) or vehicle. Induction of apoptosis as positive control was performed as described in Lorz et al. [197].
Statistical analyses (Kruskall-Wallis and Mann-Whitney U-tests) were performed using SPSS 17.0 (Spss., Chicago, IL). P values < 0.05 were considered to indicate statistically significant results.

Results

Mechanisms that promote cell survival or prevent apoptosis are considered to promote cell proliferation. An antiapoptotic effect of periostin was found in our experiments (Figure 4). The number of apoptotic cells was reduced by 9.3% and 9.7% when incubated with 100 ng/ml and 1000 ng/ml periostin, respectively. This result corresponded to other reports with different cell types [198, 199].

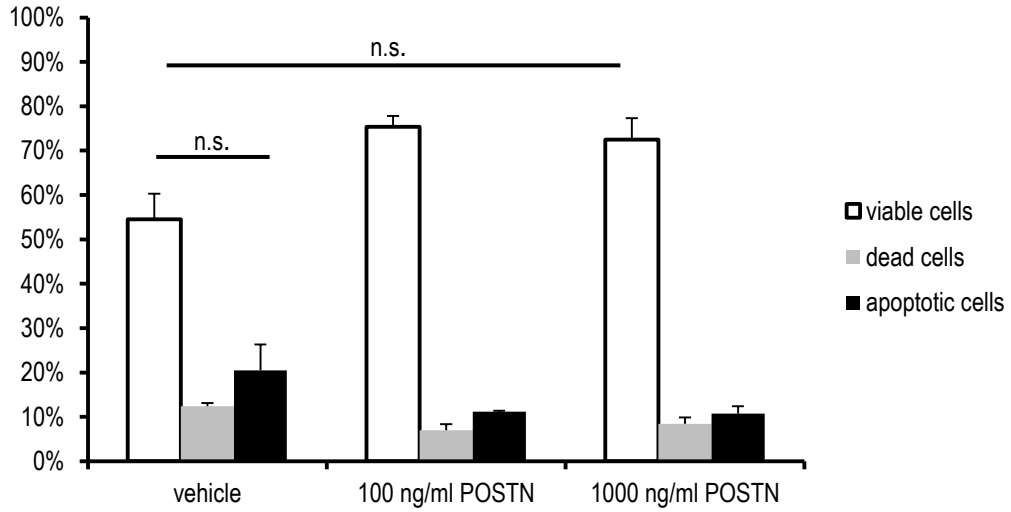

Figure 4: Effects of periostin on apoptosis

Cultured human mesangial cells (HMC) were incubated in 0.5% FBS control media or media containing 100 ng/ml to 1000 ng/ml recombinant periostin. The number of apoptotic cells was reduced when incubated with recombinant periostin. n=2; n.s. not significant

Periostin-deficient mice

In our human renal biopsies periostin was expressed in healthy human glomeruli. In patients with proteinuric glomerulopathies we found increased expression in glomeruli and in the fibrotic tubular interstitium.

Material and Methods

Periodic acid-Schiff (PAS) silver staining was performed to study the renal morphology in periostin-deficient mice. Immunohistochemistry for periostin was established in murine renal tissue as previously described [200]. In brief, dewaxed and rehydrated tissue sections were incubated in 3% hydrogen peroxide to block endogenous peroxidases. The Avidin/Biotin blocking kit was used to block endogenous biotin (Vector Laboratories, Burlingame, CA). Antigen retrieval was performed in a microwave oven in hydrochloric acid solution with a pH of 0.9 for periostin and in an autoclave oven in an antigen unmasking solution with a pH of 6 (Vector Laboratories) for α-smooth muscle actin (α-SMA, M0851; DAKO, Glostrup, Denmark), respectively. The primary antibody was applied for 1 hour, and incubation with the biotinylated secondary antibody for 30 minutes was followed by the ABC reagent (Vector Laboratories). 3,3′-Diaminobenzidine (Sigma, Taufkirchen, Germany) with metal enhancement (resulting in a black product) was used as a detection system. A monoclonal rat anti-mouse periostin antibody was used (MAB3548; R&D Systems, Germany). Blocking experiments were performed with a recombinant periostin protein (2955-F2; R&D Systems), which completely abolished the signal.

Renal tissue from periostin-deficient and wildtype mice (4- and 12-weeks old) were received from Dr. Simon Conway (Herman B Wells Center for Pediatric Research, Department of Pediatrics, Indiana University of Medicine, Indianapolis) [201].
Serum analyses from mice were performed with the Piccolo Xpress chemistry analyzer (Abaxis, Griesheim, Germany) using the renal function panel. Serum samples from wildtype (6-weeks old n=14, 24-weeks old n=9) and periostin-deficient mice (6-weeks old n=17, 24-weeks old n=9) were obtained from Dr. Nicolas Bonnet and Dr. Serge Ferrari (University Geneva Hospital, Service of Bone Diseases, Switzerland) [202].

Results

Periodic acid-Schiff (PAS) silver staining and immunohistochemistry for α-smooth muscle actin (α-SMA) was performed in murine renal tissue of wildtype and periostin-deficient mice.

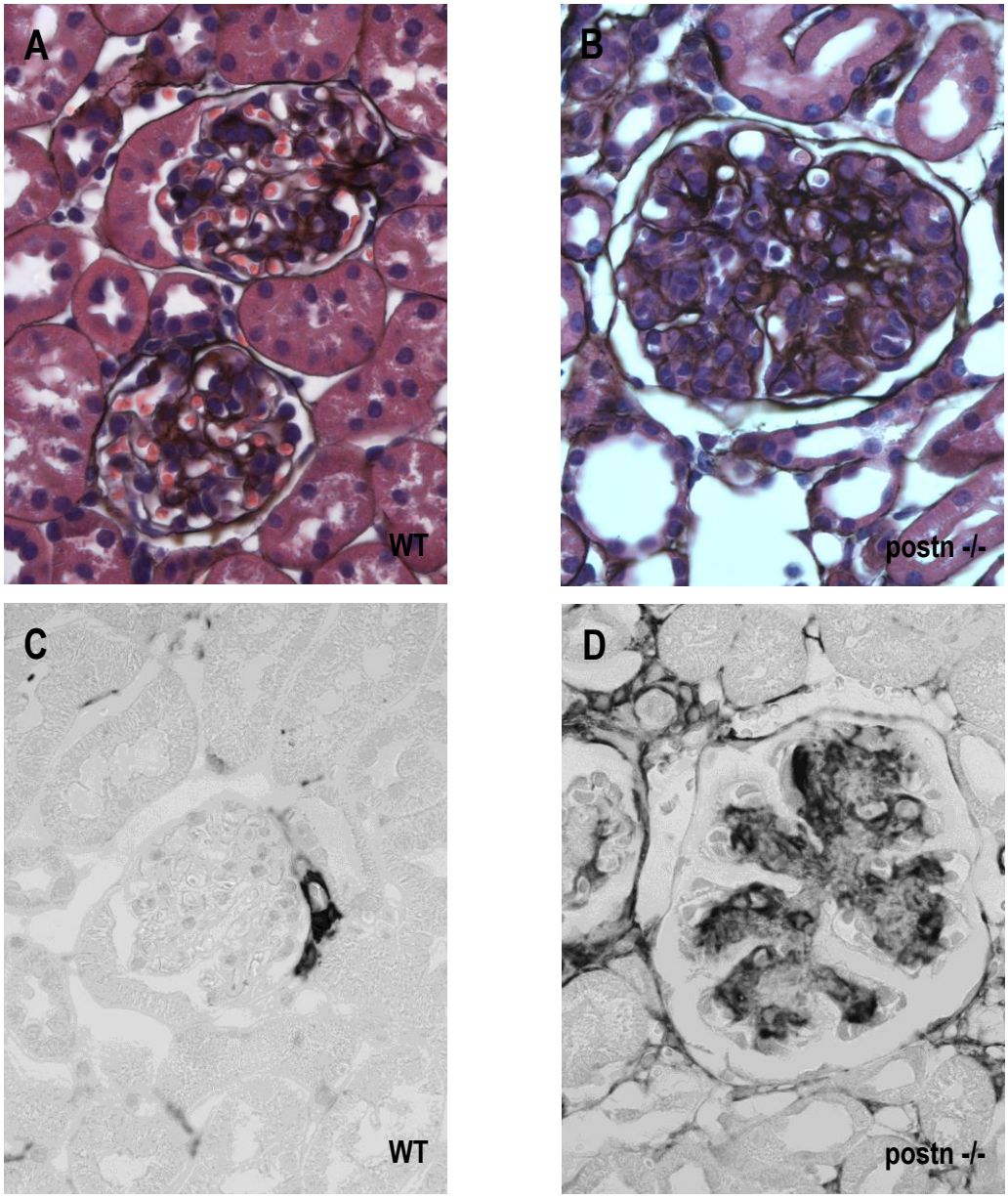

Figure 5: PAS silver staining

PAS silver staining of renal tissue from adult (12-weeks old) mice showed enlarged glomeruli in periostin-deficient (postn -/-) mice (B) compared to wildtype (WT) mice (A). 40x

Immunohistochemistry staining for α-smooth muscle actin (α-SMA) showed a proliferative mesangium (D) in the periostin-deficient glomeruli.

To study the expression and localization of the periostin protein in renal tissue from healthy wildtype mice, immunohistochemistry was established on formalin-fixed, paraffin-embedded murine renal tissue (Figure 6). A similar staining pattern as in human renal tissue was found.

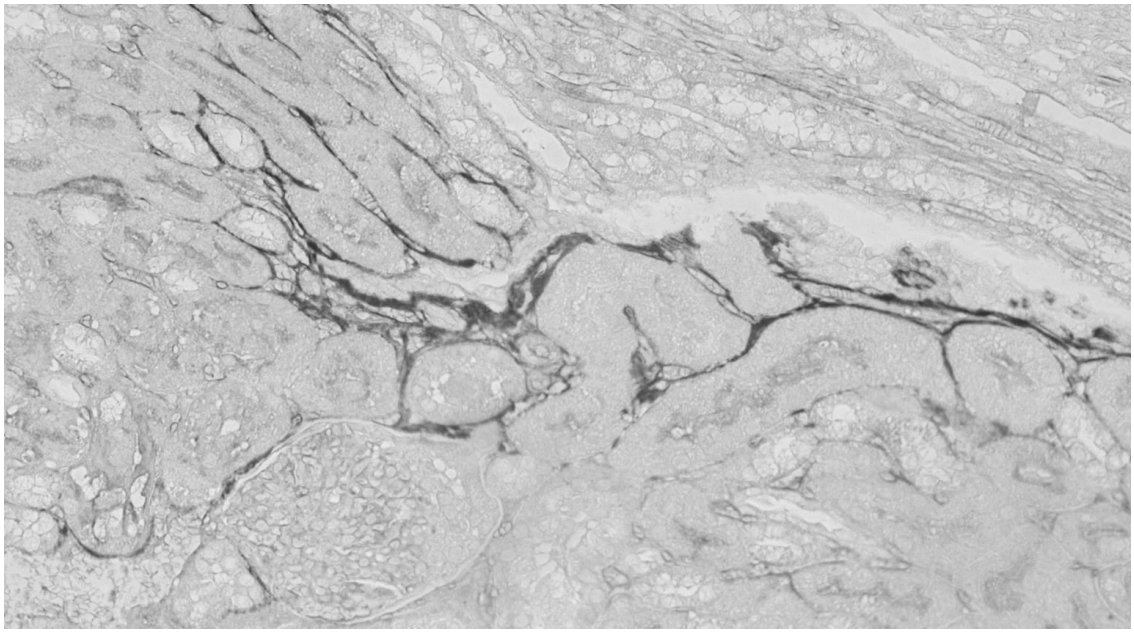

Figure 6: Localization of periostin in murine renal tissue

Adult murine renal tissue was used to establish a staining protocol for periostin in mice. Periostin was found to be expressed along the Bowman's capsule and in regions with interstitial fibrosis. 20x

As our previous *in-vitro* and *ex-vivo* human studies on periostin showed that serum marker levels differentiate, further studies on murine serum samples were performed. We compared serum data from wildtype mice and periostin-deficient mice with age of six and twelve weeks.

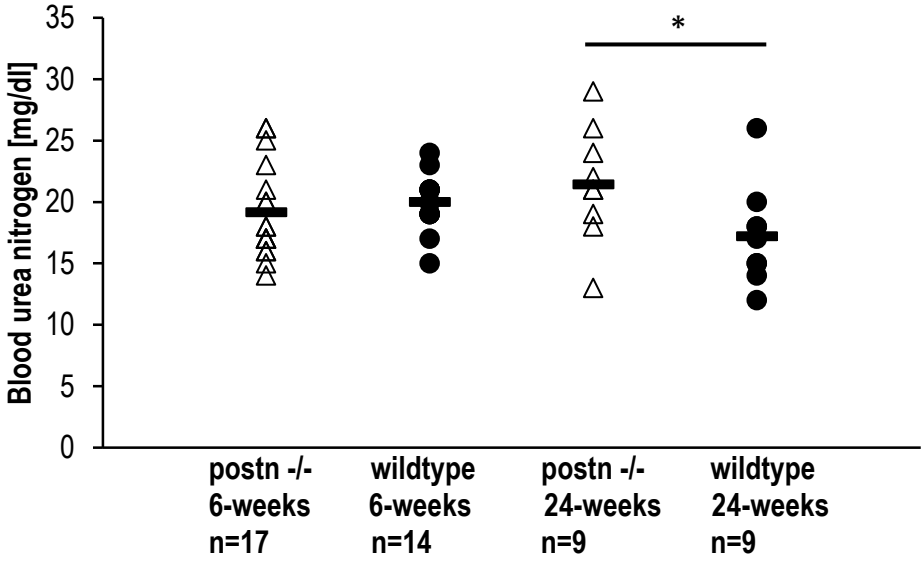

Figure 7: Blood urea nitrogen level

*The blood urea nitrogen (BUN) level was significantly higher in adult periostin-deficient mice (postn -/-) compared to wildtype mice. * $p<0.05$*

Unexpected, but according to our previous renal morphology studies periostin-deficient mice showed worse renal function (Figure 5 and 7). As example the blood urea nitrogen (BUN) value was increased which indicates an existing renal damage. The level of BUN was significantly higher in adult periostin-deficient mice 21.4 ± 4.7 mg/dl versus wildtype 17.2 ± 4.1 mg/dl (Figure 7).

This unexpected result accorded with our renal biopsy studies as the PAS silver staining revealed worse renal constitution in periostin-deficient mice (Figure 5). Comparison of the other serum data showed no significant aberrations (Table 1).

Table 1: Renal values

Elevated blood urea nitrogen level was measured in periostin-deficient mice (postn -/-) compared to wildtype mice.

postn -/- 6-weeks old n=17; wildtype 6-weeks old n=14; postn -/- 24-weeks old n=9; wildtype 24-weeks old n=9

Abbreviations: *GLU=Glucose; BUN=Blood Urea Nitrogen; CA=Calcium; CRE=Creatinine; ALB=Albumin; PHOS=Phosphorus; Na+=Sodium; K+=Potassium; Cl-=Chloride; tC02=Total Carbon Dioxide*

Genotype	Age	GLU [mg/dl]	BUN [mg/dl]	CA [mg/dl]	CRE [mg/dl]	ALB [g/dl]
postn -/-	6 weeks	188.4 ± 43.8	19.2 ± 3.8	9.5 ± 0.3	<0.2	1.9 ± 0.1
wildtype	6 weeks	218.4 ± 36.2	19.9 ± 2.3	9.8 ± 0.4	<0.2	1.9 ± 0.1
postn -/-	24 weeks	169.4 ± 21.9	21.4 ± 4.7	8.7 ± 0.5	<0.2	1.9 ± 0.2
wildtype	24 weeks	171.0 ± 23.1	17.2 ± 4.1	8.6 ± 0.3	<0.2	1.7 ± 0.3

Genotype	Age	PHOS [mmol/l]	Na^+ [mmol/l]	K^+ [mmol/l]	Cl^- [mg/dl]	tCO_2 [mmol/l]
postn -/-	6 weeks	8.6 ± 0.8	145.2 ± 1.7	5.4 ± 0.5	102.8 ± 1.0	19.5 ± 3.2
wildtype	6 weeks	7.8 ± 0.7	145.4 ± 2.9	5.3 ± 0.3	103.1 ± 2.4	19.5 ± 3.8
postn -/-	24 weeks	6.1 ± 0.6	146.0 ± 1.7	6.7 ± 1.2	103.3 ± 2.0	13.0 ± 1.9
wildtype	24 weeks	6.5 ± 1.0	144.3 ± 3.0	5.8 ± 0.5	103.4 ± 1.9	13.9 ± 2.2

CHAPTER VI

PRELIMINARY DATA: TSC22D3 – a glucocorticoid-induced leucine zipper repressed in renal disease

INTRODUCTION

Glucocorticoids are involved in physiological regulation of a variety of processes, including immune responses, metabolism, cell growth, and development [203]. Patients with renal diseases are initially treated with glucocorticoids and a majority of them respond rapidly with improvement of proteinuria or even full remission.

On our transcriptomic approach to study mechanisms involved in renal diseases, TSC22D3 was found to be significantly repressed in the main acquired proteinuric diseases MCD, FSGS and MGN. TSC22D3, also known as glucocorticoid-induced leucine zipper (GILZ), was first identified in a study with thymocytes and T-cells [204]. Several studies indicated that TSC22D3 has a key role in anti-inflammatory and immunosuppressive processes. In the kidney, up-regulation of TSC22D3 was stimulated by aldosterone in a mouse kidney collecting duct principal cell (mCCD) line. Furthermore, TSC22D3 was associated with up-regulation of the α-subunit of the renal ENaC channel [205].

The main aim of the study was to investigate the role of TSC22D3 in cultured glomerular epithelial cells, so called podocytes. In addition to the *in-vitro* experiments also very pre-functional studies in drosophila flies were initiated.

MATERIAL AND METHODS

Renal Biopsies for mRNA Analysis and Quantitative Real-Time RT-PCR

As described before in Sen et al. [196]. Predeveloped TaqMan reagents were used for human TSC22D3 (Hs00933671_m1; Applied Biosystems Europe, Rotkreuz, Switzerland). For the human TSC22D3 variants the following oligonucleotide primers and probe were used: TSC22D3-1 sense primer 5'-ACCAGACCATGCTCTCCATC-3', antisense primer 5'-GGCCTGTTCGATCTTGTTGT-3', fluorescence labeled probe (6-FAM) 5'-TCTTCTTCCACAGTGCCTCC-3'; TSC22D3-2 sense primer 5'-CTTGGAGGGGATGTGGTTT-3', antisense primer 5'-GGCCTGTTCGATCTTGTTGT-3', fluorescence labeled probe (6-FAM) 5'-AAGCTGGACAACAGTGCCTC-3'; TSC22D3-3 sense primer 5'-GCTTACCAGCCGAGAAGGA-3', antisense primer 5'-GGCCTGTTCGATCTTGTTGT-3', fluorescence labeled probe (6-FAM) 5'-TAGCTAGCTTCAGAGCCGGTGCCTC-3'. The expression was normalized by two reference genes, 18S rRNA and GAPDH.

Immunohistochemistry

Dewaxed and rehydrated tissue sections were incubated in 3% hydrogen peroxide to block endogenous peroxidases. The Avidin/Biotin blocking kit was used to block endogenous biotin (Vector Laboratories, Burlingame, CA). Antigen retrieval was performed in a microwave oven in an antigen unmasking solution with a pH of 6 (Vector Laboratories). The primary antibody (1:50; 14-4033-80; eBioscience, San Diego, CA) was applied for 1 hour, and incubation with the biotinylated secondary antibody for 30 minutes was followed by the ABC reagent (Vector Laboratories). 3,3'-Diaminobenzidine (Sigma, Taufkirchen, Germany) with metal enhancement (resulting in a black product) was used as a detection system. Human transplant nephrectomy tissue and murine renal tissue were used to establish the staining protocol.

Immunofluorescence

Multicolor immunofluorescence was performed for TSC22D3 and Wilms tumor 1 (WT1) on kidney transplant nephrectomy tissue. The monoclonal antibody for TSC22D3 (1:500; H00001831-M01; Abnova, Walnut, CA) was visualized with a Cy3-labeled secondary antibody (Invitrogen, Basel, Switzerland). WT1 (sc-192; Santa Cruz Biotechnology, Santa Cruz, CA) was visualized by a biotinylated secondary antibody and labeled with fluorescein isothiocyanate bound to streptavidin (Vector Laboratories).

Western Blot Analysis

Cultured human (AB81) and murine (K5P5) podocytes were harvested with radioimmunoprecipitation assay buffer (Ripa) composed of 150 mmol/L NaCl, 1% (v/v) Nonidet P40, 0.5% (v/v) sodium deoxycholate, 0.1% (v/v) SDS, and 50 mmol/L Tris (pH 8) or cell lysis buffer (CLB) composed of 1 mmol/L EDTA (pH 8), 400 mmol/L NaCl, 0.1% (v/v) Nonidet P40 and 10 mmol/L Tris (pH 8) (Gibco, Invitrogen). The protein concentrations of the lysates were determined by the Bradford method (Bio-Rad Laboratories, Hercules, CA). Extracted proteins were boiled in loading buffer for 5 minutes, resolved by 15% SDS-polyacrylamide gel electrophoresis under reducing conditions, and transferred to an Immobilon-P membrane (Millipore, Eschborn, Germany). Membranes were blocked for 1 hour with Tris-buffered saline/3% fat-free skim milk and then incubated with a monoclonal rat antibody raised against human/mouse TSC22D3 (2 μg/ml; eBioscience) overnight at 4°C and rinsed with Tris-buffered saline containing 0.1% Tween. For detection, a horseradish peroxidase-linked anti-rat IgG antibody (1:10’000, 1 hour at room temperature; eBioscience) and enhanced chemiluminescence substrate (PerkinElmer Life and Analytical Sciences, Waltham, MA) were used. The protocol was also used with a polyclonal rabbit antibody raised against mouse TSC22D3 (1:3’000, obtained from Dr. David Pearce; University of California, San Francisco, USA) [206].

Cell Culture

Murine podocytes (K5P5) were grown on type 1 collagen-coated flasks in RPMI-1640 medium (Gibco, Invitrogen) containing 10% fetal bovine serum (FBS) and 1% penicillin/streptomycin (P/S; Gibco, Invitrogen). Cells were incubated at 37°C in a humidified atmosphere of 5% CO2 in air for a minimum of five days to differentiate.

Dexamethasone stimulation

Murine podocytes (K5P5) were starved in serum-free medium 24 hours before incubation with 1000 nM Dexamethasone (D4902; Sigma, Taufkirchen, Germany) for 8, 12, and 24 hours, respectively. This time-dependent analysis showed highest induction at 12 hours, hence dose-dependence was tested at 12 hours with 0.1 to 1000 nM Dexamethasone. Total cellular RNA was extracted using Qiagen RNeasy kit (Qiagen, Hombrechtikon, Switzerland). The mRNA expression was analyzed by real-time RT-PCR. Predeveloped TaqMan reagents were used for murine Tsc22d3 (Mm00726417_s1; Applied Biosystems Europe, Rotkreuz, Switzerland).

Statistics

Statistical analyses (Kruskall-Wallis and Mann-Whitney U-tests) were performed using SPSS 17.0 (Spss., Chicago, IL). P values < 0.05 were considered to indicate statistically significant results.

RESULTS

Glomerular expression of TSC22D3 mRNA

To confirm that TSC22D3 mRNA is overrepresented in healthy glomeruli compared to the tubulointerstitial compartment, we performed quantitative real-time RT-PCR for TSC22D3 mRNA on microdissected glomeruli and tubulointerstitium of pretransplant biopsies from living renal allograft donors (n=13). Consistent with the data of Lindenmeyer et al. [207], TSC22D3 demonstrated a 3.9-fold (± 1.1, $p < 0.01$) higher expression in microdissected glomeruli than in tubulointerstitial specimens (Figure 8). Additional quantitative real-time RT-PCR for the three splicing variants of TSC22D3 confirmed the result.

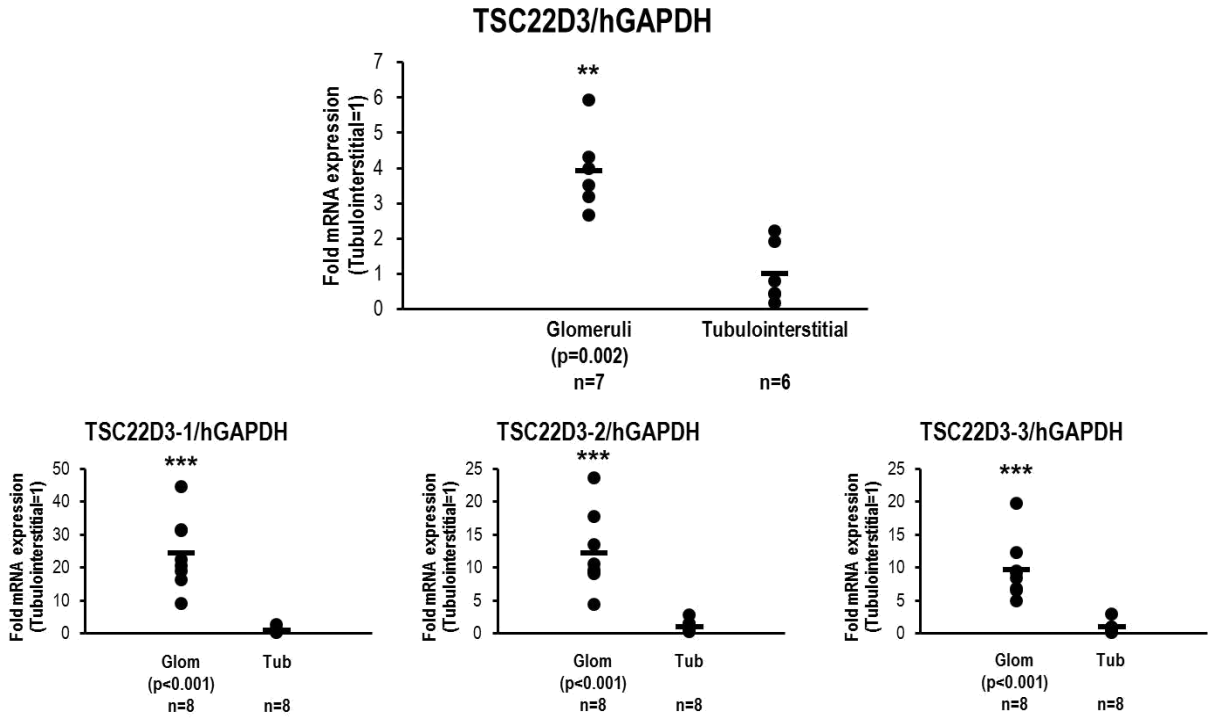

Figure 8: TSC22D3 in healthy human kidneys

*Expression of TSC22D3 mRNA in microdissected samples of allograft donors normalized to the tubulointerstitial expression. **p<0.01; ***p<0.001*

TSC22D3 in healthy kidneys

Two antibodies (eBioscience and Dr. Pearce group) were used to localize TSC22D3 by immunohistochemistry in human und murine renal tissue. In human transplant nephrectomies podocytes and some distal tubules were positive for TSC22D3; in murine renal tissue only the distal tubules were positive (Figure 9a).

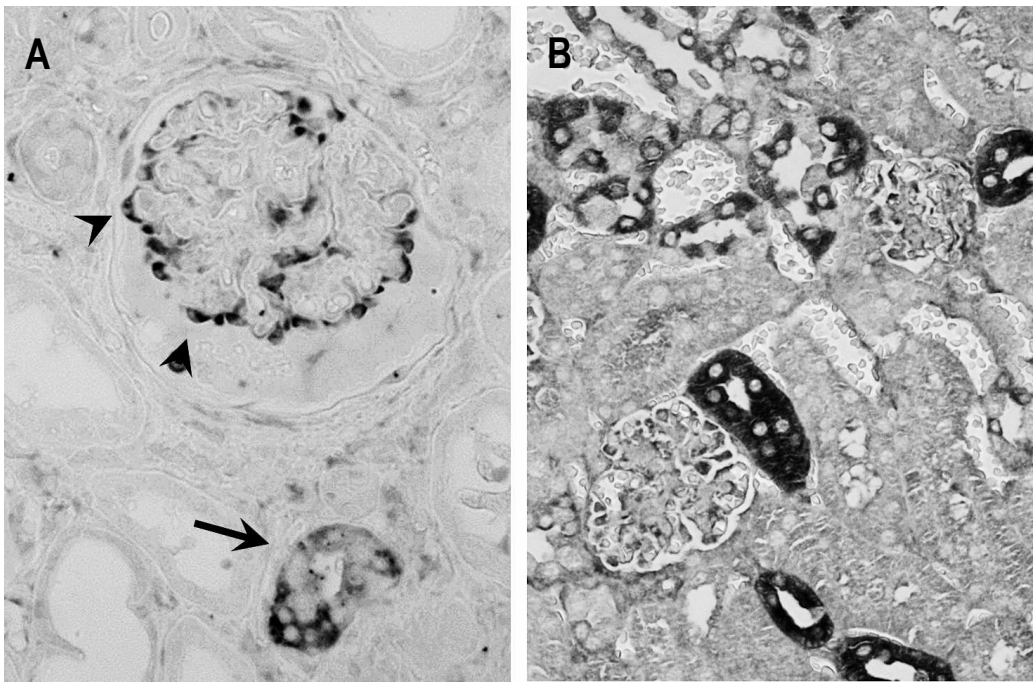

Figure 9a: TSC22D3 staining

To study the renal localization of TSC22D3, immunohistochemistry was performed with a monoclonal antiserum against TSC22D3 (eBioscience) on renal tissue. 40x

***(A)** In human transplant nephrectomies podocytes and some distal tubules were positive for TSC22D3.*

***(B)** In murine renal tissue only the distal tubules were positive.*

TSC22D3 localization in the human glomerulus

By co-immunofluorescence with WT1, a podocyte marker, a clear overlap with TSC22D3 was seen (Figure 9b).

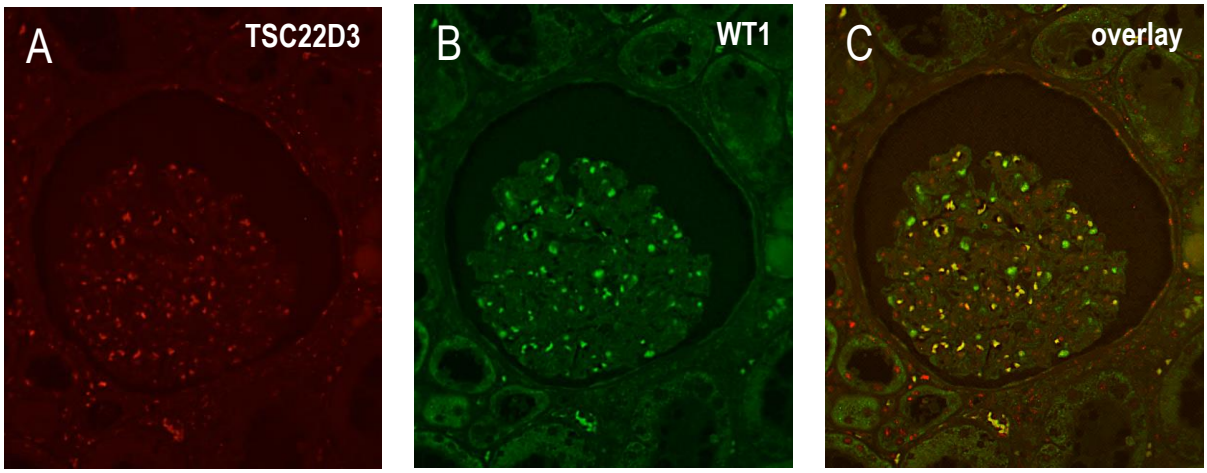

Figure 9b: Co-immunofluorescence for TSC22D3 and WT1

A human transplant nephrectomy was stained for TSC22D3 (A) and WT1 (B). The merge (C) indicated a clear overlap of both signals.

According to the staining pattern, human and murine podocyte cell lysate were found to be positive for TSC22D3 by Western blot analysis (Figure 10).

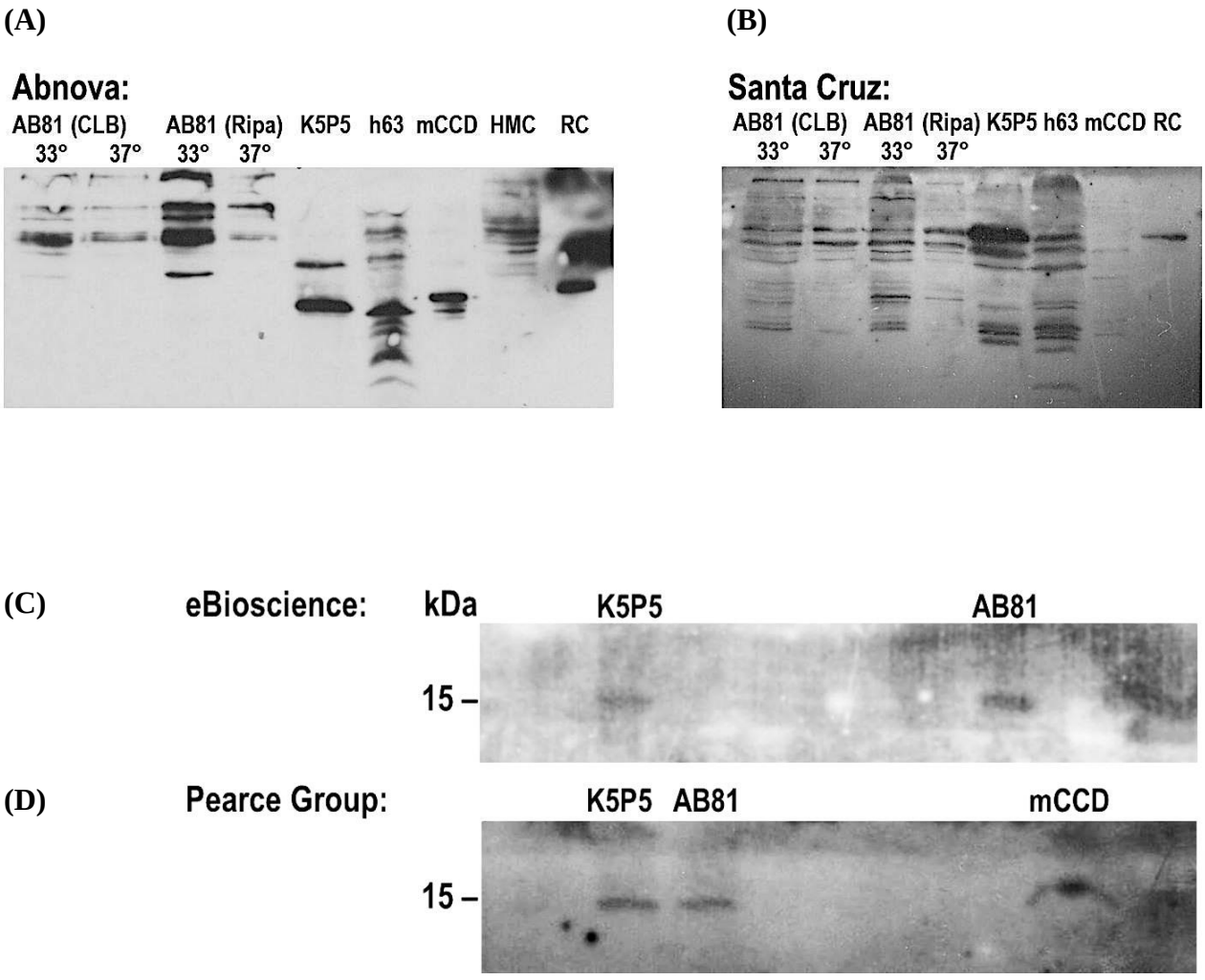

Figure 10: Western blot analysis of TSC22D3 with different antibodies

(A), (B) *Multiple unspecific bands were found with commercial available antibodies to TSC22D3 from Abnova and Santa Cruz. AB81, h63=human podocytes; K5P5=murine podocytes; mCCD=murine cortical collecting duct cells; HMC=human mesangial cells; RC=recombinant protein for TSC22D3*

(C), (D) *A single band of the expected size was found in a human (AB81) and murine podocyte cell line (K5P5); a murine cortical collecting duct cell line (mCCD) served as positive control. Antibodies obtained from eBioscience and Research Group Dr. Pearce, San Francisco, USA [206].*

TSC22D3 in glomerulopathies

In Figure 11, the expression of TSC22D3 mRNA in different proteinuric glomerulonephropathies is shown as fold-change compared with living donors (LD). Corresponding to our previously reported microarray data, the mRNA expression was found to be significantly decreased in the progressive glomerulonephropathies such as LN, FSGS and MGN ($p < 0.001$) but not significantly in non-progressive MCD.

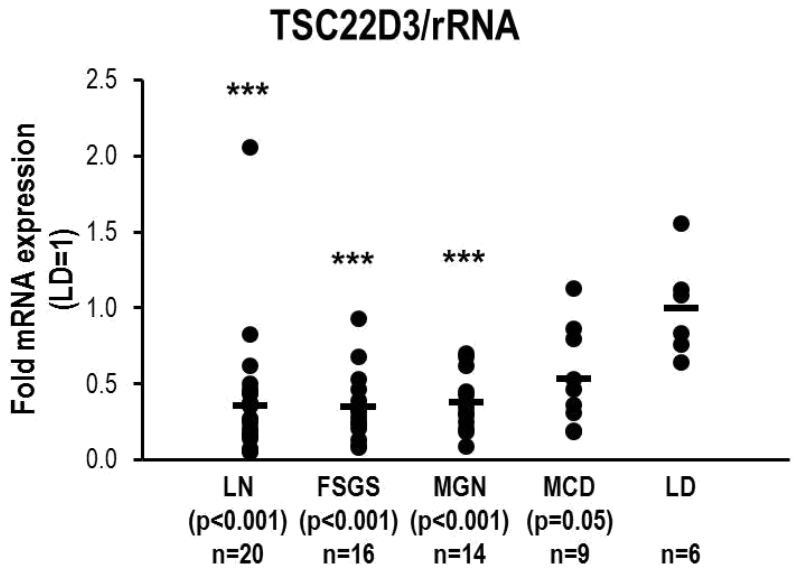

Figure 11: TSC22D3 in glomerulonephropathies

*Expression of TSC22D3 mRNA in different renal diseases normalized to healthy living donors (LD) (LN: Lupus nephritis III-IV; FSGS: focal-segmental glomerulosclerosis; MGN: membranous glomerulonephropathy; MCD: minimal change disease). ***p<0.001*

TSC22D3 in glomerulopathies treated with corticosteroids

Interestingly, the renal biopsies from patients diagnosed with a progressive proteinuric glomerulopathy preceding glucocorticoid treatment were prone to a higher mRNA expression level (Figure 12) than the untreated group. This result corresponds to previous studies that considered TSC22D3 as a glucocorticoid-inducible gene [208].

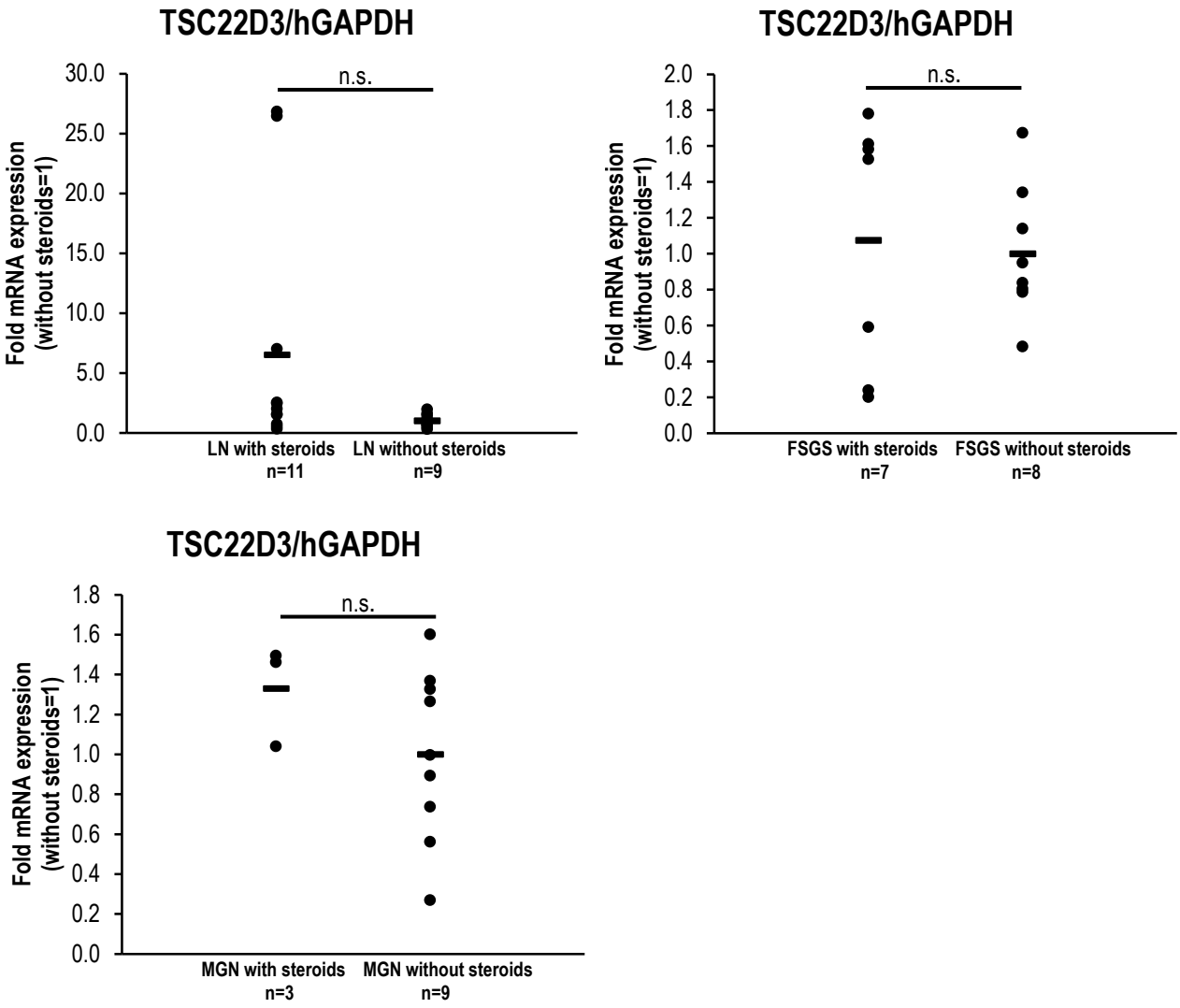

Figure 12: TSC22D3 in glomerulonephropathies treated with corticosteroids

Expression of TSC22D3 mRNA in different renal diseases treated with steroids normalized to the disease group without steroids (LN: Lupus nephritis III-IV; FSGS: focal-segmental glomerulosclerosis; MGN: membranous glomerulopathy). n.s. not significant

In-vitro stimulation experiments

TSC22D3 was originally discovered in studies aimed at characterizing genes targeted by dexamethasone. *In-vitro* stimulation experiments of murine podocytes by dexamethasone resulted in a time- and dose-dependent induction of TSC22D3 (Figure 13).

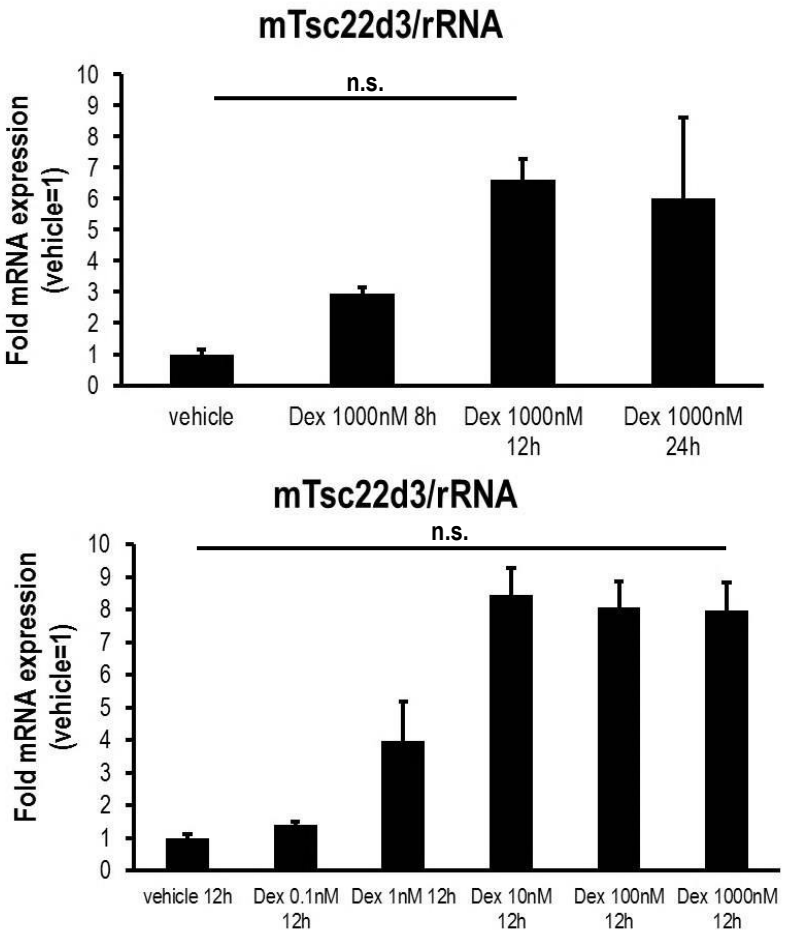

Figure 13: In-vitro stimulation by dexamethasone

Dexamethasone enhanced Tsc22d3 mRNA expression in murine epithelial cells (podocytes) time- and dose-dependently. n=3, shown are the means and standard deviations, n.s. not significant

Functional studies in drosophila melanogaster

Weavers et al. described a podocyte-like cell type in *Drosophila melanogaster*. The podocyte and nephrocyte filtration barriers are morphologically and functionally similar (Figure 14). The nephrocyte is very similar to the mammalian podocytes, including the nephrin-based slit diaphragm and is a simple model to study podocyte biology. Slit diaphragm specific genes such as nephrin (kirre) and podocin (mec2) are all expressed by the nephrocytes and loss of function leads to loss of slit diaphragm. A functional test of drosophila nephrocytes may be performed with the silver-nitrate ($AgNO_3$) method as dysfunctional nephrocytes are unable to eliminate the toxic $AgNO_3$ by endocytosis [209].

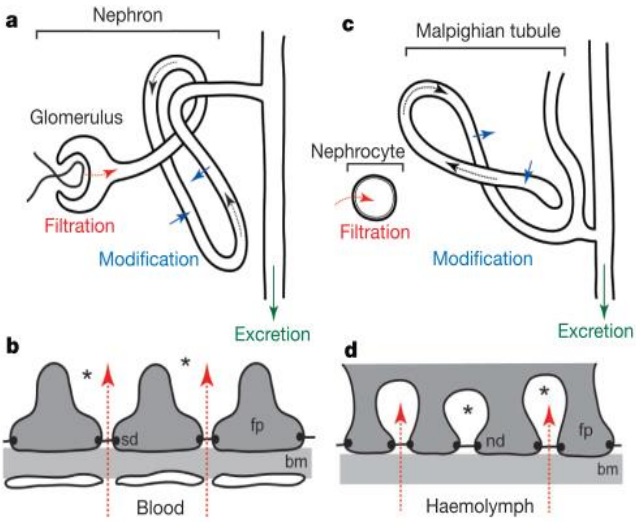

Figure 14:

*Vertebrate nephron (**a**), glomerular filtration barrier (**b**), insect excretory system (**c**) and nephrocyte filtration barrier (**d**). bm=basement membrane; fp=foot process; nd=nephrocyte diaphragm; sd=slit diaphragm. Taken from Weavers et al., Nature 2009 [209].*

The group of Hugo Stocker identified bunched A (BunA), the drosophila homolog of TSC22D3, to promote cellular growth [210]. BunA deletion mutants showed growth deficits and their eyes were smaller with a reduced cell size compared to wildtypes [211].

In our very preliminary studies, cDNA samples from two BunA (drosophila homolog of TSC22D3) mutants and wildtype flies were analyzed (obtained from the Group of Dr. Hugo Stocker) [211]. Real-time RT-PCR showed a reduction of BunA expression in both mutants confirming the deletion of BunA specific sequence. To further study the role of the bunched isoforms in drosophila, larvae were fed with normal yeast, high salt yeast or starved (n=1). A decreased expression for BunA and BunB was detected in mutants with BunC deletion compared to the controls (wildtype) under normal feeding conditions suggesting a functional interference among the different isoforms.

DISCUSSION AND OUTLOOK

Proteinuric glomerulopathies are associated with an increased risk for the development of renal failure. The molecular mechanisms leading to proteinuric glomerulopathies are intensely researched and progress has been made in diagnostic analysis and medical treatment. Nevertheless, the identification of responsible gene transcripts is still needed to understand the underlying biological processes involved in glomerular pathobiology. Several studies found genes that are responsible for a certain renal disease [212, 213].
The primary aim of these PhD project was to find candidate gene transcripts and to analyze the related biological processes involved in human proteinuric glomerulopathies.

For that purpose, we first generated a dataset of gene transcripts specifically enriched in the renal glomerulus:

PUBLICATED DATA (CHAPTERS I-IV)

REGGED – a unique glomerulus-enriched dataset

In chapter I, we started with the comparison of microarray gene expression data from human glomeruli and tubulointerstitium to generate a human glomerulus-enriched gene expression dataset (REGGED). Comparison with an earlier report of He et al. showed that our database with 677 genes is highly enriched for known podocyte- and glomerulus-enriched genes such as *MYH9* [214]. REGGED allowed us to select gene transcripts expressed in the human glomerulus and to compare these gene transcripts to our gene expression profiles of different glomerulopathies (ERCB-KFB).
Several studies confirmed their candidate gene transcripts to be enriched in the glomerulus with our dataset [215, 216]. Hwang et al. strengthened their study on anomalies of the kidney and urinary tract as podocytes were described and confirmed as ROBO2-expressing cells [216]. They identified two mutations in SRGAP1, an important player in the SLIT2-ROBO2 signaling pathway during the kidney development. Interestingly, in our study ROBO2 mRNA was expressed low in diabetic nephropathy compared to control pretransplant biopsies. From previous rodent studies it is known that disruption of ROBO2 is associated with urinary tract anomalies [217, 218].
Other reports focused on glomerulus-specific transcripts and obtained a very similar list with known glomerular expressed genes such as *CDKN1, PLA2R1*, *NPHS1* and *NPHS2* [219].

REGGED identified established and novel gene transcripts expressed in the human glomerulus and the subsequent systematic analyses of the selected gene transcripts are part of this doctoral thesis.

Hypoxia – a promotor of glomerular damage in nephrosclerosis

Chronic hypoxia contributes to renal fibrosis and was hypothesized to be involved in nephrosclerosis (NSC), also known as hypertensive nephropathy. To comprehend the biological processes involved in hypoxia-related glomerulosclerosis, we performed specific studies in chapter II.

In human nephrosclerosis (NSC), a cause for end-stage renal disease, hardening of the small blood vessels and association with diabetes and hypertension are characteristic. Chronic hypoxia was proposed to be coincidentally cause and consequence of chronic kidney disease and renal failure [220-222]. Reduced oxygen delivery leads to activation of pathological processes such as development of interstitial renal fibrosis and vasoconstriction.

In an experimental unilateral ureteral obstruction (UUO) model, epithelial HIF1 (hypoxia inducible factor) has been identified as a promotor of renal fibrosis [113]. Recently, Shved et al. found significant correlations of HIF target genes with eGFR in patients with chronic kidney disease [223]. Hypoxic conditions led to HIF activation and known HIF target genes such as CXCR4 were increased. In our patients with NSC, induction of CXCR4 mRNA was seen. In kidney biopsies of these patients CXCR4 was localized to podocytes with a positive nuclear staining for HIF1α suggesting a transcriptional activity of HIF1α. These findings indicated that hypoxic processes contribute both to tubulointerstitial fibrosis and also to glomerular damage.

Periostin – a matricellular protein contributing to the progression of human nephropathies

In a further step, our REGGED dataset was used to select a glomerular gene transcript with the highest induction mainly in the progressive glomerulopathies FSGS and MGN. Progressive kidney disease is characterized by extracellular matrix deposition, inflammatory processes and loss of nephrons [71]. Earlier studies identified matricellular proteins such as SPARC to be regulators of fibrosis, cell-matrix changes and angiogenesis [195].

In our dataset the expression of matricellular proteins were low in healthy kidneys but very high in progressive glomerulopathies. We therefore selected the matricellular protein periostin (POSTN) with the highest fold of expression as an interesting candidate gene transcript for our studies in human glomerulopathies (chapter III). It is known that periostin is involved in fibrotic alterations in cardiac valves and bone tissues [224, 225]. In our study, progression of renal disease correlated significantly to the expression of periostin. Guerrot et al. also demonstrated in an experimental model a correlation of periostin expression and progression of hypertensive nephropathy [226]. Similarly, current data revealed a correlation between periostin renal biopsy staining score and renal function in lupus nephritis patients [227]. This result is consistent with our highest periostin mRNA induction in our lupus nephritis patients compared to the living donors. Satirapoj et al. found excretion of urinary periostin in proteinuric and non-proteinuric CKD patients and higher urinary periostin levels in chronic allograft nephropathy patients compared to transplant controls [228, 229]. Furthermore, urinary periostin correlated with serum creatinine. Thus, urinary periostin may be a promising biomarker of progressive renal injury. Other studies in a polycystic kidney disease mouse model showed that periostin-deficient mice had a reduction of cysts and less interstitial fibrosis leading to a longer survival rate [230].
Further investigation with clinical and histological follow-up data from our glomerulopathy patient cohort may bring new insights to progression of disease and define disease specific expression profiles of periostin in CKD patients.

In chapter IV, we continued our studies on periostin by performing staining series on biopsies from end-stage renal disease patients under peritoneal dialysis (PD) treatment. A complication of this treatment for end-stage renal disease (ESRD) patients is peritoneal fibrosis and encapsulating peritoneal sclerosis (EPS). In our EPS biopsies the periostin-positive area were larger and more fibrotic than in control biopsies. Nam et al. [231] found increased expression of periostin in the peritoneum in mice treated with PD solution. Corresponding to our results the thickness of the submesothelial layer was also increased and more fibrotic. The intraperitoneal administration of a periostin-binding DNA aptamer (PA) abolished the changes. This raises the question whether a periostin-binding DNA aptamer could be a potential therapeutic treatment for the prevention of fibrosis in PD patients.

In addition, we found significantly increased periostin levels in the dialysate of PD patients without signs of EPS. Interestingly, only low levels of periostin could be detected in dialysate of PD patients with already developed EPS. Consequently, measuring of periostin concentration in dialysate might be used as a biomarker indicating progression of complication in PD treatment.

Nevertheless, therapeutic options for renal fibrosis are still lacking. Periostin is an obvious marker for progression of proteinuric renal disease and inhibition of periostin expression in early stages of CKD development could be a therapeutic approach.

PRELIMINARY DATA (CHAPTERS V-VI)

Periostin – a matricellular protein involved in renal injury

Our previous studies (chapters III and IV) aimed us to study further on periostin. Periostin plays an important role in cell-matrix interactions and in the development of fibrosis. This matricellular protein has been studied intensely in bone, heart and lung. In chapter V, we performed pre-functional studies on periostin:

Periostin was found to be highly expressed in different cancer cell lines [232-234] where it was proposed to be an important factor during cell proliferation and cell migration [235, 236]. In our cell cycle studies with human and murine mesangial cells periostin showed an antiapoptotic effect (Figure 4). This result corresponded to other reports with different cell types [198, 199]. Liu et al. inhibited periostin gene expression via RNA interference. Proliferation and invasion of cancer cells were suppressed [237]. This may be a new research approach to pursue in progressive chronic kidney disease. It would be necessary to study whether total inhibition of periostin expression would affect the progression of human renal disease. Existing renal fibrosis cannot be revoked but slowing the development of fibrosis in patients with progressive glomerulopathies could be life prolonging. Earlier studies demonstrated that disruption of the TGF-β/Smad3 signaling pathway protected from renal tubulointerstitial fibrosis [108, 238]. A correlation was shown between periostin and induction of the TGF-β signaling pathway. In a diabetic mouse model, the matricellular protein SPARC was associated with glomerulosclerosis and tubulointerstitial damage due to increased TGF-β1 expression [194]. In addition, another matricellular protein thrombospondin was also shown to change renal pathophysiological processes via activation of TGF-β [239].

In our human renal biopsies periostin was expressed in healthy human glomeruli. We found increased expression of periostin in the glomeruli and also in the fibrotic tubular interstitium of patients with progressive glomerulopathies (chapter III). Unexpectedly, in our studies the renal morphology in periostin-deficient mice showed worse renal constitution compared to wildtype mice. This result accorded with the increased blood urea nitrogen (BUN) levels of adult periostin-deficient mice as elevated BUN levels suggest renal function alterations. The other serum values were comparable and inconspicuous. Additionally, future examination of

the urinary samples of our periostin-deficient mice is required as it would be interesting to know whether different excretory products are occurring.

Our preliminary studies on periostin-deficient mice indicated that periostin might be necessary for the renal development. Although mice lacking the periostin gene showed less interstitial fibrosis and inflammation in an UUO model, periostin seems to be important for the regulation of cell-matrix interactions and accumulation [240]. Periostin-deficient mice showed anomalies in teeth and periodontal apparatus and the survival rate was reduced compared to the wildtype littermates [201]. This potential developmental relevance of periostin for the kidneys corresponded to our immunohistochemical stainings of human fetal kidney tissue (not shown) where periostin was found to be strongly present in the developing renal region.

In summary, in different animal models of CKD expression of periostin is constantly associated with inflammatory processes, interstitial fibrosis and decline of renal function [226, 228, 230, 240, 241]. Further studies in renal morphology and physiology in periostin-deficient mice with or without an experimental nephropathy would give new insights to the role of periostin in the kidney.

TSC22D3 – a glucocorticoid-induced leucine zipper involved in renal injury

From clinical data, it is known that patients with certain glomerulopathies such as minimal change disease (MCD) respond positively with full remission to corticosteroid therapy [242, 243]. A primary dysfunction of the podocytes such as foot process effacement is leading to proteinuria and is specific for those corticosteroid-sensitive glomerulopathies. Seeking for a corticosteroid-stimulated REGGED gene transcript, we found TSC22D3 mRNA to be significantly decreased in the progressive glomerulopathies such as LN, FSGS and MGN.
In chapter VI, the second candidate gene transcript TSC22D3 was studied *ex-vivo* in humans and *in-vitro* in human and murine cells. TSC22D3, also known as glucocorticoid-induced leucine zipper (GILZ), was first found to be expressed in lymphocytes from thymus [204]. Murine thymocytes stimulated with the corticosteroid dexamethasone showed an increased expression of TSC22D3 and cells overexpressing TSC22D3 were resistant to TCR/CD3-activated apoptosis. Asselin-Labat et al. showed that TSC22D3 delays apoptosis in activated T lymphocytes and that interleukins induce the expression of TSC22D3 [208].

In our studies, TSC22D3 was localized in podocytes and distal tubules but not in mesangial cells. This localization of TSC22D3 in distal tubules in murine and human tissue corresponded to earlier studies with mouse cortical collecting duct cells (mCCD) [244]. Hormone-regulated sodium (Na+) transport is essential for the control of circulatory volume, blood pressure and extracellular fluid composition. A correlation between TSC22D3 mRNA expression and urinary excretion of sodium and potassium was found in adrenalectomized rats after treatment with aldosterone and dexamethasone [205]. Moreover, the transepithelial transport through ENaC is inhibited by activated ERK1/2 and Tsc22d3 stimulates this transport by inhibition of ERK activation [206].
The increasing effect of corticosteroids on mRNA levels in glomerulopathies prompted us to *in-vitro* stimulation experiments. Incubation of murine podocytes with dexamethasone resulted in a time- and dose-dependent induction of Tsc22d3 mRNA. This result accorded with the study in a murine T lymphocyte cell line [208]. Asselin-Labat et al. showed that addition of RU-486, a glucocorticoid receptor antagonist, totally inhibited dexamethasone-induced Tsc22d3 expression. Tsc22d3 induction therefore requires a functional glucocorticoid receptor. As a consequence, TSC22D3 acts as a mediator for anti-inflammatory and immunosuppressive activities.

Experimental animal models to investigate the role of TSC22D3 in the kidney are only a few available [245-247]. Mice lacking Tsc22d3 have electrolyte abnormalities, increased plasma potassium concentration and alterations in sodium delivery to the ENaC.

Weavers et al. [209] described a podocyte-like cell type, the *Drosophila* nephrocytes, which acts as a filtration barrier. Functional studies can be performed with the silver-nitrate method to find differences among the mutant and wildtype flies in renal function. In *Drosophila* melanogaster, the *TSC22D3* homolog *bunched* (Bun, Shs) has been examined with different feeding conditions [210, 248]. In our very preliminary studies real-time RT-PCR showed a decreased expression for BunA and B in mutants with BunC deletion compared to the controls under normal feeding conditions suggesting functional interference among the different isoforms. We speculated that mutants with deletion of bunched have dysfunctional nephrocytes and therefore would be unable to eliminate toxic substances such as silver-nitrate by endocytosis. Various experimental approaches with different feeding conditions and addition of glucocorticoids should be pursued to achieve advanced knowledge about its renal function.

A further interesting method to study podocyte dysfunctions was established in a zebrafish model. Sugano et al. followed a similar research approach to our TSC22D3 study by selecting a glomerulus-enriched REGGED gene transcript with glucocorticoid-induced regulation [249]. The glomerulus-enriched Rho-GTPase binding protein IQGAP2 was found to be expressed in human and zebrafish podocytes and a repressed gene expression was detected in biopsies of patients with nephrotic syndrome. In this experimental iqgap2-knockdown model a mild foot process effacement with impaired permeability of the glomerular filter was observed.

In conclusion, we generated a unique glomerulus-enriched gene expression dataset and we found two candidate gene transcripts with promising molecular importance in proteinuric glomerulopathies. For Periostin, further functional studies in renal experimental models such as a periostin-overexpressing mouse and analyses of clinical follow-up data from patients with progressive glomerulopathies would give further insights to this matricellular protein.

The glucocorticoid-induced gene transcript TSC22D3 may represent a therapeutic target for steroid-sensitive podocytopathies. Renal studies in the drosophila fly model with its malpighian tubule and nephrocytes or a knockdown model in zebrafish larvae could demonstrate the role of TSC22D3 in the renal system.

REFERENCES

1. Hall JE. Textbook of Medical Physiology. 12th ed: Saunders Elsevier; 2011.
2. Thomson SC, Blantz RC. Glomerulotubular balance, tubuloglomerular feedback, and salt homeostasis. J Am Soc Nephrol. 2008;19(12):2272-5.
3. Nielsen S, Frøkiaer J, Marples D, Kwon TH, Agre P, Knepper MA. Aquaporins in the kidney: from molecules to medicine. Physiol Rev. 2002;82(1):205-44.
4. Schafer JA. Abnormal regulation of ENaC: syndromes of salt retention and salt wasting by the collecting duct. Am J Physiol Renal Physiol. 2002;283(2):F221-35.
5. Wright EM. Renal Na(+)-glucose cotransporters. Am J Physiol Renal Physiol. 2001;280(1):F10-8.
6. Dominguez JH, Song B, Maianu L, Garvey WT, Qulali M. Gene expression of epithelial glucose transporters: the role of diabetes mellitus. J Am Soc Nephrol. 1994;5(5 Suppl 1):S29-36.
7. Tryggvason K, Patrakka J, Wartiovaara J. Hereditary proteinuria syndromes and mechanisms of proteinuria. N Engl J Med. 2006;354(13):1387-401.
8. Levey AS, Stevens LA, Schmid CH, Zhang YL, Castro AF, Feldman HI, et al. A new equation to estimate glomerular filtration rate. Ann Intern Med. 2009;150(9):604-12.
9. Levey AS, Bosch JP, Lewis JB, Greene T, Rogers N, Roth D. A more accurate method to estimate glomerular filtration rate from serum creatinine: a new prediction equation. Modification of Diet in Renal Disease Study Group. Ann Intern Med. 1999;130(6):461-70.
10. Michels WM, Grootendorst DC, Verduijn M, Elliott EG, Dekker FW, Krediet RT. Performance of the Cockcroft-Gault, MDRD, and new CKD-EPI formulas in relation to GFR, age, and body size. Clin J Am Soc Nephrol. 2010;5(6):1003-9.
11. Levey AS, de Jong PE, Coresh J, El Nahas M, Astor BC, Matsushita K, et al. The definition, classification, and prognosis of chronic kidney disease: a KDIGO Controversies Conference report. Kidney Int. 2011;80(1):17-28.
12. Levin A, Stevens PE. Summary of KDIGO 2012 CKD Guideline: behind the scenes, need for guidance, and a framework for moving forward. Kidney Int. 2014;85(1):49-61.
13. Shoji T, Masakane I, Watanabe Y, Iseki K, Tsubakihara Y, Committee of Renal Data Registry JpSfDT. Elevated non-high-density lipoprotein cholesterol (non-HDL-C) predicts atherosclerotic cardiovascular events in hemodialysis patients. Clin J Am Soc Nephrol. 2011;6(5):1112-20.
14. Abboud H, Henrich WL. Clinical practice. Stage IV chronic kidney disease. N Engl J Med. 2010;362(1):56-65.
15. Levey AS. Clinical practice. Nondiabetic kidney disease. N Engl J Med. 2002;347(19):1505-11.
16. Coresh J, Selvin E, Stevens LA, Manzi J, Kusek JW, Eggers P, et al. Prevalence of chronic kidney disease in the United States. JAMA. 2007;298(17):2038-47.
17. López-Hernández FJ, López-Novoa JM. Role of TGF-β in chronic kidney disease: an integration of tubular, glomerular and vascular effects. Cell Tissue Res. 2012;347(1):141-54.
18. Remuzzi G, Schieppati A, Ruggenenti P. Clinical practice. Nephropathy in patients with type 2 diabetes. N Engl J Med. 2002;346(15):1145-51.
19. Liu Y. Renal fibrosis: new insights into the pathogenesis and therapeutics. Kidney Int. 2006;69(2):213-7.
20. Hall JE, Crook ED, Jones DW, Wofford MR, Dubbert PM. Mechanisms of obesity-associated cardiovascular and renal disease. Am J Med Sci. 2002;324(3):127-37.

21. Wang Y, Chen X, Song Y, Caballero B, Cheskin LJ. Association between obesity and kidney disease: a systematic review and meta-analysis. Kidney Int. 2008;73(1):19-33.
22. Kaplan C, Pasternack B, Shah H, Gallo G. Age-related incidence of sclerotic glomeruli in human kidneys. Am J Pathol. 1975;80(2):227-34.
23. Morrison AB, Howard RM. The functional capacity of hypertrophied nephrons. Effect of partial nephrectomy on the clearance of inulin and PAH in the rat. J Exp Med. 1966;123(5):829-44.
24. Shimamura T, Morrison AB. A progressive glomerulosclerosis occurring in partial five-sixths nephrectomized rats. Am J Pathol. 1975;79(1):95-106.
25. Moriya T, Tsuchiya A, Okizaki S, Hayashi A, Tanaka K, Shichiri M. Glomerular hyperfiltration and increased glomerular filtration surface are associated with renal function decline in normo- and microalbuminuric type 2 diabetes. Kidney Int. 2012;81(5):486-93.
26. Stanescu HC, Arcos-Burgos M, Medlar A, Bockenhauer D, Kottgen A, Dragomirescu L, et al. Risk HLA-DQA1 and PLA(2)R1 alleles in idiopathic membranous nephropathy. N Engl J Med. 2011;364(7):616-26.
27. Prunotto M, Carnevali ML, Candiano G, Murtas C, Bruschi M, Corradini E, et al. Autoimmunity in membranous nephropathy targets aldose reductase and SOD2. J Am Soc Nephrol. 2010;21(3):507-19.
28. Beck LH, Bonegio RG, Lambeau G, Beck DM, Powell DW, Cummins TD, et al. M-type phospholipase A2 receptor as target antigen in idiopathic membranous nephropathy. N Engl J Med. 2009;361(1):11-21.
29. Debiec H, Guigonis V, Mougenot B, Decobert F, Haymann JP, Bensman A, et al. Antenatal membranous glomerulonephritis due to anti-neutral endopeptidase antibodies. N Engl J Med. 2002;346(26):2053-60.
30. Kao WH, Klag MJ, Meoni LA, Reich D, Berthier-Schaad Y, Li M, et al. MYH9 is associated with nondiabetic end-stage renal disease in African Americans. Nat Genet. 2008;40(10):1185-92.
31. Kopp JB, Smith MW, Nelson GW, Johnson RC, Freedman BI, Bowden DW, et al. MYH9 is a major-effect risk gene for focal segmental glomerulosclerosis. Nat Genet. 2008;40(10):1175-84.
32. Bhavnani SK, Eichinger F, Martini S, Saxman P, Jagadish HV, Kretzler M. Network analysis of genes regulated in renal diseases: implications for a molecular-based classification. BMC Bioinformatics. 2009;10 Suppl 9:S3.
33. Ju W, Eichinger F, Bitzer M, Oh J, McWeeney S, Berthier CC, et al. Renal gene and protein expression signatures for prediction of kidney disease progression. Am J Pathol. 2009;174(6):2073-85.
34. Martini S, Eichinger F, Nair V, Kretzler M. Defining human diabetic nephropathy on the molecular level: integration of transcriptomic profiles with biological knowledge. Rev Endocr Metab Disord. 2008;9(4):267-74.
35. Köttgen A, Pattaro C, Böger CA, Fuchsberger C, Olden M, Glazer NL, et al. New loci associated with kidney function and chronic kidney disease. Nat Genet. 2010;42(5):376-84.
36. Köttgen A, Glazer NL, Dehghan A, Hwang SJ, Katz R, Li M, et al. Multiple loci associated with indices of renal function and chronic kidney disease. Nat Genet. 2009;41(6):712-7.
37. Devuyst O, Olinger E, Rampoldi L. Uromodulin: from physiology to rare and complex kidney disorders. Nat Rev Nephrol. 2017;13(9):525-44.

38. Trudu M, Schaeffer C, Riba M, Ikehata M, Brambilla P, Messa P, et al. Early involvement of cellular stress and inflammatory signals in the pathogenesis of tubulointerstitial kidney disease due to UMOD mutations. Sci Rep. 2017;7(1):7383.
39. Böger CA, Chen MH, Tin A, Olden M, Köttgen A, de Boer IH, et al. CUBN is a gene locus for albuminuria. J Am Soc Nephrol. 2011;22(3):555-70.
40. USRDS. Annual Data Report: Atlas of Chronic Kidney Disease & End-Stage Renal Disease in the United States. Bethesda, MD, National Institutes of Health, National Institute of Diabetes and Digestive and Kidney Diseases; 2011.
41. Levey AS, Coresh J, Balk E, Kausz AT, Levin A, Steffes MW, et al. National Kidney Foundation practice guidelines for chronic kidney disease: evaluation, classification, and stratification. Ann Intern Med. 2003;139(2):137-47.
42. Levey AS, Eckardt KU, Tsukamoto Y, Levin A, Coresh J, Rossert J, et al. Definition and classification of chronic kidney disease: a position statement from Kidney Disease: Improving Global Outcomes (KDIGO). Kidney Int. 2005;67(6):2089-100.
43. Iseki K. Gender differences in chronic kidney disease. Kidney Int. 2008;74(4):415-7.
44. Zoccali C, Kramer A, Jager KJ. Chronic kidney disease and end-stage renal disease-a review produced to contribute to the report 'the status of health in the European union: towards a healthier Europe'. NDT Plus. 2010;3(3):213-24.
45. Go AS, Chertow GM, Fan D, McCulloch CE, Hsu CY. Chronic kidney disease and the risks of death, cardiovascular events, and hospitalization. N Engl J Med. 2004;351(13):1296-305.
46. Koren MJ, Davidson MH, Wilson DJ, Fayyad RS, Zuckerman A, Reed DP, et al. Focused atorvastatin therapy in managed-care patients with coronary heart disease and CKD. Am J Kidney Dis. 2009;53(5):741-50.
47. de Zeeuw D, Remuzzi G, Parving HH, Keane WF, Zhang Z, Shahinfar S, et al. Proteinuria, a target for renoprotection in patients with type 2 diabetic nephropathy: lessons from RENAAL. Kidney Int. 2004;65(6):2309-20.
48. Cattran DC. Historical aspects of proteinuria. Adv Chronic Kidney Dis. 2011;18(4):224-32.
49. Schmieder RE, Mann JF, Schumacher H, Gao P, Mancia G, Weber MA, et al. Changes in albuminuria predict mortality and morbidity in patients with vascular disease. J Am Soc Nephrol. 2011;22(7):1353-64.
50. Ruggenenti P, Perticucci E, Cravedi P, Gambara V, Costantini M, Sharma SK, et al. Role of remission clinics in the longitudinal treatment of CKD. J Am Soc Nephrol. 2008;19(6):1213-24.
51. Mann JF, Schmieder RE, McQueen M, Dyal L, Schumacher H, Pogue J, et al. Renal outcomes with telmisartan, ramipril, or both, in people at high vascular risk (the ONTARGET study): a multicentre, randomised, double-blind, controlled trial. Lancet. 2008;372(9638):547-53.
52. Ruggenenti P, Perna A, Gherardi G, Garini G, Zoccali C, Salvadori M, et al. Renoprotective properties of ACE-inhibition in non-diabetic nephropathies with non-nephrotic proteinuria. Lancet. 1999;354(9176):359-64.
53. Eijkelkamp WB, Zhang Z, Brenner BM, Cooper ME, Devereux RB, Dahlöf B, et al. Renal function and risk for cardiovascular events in type 2 diabetic patients with hypertension: the RENAAL and LIFE studies. J Hypertens. 2007;25(4):871-6.
54. Parving HH, Persson F, Lewis JB, Lewis EJ, Hollenberg NK, Investigators AS. Aliskiren combined with losartan in type 2 diabetes and nephropathy. N Engl J Med. 2008;358(23):2433-46.
55. Mauer M, Zinman B, Gardiner R, Suissa S, Sinaiko A, Strand T, et al. Renal and retinal effects of enalapril and losartan in type 1 diabetes. N Engl J Med. 2009;361(1):40-51.

56. Mancia G, Parati G, Bilo G, Gao P, Fagard R, Redon J, et al. Ambulatory blood pressure values in the Ongoing Telmisartan Alone and in Combination with Ramipril Global Endpoint Trial (ONTARGET). Hypertension. 2012;60(6):1400-6.
57. Haller H, Ito S, Izzo JL, Januszewicz A, Katayama S, Menne J, et al. Olmesartan for the delay or prevention of microalbuminuria in type 2 diabetes. N Engl J Med. 2011;364(10):907-17.
58. Fried LF, Emanuele N, Zhang JH, Brophy M, Conner TA, Duckworth W, et al. Combined angiotensin inhibition for the treatment of diabetic nephropathy. N Engl J Med. 2013;369(20):1892-903.
59. Perkovic V, Verdon C, Ninomiya T, Barzi F, Cass A, Patel A, et al. The relationship between proteinuria and coronary risk: a systematic review and meta-analysis. PLoS Med. 2008;5(10):e207.
60. Matsushita K, van der Velde M, Astor BC, Woodward M, Levey AS, de Jong PE, et al. Association of estimated glomerular filtration rate and albuminuria with all-cause and cardiovascular mortality in general population cohorts: a collaborative meta-analysis. Lancet. 2010;375(9731):2073-81.
61. Moe SM. Vascular calcification: Hardening of the evidence. Kidney Int. 2006;70(9):1535-7.
62. Ganesh SK, Stack AG, Levin NW, Hulbert-Shearon T, Port FK. Association of elevated serum PO(4), Ca x PO(4) product, and parathyroid hormone with cardiac mortality risk in chronic hemodialysis patients. J Am Soc Nephrol. 2001;12(10):2131-8.
63. Meijers BK, Claes K, Bammens B, de Loor H, Viaene L, Verbeke K, et al. p-Cresol and cardiovascular risk in mild-to-moderate kidney disease. Clin J Am Soc Nephrol. 2010;5(7):1182-9.
64. Mihai S, Codrici E, Popescu ID, Enciu AM, Rusu E, Zilisteanu D, et al. Proteomic Biomarkers Panel: New Insights in Chronic Kidney Disease. Dis Markers. 2016;2016:3185232.
65. Faul C, Amaral AP, Oskouei B, Hu MC, Sloan A, Isakova T, et al. FGF23 induces left ventricular hypertrophy. J Clin Invest. 2011;121(11):4393-408.
66. Koh N, Fujimori T, Nishiguchi S, Tamori A, Shiomi S, Nakatani T, et al. Severely reduced production of klotho in human chronic renal failure kidney. Biochem Biophys Res Commun. 2001;280(4):1015-20.
67. Dai B, David V, Martin A, Huang J, Li H, Jiao Y, et al. A comparative transcriptome analysis identifying FGF23 regulated genes in the kidney of a mouse CKD model. PLoS One. 2012;7(9):e44161.
68. Hu MC, Shi M, Zhang J, Quiñones H, Griffith C, Kuro-o M, et al. Klotho deficiency causes vascular calcification in chronic kidney disease. J Am Soc Nephrol. 2011;22(1):124-36.
69. Titan SM, Zatz R, Graciolli FG, dos Reis LM, Barros RT, Jorgetti V, et al. FGF-23 as a predictor of renal outcome in diabetic nephropathy. Clin J Am Soc Nephrol. 2011;6(2):241-7.
70. Shankland SJ. The podocyte's response to injury: role in proteinuria and glomerulosclerosis. Kidney Int. 2006;69(12):2131-47.
71. Schlondorff DO. Overview of factors contributing to the pathophysiology of progressive renal disease. Kidney Int. 2008;74(7):860-6.
72. Zhou XJ, Rakheja D, Yu X, Saxena R, Vaziri ND, Silva FG. The aging kidney. Kidney Int. 2008;74(6):710-20.
73. Segerer S, Schlöndorff D. Role of chemokines for the localization of leukocyte subsets in the kidney. Semin Nephrol. 2007;27(3):260-74.

74. Halbesma N, Jansen DF, Heymans MW, Stolk RP, de Jong PE, Gansevoort RT, et al. Development and validation of a general population renal risk score. Clin J Am Soc Nephrol. 2011;6(7):1731-8.
75. Klahr S, Schreiner G, Ichikawa I. The progression of renal disease. N Engl J Med. 1988;318(25):1657-66.
76. Praga M, Morales E. Obesity, proteinuria and progression of renal failure. Curr Opin Nephrol Hypertens. 2006;15(5):481-6.
77. Hallan SI, Coresh J, Astor BC, Asberg A, Powe NR, Romundstad S, et al. International comparison of the relationship of chronic kidney disease prevalence and ESRD risk. J Am Soc Nephrol. 2006;17(8):2275-84.
78. Whaley-Connell AT, Chowdhury NA, Hayden MR, Stump CS, Habibi J, Wiedmeyer CE, et al. Oxidative stress and glomerular filtration barrier injury: role of the renin-angiotensin system in the Ren2 transgenic rat. Am J Physiol Renal Physiol. 2006;291(6):F1308-14.
79. Eddy AA, Fogo AB. Plasminogen activator inhibitor-1 in chronic kidney disease: evidence and mechanisms of action. J Am Soc Nephrol. 2006;17(11):2999-3012.
80. Tang WW, Ulich TR, Lacey DL, Hill DC, Qi M, Kaufman SA, et al. Platelet-derived growth factor-BB induces renal tubulointerstitial myofibroblast formation and tubulointerstitial fibrosis. Am J Pathol. 1996;148(4):1169-80.
81. Kato H, Osajima A, Uezono Y, Okazaki M, Tsuda Y, Tanaka H, et al. Involvement of PDGF in pressure-induced mesangial cell proliferation through PKC and tyrosine kinase pathways. Am J Physiol. 1999;277(1 Pt 2):F105-12.
82. Harris RC, Cheng HF. The intrarenal renin-angiotensin system: a paracrine system for the local control of renal function separate from the systemic axis. Exp Nephrol. 1996;4 Suppl 1:2-7.
83. Navar LG, Imig JD, Zou L, Wang CT. Intrarenal production of angiotensin II. Semin Nephrol. 1997;17(5):412-22.
84. Cameron JS. Proteinuria and progression in human glomerular diseases. Am J Nephrol. 1990;10 Suppl 1:81-7.
85. Orth SR, Ritz E. The nephrotic syndrome. N Engl J Med. 1998;338(17):1202-11.
86. Gorriz JL, Martinez-Castelao A. Proteinuria: detection and role in native renal disease progression. Transplant Rev (Orlando). 2012;26(1):3-13.
87. Rossing P, Hommel E, Smidt UM, Parving HH. Reduction in albuminuria predicts a beneficial effect on diminishing the progression of human diabetic nephropathy during antihypertensive treatment. Diabetologia. 1994;37(5):511-6.
88. Apperloo AJ, de Zeeuw D, de Jong PE. Short-term antiproteinuric response to antihypertensive treatment predicts long-term GFR decline in patients with non-diabetic renal disease. Kidney Int Suppl. 1994;45:S174-8.
89. Benigni A, Remuzzi G. How renal cytokines and growth factors contribute to renal disease progression. Am J Kidney Dis. 2001;37(1 Suppl 2):S21-4.
90. Birn H, Christensen EI. Renal albumin absorption in physiology and pathology. Kidney Int. 2006;69(3):440-9.
91. Bennett WM. Efficacy and safety of cyclosporine in renal-transplant recipients. N Engl J Med. 1994;331(26):1777; author reply -8.
92. Harris RC, Breyer MD. Update on cyclooxygenase-2 inhibitors. Clin J Am Soc Nephrol. 2006;1(2):236-45.
93. Brater DC. Update in diuretic therapy: clinical pharmacology. Semin Nephrol. 2011;31(6):483-94.
94. Liu Y. Cellular and molecular mechanisms of renal fibrosis. Nat Rev Nephrol. 2011;7(12):684-96.

95. Lewis MP, Norman JT. Differential response of activated versus non-activated renal fibroblasts to tubular epithelial cells: a model of initiation and progression of fibrosis? Exp Nephrol. 1998;6(2):132-43.
96. Gilbert RE, Cooper ME. The tubulointerstitium in progressive diabetic kidney disease: more than an aftermath of glomerular injury? Kidney Int. 1999;56(5):1627-37.
97. Eckes B, Kessler D, Aumailley M, Krieg T. Interactions of fibroblasts with the extracellular matrix: implications for the understanding of fibrosis. Springer Semin Immunopathol. 1999;21(4):415-29.
98. Meran S, Steadman R. Fibroblasts and myofibroblasts in renal fibrosis. Int J Exp Pathol. 2011;92(3):158-67.
99. Qi W, Chen X, Polhill TS, Sumual S, Twigg S, Gilbert RE, et al. TGF-beta1 induces IL-8 and MCP-1 through a connective tissue growth factor-independent pathway. Am J Physiol Renal Physiol. 2006;290(3):F703-9.
100. Hinz B, Phan SH, Thannickal VJ, Galli A, Bochaton-Piallat ML, Gabbiani G. The myofibroblast: one function, multiple origins. Am J Pathol. 2007;170(6):1807-16.
101. Wang SN, LaPage J, Hirschberg R. Role of glomerular ultrafiltration of growth factors in progressive interstitial fibrosis in diabetic nephropathy. Kidney Int. 2000;57(3):1002-14.
102. Böttinger EP. TGF-beta in renal injury and disease. Semin Nephrol. 2007;27(3):309-20.
103. Malmström J, Larsen K, Malmström L, Tufvesson E, Parker K, Marchese J, et al. Proteome annotations and identifications of the human pulmonary fibroblast. J Proteome Res. 2004;3(3):525-37.
104. Prunotto M, Ghiggeri G, Bruschi M, Gabbiani G, Lescuyer P, Hocher B, et al. Renal fibrosis and proteomics: current knowledge and still key open questions for proteomic investigation. J Proteomics. 2011;74(10):1855-70.
105. Kopp JB, Factor VM, Mozes M, Nagy P, Sanderson N, Böttinger EP, et al. Transgenic mice with increased plasma levels of TGF-beta 1 develop progressive renal disease. Lab Invest. 1996;74(6):991-1003.
106. Zhong X, Chung AC, Chen HY, Meng XM, Lan HY. Smad3-mediated upregulation of miR-21 promotes renal fibrosis. J Am Soc Nephrol. 2011;22(9):1668-81.
107. Wang W, Huang XR, Canlas E, Oka K, Truong LD, Deng C, et al. Essential role of Smad3 in angiotensin II-induced vascular fibrosis. Circ Res. 2006;98(8):1032-9.
108. Meng XM, Huang XR, Chung AC, Qin W, Shao X, Igarashi P, et al. Smad2 protects against TGF-beta/Smad3-mediated renal fibrosis. J Am Soc Nephrol. 2010;21(9):1477-87.
109. Choi YJ, Chakraborty S, Nguyen V, Nguyen C, Kim BK, Shim SI, et al. Peritubular capillary loss is associated with chronic tubulointerstitial injury in human kidney: altered expression of vascular endothelial growth factor. Hum Pathol. 2000;31(12):1491-7.
110. Higgins DF, Kimura K, Iwano M, Haase VH. Hypoxia-inducible factor signaling in the development of tissue fibrosis. Cell Cycle. 2008;7(9):1128-32.
111. Gunaratnam L, Bonventre JV. HIF in kidney disease and development. J Am Soc Nephrol. 2009;20(9):1877-87.
112. Rudnicki M, Eder S, Perco P, Enrich J, Scheiber K, Koppelstätter C, et al. Gene expression profiles of human proximal tubular epithelial cells in proteinuric nephropathies. Kidney Int. 2007;71(4):325-35.
113. Higgins DF, Kimura K, Bernhardt WM, Shrimanker N, Akai Y, Hohenstein B, et al. Hypoxia promotes fibrogenesis in vivo via HIF-1 stimulation of epithelial-to-mesenchymal transition. J Clin Invest. 2007;117(12):3810-20.

114. Haase VH. Hypoxia-inducible factor signaling in the development of kidney fibrosis. Fibrogenesis Tissue Repair. 2012;5(Suppl 1):S16.
115. Haase VH. The VHL/HIF oxygen-sensing pathway and its relevance to kidney disease. Kidney Int. 2006;69(8):1302-7.
116. Meyer TW, Hostetter TH. Uremia. N Engl J Med. 2007;357(13):1316-25.
117. Oh HJ, Shin DH, Lee MJ, Koo HM, Doh FM, Kim HR, et al. Early initiation of continuous renal replacement therapy improves patient survival in severe progressive septic acute kidney injury. J Crit Care. 2012;27(6):743.e9-18.
118. Rosansky SJ, Clark WF, Eggers P, Glassock RJ. Initiation of dialysis at higher GFRs: is the apparent rising tide of early dialysis harmful or helpful? Kidney Int. 2009;76(3):257-61.
119. Cooper BA, Branley P, Bulfone L, Collins JF, Craig JC, Fraenkel MB, et al. A randomized, controlled trial of early versus late initiation of dialysis. N Engl J Med. 2010;363(7):609-19.
120. Himmelfarb J, Ikizler TA. Hemodialysis. N Engl J Med. 2010;363(19):1833-45.
121. Daugirdas JT, Chertow GM, Larive B, Pierratos A, Greene T, Ayus JC, et al. Effects of frequent hemodialysis on measures of CKD mineral and bone disorder. J Am Soc Nephrol. 2012;23(4):727-38.
122. Moist LM, Port FK, Orzol SM, Young EW, Ostbye T, Wolfe RA, et al. Predictors of loss of residual renal function among new dialysis patients. J Am Soc Nephrol. 2000;11(3):556-64.
123. van Biesen W, Claes K, Covic A, Fan S, Lichodziejewska-Niemierko M, Schoder V, et al. A multicentric, international matched pair analysis of body composition in peritoneal dialysis versus haemodialysis patients. Nephrol Dial Transplant. 2013;28(10):2620-8.
124. Devuyst O, Margetts PJ, Topley N. The pathophysiology of the peritoneal membrane. J Am Soc Nephrol. 2010;21(7):1077-85.
125. Jaar BG, Coresh J, Plantinga LC, Fink NE, Klag MJ, Levey AS, et al. Comparing the risk for death with peritoneal dialysis and hemodialysis in a national cohort of patients with chronic kidney disease. Ann Intern Med. 2005;143(3):174-83.
126. Macdonald JA, McDonald SP, Hawley CM, Rosman J, Brown F, Wiggins KJ, et al. Recovery of renal function in end-stage renal failure--comparison between peritoneal dialysis and haemodialysis. Nephrol Dial Transplant. 2009;24(9):2825-31.
127. Andrikos E, Tseke P, Balafa O, Pappas M. Five-year survival in comparable HD and PD patients: one center's experience. Int J Artif Organs. 2008;31(8):737-41.
128. Jansen MA, Hart AA, Korevaar JC, Dekker FW, Boeschoten EW, Krediet RT, et al. Predictors of the rate of decline of residual renal function in incident dialysis patients. Kidney Int. 2002;62(3):1046-53.
129. Mateijsen MA, van der Wal AC, Hendriks PM, Zweers MM, Mulder J, Struijk DG, et al. Vascular and interstitial changes in the peritoneum of CAPD patients with peritoneal sclerosis. Perit Dial Int. 1999;19(6):517-25.
130. Fielding CA, Topley N. Piece by piece: solving the puzzle of peritoneal fibrosis. Perit Dial Int. 2008;28(5):477-9.
131. Williams SW, Tell GS, Zheng B, Shumaker S, Rocco MV, Sevick MA. Correlates of sleep behavior among hemodialysis patients. The kidney outcomes prediction and evaluation (KOPE) study. Am J Nephrol. 2002;22(1):18-28.
132. Combet S, Ferrier ML, Van Landschoot M, Stoenoiu M, Moulin P, Miyata T, et al. Chronic uremia induces permeability changes, increased nitric oxide synthase expression, and structural modifications in the peritoneum. J Am Soc Nephrol. 2001;12(10):2146-57.

133. Zhou Q, Bajo MA, Del Peso G, Yu X, Selgas R. Preventing peritoneal membrane fibrosis in peritoneal dialysis patients. Kidney Int. 2016;90(3):515-24.
134. Kawaguchi Y, Kawanishi H, Mujais S, Topley N, Oreopoulos DG. Encapsulating peritoneal sclerosis: definition, etiology, diagnosis, and treatment. International Society for Peritoneal Dialysis Ad Hoc Committee on Ultrafiltration Management in Peritoneal Dialysis. Perit Dial Int. 2000;20 Suppl 4:S43-55.
135. Group KDIGOKTW. KDIGO clinical practice guideline for the care of kidney transplant recipients. Am J Transplant. 2009;9 Suppl 3:S1-155.
136. Galichon P, Xu-Dubois YC, Finianos S, Hertig A, Rondeau E. Clinical and histological predictors of long-term kidney graft survival. Nephrol Dial Transplant. 2013;28(6):1362-70.
137. El-Zoghby ZM, Stegall MD, Lager DJ, Kremers WK, Amer H, Gloor JM, et al. Identifying specific causes of kidney allograft loss. Am J Transplant. 2009;9(3):527-35.
138. Nankivell BJ, Alexander SI. Rejection of the kidney allograft. N Engl J Med. 2010;363(15):1451-62.
139. Solez K, Axelsen RA, Benediktsson H, Burdick JF, Cohen AH, Colvin RB, et al. International standardization of criteria for the histologic diagnosis of renal allograft rejection: the Banff working classification of kidney transplant pathology. Kidney Int. 1993;44(2):411-22.
140. Habib R, Kleinknecht C, Gubler MC, Maiz HB. Idiopathic membranoproliferative glomerulonephritis. Morphology and natural history. Perspect Nephrol Hypertens. 1973;1 Pt 1:491-514.
141. Eddy AA, Symons JM. Nephrotic syndrome in childhood. Lancet. 2003;362(9384):629-39.
142. Mundel P, Reiser J. Proteinuria: an enzymatic disease of the podocyte? Kidney Int. 2010;77(7):571-80.
143. Wei C, Reiser J. Minimal change disease as a modifiable podocyte paracrine disorder. Nephrol Dial Transplant. 2011;26(6):1776-7.
144. Wiggins RC. The spectrum of podocytopathies: a unifying view of glomerular diseases. Kidney Int. 2007;71(12):1205-14.
145. Hricik DE, Chung-Park M, Sedor JR. Glomerulonephritis. N Engl J Med. 1998;339(13):888-99.
146. Kestilä M, Lenkkeri U, Männikkö M, Lamerdin J, McCready P, Putaala H, et al. Positionally cloned gene for a novel glomerular protein--nephrin--is mutated in congenital nephrotic syndrome. Mol Cell. 1998;1(4):575-82.
147. Boute N, Gribouval O, Roselli S, Benessy F, Lee H, Fuchshuber A, et al. NPHS2, encoding the glomerular protein podocin, is mutated in autosomal recessive steroid-resistant nephrotic syndrome. Nat Genet. 2000;24(4):349-54.
148. Michaud JL, Chaisson KM, Parks RJ, Kennedy CR. FSGS-associated alpha-actinin-4 (K256E) impairs cytoskeletal dynamics in podocytes. Kidney Int. 2006;70(6):1054-61.
149. Hinkes B, Wiggins RC, Gbadegesin R, Vlangos CN, Seelow D, Nürnberg G, et al. Positional cloning uncovers mutations in PLCE1 responsible for a nephrotic syndrome variant that may be reversible. Nat Genet. 2006;38(12):1397-405.
150. Mucha B, Ozaltin F, Hinkes BG, Hasselbacher K, Ruf RG, Schultheiss M, et al. Mutations in the Wilms' tumor 1 gene cause isolated steroid resistant nephrotic syndrome and occur in exons 8 and 9. Pediatr Res. 2006;59(2):325-31.
151. Winn MP, Conlon PJ, Lynn KL, Farrington MK, Creazzo T, Hawkins AF, et al. A mutation in the TRPC6 cation channel causes familial focal segmental glomerulosclerosis. Science. 2005;308(5729):1801-4.

152. Meadow SR, Sarsfield JK. Steroid-responsive and nephrotic syndrome and allergy: clinical studies. Arch Dis Child. 1981;56(7):509-16.
153. Floege J, Johnson RJ, Feehally J. Comprehensive Clinical Nephrology. 4th ed: Saunders Elsevier; 2010.
154. Reiser J, von Gersdorff G, Loos M, Oh J, Asanuma K, Giardino L, et al. Induction of B7-1 in podocytes is associated with nephrotic syndrome. J Clin Invest. 2004;113(10):1390-7.
155. Wada T, Pippin JW, Marshall CB, Griffin SV, Shankland SJ. Dexamethasone prevents podocyte apoptosis induced by puromycin aminonucleoside: role of p53 and Bcl-2-related family proteins. J Am Soc Nephrol. 2005;16(9):2615-25.
156. Garin EH, Mu W, Arthur JM, Rivard CJ, Araya CE, Shimada M, et al. Urinary CD80 is elevated in minimal change disease but not in focal segmental glomerulosclerosis. Kidney Int. 2010;78(3):296-302.
157. Zhang SY, Kamal M, Dahan K, Pawlak A, Ory V, Desvaux D, et al. c-mip impairs podocyte proximal signaling and induces heavy proteinuria. Sci Signal. 2010;3(122):ra39.
158. Clement LC, Avila-Casado C, Macé C, Soria E, Bakker WW, Kersten S, et al. Podocyte-secreted angiopoietin-like-4 mediates proteinuria in glucocorticoid-sensitive nephrotic syndrome. Nat Med. 2011;17(1):117-22.
159. Schwartz MM, Korbet SM. Primary focal segmental glomerulosclerosis: pathology, histological variants, and pathogenesis. Am J Kidney Dis. 1993;22(6):874-83.
160. D'Agati VD, Fogo AB, Bruijn JA, Jennette JC. Pathologic classification of focal segmental glomerulosclerosis: a working proposal. Am J Kidney Dis. 2004;43(2):368-82.
161. Kitiyakara C, Eggers P, Kopp JB. Twenty-one-year trend in ESRD due to focal segmental glomerulosclerosis in the United States. Am J Kidney Dis. 2004;44(5):815-25.
162. Kaplan JM, Kim SH, North KN, Rennke H, Correia LA, Tong HQ, et al. Mutations in ACTN4, encoding alpha-actinin-4, cause familial focal segmental glomerulosclerosis. Nat Genet. 2000;24(3):251-6.
163. Dantal J, Bigot E, Bogers W, Testa A, Kriaa F, Jacques Y, et al. Effect of plasma protein adsorption on protein excretion in kidney-transplant recipients with recurrent nephrotic syndrome. N Engl J Med. 1994;330(1):7-14.
164. Marszal J, Saleem MA. The bioactivity of plasma factors in focal segmental glomerulosclerosis. Nephron Exp Nephrol. 2006;104(1):e1-5.
165. Wei C, El Hindi S, Li J, Fornoni A, Goes N, Sageshima J, et al. Circulating urokinase receptor as a cause of focal segmental glomerulosclerosis. Nat Med. 2011;17(8):952-60.
166. Kerjaschki D. Pathomechanisms and molecular basis of membranous glomerulopathy. Lancet. 2004;364(9441):1194-6.
167. Farquhar MG, Saito A, Kerjaschki D, Orlando RA. The Heymann nephritis antigenic complex: megalin (gp330) and RAP. J Am Soc Nephrol. 1995;6(1):35-47.
168. Debiec H, Nauta J, Coulet F, van der Burg M, Guigonis V, Schurmans T, et al. Role of truncating mutations in MME gene in fetomaternal alloimmunisation and antenatal glomerulopathies. Lancet. 2004;364(9441):1252-9.
169. Qin W, Beck LH, Zeng C, Chen Z, Li S, Zuo K, et al. Anti-phospholipase A2 receptor antibody in membranous nephropathy. J Am Soc Nephrol. 2011;22(6):1137-43.
170. Beck LH. Monoclonal anti-PLA2R and recurrent membranous nephropathy: another piece of the puzzle. J Am Soc Nephrol. 2012;23(12):1911-3.
171. Stahl R, Hoxha E, Fechner K. PLA2R autoantibodies and recurrent membranous nephropathy after transplantation. N Engl J Med. 2010;363(5):496-8.

172. Hoxha E, Kneißler U, Stege G, Zahner G, Thiele I, Panzer U, et al. Enhanced expression of the M-type phospholipase A2 receptor in glomeruli correlates with serum receptor antibodies in primary membranous nephropathy. Kidney Int. 2012;82(7):797-804.
173. Debiec H, Ronco P. PLA2R autoantibodies and PLA2R glomerular deposits in membranous nephropathy. N Engl J Med. 2011;364(7):689-90.
174. Higgins JP, Wang L, Kambham N, Montgomery K, Mason V, Vogelmann SU, et al. Gene expression in the normal adult human kidney assessed by complementary DNA microarray. Mol Biol Cell. 2004;15(2):649-56.
175. Kainz A, Mitterbauer C, Hauser P, Schwarz C, Regele HM, Berlakovich G, et al. Alterations in gene expression in cadaveric vs. live donor kidneys suggest impaired tubular counterbalance of oxidative stress at implantation. Am J Transplant. 2004;4(10):1595-604.
176. Schmid H, Boucherot A, Yasuda Y, Henger A, Brunner B, Eichinger F, et al. Modular activation of nuclear factor-kappaB transcriptional programs in human diabetic nephropathy. Diabetes. 2006;55(11):2993-3003.
177. Rossing K, Mischak H, Dakna M, Zürbig P, Novak J, Julian BA, et al. Urinary proteomics in diabetes and CKD. J Am Soc Nephrol. 2008;19(7):1283-90.
178. Cohen CD, Frach K, Schlöndorff D, Kretzler M. Quantitative gene expression analysis in renal biopsies: a novel protocol for a high-throughput multicenter application. Kidney Int. 2002;61(1):133-40.
179. Cohen CD, Gröne HJ, Gröne EF, Nelson PJ, Schlöndorff D, Kretzler M. Laser microdissection and gene expression analysis on formaldehyde-fixed archival tissue. Kidney Int. 2002;61(1):125-32.
180. Gibson UE, Heid CA, Williams PM. A novel method for real time quantitative RT-PCR. Genome Res. 1996;6(10):995-1001.
181. Lockhart DJ, Dong H, Byrne MC, Follettie MT, Gallo MV, Chee MS, et al. Expression monitoring by hybridization to high-density oligonucleotide arrays. Nat Biotechnol. 1996;14(13):1675-80.
182. Yasuda Y, Cohen CD, Henger A, Kretzler M, Consortium ERcBE. Gene expression profiling analysis in nephrology: towards molecular definition of renal disease. Clin Exp Nephrol. 2006;10(2):91-8.
183. Henger A, Kretzler M, Doran P, Bonrouhi M, Schmid H, Kiss E, et al. Gene expression fingerprints in human tubulointerstitial inflammation and fibrosis as prognostic markers of disease progression. Kidney Int. 2004;65(3):904-17.
184. Lindenmeyer MT, Kretzler M, Boucherot A, Berra S, Yasuda Y, Henger A, et al. Interstitial vascular rarefaction and reduced VEGF-A expression in human diabetic nephropathy. J Am Soc Nephrol. 2007;18(6):1765-76.
185. Segerer S, Banas B, Wörnle M, Schmid H, Cohen CD, Kretzler M, et al. CXCR3 is involved in tubulointerstitial injury in human glomerulonephritis. Am J Pathol. 2004;164(2):635-49.
186. Eitner F, Ostendorf T, Kretzler M, Cohen CD, Eriksson U, Gröne HJ, et al. PDGF-C expression in the developing and normal adult human kidney and in glomerular diseases. J Am Soc Nephrol. 2003;14(5):1145-53.
187. Sever S, Altintas MM, Nankoe SR, Möller CC, Ko D, Wei C, et al. Proteolytic processing of dynamin by cytoplasmic cathepsin L is a mechanism for proteinuric kidney disease. J Clin Invest. 2007;117(8):2095-104.
188. Ding M, Cui S, Li C, Jothy S, Haase V, Steer BM, et al. Loss of the tumor suppressor Vhlh leads to upregulation of Cxcr4 and rapidly progressive glomerulonephritis in mice. Nat Med. 2006;12(9):1081-7.

189. Chabardès-Garonne D, Mejéan A, Aude JC, Cheval L, Di Stefano A, Gaillard MC, et al. A panoramic view of gene expression in the human kidney. Proc Natl Acad Sci U S A. 2003;100(23):13710-5.
190. Cuellar LM, Fujinaka H, Yamamoto K, Miyamoto M, Tasaki M, Zhao L, et al. Identification and localization of novel genes preferentially expressed in human kidney glomerulus. Nephrology (Carlton). 2009;14(1):94-104.
191. Nyström J, Fierlbeck W, Granqvist A, Kulak SC, Ballermann BJ. A human glomerular SAGE transcriptome database. BMC Nephrol. 2009;10:13.
192. Nangaku M, Eckardt KU. Hypoxia and the HIF system in kidney disease. J Mol Med (Berl). 2007;85(12):1325-30.
193. Rosenberger C, Khamaisi M, Abassi Z, Shilo V, Weksler-Zangen S, Goldfarb M, et al. Adaptation to hypoxia in the diabetic rat kidney. Kidney Int. 2008;73(1):34-42.
194. Taneda S, Pippin JW, Sage EH, Hudkins KL, Takeuchi Y, Couser WG, et al. Amelioration of diabetic nephropathy in SPARC-null mice. J Am Soc Nephrol. 2003;14(4):968-80.
195. Socha MJ, Manhiani M, Said N, Imig JD, Motamed K. Secreted protein acidic and rich in cysteine deficiency ameliorates renal inflammation and fibrosis in angiotensin hypertension. Am J Pathol. 2007;171(4):1104-12.
196. Sen K, Lindenmeyer MT, Gaspert A, Eichinger F, Neusser MA, Kretzler M, et al. Periostin is induced in glomerular injury and expressed de novo in interstitial renal fibrosis. Am J Pathol. 2011;179(4):1756-67.
197. Lorz C, Ortiz A, Justo P, González-Cuadrado S, Duque N, Gómez-Guerrero C, et al. Proapoptotic Fas ligand is expressed by normal kidney tubular epithelium and injured glomeruli. J Am Soc Nephrol. 2000;11(7):1266-77.
198. Bao S, Ouyang G, Bai X, Huang Z, Ma C, Liu M, et al. Periostin potently promotes metastatic growth of colon cancer by augmenting cell survival via the Akt/PKB pathway. Cancer Cell. 2004;5(4):329-39.
199. Zhu M, Fejzo MS, Anderson L, Dering J, Ginther C, Ramos L, et al. Periostin promotes ovarian cancer angiogenesis and metastasis. Gynecol Oncol. 2010;119(2):337-44.
200. Segerer S, Cui Y, Eitner F, Goodpaster T, Hudkins KL, Mack M, et al. Expression of chemokines and chemokine receptors during human renal transplant rejection. Am J Kidney Dis. 2001;37(3):518-31.
201. Rios H, Koushik SV, Wang H, Wang J, Zhou HM, Lindsley A, et al. periostin null mice exhibit dwarfism, incisor enamel defects, and an early-onset periodontal disease-like phenotype. Mol Cell Biol. 2005;25(24):11131-44.
202. Bonnet N, Standley KN, Bianchi EN, Stadelmann V, Foti M, Conway SJ, et al. The matricellular protein periostin is required for sost inhibition and the anabolic response to mechanical loading and physical activity. J Biol Chem. 2009;284(51):35939-50.
203. Ayroldi E, Riccardi C. Glucocorticoid-induced leucine zipper (GILZ): a new important mediator of glucocorticoid action. FASEB J. 2009;23(11):3649-58.
204. D'Adamio F, Zollo O, Moraca R, Ayroldi E, Bruscoli S, Bartoli A, et al. A new dexamethasone-induced gene of the leucine zipper family protects T lymphocytes from TCR/CD3-activated cell death. Immunity. 1997;7(6):803-12.
205. Muller OG, Parnova RG, Centeno G, Rossier BC, Firsov D, Horisberger JD. Mineralocorticoid effects in the kidney: correlation between alphaENaC, GILZ, and Sgk-1 mRNA expression and urinary excretion of Na+ and K+. J Am Soc Nephrol. 2003;14(5):1107-15.
206. Soundararajan R, Zhang TT, Wang J, Vandewalle A, Pearce D. A novel role for glucocorticoid-induced leucine zipper protein in epithelial sodium channel-mediated sodium transport. J Biol Chem. 2005;280(48):39970-81.

207. Lindenmeyer MT, Eichinger F, Sen K, Anders HJ, Edenhofer I, Mattinzoli D, et al. Systematic analysis of a novel human renal glomerulus-enriched gene expression dataset. PLoS One. 2010;5(7):e11545.
208. Asselin-Labat ML, Biola-Vidamment A, Kerbrat S, Lombès M, Bertoglio J, Pallardy M. FoxO3 mediates antagonistic effects of glucocorticoids and interleukin-2 on glucocorticoid-induced leucine zipper expression. Mol Endocrinol. 2005;19(7):1752-64.
209. Weavers H, Prieto-Sánchez S, Grawe F, Garcia-López A, Artero R, Wilsch-Bräuninger M, et al. The insect nephrocyte is a podocyte-like cell with a filtration slit diaphragm. Nature. 2009;457(7227):322-6.
210. Gluderer S, Oldham S, Rintelen F, Sulzer A, Schütt C, Wu X, et al. Bunched, the Drosophila homolog of the mammalian tumor suppressor TSC-22, promotes cellular growth. BMC Dev Biol. 2008;8:10.
211. Gluderer S, Brunner E, Germann M, Jovaisaite V, Li C, Rentsch CA, et al. Madm (Mlf1 adapter molecule) cooperates with Bunched A to promote growth in Drosophila. J Biol. 2010;9(1):9.
212. Hildebrandt F. Genetic kidney diseases. Lancet. 2010;375(9722):1287-95.
213. Keller BJ, Martini S, Sedor JR, Kretzler M. A systems view of genetics in chronic kidney disease. Kidney Int. 2012;81(1):14-21.
214. He L, Sun Y, Takemoto M, Norlin J, Tryggvason K, Samuelsson T, et al. The glomerular transcriptome and a predicted protein-protein interaction network. J Am Soc Nephrol. 2008;19(2):260-8.
215. Prakash S, Papeta N, Sterken R, Zheng Z, Thomas RL, Wu Z, et al. Identification of the nephropathy-susceptibility locus HIVAN4. J Am Soc Nephrol. 2011;22(8):1497-504.
216. Hwang DY, Kohl S, Fan X, Vivante A, Chan S, Dworschak GC, et al. Mutations of the SLIT2-ROBO2 pathway genes SLIT2 and SRGAP1 confer risk for congenital anomalies of the kidney and urinary tract. Hum Genet. 2015;134(8):905-16.
217. Lu W, van Eerde AM, Fan X, Quintero-Rivera F, Kulkarni S, Ferguson H, et al. Disruption of ROBO2 is associated with urinary tract anomalies and confers risk of vesicoureteral reflux. Am J Hum Genet. 2007;80(4):616-32.
218. Grieshammer U, Le Ma, Plump AS, Wang F, Tessier-Lavigne M, Martin GR. SLIT2-mediated ROBO2 signaling restricts kidney induction to a single site. Dev Cell. 2004;6(5):709-17.
219. Woroniecka KI, Park AS, Mohtat D, Thomas DB, Pullman JM, Susztak K. Transcriptome analysis of human diabetic kidney disease. Diabetes. 2011;60(9):2354-69.
220. Fine LG, Norman JT. Chronic hypoxia as a mechanism of progression of chronic kidney diseases: from hypothesis to novel therapeutics. Kidney Int. 2008;74(7):867-72.
221. Fine LG, Bandyopadhay D, Norman JT. Is there a common mechanism for the progression of different types of renal diseases other than proteinuria? Towards the unifying theme of chronic hypoxia. Kidney Int Suppl. 2000;75:S22-6.
222. Eckardt KU, Bernhardt WM, Weidemann A, Warnecke C, Rosenberger C, Wiesener MS, et al. Role of hypoxia in the pathogenesis of renal disease. Kidney Int Suppl. 2005(99):S46-51.
223. Shved N, Warsow G, Eichinger F, Hoogewijs D, Brandt S, Wild P, et al. Transcriptome-based network analysis reveals renal cell type-specific dysregulation of hypoxia-associated transcripts. Sci Rep. 2017;7(1):8576.
224. Kruzynska-Frejtag A, Machnicki M, Rogers R, Markwald RR, Conway SJ. Periostin (an osteoblast-specific factor) is expressed within the embryonic mouse heart during valve formation. Mech Dev. 2001;103(1-2):183-8.

225. Merle B, Garnero P. The multiple facets of periostin in bone metabolism. Osteoporos Int. 2012;23(4):1199-212.
226. Guerrot D, Dussaule JC, Mael-Ainin M, Xu-Dubois YC, Rondeau E, Chatziantoniou C, et al. Identification of periostin as a critical marker of progression/reversal of hypertensive nephropathy. PLoS One. 2012;7(3):e31974.
227. Wantanasiri P, Satirapoj B, Charoenpitakchai M, Aramwit P. Periostin: a novel tissue biomarker correlates with chronicity index and renal function in lupus nephritis patients. Lupus. 2015;24(8):835-45.
228. Satirapoj B, Wang Y, Chamberlin MP, Dai T, LaPage J, Phillips L, et al. Periostin: novel tissue and urinary biomarker of progressive renal injury induces a coordinated mesenchymal phenotype in tubular cells. Nephrol Dial Transplant. 2012;27(7):2702-11.
229. Satirapoj B, Witoon R, Ruangkanchanasetr P, Wantanasiri P, Charoenpitakchai M, Choovichian P. Urine periostin as a biomarker of renal injury in chronic allograft nephropathy. Transplant Proc. 2014;46(1):135-40.
230. Wallace DP, White C, Savinkova L, Nivens E, Reif GA, Pinto CS, et al. Periostin promotes renal cyst growth and interstitial fibrosis in polycystic kidney disease. Kidney Int. 2014;85(4):845-54.
231. Nam BY, Park JT, Kwon YE, Lee JP, Jung JH, Kim Y, et al. Periostin-Binding DNA Aptamer Treatment Ameliorates Peritoneal Dialysis-Induced Peritoneal Fibrosis. Mol Ther Nucleic Acids. 2017;7:396-407.
232. Puglisi F, Puppin C, Pegolo E, Andreetta C, Pascoletti G, D'Aurizio F, et al. Expression of periostin in human breast cancer. J Clin Pathol. 2008;61(4):494-8.
233. Sasaki H, Dai M, Auclair D, Fukai I, Kiriyama M, Yamakawa Y, et al. Serum level of the periostin, a homologue of an insect cell adhesion molecule, as a prognostic marker in nonsmall cell lung carcinomas. Cancer. 2001;92(4):843-8.
234. Tischler V, Fritzsche FR, Wild PJ, Stephan C, Seifert HH, Riener MO, et al. Periostin is up-regulated in high grade and high stage prostate cancer. BMC Cancer. 2010;10:273.
235. Wallace DP, Quante MT, Reif GA, Nivens E, Ahmed F, Hempson SJ, et al. Periostin induces proliferation of human autosomal dominant polycystic kidney cells through alphaV-integrin receptor. Am J Physiol Renal Physiol. 2008;295(5):F1463-71.
236. Kyutoku M, Taniyama Y, Katsuragi N, Shimizu H, Kunugiza Y, Iekushi K, et al. Role of periostin in cancer progression and metastasis: inhibition of breast cancer progression and metastasis by anti-periostin antibody in a murine model. Int J Mol Med. 2011;28(2):181-6.
237. Liu C, Huang SJ, Qin ZL. Inhibition of periostin gene expression via RNA interference suppressed the proliferation, apoptosis and invasion in U2OS cells. Chin Med J (Engl). 2010;123(24):3677-83.
238. Sato M, Muragaki Y, Saika S, Roberts AB, Ooshima A. Targeted disruption of TGF-beta1/Smad3 signaling protects against renal tubulointerstitial fibrosis induced by unilateral ureteral obstruction. J Clin Invest. 2003;112(10):1486-94.
239. Bige N, Shweke N, Benhassine S, Jouanneau C, Vandermeersch S, Dussaule JC, et al. Thrombospondin-1 plays a profibrotic and pro-inflammatory role during ureteric obstruction. Kidney Int. 2012;81(12):1226-38.
240. Mael-Ainin M, Abed A, Conway SJ, Dussaule JC, Chatziantoniou C. Inhibition of periostin expression protects against the development of renal inflammation and fibrosis. J Am Soc Nephrol. 2014;25(8):1724-36.
241. Prakoura N, Kavvadas P, Kormann R, Dussaule JC, Chadjichristos CE, Chatziantoniou C. NFκB-Induced Periostin Activates Integrin-β3 Signaling to Promote Renal Injury in GN. J Am Soc Nephrol. 2017;28(5):1475-90.

242. Waldman M, Crew RJ, Valeri A, Busch J, Stokes B, Markowitz G, et al. Adult minimal-change disease: clinical characteristics, treatment, and outcomes. Clin J Am Soc Nephrol. 2007;2(3):445-53.
243. Pozzi C, Bolasco PG, Fogazzi GB, Andrulli S, Altieri P, Ponticelli C, et al. Corticosteroids in IgA nephropathy: a randomised controlled trial. Lancet. 1999;353(9156):883-7.
244. Robert-Nicoud M, Flahaut M, Elalouf JM, Nicod M, Salinas M, Bens M, et al. Transcriptome of a mouse kidney cortical collecting duct cell line: effects of aldosterone and vasopressin. Proc Natl Acad Sci U S A. 2001;98(5):2712-6.
245. Suarez PE, Rodriguez EG, Soundararajan R, Mérillat AM, Stehle JC, Rotman S, et al. The glucocorticoid-induced leucine zipper (gilz/Tsc22d3-2) gene locus plays a crucial role in male fertility. Mol Endocrinol. 2012;26(6):1000-13.
246. Bruscoli S, Velardi E, Di Sante M, Bereshchenko O, Venanzi A, Coppo M, et al. Long glucocorticoid-induced leucine zipper (L-GILZ) protein interacts with ras protein pathway and contributes to spermatogenesis control. J Biol Chem. 2012;287(2):1242-51.
247. Rashmi P, Colussi G, Ng M, Wu X, Kidwai A, Pearce D. Glucocorticoid-induced leucine zipper protein regulates sodium and potassium balance in the distal nephron. Kidney Int. 2017;91(5):1159-77.
248. Wu X, Yamada-Mabuchi M, Morris EJ, Tanwar PS, Dobens L, Gluderer S, et al. The Drosophila homolog of human tumor suppressor TSC-22 promotes cellular growth, proliferation, and survival. Proc Natl Acad Sci U S A. 2008;105(14):5414-9.
249. Sugano Y, Lindenmeyer MT, Auberger I, Ziegler U, Segerer S, Cohen CD, et al. The Rho-GTPase binding protein IQGAP2 is required for the glomerular filtration barrier. Kidney Int. 2015;88(5):1047-56.

LIST OF PUBLICATIONS

Lindenmeyer MT, Eichinger F, Sen K, Anders HJ, Edenhofer I, Mattinzoli D, Kretzler M, Rastaldi MP, Cohen CD. Systematic analysis of a novel human renal glomerulus-enriched gene expression dataset. PLoS One. 2010;5(7):e11545.

Neusser MA, Lindenmeyer MT, Moll AG, Segerer S, Edenhofer I, Sen K, Stiehl DP, Kretzler M, Gröne HJ, Schlöndorff D, Cohen CD. Human nephrosclerosis triggers a hypoxia-related glomerulopathy. Am J Pathol. 2010;176(2):594-607.

Sen K, Lindenmeyer MT, Gaspert A, Eichinger F, Neusser MA, Kretzler M, Segerer S, Cohen CD. Periostin is induced in glomerular injury and expressed de novo in interstitial renal fibrosis. Am J Pathol. 2011;179(4):1756-67.

Braun N, Sen K, Alscher MD, Fritz P, Kimmel M, Morelle J, Goffin E, Jörres A, Wüthrich RP, Cohen CD, Segerer S. Periostin: a matricellular protein involved in peritoneal injury during peritoneal dialysis. Perit Dial Int. 2013;33(5):515-28.

ACKNOWLEDGEMENTS

First of all, I would like to thank my supervisor Prof. Dr. Clemens D. Cohen for accepting me as his PhD student and supporting me with great dedication during those years.

I would also like to thank Prof. Dr. Carsten A. Wagner for being my responsible faculty member and for giving me the chance to finish my PhD.

Furthermore my thanks go to the other committee members: Prof. Dr. Rudolf Wüthrich, Prof. Dr. Johannes Loffing and Prof. Dr. Matthias Kretzler for their advice and support.

Many thanks to the former members of the Nephrology group: PD Dr. Maja Lindenmeyer, Ilka Edenhofer, Stefanie Gaiser, Prof. Dr. Stephan Segerer, Dr. Matthias Neusser, Dr. Anna Moser, Dr. Ivana Pavik Mezzour, Dr. Pietro Cippà and Shagun Raina.

Special thanks go to Katerina Svozilova for her encouraging and supportive words.

My biggest thanks go to my parents and my brother for believing in me and supporting me during my entire education.